Studies On Copper Extraction With Hydroxyoxime Extractants For The Design Of Hollow Fibre Membrane Based Extraction Processes

by

Salman Ghanem Rashid

A thesis submitted in partial fulfilment of the requirements

of the University of Glamorgan

for the degree of Doctor of Philosophy

University Of Glamorgan

School Of Applied Sciences

Chemical Engineering and Technology Division

This research work programme was carried out in collaboration with the Department of Food Studies, Biotechnology Division, University of Reading

April 1999

Declaration

This is certify that, except where specific reference is made, the work describe in this thesis is the result of the candidate. Neither this thesis, nor any part of it has been presented, or is concurrently submitted in candidature for any other degree at any other University.

Signed 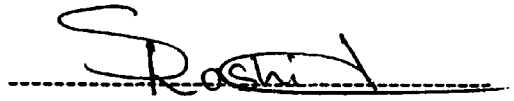

Candidate

Signed 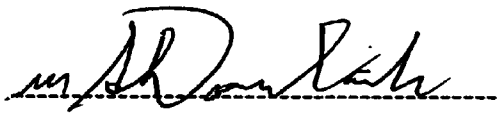

Director of Studies

Signed 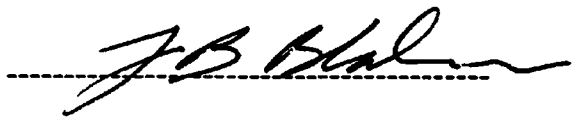

Director of Studies

Date 28 - 4 - 1999

To my family
and to all the people who helped,
encourage, enlightened, and inspired me.

ABSTRACT

This work has included a review of the most relevant aspects of measurement techniques and mathematical models proposed in the literature to assess the equilibrium and mass transfer data of metal extraction by the use of chelating agents. The limitations of these techniques and models have been highlighted.

Three chelating extractants diluted in Escaid110 were used to study the extraction equilibrium of copper. The extractants are 5-nonylacetophenone oxime (LIX84®), 5-dodeylsalicylaldoxime (LIX860®) and 50/50 v/v mixture of both oximes (LIX984®). The copper concentration changes in the aqueous and the organic phases were monitored by using atomic absorption spectrophotometer.

Two mathematical models (a chemical model and a semi-empirical model) have been developed in this study to predict the equilibrium data of copper sulfate/ hydroxyoxime system. The chemical model was found to fit all the three equilibrium systems ($CuSO_4$/ LIX84®, LIX860®and LIX984®) equally. The semi-empirical model based on Freundlich's adsorption equation was also found to fit the three systems but with less accuracy.

The mass transfer characteristics and properties of copper extraction and recovery from an aqueous solution using LIX984® were studied using dispersion-based (rising drops) and dispersion-free techniques. In the dispersion-based technique the organic phase was dispersed in form of drops at the tip of hypodermic needle while the aqueous solution was used as a continuous phase. The extraction process was carried out in four different height columns under wide range of conditions. The effects of the columns' height, the dispersed and the continuous phases concentrations on the metal rate of mass transfer were investigated. It has been found in that the metal's rate of mass transfer and system's overall mass transfer coefficient have remained constant in all four columns. A model utilising the

two-film theory, some of the dimensionless groups and the experimental results has been proposed in this work to calculate the local mass transfer coefficients in the dispersed phase and the continuous phase. The overall mass transfer coefficient and the calculated local coefficients were used to account for the reaction rate constant at the interface from the sum of the individual resistances to mass transfer.

A dispersion-free technique consisting of a microporous hollow fibre module was used in this study to examine the mass transfer properties of the extraction and stripping processes of copper across an immobilised interface system. The extraction and re-extraction (stripping) processes in this system were conducted under a wide range of operating conditions and produced satisfactory results. In general it has been found that counter current flow arrangement gave higher concentration driving forces which were reflected in form higher metal concentrations at the extract phase.

A generalised mathematical model was developed in this study which utilised Wilson's method, the experimental data, some dimensionless groups and the two-film theory to account for local resistances and predict the system's overall mass transfer coefficient. A correlation was established first to calculate mass transfer coefficients using a form of Leveque's equation which relates the two phase's physical properties and the system's parameters. The membrane mass transfer coefficient was calculated from the structural properties of the membrane material. While the resistance at the reaction interface was calculated under set of experimental conditions. The individual coefficients were then used to predict the overall mass transfer coefficient under any set of conditions by using the aditivity approach of the individual resistances to mass transfer. However, further checks and investigations are necessary to validate this model over variety of extraction systems and membrane configurations.

Acknowledgements

A thankful prayer to almighty Allah for giving me the faith, the health and the knowledge.

I am greatly indebted to Dr .M. S. Doulah and Mr. F. B. Blackemore for their intellectual contribution, enthusiastic support and accessibility throughout the course of this study. I would like to extend my thank to Dr. F. Y. Addo-Yobo of Reading University for the help, guidance and support he provided at the early stage of this work. The Chemical Engineering Division at the School of Applied Sciences of the University of Glamorgan provided an intellectually stimulating environment in which to work and develop ideas. I am grateful to the former and current Head of School Professor J. R. Dixon and Dr. P. McIntyre respectively. Further, I gratefully acknowledge the skilled support provided by Mr. B. Evans and the technical staff in this department for the construction of the experimental rig.

Special thanks are due to Mr. D. Koppl of Henkel CO. in Germany and Exxon Chemical Ltd. UK for their generous donations of the organic solvent and the diluent Escaid110.

I am particularly thankful to my friends Hishamudin, Ja'ffar, Samir, Harith, Faisal, Ahmed, Ali, Fauzi, and Johannes for their support and encouragement throughout all times. Importantly I would like to thank Vasso for her friendship, support, neat typing and marvellous cooking.

Finally my heartfelt thank goes to my family who provided me with love and the inspiration to take on challenges in life and overcome its difficulties.

"In The Name Of Allah, Most Gracious, Most Merciful"

(Moses Said:) "O my lord! Expand me my breast, ease my task for me and remove the impediment of my speech so they may understand what I say"

The Holy Qur'an, Surah 20: Taha.

CONTENTS

List of figures

List of tables

NOMENCLATURE

Symbol	Definition	Units
A	The surface area of transfer	cm^2
A_c	The surface area where the contact between	
	the two phase occurs	cm^2
A_d	Drop surface area	cm^2
C^{i}_{HR}	The interfacial concentration of LIX984 at time (t)	g/cm^3
C^{*}_{aCu}	A hypothetical copper concentration in the aqueous.	g/cm^3
	phase interface in equilibrium with the bulk organic phase.	g/cm^3
C^{*}_{oCu}	A hypothetical copper concentration in the organic phase	
	interface in equilibrium with the bulk aqueous phase.	g/cm^3
C^{ab}_{Cu}	The copper concentration at the bulk aqueous phase.	g/cm^3
C_{aqs}^{in} , C_{aqs}^{out}	The copper concentrations at the stripping phase	
	flowing into and out of the MPHF membrane.	g/cm^3
C^{i}_{Cu}	The copper concentration at the aqueous phase-	
	membrane interface.	g/cm^3
C^{i}_{CuR2}	The (copper-LIX) formed complex concentration at	g/cm^3
	(the aqueous phase-inner surface of the fibre) interface.	
C^{i}_{HR}	The interfacial concentration of the chelating active reagent.	g/cm^3
$C^{i}_{H^+}$	The interfacial concentration of hydrogen generated during the	
	reaction.	g/cm^3
C^{in}_{aq}	Initial copper concentration at the aqueous feed stream.	g/cm^3

C^{in}_{HR}	The initial concentration of the droplet organic phase LIX984 in Escaid110.	g/cm^3
C_L	The column height.	cm
C^{om}_{CuR2}	The (copper-LIX) formed complex concentration at (the outer surface of the fibre-organic phase) interface.	g/cm^3
C_{orge}^{in} , C_{orge}^{out}	Copper concentrations at the organic (extract) phase flowing into and out the MPHF membrane.	g/cm^3
C_{org}^{out}	Copper concentration at the droplet organic phase (LIX984) at the top of the column.	g/cm^3
C^{out}_{aq}	Copper concentration at the aqueous outlet stream (the raffinate).	g/cm^3
C^{r}_{HR}	The reacted concentration of LIX984 to form the metal-organic complex.	mole/l
C^{si}_{Cu}, C^{si}_{HR}, $C^{si}_{H^+}$ and C^{si}_{CuR2}	The interfacial concentrations during a stripping process in a MPHF module of copper, the LIX reagent, the hydrogen generated during the reaction and the copper-LIX reagent formed at the interface respectively	mole/l
D_{aq}, D_{org}	The diffusion coefficient of copper at the aqueous phase and the organic phase respectively.	cm^2/s
D_{cu}	Diffusivity of copper ion in the aqueous phase.	m^2/s
d_c	The column internal diameter	m
$D_{eff\,CuR2}$, D_{CuR2}	The (copper-LIX formed complex) effective diffusion and diffusion coefficient respectively.	cm^2/s

d_f	The drop flow rate (drops per minutes).	Drop/min
d_h	The shell hydraulic diameter.	cm
D_{HR}	The diffusivity coefficient of LIX984 in Escaid 110.	cm^2/s
d_i	Fibre tube internal diameter.	cm
d_{is}	The inner diameter of the membrane shell.	cm
d_{it}	The fibre tube internal diameter.	cm.
d_m	Fibre tube external diameter.	cm
d_o:	The shell side internal diameter.	cm
D^o_{HR}	The mutual diffusivity coefficient of species.	-
d_{ot}	The outer diameter of fibre tube.	cm.
d_p	Drop diameter	cm
F_{aq}, F_{org}	The volumetric flow rates of the aqueous and organic phases respectively.	cm^3/s
F_{aqs}	The stripping phase volumetric flow rate.	cm^3/s
F_{orge}	The rich copper organic (extract) phase volumetric flow rate.	cm^3/s
J	The mass flux of solute throughout the membrane module.	g/s
k_{aq}	The aqueous phase mass transfer coefficient.	cm/s
k_m	Mass transfer coefficient across the membrane wall.	cm/s
k_{org}	The organic phase mass transfer coefficient.	cm/s
K_{ov}	The overall mass transfer coefficient.	cm/s
K_{ovc}	The calculated value of the overall mass transfer coefficient	cm/s

K_{ovf}	The overall mass transfer coefficient value found experimentally.	cm/s
k_r, K_{ex}	The reaction rate constant and the equilibrium constant respectively.	-
k_s	The stripping reaction rate constant.	-
K_w	The overall mass transfer coefficient based on the aqueous phase.	cm/s
k_{wt}	The aqueous phase mass transfer coefficient.	cm/s
L	The membrane module length.	cm
M_{Cu}	Total mass of copper extracted in single drop of the organic phase	g
M_s	The molecular weight of Escaid110.	-
n	Number of fibre tubes inside the membrane module.	-
N_a	The overall rate of mass transfer per unit area per unit time.	g/cm^2s
N_{AB}	The number of drops sufficient to fill $1cm^3$ volume of the capillary tube.	drops
N_{Res}	The Reynolds number of the organic phase in the shell side.	-
N_{Ret}	The Reynolds number of the aqueous phase inside the fibre tube	-
N_{Scs}	Schmidt number of the organic phase in the shell side	-
N_{Sct}	Schmidt number of the aqueous phase inside the fibre tube	-

N_{Shs}	Sherwood number of the organic phase in the shell side	-
N_{Sht},	Sherwood number of the aqueous phase inside the fibre tube	-
r_d	The drop radius.	cm
SME529™	A commercial name used to define 2-hydroxy-5nonyl acetophenone, which produced by Shell.	-
T	The room temperature during experiment time, in Kelvin.	K
t_m	The membrane fibre wall thickness.	cm
t_r	Drop rising time.	s
V	The drop's average linear velocity.	m/s
V_c	The volume of the capillary tube, (section AB in figure. 3.1).	cm^3
V_d	The volume of single drop.	cm^3
v_{HR}	The molar volume of LIX984.	-
V_{org}	Volume of the loaded organic phase in the capillary tube section.	cm^3
V_t	The drop's terminal velocity.	m/s
a, b, γ and β	Constants.	-
ΔC_{LM}	The logarithmic mean driving force for copper concentration at both ends of the MPHF membrane contactor.	g/cm^3
ε_m	The membrane porosity.	-
η	Kinematic viscosity.	cm^2/s
θ_f	Association factor of the organic solvent.	-
σ	The continuous phase interfacial tension.	N/m^2.

μ_c	The continuous phase viscosity.	Ns/m^2
μ_D	The dispersed phase viscosity.	Ns/m^2
μ_s	The viscosity of Escaid 110	Ns/m^2
ρ_c	The continuous phase density.	kg/m^3
τ_m	The tortuosity of the membrane pores.	-

CHAPTER ONE

1 INTRODUCTION

Liquid-liquid extraction is a process in which a solute is transferred between two partially miscible or immscible liquid phases due to its solubility or chemical potential. This process has achieved considerable progress in replacing conventional thermal based processes such as distillation especially in the separation or purification of products which could be damaged by thermal processing [1,2].

1.1 Liquid-Liquid Extraction of Metals

The recovery of metal through liquid-liquid extraction process has attracted world wide attention from scientific and commercial sectors. This is due to the rapid success and effective cost reduction it offers in metal extraction in comparison to pyrometallurigical techniques. The technological advances in this area taken place so far in the improvement of new extraction reagents i.e. solvents. These solvents should have set of properties to be suitable for metals extraction; these properties can be summarised as follows:

1. High selectivity toward the metal species to be extracted
2. Low solubility in the aqueous phase
3. Free or low toxicity of the solvent through out the extraction process and in the downstream biological treatment facilities.
4. Easy to strip and recover from the aqueous phase and highly stable to be recycled within close loop.
5. Low cost and highly effective even with lower concentration levels (in a suitable carrier or diluent).

To achieve the fullest potential of the extraction process, research work is needed in the area of extraction mechanisms. The foremost requirement for a separation process i.e. liquid-liquid extraction is the phase equilibrium between phases involved. The equilibrium characteristics of an aqueous solution containing metal ions with an organic solvent containing an extractive reagent are the main focus of many research works [1-17]. The wider interests include developing means of minimising the cost of predicting system equilibria through mathematical modelling. This is due to the fact that establishing equilibrium data by experimental means is often time consuming, with costly materials and labour and is remarkably difficult in some cases. Hence, it is often the case a limited amount of experimental data are generated and then correlation equations are used to estimate and predict the essential data over the required range of concentrations.

Some of these models are chemically and thermodynamically based while others are of an empirical nature. However, these models are still falling short of predicting precisely all changes in physical and chemical properties of systems involved. Some new mathematical models for the prediction of copper-hydroxyoxime system's equilibria that take into account the process main variables have been proposed in this work. Further to the phase equilibria, the characteristics of metal mass transfer and the influence of contacting technique on the output of the extraction process are also important.

1.1.1 Overall rate of mass transfer

The rate of mass transfer in liquid-liquid extraction of metals has important implications for the performance of extraction process. The knowledge of the overall rate of mass transfer is essential for the design of an extraction process and process equipment. Mass transfer in metal extraction usually involves chemical reaction between the metal ions (in the aqueous phase) and the extracting reagent (in the organic phase). Since a chemical reaction is involved, the rate of mass transfer between the two phases will depend upon both the rate of actual physical transport of the reactants and the products in both phases and the kinetics of the reaction. The theoretical aspects of mass transfer accompanied by chemical reactions follow the same principles of well known theories of mass transfer namely; the two-film theory, surface renewal theories and the penetration theories.

The process of mass transfer from the bulk phases across the boundary layer to the interface is through diffusional means unless enhanced by external disturbances such as mixing. While mass transfer where chemical reaction is involved should include the site of the chemical reaction between the metal species and the extractant at the aqueous phase or at the interface depending on the chemical nature of the reactants.

If the chemical reaction is much faster than the diffusion process, the overall rate of mass transfer will be controlled by diffusion of the reactants and the products. On the other hand, when the diffusion process is much faster than any of the chemical reaction steps, the overall mass transfer may be limited by chemical kinetics. Generally most liquid-liquid metal extraction processes appear to incorporate kinetic and diffusional regimes [18].

Many techniques have been employed to study mass transfer characteristics in liquid-liquid extraction of metals. The reported results from these techniques are varied due to the differences in contacting scheme and the hydrodynamic feature of these techniques. The single drop technique is one of the chosen techniques for studying mass transfer and kinetic

properties of copper sulfate-hydroxyoxime system in this work. This technique is chosen because of the advantages it offers i.e. known interfacial area and easy to construct and operate. However, all existing techniques for kinetic and mass transfer studies still suffer limitations and shortcomings. Therefore, the demand for an efficient and cost effective technique is strong.

1.2 Membranes Applications

One of the newly emerging techniques is free-dispersion membrane based liquid-liquid extraction, particularly microporous hollow fibre membranes. This technique is used extensively in this study and it offers enormous advantages in comparisons to conventional techniques especially in overcoming the operational and scaling-up limitations.

Membranes in general are permeable or semi-permeable materials made of polymer, inorganic or metals which are capable of hindering the motions of certain species. These membranes are diverse in their geometrical shapes and sizes ranging from thin flat sheets to large microporous hollow fibre contactors.

The uses of these membranes have increased significantly in recent years driven by new environmental legislation on waste gases and effluent treatment to cover traditional unit operations in the process industries such as gas absorption and liquid-liquid extraction beside the well established applications like filtration.

The intensive demands for larger applications of membranes technology in liquid-liquid extraction processes in general and in toxic and precious metals removal and recovery in particular have increased the need for a thorough investigation to determine membrane operational and technical parameters. This study concentrates on establishing mass transfer parameters of copper extraction and recovery of copper from an aqueous solution under variable conditions using a microporous hollow fibre membrane. The microporous hollow fibre membrane module, which is referred to here and after, as MPHF, is the unit where the

free-dispersion extraction and stripping takes place. This technique immobilises two-immscible phase's interface at the pores mouths in one side of the microporous membrane. The location of the interface depends on membranes wetability and pores size. Through this immobilised interface the required solutes are transferred between the two phases driven by a chemical reaction across the membrane wall, while the two phases flow on opposite sides of the membrane. A wide range of copper concentrations ranging between low level concentrations 25 ppm to relatively high concentrations of 3g/l have been used in this study.

It is important here to emphasis the fact that the equilibrium studies and mass transfer characterisations of copper sulfate-hydroxyoxime system which have been carried out in this work are useful for the construction of conventional metal extraction equipment as well as for the design of membrane based metal extraction processes. The experimental work in this study covers some aspects of metal extraction mass-transfer features in a single drop technique and a hollow fibre membrane. The promising features of a MPHF membrane based metal extraction process and its ability to replace existing conventional technique i.e. mixer settler is one of the motivations behind this study.

As part of this study a survey of the relevant literature indicated a need for an understanding of copper extraction with chelating agents. Hence, the experimental work in this thesis is planed to focus on the following areas:

1. Determine and clarify all operating conditions on phase equilibria between aqueous solutions of copper and newly introduced hydroxyoximes (LIX) reagents, such as LIX84®, LIX860® or LIX984®.
2. Development of mathematical models, which can estimate efficiently the concentrations of copper to be extracted by these hydroxyoximes under set equilibrium conditions.

3. Clarify through detailed experimental work the reaction and mass transfer mechanisms of copper extraction with the above extractants, which have not been investigated or reported in the literature.
4. Characterisation and measurement of the overall mass transfer coefficient of copper in LIX984 over a wide range of conditions in both single-drop technique and MPHF contactors.
5. Development of general mathematical equations for MPHF membrane based extraction unit for the extraction of heavy metal such as copper from wastewater and weak leached mine deposit.

The results of the equilibrium stage and mass transfer mechanisms in the dispersion-based and dispersion-free techniques (i.e. rising single drop and microporous hollow fibre membrane respectively) are listed in Chapter 4. While the data analysis and thorough discussion of this study finding are presented in Chapter 5.

CHAPTER TWO

2 LITERATURE SURVEY

2.1 An introduction to liquid-liquid extraction

Liquid-liquid extraction is a process in which a solute is transferred from one liquid phase (called the feed) into partially miscible or totally immscible liquid phase (called the solvent). The remaining of the feed solution after the contacting stage is called the raffinate, and the solvent containing the desired component is called the extract [1-4]. Liquid-liquid extraction is used to separate solutes which are either difficult or impossible to separate by conventional thermal techniques such as distillation. Therefore this process is widely used in the following fields:

- Separation of close boiling point mixtures such as isomers.
- Separation of heat sensitive components to avoid temperature damage that might be caused by thermally driven separation.
- Removal of organic from wastewater which has better prospect of energy saving over ordinary separation by evaporation.
- Recovery of non-volatile materials as in extracting metals from their mineral deposits.

The employment of solvent extraction has grown rapidly in the petrochemical industry (refining of lubricating oil, and production of aromatic hydrocarbons), at the same time it is widely used in the pharmaceutical industry for the purification of anti-biotics [2]. While in metal processing, solvent extraction was first reported as an analytical tool for the separation of most metals in the periodic table[5-8]. An enormous number of publications covering both the engineering and the chemistry aspects of extraction are reported in literature[1,2,6-16] .In contrast the practical and design aspects of solvent extraction processes

are not widely publicised, partly because the equipment and systems design have been largely in the hands of equipment suppliers. Nevertheless many authors have explained in some details the design principles and the main parameters for some extraction equipment[3,15,19].

2.1.1 Metals separation by liquid-liquid extraction

Solvent extraction of metals was first reported as an analytical method in many parts of the world[20,21]. This process was rapidly developed as a consequence of a parallel development of inexpensive effective organic reagents (extractant). These subsequently led to the establishment of large scale processes for the extraction of copper, rare-earth metals and actinide and other metals from the hydrometallurgical leach liqours[19,22-23]. Liquid-Liquid extraction process is used for both purification and concentration in metal separation. It is a purification process because a single metal solute can be selectively removed from a mixture of metals solutes by choice of the organic extractant. It can be used as a concentration process because a small volume of an organic solvent can be loaded with a large concentration of the required metal from a diluted aqueous solution. There are many reasons for the commercial growth of metal separation by liquid-liquid extraction also known as (Hydrometallurgy) which can be summarised as follows:

1. It is suitable for the treatment of low grade ores and complex ores, especially in the metal industry as a gradual exhaustion of natural resources and the declining of the ore grade of many metals become eminent.
2. Environmental legislation of anti-pollution "clean technology" has set the limits for maximum metals concentrations in discharged effluent streams in which hydrometallurgical processes have proved successful in comparison to conventional processes.

3. Hydrometallurgy requires low capital and operating cost, because of the recycling of organic solvents and by product recovery.
4. Almost complete recovery of metal from ores is possible.
5. Liquid-liquid extraction processes for metal recovery are amenable to automatic controls resulting in lower labour cost.

The development of liquid-liquid extraction processes has been considerably enhanced by the recent availability of variety of extractants which by chelation, ion exchange or solvation selectively separate metals from aqueous solutions. This has led to solvent extraction gaining favour in the metal industry, so that in recent years some over 100 plants of different size are in operation and more are under construction throughout the world in the processing of 25 different metals[3].

2.1.2 Copper extraction technology

Primitive Hydrometallurigical processing of pyrites containing copper sulfate was practised at Rio-Tinto in Spain since the 1700's where the first large scale leaching process was reported [24]. In the last 50 years copper production has increased world-wide especially after the successful use of highly selective reagents and electrowinning compound processes. This is reflected in the size and magnitude of copper extraction plants, which are larger than any other type of solvent extraction plants presently in operation.

Copper extraction from its ores listed in table 2.1, has been described by Ritcey (1984) as a three steps process; extraction, scrubbing and stripping [25]. The aqueous solution (feed) containing the metal and the organic solvent is fed in a counter current manner into the extraction stage. In this stage a mass transfer process takes place in which the required metal is transferred from the aqueous phase to the organic solvent. The aqueous phase outlet (Raffinate) is either further re-extracted in another extraction stage or recycled to the

heap. While the outgoing organic phase (extract) is fed counter currently into another contactor where it is scrubbed with a suitable scrub solution to remove any impurities. Normally scrubbing is achieved by water or diluted acid[23]. The scrubbed loaded solvent is then pumped into the stripping stage where the final phase of mass-transfer takes place. In this stage the metal is transferred from the organic phase into a low pH aqueous phase. The concentrated aqueous solution produced here is then pumped to the electrowinning unit in which the copper metal is deposited at the cathodes. The first plant to use liquid extraction electrowinning sequence was the Ranchers Bluebird mine at Arizona[26-27]. While the largest copper plant using this process went into production in 1974 in Zambia[3].

Table 2. 1: Summarises the main source of copper deposits.

Minerals	**Compositions**	**Copper percentage of the mineral**	**Reference**
Chalcocite	Cu_2S	78.8%	26
Chalcopyrite	$CuFeS_2$	34.5%	26
Bornite	Cu_5FeS_4	63.3%	26
Enargite	Cu_3AsS_4	48.3%	26
Antlerite	$3CuS.As_2S_5$	65.8%*	26
Tetrahedrite	$4(Cu_2S).Sb_2S_3$	21.9%*	26
Azurite	$2CuCO_3.(CuOH)_2$	94.5%*	26
Malachite	$CuCO_3.Cu(OH)_3$	90.2%*	26
Cuprite	Cu_2O	85.5%*	26
Bornite	$FeS.2Cu_2S.CuS$	70.0%*	26

* Percentage dissolved in cyanide after 24 hours

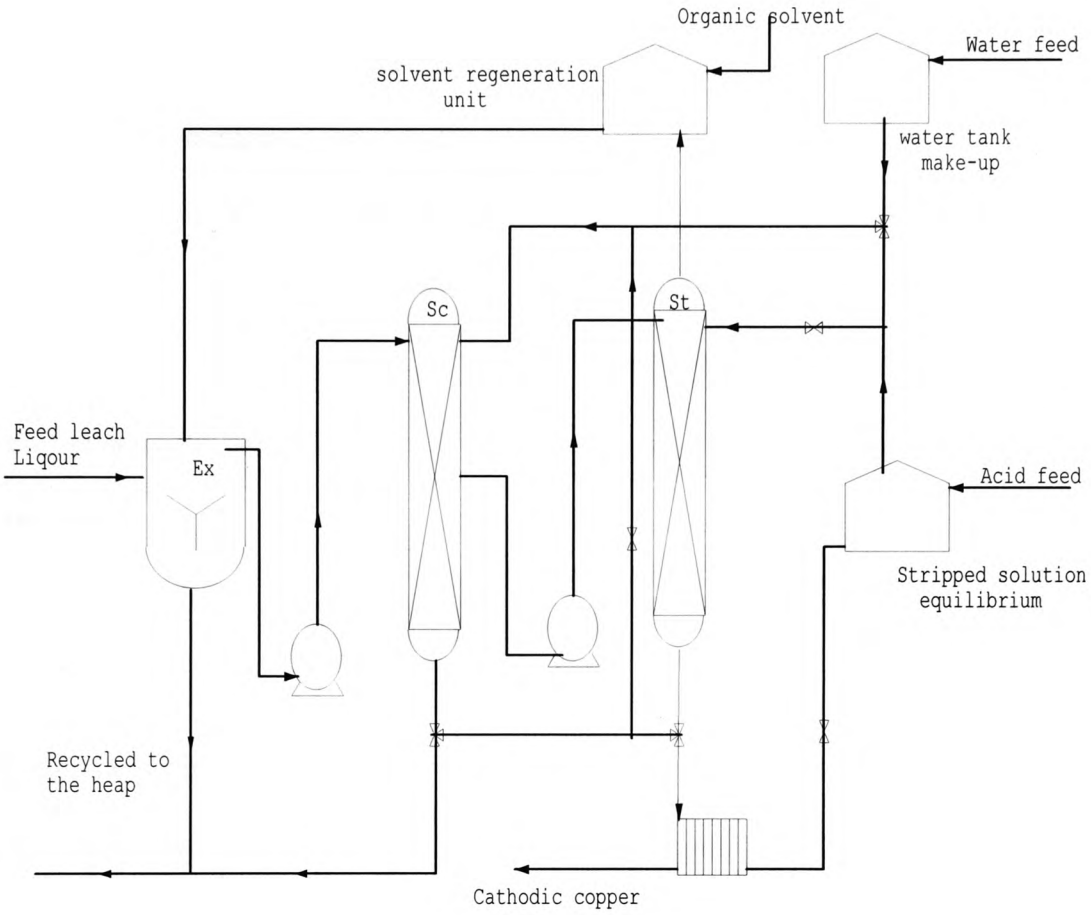

Figure 2. 1: General process of copper extraction, where the symbols; (Ex) is extraction stage, (Sc) is scubbing stage and (St) is stripping stage. Source is Ritcey and Ashbrook[23].

2.2 THE IMPORTANCE OF PHASE EQUILIBRIA IN LIQUID-LIQUID EXTRACTION

An initial requirement for the design of a liquid-liquid extraction plant is the knowledge of solute distribution behaviour under the proposed operating conditions. This and the search for a better understanding of solute transfer mechanisms were the reasons for many publications on this subject [1-3,13,19]. The various ways in which distribution equilibria can be treated have been covered by Marcus and Kertes[18]. Extraction equilibrium studies of a metal species are often described in terms of metal distribution coefficient (E , D or m) between the aqueous and organic phases which has appeared in many publications[25,28-29] as follows:

$$m = \frac{\text{Concentration of metal in the organic phase}}{\text{Concentration of metal in the aqueous phase}}$$

This Coefficient is useful in guiding the selection of the organic solvent (extractant) especially when the aqueous solution contains more than one metal species, each of which has different tendencies towards different extractants, see figure 2.2.A and B.

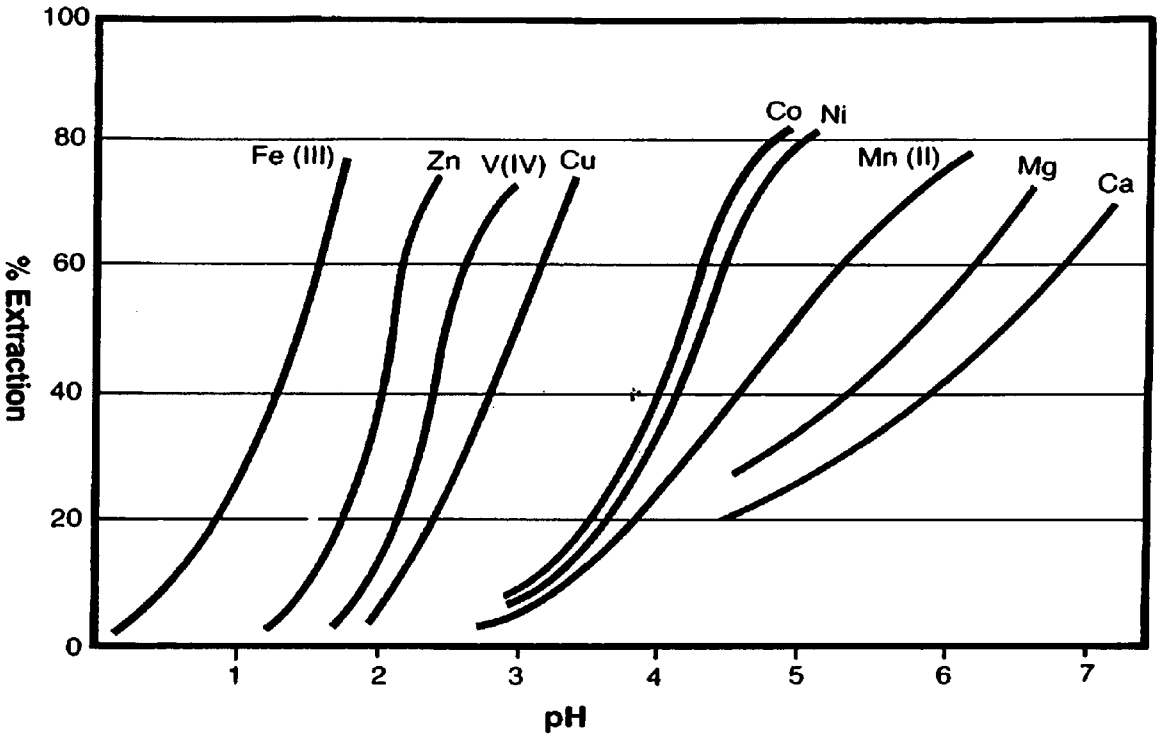

(A)

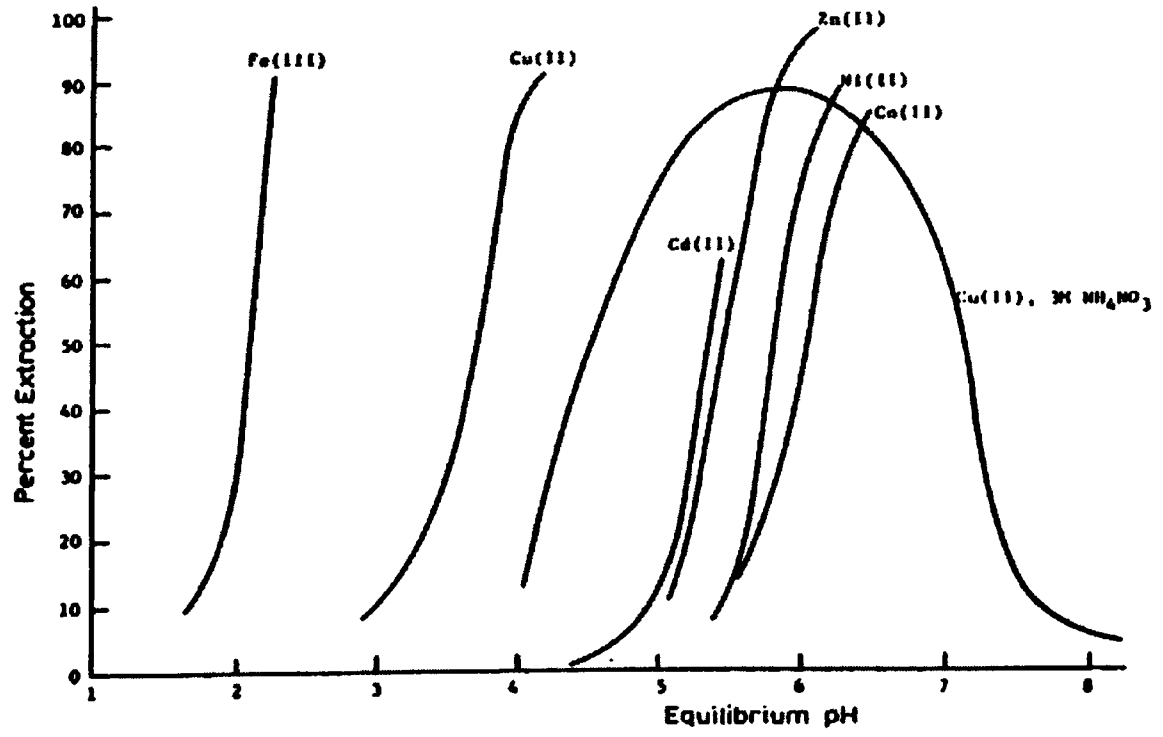

(B)

Figure 2. 2: The extraction tendencies of different metals in two different extractants, (A) in D2EHPA and (B) in Nephthaneic acid [23,30].

In general metal extraction equilibria can be described by the following equations:

$$M^{n+}{}_{aq} + nHR_{org} \rightleftharpoons MR_{norg} + nH_2{}^{+}{}_{aq} \qquad 2.1$$

The equilibrium constant for this equation is:

$$K_{ex} = \frac{[MR_{n_{org}}][H^{+}_{aq}]^n}{[M^{n+}_{aq}][HR_{org}]^n} \qquad 2.2$$

$$m = \frac{[MR_{n_{org}}]}{[M^{n+}_{aq}]} \qquad 2.3$$

Then equation 2.2 could be rearranged as follows:

$$K_{ex} = m \times \frac{[H^{+}_{aq}]^n}{[HR_{org}]^n} \qquad 2.4$$

Taking the log of both sides will result:

$$Logm = LogK_{ex} + nLog[HR_{org}] - nLog[H^{+}_{aq}] \qquad 2.5$$

or $$Logm = LogK_{ex} + nLog[HR_{org}] - npH \qquad 2.6$$

From these equations it is clear that equilibrium data are unique to the conditions under which they are generated. These equations also show the important relationships, which exist, between various parameters during equilibrium studies and indeed throughout the process of metal extraction. According to commercial research carried out by the Henkel Co.[34],and others [30] With various metals using hydroxyoxime (LIX84®), the order of metal extraction reaction (n) appears to be a function of the equilibrium pH, as can be seen in figure 2.3.

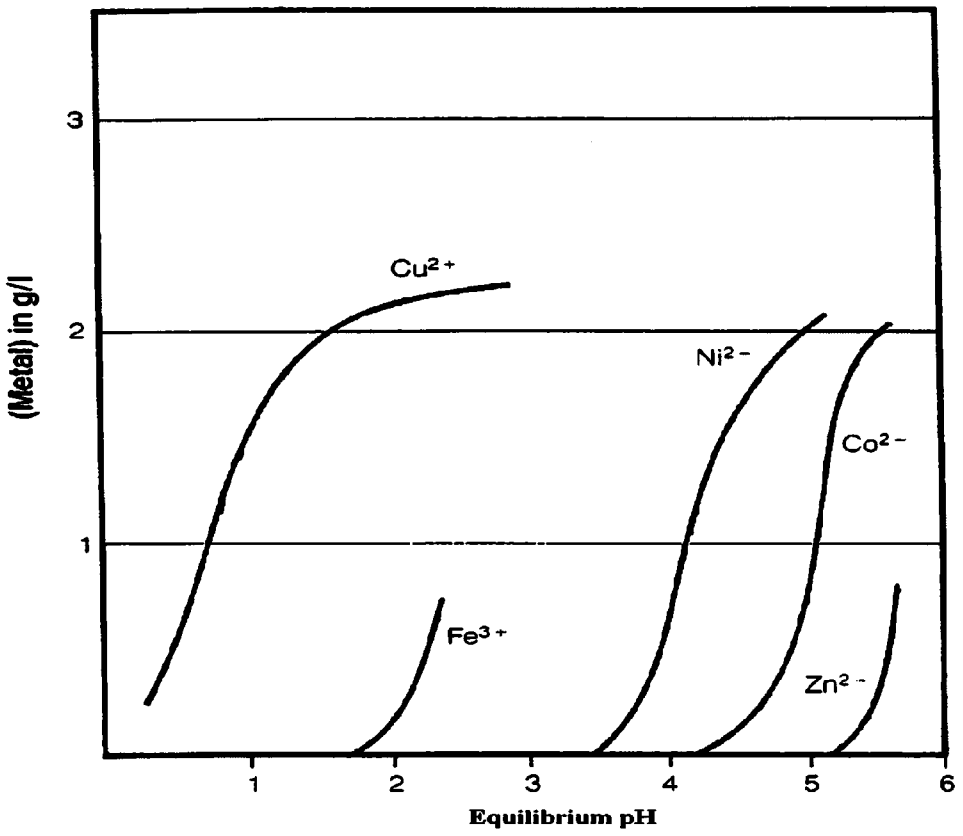

Figure 2. 3: The positions of the equilibrium isotherm of different metals in LIX84 correspond to the equilibrium pH [30].

2.2.1 Modelling of phase equilibria

The published work on modelling the equilibria of liquid-liquid extraction of metal can be classified into the following categories:

1. Chemically based models which seek to model the data on the basis of known chemistry of extraction reaction and its conditions.

2. Thermodynamic relationships which consider the system behaviour based on an activity coefficient as a function of concentration and the Gibbs-Duhem equation.

3. Semi or totally empirical models which use generalised mathematical expressions in relation to the system conditions.

2.2.1.1 Chemical based models

The earliest chemically based models considered the ion exchange mechanism for the extraction of metals with various reagents; hydroxyoxime (LIX series), di-2-ethylhexyl phosphoric acid (D2EHPA), trybutyl phosphate (TBP) etc.[31-35]. The general form of this model can be expressed in a reaction equation as in equation (2.1). The equilibrium constant and the distribution coefficient for the reaction equation are given in equations (2.2) and (2.3) respectively.

During early sixties Madigan[36] worked on the extraction of some heavy metals using D2EHPA and was able to develop expressions similar to equations (2.2) and (2.5). He suggested the following steps for the reaction equations:

1. The partition of the extractant between the organic and aqueous phases.

$$HR_{org} \rightleftharpoons HR_{aq} \qquad 2.7$$

$$K_1 = \frac{[HR_{aq}]}{[HR_{org}]} \qquad 2.8$$

2. The dissociation of the extractant into anion and cation:

$$HR_{aq} \rightleftharpoons H^+ + R^- \qquad 2.9$$

$$K_2 = \frac{[H^+][R^-]}{[HR_{aq}]} \qquad 2.10$$

3. The formation of metal complex at the aqueous phase:

$$M^{n+} + nR^- \rightleftharpoons MR_{n\,aq} \qquad 2.11$$

$$K_3 = \frac{[MR_{n_{aq}}]}{[M^{n+}][R^-]} \qquad 2.12$$

4. Partition of the formed metal complex between the two phases:

$$MR_{n\ aq} \rightleftharpoons MR_{org} \qquad 2.13$$

$$K_4 = \frac{[MR_{n_{org}}]}{[MR_{n_{aq}}]} \qquad 2.14$$

Finally he concluded that the equilibrium constant is:

$$K_{ex} = K_1^{n}.K_2^{n}.K_3.K_4 \qquad 2.15$$

Robinson and Paynter[33] studied the operating characteristics of LIX65N® for various copper concentrations in the feed solution. They observed that modelling such equilibrium was affected by three variables, these are:

1. The copper concentration fed to the system. They asserted that a high initial copper concentration in the feed would result in a less favourable equilibrium curve (i.e. low concentrations of copper at the extract phase).

2. The acid concentration in the aqueous feed. They suggested that the equilibrium be strongly affected by the amount of sulphuric acid in the aqueous solution. Where solutions with a low pH tended to depress the equilibrium curve.

3. The concentration of the active oxime, in the organic phase fed to the system, where they found the higher the LIX65N concentration the more favourable the equilibrium curve (i.e. high concentration of copper at the extract phase).

Interpolation of Robinson's results through a polynomial mathematical model by Hughes et al. (1975) gave an average error of 2.5% from the experimental data[37]. Flett et al., (1973)[38] suggested a reaction mechanism for copper extraction with LIX65N similar to

that proposed by Madigan [36]. They found that a graphical relationship between the distribution coefficient in form of (Log m) and the system's pH at constant acid concentrations was a straight line with a slope of 2 which represent the metal valency in the case of Co and Ni but greater that 2 for copper. They concluded that equilibrium reaction equation still could be presented as in equation 2.1.

All chemical based models which have been reviewed here and others reviewed before[25,39], have suffered limitations of accuracy in representing a system equilibria. These limitations can be summarised as follows:

- The models are based on the chemistry of the system, therefore a prior knowledge of the reactants physical and chemical properties is required which is quite difficult especially for a commercial reagent mixtures.
- A great deal of experimental effort is required to determine the reactants behaviours in the reaction system which is perhaps not worthwhile when other simpler models can give just as good a fit.

2.2.1.2 Thermodynamic based models

At equilibrium if the activity coefficient of a solute is equal in both liquid phases as expressed by equation (2.16), the solute will partition evenly between the two phases [3].

$$(\gamma_i x_i)_{aqu} = (\gamma_i y_i)_{org} \qquad 2.16$$

and $m = y_i/x_I = (\gamma_i)_{aqu} / (\gamma_i)_{org}$

Where γ_i is the activity coefficient of the solute i, x, y are the mole fraction of component i in the aqueous and organic phase respectively.

But if the activity coefficient is high at the aqueous feed phase and low at the organic (extractant), then mole fraction ratio of the extract to the raffinate will be high and consequently the distribution coefficient (m) will be desirably high. Thus a solvent with this property is more suitable for a selective extraction process.

Numerous mathematical models have been proposed to predict the equilibrium of liquid system behaviour based on the activity coefficients and the molar free Gibbs energy of its composition. Brisk and McManamey [39,40], Bromley [41,42] and Renon [43] were among the early researchers who proposed simple empirical equations relating activity coefficients to binary liquid compositions. Brisk et al.[39,40] studied the distribution of metals on dimeric acidic reagents and suggested the following relationship of activity coefficient for thermodynamic equilibrium constant:

$$K_{ex} = \frac{[M_{org}][H^+]^2 \gamma_{M_{org}}}{[M_{aq}][H_2R_{2_{org}}]^2 \gamma_{M_{aq}}} \qquad 2.17$$

Where $\gamma_{M\ orq}$, $\gamma_{M\ aqu}$ are the activity coefficients of metal in the organic and aqueous phases.

Flory [44] and Huggins [45] investigated the thermodynamic behaviours of polymer (non-crystalline) in a solvent and proposed the following equation for the relation of the system compositions in respect to Gibbs free energy:

$$\frac{Ge}{RT} = \sum_{i=1}^{n} x_i Ln \frac{V_i}{x_i} \qquad 2.18$$

$$Where. V_i = \frac{v_i x_i}{\sum_{i=1}^{n} x_i v_i} \qquad 2.19$$

Ge is free Gibbs energy, V_i, x_i are the volume and mole fraction of the component i respectively, and v_i is the molar liquid volume of pure i.

Mahmood [46] has reviewed most of Gibbs free energy based models and proposed a correlation for phase equilibria of solvent extraction of metal based on a thermodynamic approach employing relationships between the activity coefficient of the elements and phase concentrations. While the enthalpy and entropy changes and their effects on extraction equilibria have been discussed in detail by Marcus [47].

In spite of the enormous efforts to model the equilibrium data based on the system thermodynamic properties, it is still a very difficult and time consuming process to establish for every system the precise thermodynamic changes throughout the extraction process especially for those systems that involve reaction and complexation processes.

2.2.1.3 Semi or totally empirical models

Semi-empirical models for liquid-liquid equilibria are usually based on its analogies to two phase systems such as vapour-liquid equilibria and gas adsorption equilibria. Ellis has proposed that the curvature of the liquid-liquid equilibrium curves are similar to the adsorption isotherm[48]. He assumed that the curvature was due to the reduction of the extractant concentration as a result of the reaction between the extracted substance and the extractant. Ioannou et al.[49] studied the equilibrium behaviour of lanthanide metals in D2EHPA solutions. They suggested a model consisting of a series of linear terms similar to Raoult's law and a series of non-linear terms to correlate and predict the deviation of their multi component systems. Raoult's law for a vapour-liquid system can be expressed as follows:

$$p_i = Pv_i x_i$$

Where p_i is the partial pressure of component (i) in the vapour phase, Pv_i is the vapour pressure of pure (i) and x_i is the mole fraction of component i in liquid phase. They

proposed that for a liquid-liquid system the Pv_ix_i term could be substituted with $y^{\neq}_i x_i$ or as :

$$Y_{org} = y^{\neq}_i x_{iaq} \qquad (2.20)$$

Where (Y_{org}) the concentration of component i in the organic phase, $y^{\neq}_i$ is the molarity of the component i in the equilibrated organic phase for a single solute system, and (x_{iaq}) is the mole fraction of component i in the aqueous phase.

While for a binary system they proposed they following equation:

$$(Y_T)_{org} = (y^{\neq}_i x_{iaq}) + (y^{\neq}_j x_{jaq}) + \Delta y_i + \Delta y_j \qquad (2.21)$$

Y_T is the total concentration of the binary metal solutes (i, j) in the organic phase. $\Delta y_i, \Delta y_j$ are the deviations from ideality.

Ioannou et al.[49], Sharp and Smutz [50] and Goto [51] all have proposed totally empirical models based on polynomial relations to interpolate their equilibrium data. These models were reported to be able to predict the behaviour of multi component system, i.e., five lanthanide solutions in Sharp work [50]. However, I believe these model can not be reliably used beyond the range of experimental data used to generate the polynomial, since the chemistry of the process may begin to change in this extrapolated range of conditions.

2.3 THE CHEMISTRY OF REACTIVE EXTRACTION OF METALS

Liquid-liquid extraction chemistry of metals has developed rapidly in the last quarter of a century, this can be seen from the number of papers discussing this process in the international conferences and publications [1-3,13,18-20,22-25,52]. The chemistry of metal extraction process has been classified into many divisions. Some of them based on the type of reaction controlling the transfer of metal species from the aqueous into the organic phase, others classified according to the type of the extractants or solvent used [18,19,25,52].

Metal salts are generally soluble in an aqueous solution due to the high dielectric constant of water (which reduces the energy required to separate oppositely charged ions), and also because of solvation of metal ions in water. In order that metal ions can transfer to the organic phase, the solvated water must be displaced with a neutrally charged species preferably containing a hydrophobic group such as long hydrocarbon chain. Extractants which react with metal ions to convert them to extractable complexes are always diluted in an organic carrier (diluent).

2.3.1 Types of extractants and their requirements

Many classifications for commercial extractants have been proposed [18,53,54], but according to Ritcey's [25] classification there are three main groups, namely:

- Acidic extractants
- Chelating extractants
- Extractants containing phosphorous-sulphur bonds

Generally for any extractant to be successful in metal extraction applications it has to fulfil the following requirements:

1. It must be immscible or have a very low solubility in the aqueous solution.
2. Extractants should have good solubility in organic diluents and be capable of withstanding long periods of recycling in the extraction circuit without decomposition or degrading and have a defined kinetics.
3. It should not form emulsions during contacting process such as mixing and should have good coalescing properties.
4. Extractants must have a high metal loading capacity, and can be easily stripped of the extracted metal.
5. Extractants should be non-toxic, non-volatile and non-flammable since these properties are very important for safety and operational conditions.

6. It should be inexpensive and its starting materials should be readily available.

All commercial extractants are diluted with organic carriers (diluents) before they are fed to the extraction process. These diluents are either pure organic solvents e.g. hexane, toluene or crude oil mixtures of aromatic and aliphatic fractions such as kerosene.

In this work chelating extractants were used especially hydroxyoximes (known as LIX as in LIX84®, LIX860® and LIX984®) due to their high stability and high extraction tendencies for copper from acidic leach liquor [30]. Therefore a brief summary of their extraction mechanism is reviewed. Chelating agents molecules have two functional groups participating in the reaction with the metal ions. One of those groups is an OH or HS, and the other is a basic functional group such as nitrogen, oxygen or sulphur atoms capable of co-ordinating with its donor properties to the metal. Marcus et al.[18] suggested that the solubility of the chelating agents depend on the basic nature of the co-ordination site and the acidity of the OH group and also metal co-ordination ability. Structural features of the chelating molecule affected by both the acidic nature of the OH group and the basic strength of the donor atom, which will then affect the extractive effectiveness of the chelating extractant. The general reaction equation is given by:

$$(M^{n+})_{aqu} + (nRH)_{org} \rightleftharpoons (MR_n)_{org} + (nH^+)_{aq}$$

The reaction between metal cation and any of the chelating agents will involve release of hydrogen ions into the aqueous phase at the instant a neutral metal complex is formed. Therefore, the degree of metal extraction depends to a large extent on the pH of the aqueous phase. Cox et al.[53] suggested that an increasing charge to radius ratio of the metal

cation will increase the degree of metal extraction. The mechanism of the reaction between the metal species and the chelating extractants is largely characterised by the location of such a reaction, this will be discussed further in the kinetic section of this work.

2.4 THE LOCATION OF THE CHEMICAL REACTION AND ITS KINETICS IN METAL EXTRACTION

There is a considerable disagreement among many of those who are working on metal extraction concerning the precise site and mechanism of the reaction and transfer of metal species. The main disagreement in the literature can be divided into three groups and these are:

1. Researchers who have interpreted their kinetic data with the help of reaction orders with respect to the metal ion, extractant and the solution's pH [55]. They concluded that the rate of metal transfer process is accompanied by a diffusion process, but they could not determine where or how such a process proceeded. The mechanism of metal transfer, therefore, cannot be well understood by this approach.
2. Freire at al.[56] asserted from their kinetic data on reaction orders and the effect of diluent that the metal complex formation takes place in the aqueous phase. This could not be extended to those chelating agents and their organic diluents which have very low solubility in water.
3. Flett et al.[38] and Harada et al.[57] found that commercial chelating agents are strongly surface-active and less soluble in aqueous solutions. Therefore, they asserted that the heterogeneous complex formation reaction locus would be the interfacial zone. The mechanism of interfacial reaction has been reviewed by Harada et al.[57] and they proposed a model to explain the distribution of reactants

at the interface as in figure 2.4. This was also confirmed by Komasawa et al.[58,59] who suggested that the chelating agents have to be adsorbed at the interface and also added that the neutral complex formation at the interface is the rate controlling step.

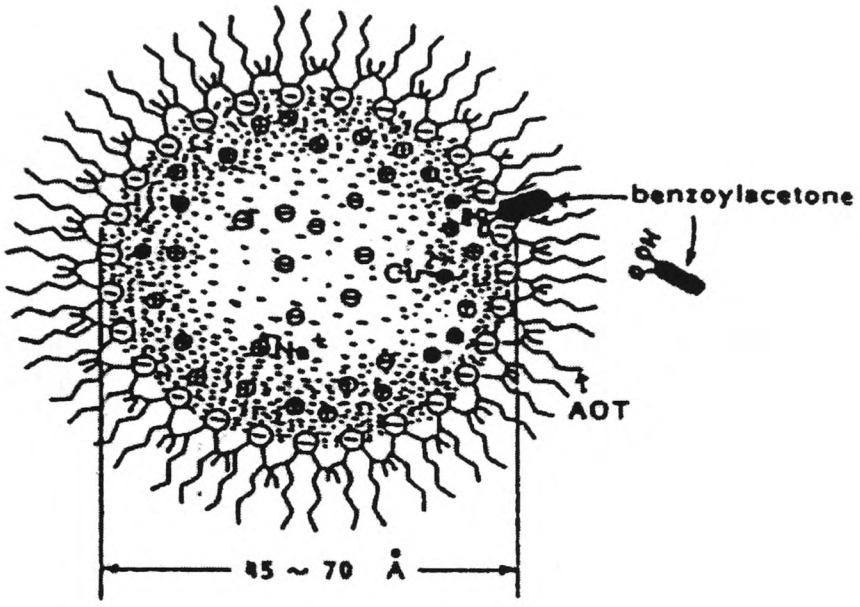

Figure 2. 4: Illustration of the ions distribution and the position of an interfacial reaction in a microemulsion droplet, proposed by Harada and Kisahda [57].

4. While others [60,61] asserted a reaction at the bulk phase or in a narrow zone adjacent to the interface in the aqueous side, as shown in figure 2.5

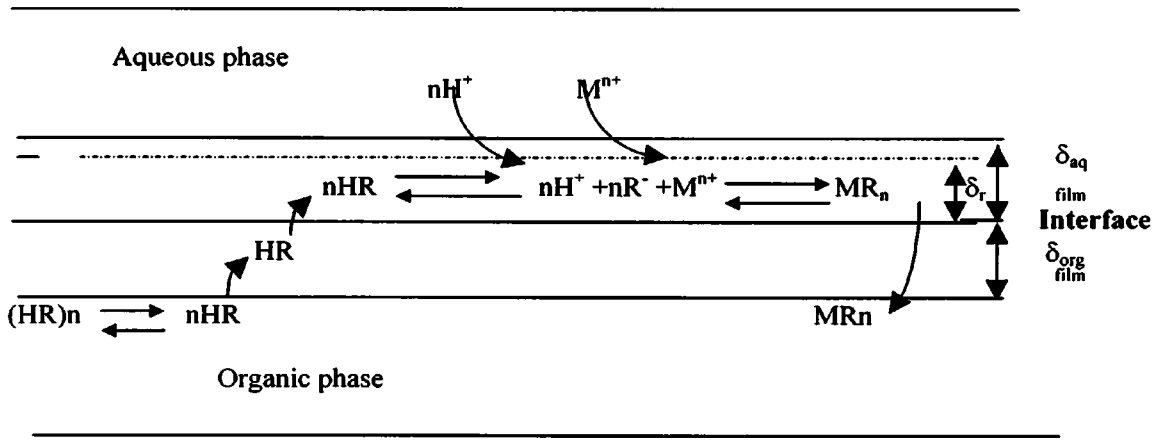

Figure 2. 5: Systematic representation of cationic metal extraction reaction at a narrow thin layer in the aqueous side of the interface, Inoue et al.[62]
* n=2 for divalent metals.

For copper extraction, Komawasa et al.[58, 59] suggested that metal-chelating agent reaction is accompanied by a diffusion process. The reactants (metal and organic active species) have to diffuse from the bulk phases to the interfacial reaction zone, and the products (hydrogen ion and the metal-organic complex) must diffuse away from the zone. The diffusional properties of those species are always affected by the hydrodynamic features of the contacting technique.

The complicated features mentioned above highlight the important factors in the rate of extraction process, these are the kinetics of the neutral complex formation reaction and its locus, the solubility and the diffusional properties of the chelating agents. These factors play the main role in the design of the process contactors. If the reaction rate is slow

then a long residence time is required and so are large mixing sections to give enough contacting time. In contrast if the reaction has fast kinetics then suitable contactors would be of rotary column or centrifugal types.

2.5 EXPERIMENTAL METHODS AND TECHNIQUES FOR THE RATE AND KINETIC STUDIES

Many studies have been performed on the rate of mass transfer of metal extraction and the kinetic behaviour of heterogeneous reactions involving metal solutes in a liquid-liquid system. It is apparent that different results were obtained from various workers studying the same chemical system. This could be attributed to the fact that the researchers have used different contacting techniques and a wide range of metal solutions and extractant concentrations. The variation on the contacting techniques would lead to variation on the hydrodynamic features of the studied system. These variations consequently affected the rate of mass transfer. Different experimental techniques have their merits and shortcomings even if they used for the same system. The most common experimental techniques which have been used for the rate of metal transfer in liquid-liquid extraction and their relevant references are summarised as follows:

1. Stirred tank; this included a mixer settler arrangement [19,23,62].
2. The AKUFVE [64].
3. Lewis cell (the stirred cell) [65,66].
4. Hahan cell (the static constant interfacial cell)[67].
5. Laminar Jets [68].
6. Growing drops[69].
7. Wetted column (falling film)[70].
8. Single drop (rising or falling drops)[51,55,71].

Many of the techniques listed above have found limited use in the studies of the rate of mass transfer of metals in liquid-liquid systems involving commercial operational conditions. In the present work, rising drop technique was used to study the properties of the rate of mass transfer and reaction kinetics of copper sulfate aqueous solution and LIX984, more details are given in chapter three.

The principles of the single drop technique are to produce drops of one phase at the tip of a stainless steel needle or capillary glass tube and the drops rise or fall through a vertical tube filled with the second phase. If the drops (dispersed phase) are lighter than the continuous phase, the drops are made to rise, otherwise the drops are made to fall through the continuous phase. The rising or falling drops then coalesce at the end of the column, from where a known number of drops is collected for analysis. The rate of mass transfer can be calculated based on the drops traveling time, the average drop size and the amount of metal transfer per unit volume of single drop.

One advantage of this technique is the ability to measure the interfacial area. The interfacial area of a single drop usually calculated on the assumption that all drops are totally spherical. Added to that, single drop equipment is very simple and easy to modify for studying the effect of other parameters such as temperature and drop size. Despite the popularity of this technique, it is still subject to some limitations. The assumption that all drops are perfectly spherical is not always valid, as the shape of drops depends on the physical properties of both phases and the hydrodynamic behaviour of the drops throughout the column. Another shortcoming of this technique that it doesn't produce drops in a situation similar to that produced in an industrial mixer-settler, but it can be used to simulate plate column contactors. Column contactors are not suitable for slow reactions

which require a long residence time as this needs a long column for any measurable rate be achieved. This will pose practical problems for experimental design and chemical analysis.

Liquid drops rising or falling usually are faster than solid spheres of the same size and density [1]. This is due to the mobility of the drop surface that is carried from the forward stagnation point to the rear by shear. The drop contents circulate internally in the manner indicated by figure (2.6). It has been reported that circulation within the drops can occur at any value of the droplet Reynold's number, if the continuous phase viscosity is high. The hydrodynamics of rising drops and the rate of mass transfer within their surface area have been under intensive investigations by many researchers [1,13,19,72]. The rate of mass transfer of a metal during extraction is strongly influenced by the reaction kinetics and its locus, as well as the internal circulation of the drops.

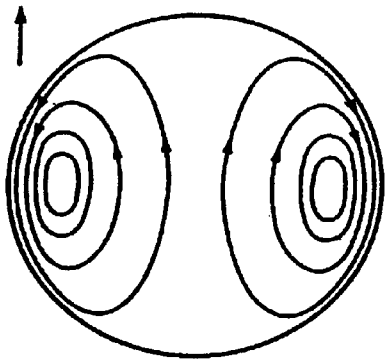

Figure 2. 6: Circulation pattern in rising drop.

2.6 ANALYSIS OF THE OVERALL RATE OF MASS TRANSFER IN LIQUID-LIQUID EXTRACTION

Many mathematical models have been proposed to describe the overall rate of mass transfer in liquid-liquid extraction systems. Any interpretation of experimental extraction data using mathematical models has to take into account the hydrodynamic features of the experimental technique used and the possible locus of any chemical reaction that may accompany the mass transfer process. Obviously the rate of mass transfer would be controlled by the slowest step. Therefore, the choice and the presentation of a model would require a prior knowledge whether the overall rate of mass transfer was controlled by diffusion mass transfer or the kinetic regime alone, or whether both processes may control which requires a mixed model of mass transfer with chemical reaction. The earliest models for mass transfer with or without chemical reaction were applied to gas absorption because of the industrial importance and the relative ease for theoretical treatment in comparison to a liquid-liquid system[73].

2.6.1 Analysis of diffusion controlled mass transfer system

The oldest diffusional mass transfer models were proposed for gas absorption by Whitman et al.[74,75], Higbie [76] and Danckwerts [77]. In liquid-liquid extraction of metals and for a process controlled by diffusional mass transfer alone, the proposed models have been based on the approximate solutions of Fick's second law of diffusion. For example Komasawa et al.[59] discussed copper extraction by hydroxyoxime and interpreted the rate of mass transfer as follows:

$$(\frac{V}{A})\frac{dC_o}{dt} = K_o(C_o^{\circ} - C_{oi}) = K_{aq}(C_{aqi} - C_{aq}^{\circ}) \qquad 2.22$$

where A= is the interfacial area.

C_o°, C_{aq}° = The initial concentration of organic and aqueous phases respectively.

C_{oi}, C_{aqi} = The interfacial concentrations of organic and aqueous phases.

K_o, K_{aq} = Mass transfer coefficients of organic and aqueous phases.

For an average time of (t), the phase concentration will be (C_t) then;

$$K_o = (\frac{V_o}{A*t}) \ln(\frac{C_o^\circ}{C_{ot}}) \qquad 2.23$$

While Krong and Brink [1] suggested the following equation for diffusion mass transfer in circulating drops:

$$\frac{C_o^\circ - C_t}{C_o^\circ - C_{oi}} = 1 - \frac{3}{8}\sum_{n=1}^{\infty} A_n^2 \exp(1 - \frac{\varphi_n 64 D_d t}{d_p^2}) = \{1 - \exp[\frac{-2.25 \times 4 D_d \pi^2 t}{d_p^2}]\}^{0.5} \qquad 2.24$$

where A_n= eigen value

C_t = concentration of the dispersed phase (droplet) at any time.

D_d = diffusivity of the dispersed phase.

d_p = the drop diameter.

φ = eigenvalue.

While mass transfer characteristics in rigid and oscillating spheres were reviewed in details by Treybal[1] and Hadamard [78].

2.6.2 Analysis of kinetic controlled mass transfer system

Systems that are identified as purely kinetically controlled are often described by models based on reaction order with respect to concentration of the reactants. The general forms of these models are as follows:

$$-\frac{d[M^{n+}]_{aq}}{dt}\alpha[M^{n+}]^{\alpha}{}_{aq}\times[HR]^{\beta}{}_{org}\times[H^{+}]^{\gamma}{}_{aq} \qquad 2.25$$

$$-\frac{d[M^{n+}]_{aq}}{dt}=K_r[M^{n+}]^{\alpha}{}_{aq}\times[HR]^{\beta}{}_{org}\times[H^{+}]^{\gamma}{}_{aq} \qquad 2.26$$

Where α,β,γ = the reaction order to be found experimentally.

Kr = is the reaction rate constant.

[] = refer to species concentration in both phases.

Hughes et al.[79] reported that the rate of mass transfer for vanadium extracted by D2EHPA was of first order with respect to $[VO^{2+}]_{aq}$ and half order in $[D2EHPA]^{1/2}{}_{org}$, but inverse first order in $[H^{+}]_{aq}$. They found the following rate equation:

$$Rate = K_r\frac{[VO^{2+}]_{aq}[D2EHPA]^{1/2}{}_{org}}{[H^{+}]_{aq}} \qquad 2.27$$

While for copper extraction process many kinetic regimes have been proposed for instance Pratt et al.[80] reported the rate of copper organic complex (CuR_2) formation with LIX65N in ethanol solution as follows:

$$Rate = K_r\frac{[Cu^{2+}]_{aq}[HR]_{org}}{[H^{+}]^{0}{}_{aq}} \qquad 2.28$$

Danesi et al.,[81] Komasawa et al.[58] and Harada et al.[82] have all suggested the following equation for the rate of mass transfer under reaction controlled system.

$$Rate = K_r \frac{[M^{n+}]_{aq}[HR]_{org}}{[H^+]_{aq}} \qquad 2.29$$

2.6.3 Analysis of mass transfer accompanied with chemical reaction

The theories and models of diffusional mass transfer accompanied by simultaneous chemical reaction are the most relevant to the present work and to many liquid-liquid extraction processes. Danckwerts[83] reviewed the principles of mass transfer with chemical reaction in heterogeneous system and applied both the two-film and the penetration models for the treatment of mass transfer accompanied by second order irreversible chemical reaction process. Laddha[13] have examined some limiting cases of very slow chemical reaction, fast reaction, instantaneous reactions, second order reactions and intermediate reaction regimes.

The phenomena of a solute i.e. (A) transformed unidirectionally a distance of (dy) by diffusion accompanied by a chemical reaction of an (n) order in one phase can be describe by the following equations[84]:

$$\frac{\partial.C_A}{\partial.t}dy = -\frac{\partial}{\partial.y}(-D\frac{\partial.C_A}{\partial.y})dy - K_r C_A{}^n dy \qquad 2.30)$$

$$\frac{\partial.C_A}{\partial.t} = D\frac{\partial^2 C_A}{\partial.y^2} - K_r C_A{}^n \qquad 2.31$$

(Accumulation) = (Molecular transport) - Reaction rate.

At a steady state process ($\frac{\partial C_A}{\partial t} = 0$), this reduce equation 2.31 to a second order differential equation of the form:

$$D\frac{\partial^2 C_A}{\partial.y^2} = K_r C_A{}^n \qquad 2.32$$

where k_r= is the reaction rate constant.

C_A= is the concentration of solute A.

Systematically the process can be represented by the following sequence:

$$\text{Reactant} \xrightarrow{\text{Diffusion (mass transfer)}} \xrightarrow[\text{Chemical reaction}]{} \xrightarrow{\text{Diffusion (mass transfer)}} \text{Product}$$

Astarita[73] has developed a model based on this basic principle and coupled with concepts of the two-film theory, he found that:

$$(N_A)_{ave} = (2D_A \int_{C_{Ab}}^{C_{Ai}} r_A dC_A)^{1/2} \qquad 2.33$$

Where (N_A) = is the average rate of mass transfer of component A per unit area.

C_{Ai}= the interfacial concentration of component A.

C_{Ab} = the bulk concentration of component A where the reaction occurs.

r_A = the rate of chemical reaction in respect to A.

Hughes et al.[85] postulated a model based on two-film theory for extraction of metal by organic acid. The model accounted for reaction zone of variable thickness, so that reaction at the interface or into the diffusion film of the aqueous side can be examined together with the two-film mass transfer coefficients.

In the present work a model based on the two-film theory accompanied with first order chemical reaction with respect to copper concentration is proposed to account for the local and overall mass transfer coefficients.

2.7 MEMBRANE TECHNOLOGY AND ITS APPLICATION IN LIQUID-LIQUID EXTRACTION

There has been growing demand for an efficient and cost effective process for the selective removal and recovery of organic pollutants and toxic metals from wastewater streams. Such a process is also needed for Hydromettalurgical extraction of valuable metals from low-grade ores. Conventional extraction techniques such as mixer-settlers, columns and centrifuges usually involve dispersion of one liquid phase into another liquid in forms of droplets to facilitate mass transfer. After the required species is transferred, the dispersed phase is usually separated by methods utilising density differences.

Membrane based liquid-liquid extraction technology, currently under rapid development, can establish a consistent, stable interface between the two phases. This feature has made membranes superior for eliminating problems associated with conventional extraction such as emulsification, flooding and loading. At the same time membrane based solvent extraction differs in principle from other membrane separations such as filtration and gas separation as there is no convective flow through the membrane pores, instead, the membrane acts as an inert support to facilitate diffusive transfer[86].

The use of membrane based liquid-liquid extraction was briefly reported for the first time in a Patent dealing particularly with dispersion-free solvent extraction using solvent-swollen membranes in 1976[87]. Baker et al. [88] studied copper extraction through a liquid membrane supported by a porous film. While Lee et al. [89] studied the principles of ion transport in a supported liquid membrane and differences to the transport in liquid surfactant membranes. They found that although the fluxes of species were similar, the liquid surfactant membranes were unstable. Descriptions of the mechanisms and reactions of carrier-mediate transport in liquid membranes have been proposed in the literatures [90-97]. Recently wider reviews have been published which cover membrane technology; history,

future development and scope [98-102]. The above authors and others have all agreed in recommending that membrane based liquid-liquid extraction processes offer enormous advantages over convention extraction techniques. These advantages can be summarised as follows:

1. Dispersion-free extraction and stripping.
2. Very high contact area per membrane unit equipment available in very compact bundle.
3. No need for power consumption for mixing of the two phases.
4. Independent variation of process streams flow rates, this is a great advantage over conventional extraction which is plagued by problems of flooding, loading and weeping.
5. The membrane modular design eases scale-up and fitting of equipment.
6. The membrane module can sustain high pressure and
7. the ability to provide several extraction stages in a single module as compared to a single stage operation provided by a mixer-settler.

These characteristics and the rapid membrane technology developments have attracted scientific and commercial attention to study and apply membranes based extraction technology into a diverse range of processes. Some of these processes are still in a laboratory scale while others in a pilot plant scale. Lists of potential areas where dispersion-free extraction have been or can be applied are summarised in Table (2.2).

Table 2. 2: Membrane based liquid-liquid extraction processes.

Industrial process	*Application*	*Reference*
Chemical Industry	• Extractive reaction • Metals extraction • Organics recovery by liquid-liquid extraction • Concentration of aqueous salt solution and acid.	103, 104, 105
Pharmaceuticals and biotechnology	• Protein extraction • Antibiotic separation	86, 105
Food and Drink	• Metals removal from edible oils • Flavour extraction • Extraction of ethanol from fermentation media • Extraction and fractionation of fatty acids from oil	86, 106
Environmental and waste treatment	• Toxic metals extraction • Organic solvents removal from wastewater	102, 107

2.7.1 Structural and configurational features of membrane extractors

The structural materials and geometrical shapes of membrane contractors depend to a large extent on the nature of the separation process, which they are utilised in. There are many forms in which membrane contactors can be built, but they have to take into account the properties of the contacted phases and the contactor long-term durability in facilitating the required species separation. Wide range of materials has been reported in the literature as suitable for building membrane extractors ranging from emulsions to synthetic cellulosic and polymeric fibres [101,106,108]. Some of these membranes contactors and their structure and configuration are described in detail in the following sections. These have been chosen due to their promising technological features in liquid-liquid extraction processes.

2.7.1.1 Emulsion liquid membrane contactors

An emulsion liquid membrane ELM is a three-phase system, which is stabilised by an emulsifier. This membrane can be formed by generating a stable dispersion of receiving (stripping) phase encapsulates within an organic phase [86]. The process of preparing the membrane emulsion phase and employing it in an extraction operation can be summarised as follows:

1. An aqueous acceptor phase either acid or an alkali is emulsified in form of small drops (1-10 μm) into relatively larger organic drops (0.1-1 mm). The organic phase may constitute of a carrier (ion exchanger) and surfactant to stabilise the emulsion.
2. Extraction stage, where the membrane emulsion is dispersed into a continuous phase solution to extract the required species.
3. Emulsion membrane separation from the spent feed [86].
4. Solute recovery and emulsion break-up. In this stage the loaded organic is separated from the internal aqueous recipient.

The organic phase is then recycled while the aqueous recipient is further processed to recover the solute it contains. Figure 2.7 is summarising the operational stages of preparing and using ELM contactor.

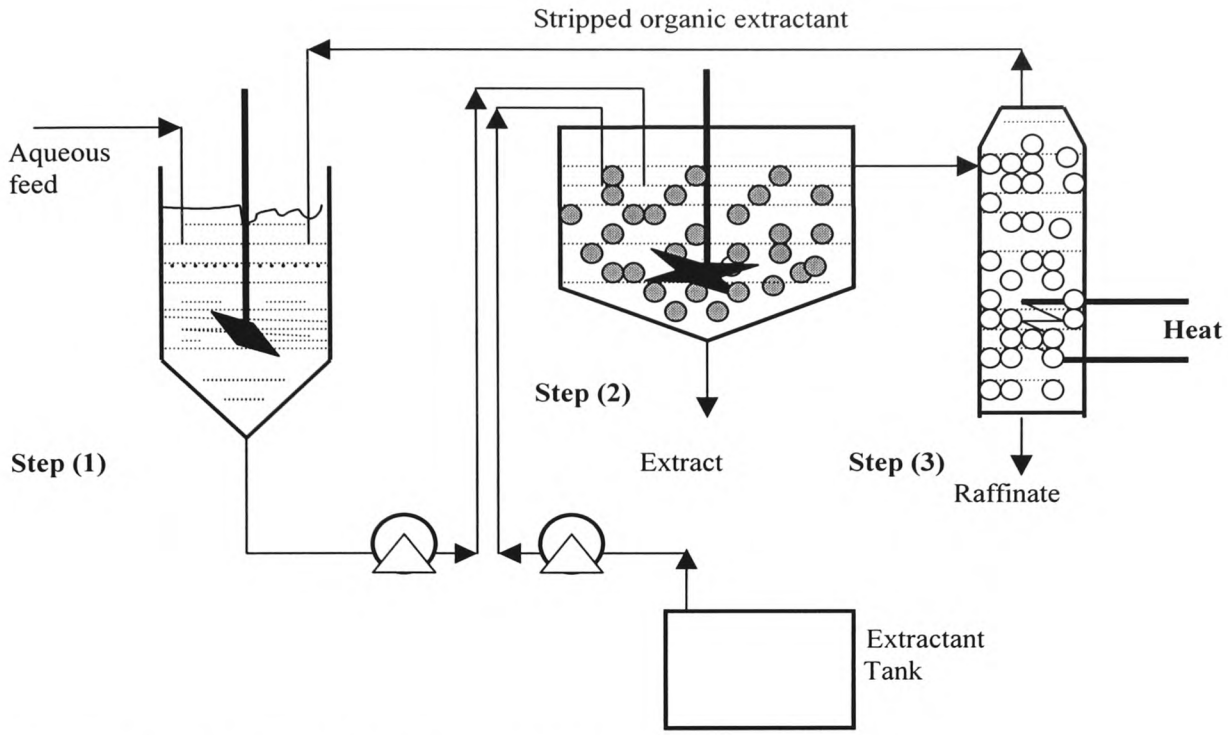

Figure 2. 7: Schematic diagram of ELM contacting process

However, ELM contacting processes have major problems, which reduce this technique efficiency and limit its uses. For example most ELM contactors suffer poor stability which causes partial rupture of the membrane emulsion drops and leakage of their content. On the other hand high stability makes it difficult to break the emulsion in the final stages of the extraction process [86,109].

2.7.1.2 Supported liquid membrane contactor

In general the supported liquid membrane (SLM) contactor consists of a three phases system; an aqueous feed phase, liquid membrane phase and a stripping phase[110]. The liquid membrane phase is immobilised in a polymeric porous film, which provides mechanical support to the liquid membrane and facilitates easy species transfer from the feed phase to the stripping phase through the liquid membrane. The membrane phase is composed of an extracting agent diluted in an inert diluent and in some cases a modifier that enhances the

pure reagents distribution coefficients. SLM contactors can be configured in several forms such as flat sheets or spiral-wond hollow fibre [98,111,113]. The support materials are chosen based on several parameters such as the support surface area, pore size, porosity, thickness and chemical stability. The supporting materials should be inert and chemically compatible (i.e. non-swelling) to all the phases present in the system for extended periods of time over the full range of likely process conditions [114]. It is also important that the liquid membrane should wet the support material so that all the pores are completely filled. Therefore, displacement of the liquid membrane will be unlikely under pressure differences between the application phases. The mechanism of species extraction and recovery in SLM contactors is be illustrated in Figure 2.8. This figure shows that there is a two step transport mechanism of species A described in equation 2.34. The reversible reaction is an ion exchange, and the solute's (A) flux is linked to the extraction reagent's flux at the interface Zone I. While the Flux of species (A) from the liquid membrane phase into the stripping phase is coupled with the stripping reagent's (B) flux at the interface Zone II.

$$A + CB \rightleftharpoons CA + B \qquad 2.34$$

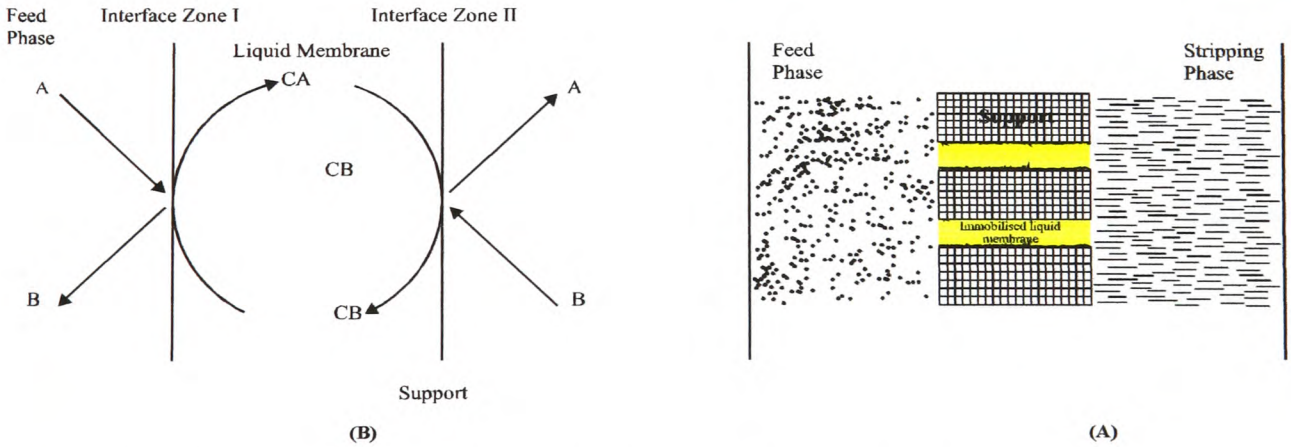

Figure 2. 8: Schematic representation of, (A) set up of polymeric SLM device (B) species transfer mechanism during extraction process in SLM device.

The liquid membrane can be introduced to the polymeric film either by pressurising the organic phase into the pores or by simply soaking the polymeric film in the organic solvent for some time, see Figure 2.8,A.

The major advantages of the SLM contactors are the easy process design, and the numerous applications that this process could fit into. However, these contactors still suffer of many problems such as: membrane stability which declines with time due to losses of membrane phase by solubility, osmotic flow of water across the liquid membrane, and membrane phase displacement from the support pores due to pressure differences between the phases[96,115]. This problem and many more technical deficiencies led to the search for more reliable techniques.

2.7.1.3 Hollow fibre containing immobilised liquid membrane (HFCLM) contactors

The HFCLM contactors have been built and developed due to their distinct features of providing mechanical support to the liquid organic membrane (solvent), and simplifying the extraction process. This technique was developed and used extensively by Sengupt et al.[115] Majumdar et al.[117,118] and others [119] for the separation of liquid or gas species. These contactors generally take the shape of a cylindrical shell which contains two well packed sets of hollow fibres. One set of the hollow fibres carries the feed solution, the other set has the stripping phase flowing through and the organic solvent is immobilised in the interstices at the two sets of fibres in the contactor shell. The two fibre sets are connected to different ends of the contactor in such a way that the feed and stripping could be pumped through them in co-current or counter-current directions. The construction materials of these contactors, depends to a large extent on the nature and conditions of the separation process. However, the materials that widely used are hydrophilic or hydrophobic polymer bases. When hydrophilic hollow fibres are used and for instance the feed phase and the stripping phase are aqueous, the pressure of both phases should be kept lower than that of

the shell side. This will help to immobilise the aqueous-organic interface at the fibres outer surface and prevent the aqueous phase from leaking into the shell side. Whereas if the fibres were made of hydrophobic substance, then the aqueous feed and strip phases should be in higher pressure than that of the organic phase contains in the shell which wets the fibre membrane walls. The extraction process using HFCLM contactors takes place into two steps. First, the immobilised organic solvent extracts the required species through the porous surfaces of the hollow fibres, which contain the feed solution by forming a complex between the extraction agent and the wanted species. The second stage is stripping off the extracted species from the organic complex through the porous surfaces of the fibres which contain the stripping solution. In the latter stage the organic solvent is regenerated for the extraction step.

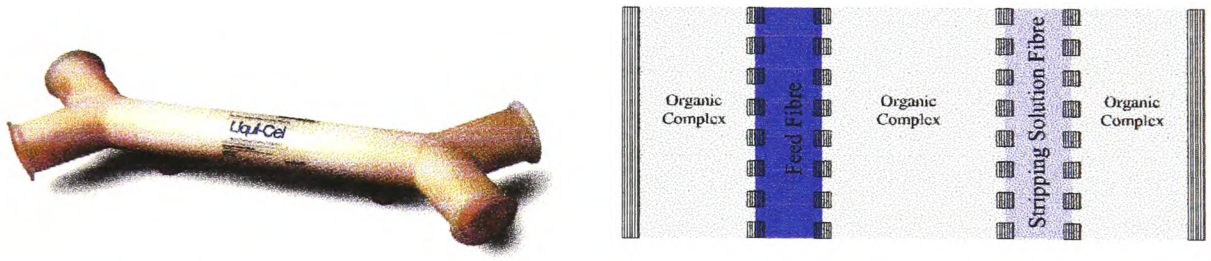

(A) **(B)**

Figure 2. 9: Illustrates; (A) a modern compact form of HFCLM contactor and (B) the extraction mechanism respectively.

The HFCLM contactors distinguishing advantages over SLM and ELM contractors can be summarised as follows:

1. The HFCLM contactors may be operated in a variety of modes much more easily than a SLM contactor [98].
2. The volumetric transfer rate of the required solute species in HFCLM devices are quite high in comparison with that of SLM and ELM contactors due to the high membrane surface packing density [98].
3. Fibre wall defects lead only to a loss of the organic solvent through the hollow fibres which can be easily detected and treated.

Despite the advantages these contactors offer, they are still under intensive investigation particularly with regard to long-term immobilised organic solvent stability and the risk of dispersion of one of the phases into another under fluctuating pressures within the shell and the hollow fibres.

2.7.1.4 Microporous Hollow fibre contactors

Microporous hollow fibre extractors (MPHF) are available in the shape of shell and tube heat exchanger. The dimensions of commercially available devices are ranging between 2.5 to 10 cm shell diameter and 30 to 120 cm module length respectively [120]. The shell can be made of nylon, polycarbonate, polypropylene, ceramic or stainless steel and contains no baffles. The shell is densely packed with hollow fibres, which are usually made of epoxy, polyurethane or polypropylene [98,120]. Figure (2.10) shows schematically the arrangement of a MPHF contactor and full details of the module which is used in this work are given in chapter three.

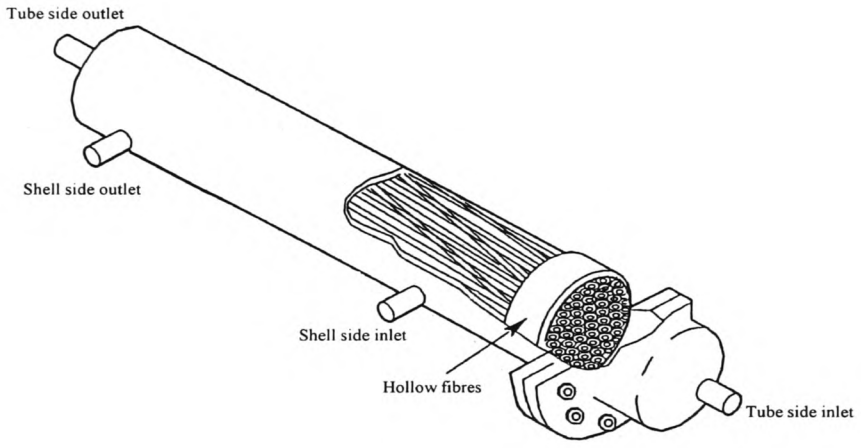

Figure 2. 10: Cut view of MPHF membrane module.

There are two types of characteristics to be considered in the selection of a MPHF module for liquid-liquid extraction process; these are chemical and physical or structural.

The chemical features to be considered can be summarised as follows:

1. Compatibility: MPHF construction materials should be chemically inert with all organic and aqueous reagents present in the system. For instance modules with epoxy potting resin and polypropylene casings can withstand most chemicals except chlorinated solvents, Ketons and dimethylformaide. Further there are some devices which can tolerate extreme pH conditions and temperature up to 80°C [98]. The presence of any incompatible reagents could lead to swelling of potting resin or casing substrates, consequently reducing the effective area of transfer which will lead to flux reduction and poor extraction [121].

2. Wetability: There are two types of MPHF membrane module construction materials i.e. hydrophilic and hydrophobic. The hydrophobicity of the hollow fibres limit to large extent the side which will be wetted by the aqueous or the organic phases. In the case of fibres made of hydrophobic substrate, the organic will wet the fibres walls which will lead to immobilisation of the organic-aqueous interface at the pores mouth in the aqueous side if the aqueous phase flows inside the fibres, see Figure 2.11,A. Whereas in the case of hydrophilic membrane, the aqueous phase will wet the hollow fibres walls, hence the organic-aqueous interface will be at the fibre outer surfaces when the aqueous phase flows inside the fibre lumen, see Figure 2.11(b). To prevent any dispersion of either of the phases into the other the pressure of the two phases should be adjusted. The organic phase pressure should be higher than the aqueous phase side in the case of hydrophilic MPHF membranes. While a higher aqueous phase pressure should be employed at hydrophobic membranes [98,122,123].

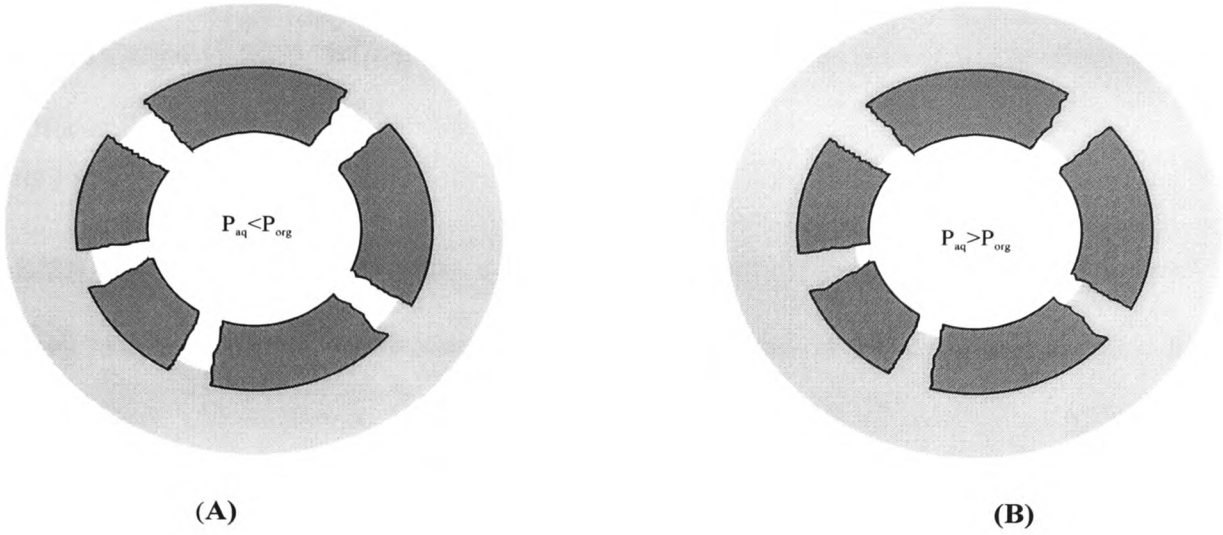

Figure 2. 11: Liquid wetting and its presser pattern in (A) Hydrophobic hollow fibre and (B) in a hydrophilic hollow fibre membrane.

The physical properties, which have to be considered during membrane selection, can be summarised as follows:

Thickness: the hollow fibre membrane thickness should be minimal so that the extracted species flow through the membrane would be unhindered. On the other hand membrane thickness should be sufficient to provide the mechanical support and sustain the fluid flow through it.

Porosity: It has been reported by Kiani et al.,[122] that membranes with a pore diameter anywhere between 10^{-2}-10^{-7} cm are suitable for liquid-liquid extraction systems [122]. The porousity of hollow fibre membranes should be as high as possible in order to maximise the effective surface area for mass transfer per unit volume of the MPHF module. Further the pores tortuousity should be minimal so that the diffusion path for the extracted species would be small and the porous surface would facilitate unhindered diffusion. This feature will decrease the time required for species diffusion through the fibre wall and increase the rate of solute transport.

From reviewing the technical literature available it has been found that a MPHF module of the type Celgard® 2400, X10 or X20 is the most suitable for the system under investigation in this study [123,124].

2.8 THEORETICAL ANALYSIS OF MASS TRANSFER IN MPHF MEMBRANES

Initial membrane based extraction studies were reported to be carried out using flat microporuos hydrophobic, hydrophilic and composite hydrophilic-hydrophobic membranes[111,122,125,126]. These studies have suggested that the overall mass transfer resistance to species transport across the membrane wall could possibly be modelled by a conventional procedure i.e. adding the local resistances. Sirkar and co-workers [125] have studied many systems of dispersion-free liquid extraction in MPHF membranes and postulated the following overall resistance equation for a Methyl isobutyl ketone (MIBK)-water-phenol in a hydrophobic membrane, (the aqueous phase flows inside the fibres):

$$\frac{1}{K_w d_i} = \frac{1}{k_{wt} d_i} + \frac{1}{m k_m d_m} + \frac{1}{m k_{os} d_o}$$

They defined K_w: the overall mass transfer coefficient based on the aqueous phase, (cm/s).

k_{wt}: the aqueous phase mass transfer coefficient, (cm/s).

k_m: mass transfer coefficient across the membrane wall, (cm/s).

k_{os}: the organic phase mass transfer coefficient, (cm/s).

d_i: fibre tube internal diameter, (cm).

d_m: fibre tube external diameter, (cm).

d_o: the shell side internal diameter, (cm).

In the equation above a new resistance to mass transfer has appeared in form of ($1/k_m$) which does not exist in conventional extraction processes, this represents the resistance to

species transfer in the hollow fibre membrane pores containing the liquid-liquid interface. In general the overall mass transfer in non-dispersive liquid-liquid extraction can be expressed in the following equation:

$$J = K\ A\ \Delta C_{LM} \qquad 2.35$$

$$J = F_{aq}(C^{in}_{aq} - C^{out}_{aq}) = F_{org}(C^{out}_{orq} - C^{in}_{org})$$

Where J: is the mass flux of solute throughout the membrane module, (g/s).

K: the overall mass transfer coefficient, (cm/s).

A: is the surface area of transfer, (cm^2).

ΔC_{LM}: the log mean concentration profile at both ends of the membrane module, (g/cm^3).

and since the inlet concentrations and flow rates of both phases could be measured, then equation (2.35) could be re-written based on the aqueous phase conditions as follows:

$$F_{aq}(C_{aq}^{in} - C_{aq}^{out}) = K\ A\ \Delta C_{LM} \qquad 2.36$$

where $\Delta C_{LM} = \dfrac{\Delta C_1 - \Delta C_2}{\ln \dfrac{\Delta C_1}{\Delta C_2}}$

The numbers 1 and 2 in this equation refer to the ends of the MPHF module where concentrations differences of both phases can be measured and at the end numbered 1 the aqueous inlet and the organic outlet are located in counter current flow arrangement.

The concentration profile in and around a microporous hollow fibre in a liquid-liquid extraction membrane module can be illustrated as in figure 2.12.

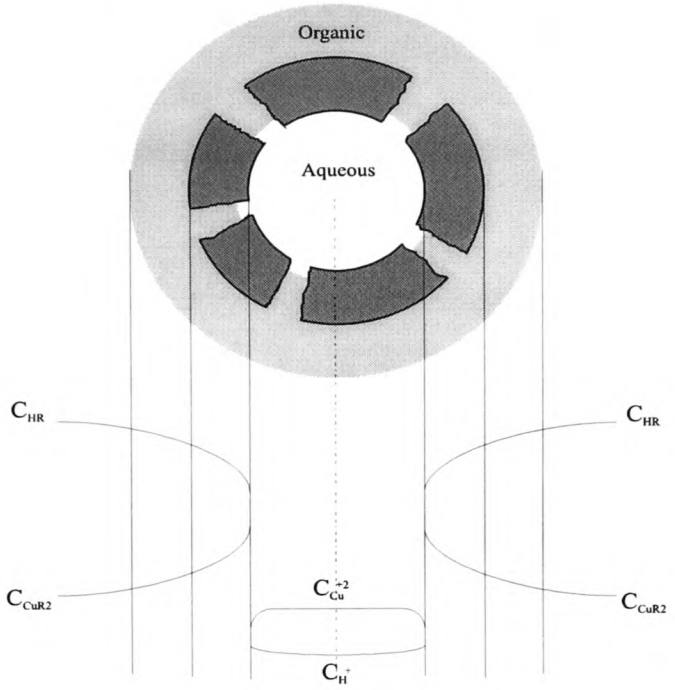

Figure 2. 12: Schematic diagram of copper concentration profile in and around a microporous hollow fibre during extraction process with chelating agent (HR).

In the figure above and in all dispersion-free liquid-liquid extraction processes in MPHF membrane modules there are elementary steps which govern the mass transfer. For a copper-chelating agent system which is the subject of this study these steps can be summarised as follows [92,95,110,127-130]:

1. Diffusion of copper ions from inside the fibre lumen to the interface zone between the organic and the aqueous phase. The interface is located at the pores inner mouths if a hydrophobic microporous fibres membrane is used and the aqueous phase flows inside the fibre lumen.

2. Diffusion of the organic solvent which contains the chelating agent through the shell side to wet the hollow fibres walls and then
3. diffusion of the organic solvent across the hollow fibres walls through the pores to the interface.
4. Reaction of copper ions and the chelating agent at the reaction zone i.e. the interface area.
5. Diffusion of the formed complex between the metal ions and the chelating agent from the reaction zone at the interface through the hollow fibre membrane wall, then through the boundary layer at the outside of the capillary fibres to the bulk of organic phase.
6. Diffusion of the hydrogen generated at the reaction zone to the aqueous bulk phase.

In broad terms liquid-liquid extraction processes in MPHF membranes can be sub-divided into three categories based on the controlling steps of solute transfer between the two liquid phases under free dispersion conditions as follows:

- Diffusion controlled non-dispersive extraction process.
- Reaction controlled non-dispersive extraction process and
- combined reaction and diffusion controlled dispersion-free extraction process.

The importance and the direct implications of diffusional and reaction forces in dispersion-free liquid-liquid extraction have been investigated by few researchers and can be summarised as follows:

2.8.1 Diffusional mass transfer and boundary-layer resistance in a MPHF module

In this section the theoretical aspects of a species diffusional mass transfer across the immobilised interface in a MPHF membrane module is considered. In systems where a species (i) transports from an aqueous phase to an organic phase through an inert porous membrane due to chemical reaction influence or due to the species (i) solubility differences in the two phases, then the diffusion path and its characteristics has to be defined. In other words diffusional flow from the bulk aqueous phase to the organic phase or vice versa would encounter local resistances in the form of stagnant layers of solution near the inner and outer fibres surfaces and through the tortuous membrane pores in addition to the reaction resistance at the interface as described in the literature [86,92,129-131]. In this study a hydrophobic membrane was used, see figure 2.12, which illustrates the concentration profile of copper, the chelating agent (HR), the copper-chelating agent complex formed, the hydrogen ions generated at the interface, and other species present in the studied system of ($CuSO_4$-LIX984). In section 2.8 the above diffusional steps of these species were highlighted in steps 1,2,3,5 and 6 under the following assumptions:

- Steady-state mass transfer through the interface with no immiscible displacement accruing through the pores.
- The organic-aqueous interface is located at the pores mouths at the aqueous-membrane interface.
- No solute transport through the non-porous surface of the MPHF membrane.
- Unhindered diffusion of species through the organic-filled microporous membrane of thickness (t_m).

The species transport (i.e. copper) in the boundary layers inside the fibres lumen and outside surface of the fibres can be simply expressed by film-type mass transfer as in equation 2.37 and 2.38 respectively:

$$N_{Cu} = \frac{D_{Cu}}{\delta_{aq}}(C_{Cu}^{ab} - C_{Cu}^{i}) \qquad 2.37$$

$$N_{CuR2} = \frac{D_{CuR2}}{\delta_{org}}(C_{CuR2}^{om} - C_{CuR2}^{ob}) \qquad 2.38$$

While copper transport through the fibres walls could be expressed as follows:

$$N_{CuR2} = \frac{D_{eff\,CuR2}}{t_m}(C_{CuR2}^{i} - C_{CuR2}^{om}) \qquad 2.39$$

Where $D_{eff\ CuR2}$ is the (copper-chelating agent complex) effective diffusion which is a function of the species diffusion coefficient, membrane's porosity (ε_m) and tortuousity (τ_m):

$D_{eff\,CuR2} = (D_{CuR2}\varepsilon_m/\tau_m)$

The above equations can be described by means of local mass transfer coefficients as follows:

$$N_{Cu} = k_{aq}(C_{Cu}^{ab} - C_{Cu}^{i}) \qquad 2.40$$

$$N_{CuR2} = k_m(C_{CuR2}^{i} - C_{CuR2}^{om}) \qquad 2.41$$

$$N_{CuR2} = k_{org}(C_{CuR2}^{om} - C_{CuR2}^{ob}) \qquad 2.42$$

Using an aqueous phase based overall mass transfer coefficient (K_{ov}) for copper transfer, the overall rate of mass transfer can be expressed as:

$$N_{Cu} = K_{ov}(C_{Cu}^{ab} - C_{aCu}^{*}) \qquad 2.43$$

Where C^{*}_{Cu} is a hypothetical aqueous phase concentration in equilibrium with the bulk organic phase concentration C^{ob}_{Cu}, and the distribution coefficient of copper between the two phases i.e. the aqueous and the organic is:

$$m = \frac{C_{Cu}^{ob}}{C_{aCu}^{*}} = \frac{C_{Cu}^{om}}{C_{Cu}^{i}} = \frac{C_{oCu}^{*}}{C_{Cu}^{ab}}$$

A relation between the overall mass-transfer coefficient and the local mass-transfer coefficients can be redrawn as follows:

$$\frac{1}{K_{ov}} = \frac{1}{k_{aq}} + \frac{1}{mk_{m}} + \frac{1}{mk_{org}} \qquad 2.44$$

Where C^{ab}_{Cu}: is copper concentration at the bulk aqueous phase, (g/cm^3).

C^{i}_{Cu}: is copper concentration at the aqueous phase-membrane interface, (g/cm^3).

C^{i}_{CuR2}: is the (copper-LIX) formed complex concentration at (the aqueous phase-inner surface of the fibre) interface, (g/cm^3).

C^{om}_{CuR2}: is the (copper-LIX) formed complex concentration at (the outer surface of the fibre-organic phase) interface, (g/cm^3).

C^{ob}_{CuR2}: is the (copper-LIX) formed complex concentration at bulk organic phase, (g/cm^3).

C^{*}_{aCu}: is a hypothetical copper concentration in the aqueous phase interface in equilibrium with the bulk organic phase, (g/cm^3).

C^{*}_{oCu}: is a hypothetical copper concentration in the organic phase interface in equilibrium with the bulk aqueous phase, (g/cm^3).

$D_{eff\,CuR2}$, D_{CuR2}: is the (copper-LIX formed complex) effective diffusion and diffusion coefficient respectively (cm^2/s).

N_{Cu}: is the rate of mass transfer of copper across the membrane-aqueous phase contact area, ($g/cm^2.s$).

N_{CuR2}: is the rate of mass transfer (copper-LIX formed complex) transfer through the membrane to the organic phase, ($g/cm^2.s$).

k_{aq}: is the aqueous phase mass transfer coefficient, (cm/s).

k_{org}: is the organic phase mass transfer coefficient, (cm/s).

K_{ov}: is the overall mass transfer coefficient, (cm/s).

Equation (2.44) shows that it is valid to represent the overall resistance to mass transfer in a MPHF membrane where species diffusion and solubility in the two phases are the main factors affecting its transfer, as has been demonstrated by Sirkar et al.[98] and Kiani et al.[122] In this study another important factor has contributed to copper transfer from the aqueous phase to the organic phase through the MPHF membrane wall. This factor is the chemical reaction between copper ions and the active component (LIX984) of the organic solvent.

2.8.2 The chemical reaction as a mass-driving force in dispersion-free extraction

In general mass-transfer occurs as a result of some potential differences or potential gradient (i.e. driving force) within the molecule surrounding which lead to molecules migration in the direction of lower potential[101]. Chemical reaction in liquid-liquid extraction has been utilised to enhance the extraction rate and refine the selectivity of the separation process. In membrane-based extraction, the reaction driving force can be considered an important factor in selective extraction of low or non-soluble species such as organic acids and metals respectively. The theoretical aspects of mass-transfer accompanied by chemical reaction have been proposed by Astarita [73] and reviewed in section 2.6.3 of this chapter.

In dispersion-free extraction the reaction front or location depends to large extent on the nature of the membrane used and the contacted phases wetability. In a hydrophobic MPHF membrane, the reaction interface between an aqueous solution and an organic solvent is located at the pores mouths at the aqueous side. Whereas, in a hydrophilic membrane the reaction zone is located inside the pores or near the organic phase side [98]. Guha et al [119]., studied copper extraction in a HFCL membrane using LIX 84, while Teramoto et al [127].,

examined copper extraction in hollow fibre liquid membrane using SME529™. These researchers have proposed the same equations to calculate the rate of mass-transfer at the reaction zone. The equation could be written for the current system (copper-LIX) as follows:

$$Cu^{+2} + 2HR \rightleftharpoons CuR_2 + 2H^+$$

$$N_{Cu} = k_r[\frac{C^i_{Cu}C^i_{HR}}{C_{H^+}} - \frac{1}{K_{ex}}\frac{C^i_{CuR_2}C^i_{H^+}}{C^i_{RH}}] \qquad 2.45$$

Where: $\frac{1}{K_{ex}}\frac{C^i_{CuR_2}C^i_{H^+}}{C^i_{RH}}$ describes the reverse reaction at the interface.

C^I_{Cu}, C^i_{HR}, $C^i_{H}{}^+$ and C^i_{CuR2}: are the interfacial concentrations of copper, the chelating reagent, the hydrogen generated during the reaction and the copper-LIX reagent formed at the interface respectively, (mole/l).

k_r, K_{ex}: are the reaction rate constant and the equilibrium constant respectively.

Guha and Sirkar[119] also postulated the following equation for the rate of mass-transfer at the stripping side of a HFCL membrane device they used:

$$N_{Cu} = k_s[C^{si}_{CuR_2}C^{si}_{H^+} - K_{eq}\frac{C^{si}_{Cu^{+2}}(C^{si}_{RH})^2}{C^{si}_{H^+}}] \qquad 2.46$$

Where C^{si}_{Cu}, C^{si}_{HR}, $C^{si}_{H}{}^+$ and C^{si}_{CuR2}: are the interfacial concentrations during a stripping process in a MPHF module of copper, the LIX reagent, the hydrogen generated during the reaction and the copper-LIX reagent formed at the interface respectively, (mole/l).

k_s: the stripping reaction rate constant.

If the chemical reaction is slow, then a new resistance (the reaction resistance) should be accounted for when calculating the overall mass-transfer coefficient based on local resistances. The reaction resistance in the current study is located at the interface in pores mouths at the aqueous side of the MPHF membrane and could be expressed as **(1/ k_r)**. Therefore, the overall resistance to copper transfer in a hydrophobic MPHF module could be written as follows:

$$\frac{1}{K_{ov}} = \frac{1}{k_{aq}} + \frac{1}{mk_m} + \frac{1}{k_r} + \frac{1}{mk_{org}} \qquad 2.47$$

2.8.3 Measurements and correlations of the overall mass-transfer coefficient in non-dispersive extraction

In a MPHF membrane-base liquid-liquid extraction system, the overall mass transfer coefficient is a weighted average of the individual mass transfer coefficients in the feed phase, at the reaction interface, across the membrane wall and in the organic phase. Previous studies on mass transfer across immobilised aqueous-organic interface in a membrane have suggested that the overall mass transfer coefficient and the local coefficients could be related together using simple film-theory[132,133]. Prasad et al[111]., have investigated the effect of eliminating the organic and aqueous boundary layer resistances on the overall mass transfer coefficient by selecting extraction systems with wide range of distribution coefficients, or by stacking a known number of flat membranes in the extraction cell [111,121]. It is obvious that the boundary layer film resistance in the aqueous and organic phases in the tube and the shell side respectively are a function of the turbulence in the system. Therefore, some methods of correlating and predicting these films resistance involve analysis of the physical properties and flow patterns of both phases by using dimensionless groups in form of Leveque solution as follows [101,107,134]:

1. The aqueous phase mass transfer (k_{aq}) in the tube side could be expressed in form of a Sherwood's number as follows:

$$N_{Sht} = \frac{k_{aq} d_t}{D_{aq}} = \gamma[\frac{d_t}{L}(N_{Re})^a (N_{Sc})^b] \qquad 2.48$$

2. The organic phase mass transfer coefficient (k_{org})in the shell side could be expressed in form of a Sherwood's number as follow:

$$N_{Shs} = \frac{k_{org} d_h}{D_{org}} = \beta[\frac{d_h}{L}(N_{Re})^a (N_{Sc})^b] \qquad 2.49$$

Where N_{Re} is the Reynolds number, N_{Sc} is Schmidt number, L is the membrane module length in cm, d_t and d_h are the fibre tubes internal diameter and the shell hydraulic diameter respectively, and a, b, γ and β are constants. The value of the constant (a) was reported to be 0.33 for laminar flow conditions and ranging between (0.6-0.8) for turbulent flow [101,107]. While the constant (b) value was reported to be unaffected by the flow pattern and relatively constant ranging between (0.3-0.33) [107].

The membrane resistance ($1/k_m$) could be accounted for by eliminating the film resistance under high flow rate of both phases in non-reactive extraction system, or by using a modified Wilson's plot, which involve plotting ($1/K_{ov}$) against $(1/N_{Re})^n$. A proper (n) value could be chosen to produce a straight line which can be extrapolated to in infinite flow rate where $(1/N_{Re})^n=0$. At that point the value of ($1/K_{ov}$) is assumed to equal to ($1/k_m$). While in a reactive extraction system the value of the intercept point at ($1/K_{ov}$) is assumed to be equal to ($1/k_r+1/k_m$) [101,107].

In this study the relationship between the local coefficients and overall mass transfer coefficient has been expressed in the form of local resistances to copper transfer which takes the form of equation (2.47) above. The local coefficients i.e. k_{aq}, k_{org}, k_r and k_m have

been calculated by combined Leveque solution and Wilson's plot. The experimental data and their discussion are given in details in chapters four and five.

CHAPTER THREE

EXPERIMENTAL STUDY

3 INTRODUCTION

This chapter includes detailed illustrations of all materials and apparatus, which were used in this study. The working conditions and the operating procedures of the experimental work are also discussed.

3.1 Materials and methods

In this section the general properties and the quantities of the experimental materials will be outlined and flow diagrams of some the experimental apparatus which were used to in the experimental work will be explained.

3.1.1 Copper sulphate solution

The aqueous solutions used for the equilibrium and mass transfer studies were prepared by dissolving known amount of copper sulphate (anhydrous copper sulphate) in a measured volume of de-ionised water. The prepared solutions pH was adjusted between 2 and 4 by adding few drops of concentrated sulphuric acid or sodium hydroxide.

3.1.2 The organic phase (Extractant)

Three different samples of alkalated phenol alkyl extracting reagents (LIX) were supplied by Henkel Corporation of Germany, which were diluted in Escaid 110™ supplied by Exxon UK. The three LIX reagents used for the equilibrium experimental investigations are namely as follows:

- LIX 84® (Ketoxime): a 5-nonylacetophenone oxime containing traces amount of 5-dodeylsalicylaldoxime in Escaid 110™.
- LIX 860® (Aldoxime): a 5-dodeylsalicylaldoxime containing traces amount of 5-nonylacetophenone oxime in Escaid 110™.
- LIX 984® (Mixture): an equivolume (50/50 v/v) mixture of LIX84® and LIX860®

The above three extractants were supplied separately by (Henkel Corporation of Germany) with original concentrations of 52- 60vol% LIX and 40-48vol% Escaid 110™, and were used separately without any further purification. In the equilibrium studies and mass transfer studies the stock samples were diluted with Escaid110™ to the required concentration.

3.2 Measurement Techniques

The following techniques were used to monitor the main variables during experimental work:

3.2.1 Measurement of copper concentrations

Copper concentrations in both phases (the extract and the raffinate) were measured by using flamed base atomic absorption spectrophotometer (Parkin Elmer PU9100 spectrophotometer) as follows:

Copper concentration at the raffinate phase was measured by taking 5-10 cm^3 of the solution and diluting it with de-ionised water in a 100cm^3 flask. Then the samples were analysed by atomic absorption spectroscopy, where their absorbances were recorded at 222.6nm wavelength. Previously standard solutions of Cu^{2+} (70-280 ppm concentration) were prepared. The absorbance of these standard solutions was also measured at 222.6nm

wavelength. Copper concentration at the raffinate phase was obtained from the calibration curve, (appendix 1) corresponding to the recorded absorbance.

Copper concentration at the extract phase was measured by the same spectrophotometer at the same conditions, but first the loaded organic phase was stripped with 2M sulphuric acid. For example 5 cm^3 of the extract was stripped with 20-30 cm^3 of acid (2M H_2SO_4). The mixture was shaken for 10-20 minutes and then poured into a separation funnel. A sample (5 cm^3) of the aqueous acidic solution layer was withdrawn and diluted with de-ionised water in a 100 cm^3 standard flask. The atomic absorption of the diluted solution was measured at 222.6 nm wavelength and the corresponding copper concentration for the found absorbance was determined from the calibration curve given in appendix 1.

3.2.2 pH measurements

Acidity of the aqueous phase was measured with a digital Jencons 3015 pH meter (Jencons scientific Ltd). The pH electrode and the glass reference combination electrode were manufactured by Jencon scientific Ltd. UK. The pH of the aqueous solutions was adjusted by adding few drops of acid or alkali to keep it in the required range.

3.2.3 Interfacial tension measurements

The interfacial tension at the aqueous-organic interface was measured by ring method using a tensiometre manufactured by (Whate Electronic and Instrumentation Company Ltd.). The average of several readings was taken at the room temperature 24 ± 1 $^{\circ}C$, but reproducibility was found to be with an average error of ± 20%.

3.3 Equilibrium Studies

Intensive experimental work is carried out in this study to establish the equilibrium data of the extraction and the stripping stages of copper into and from the chelating agents. This is illustrated in following subsection:

3.3.1 The experimental procedure of the extraction equilibrium stage

Extraction measurements of copper in three different extraction reagents (LIX84® LOT number 9084070, LIX860® LOT number I860102 and LIX984® LOT number 2984037) were carried out by contacting known volumes of the aqueous solution with similar volumes of an extractant (50 cm^3 of each). The aqueous phase concentrations are in the range between 0.25×10^{-3} to $20\times10^{-3}g/cm^3$ (0.25-20 g/l) with a pH of 2-2.5. Copper sulphate solutions (50 cm^3 each) were placed first in a 250 cm^3 flasks. The organic phase was prepared by diluting the above organic stocks with Escaid110 to produce 10 or 20v/v% LIX concentration solutions. Samples (50 cm^3) of the diluted LIX84®, LIX860® and LIX984® were added into the 250 cm^3 flasks in three separate batches. The flasks were placed in a fixed temperature 25±1°C shaking machine (Gallenkamp) and contacted for 2 hours under high speed shaking. After a total of 12 hours shaking the samples were removed and allowed to settle for 2 hours at a fixed temperature of 25°C in a water bath. The two phases then were separated in a separation funnel. The aqueous phase samples were filtered through a 0.7μm filtration paper (Whitman) to remove any remaining organic solvent and separate portions withdrawn to be analysed by atomic absorption spectrophotometer. Next 5cm^3 of each of the organic phase samples were placed in a 50 cm^3 flask and stripped with 20-30 cm^3 of (2M) sulphuric acid solution. The stripped solutions were analysed by atomic absorption spectrophotometer. Copper concentrations at

all solutions were obtained from the corresponding standard calibration curve (appendix 1). The concentrations obtained of both phases were used to find the equilibrium isotherms.

3.3.2 The experimental procedure of the stripping stage equilibrium

Metals recovery from an organic phase and concentration into an acidic aqueous solution is known as a stripping or re-extraction process. Based on the equilibrium experimental results for the three LIX reagents. LIX 984 was chosen to study the stripping process. The procedure was as follows:

A stock solution of the aqueous phase of 1000 cm^3 volume and 20 x 10^{-3} g/cm^3 copper concentration was prepared. A range of less concentrated samples were prepared by diluting known volumes of the aqueous stock solution above with de-ionised water to produce aqueous solutions of concentrations ranging between 0.25 x10^{-3} to 20 x 10^{-3} g/cm^3. A sample of 50 cm^3 for each of the diluted solutions was placed into a 250 cm^3 volume flask. An equal volume (50 cm^3) of pre-prepared LIX984 with 10v/v % concentration was added to each flask. The mixtures were shaken for 12 hours under a fixed temperature of 25 ± 1°C in the Gallenkamp shaking machine. Then the flasks were placed into a 25°C fixed temperature water bath overnight to achieve complete settling. The two layers were poured into a separator funnel where both phases were allowed to separate fully. Two samples (20 cm^3) each of the loaded organic were withdrawn carefully from each equilibrium separator funnel and placed into 50 cm^3 volume flasks. A volume (20 cm^3) of 0.5M H_2SO_4 was added to one of the 50 cm^3 flasks, while an equal volume (20 cm^3) of 2M H_2SO_4 was added to the other. The new mixtures were shaken for 12 hours in the Gallenkamp shaking machine under the same conditions as above. The samples were then transferred to a water bath and kept for 12 additional hours at 25°C fixed temperature to settle. Both layers of each sample (the stripped organic and the rich copper acid solution)

were collected through a separator funnel. The aqueous acidic solutions were analysed by atomic absorption spectrophotometer and the correspondence absorptions were used to obtain copper concentrations from the calibration curve Appendix. 1. The resultant concentrations of the stripped organic and the stripping acidic solution were used to draw the stripping equilibrium isotherm.

3.4 Mass Transfer and Kinetic Studies Using Single Drop Technique

This technique has been chosen among other dispersion-based techniques due to the advantages it offers of known interfacial area and of easy operating condition. The interfacial area and its characteristics are essential elements in dispersion and non-dispersion based contactor design. In this study using a single drop technique a dispersion-based liquid-liquid extraction process was carried out. The dispersed phase (droplet) was always LIX984® of 10v/v% to 60v/v% concentration in Escaid 110™. The continuous phase was copper sulphate aqueous solution with copper concentration ranging between (3 to 7g/l) with a pH of 2.

3.4.1 The apparatus and set-up of the single drop technique

The apparatus basically consists of the following:

1. A set of four Pyrex tube jacketed columns having internal diameter of 2.5 cm. Each column had a modified top comprising a quick fit B24 socket. The columns were of 55, 95, 149, and 187 cm length. Only one column was used at a time as in figure 3.1.
2. A Pyrex delivery unit fitted with a stainless steel needle of 21 gauge size which was fixed at the bottom end of the column. The delivery unit was connected by a polyethylene tube to the organic reservoir.

3. A collection head fitted with a capillary tube of 1 cm^3 volume in one side and a connection section to the aqueous phase reservoir on the other side. The capillary tube volume was first calibrated with water.

4. The organic reservoir is connected to a cylinder containing nitrogen-free oxygen gas using a polyethylene tube. The pressure of the system was controlled by a fine pressure control valve attached to the cylinder.

5. A thermostat water tank was used, and from there water at fixed temperature (25°C) was circulated through the column jacket by peristaltic pump.

* Full details of the experimental rig set up are given in appendix 2.

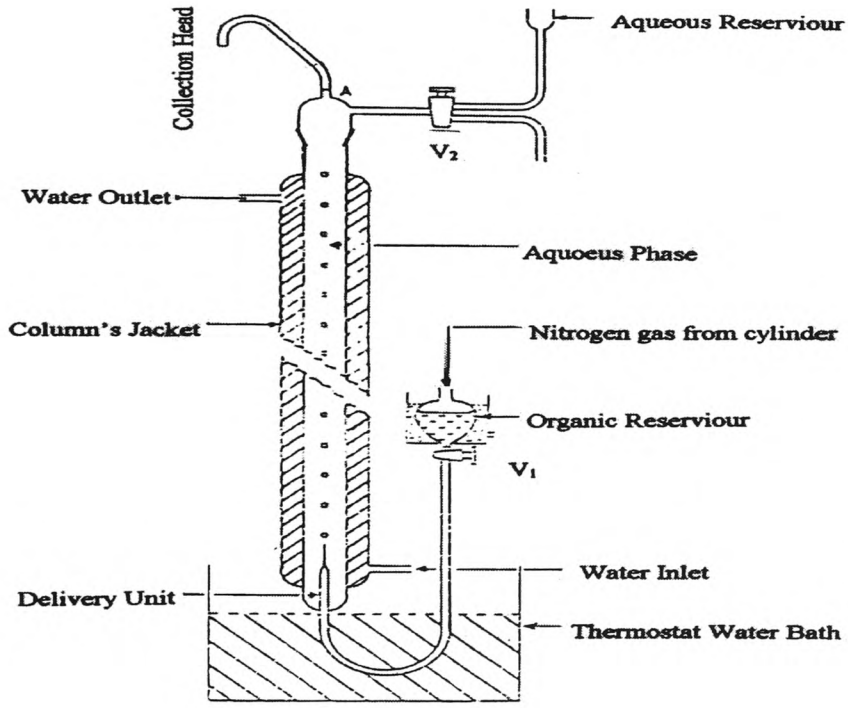

Figure 3. 1: Schematic diagram of the main parts of single drop apparatus

3.4.2 The experimental procedure for generating single drops

The following operating steps were used to generate single drops of the dispersed phase and control their flow:

1. Two litres of an aqueous solution with known copper concentration was prepared. At the same time 1 litre of LIX 984® was prepared by mixing 0.5 litre of LIX84® with 0.5 litre of LIX 860®, then 0.2 litre of this mixture was diluted with 0.8 litre Escaid110™ to produce 20v/v% LIX984® solution.
2. The columns and all the glass parts of the apparatus were washed with distilled water and acetone and then rinsed thoroughly with water several times. The apparatus were then dried with hot air for 15 minutes.
3. The thermostat tank was filled with water and the temperature was set at 25°C.
4. Columns (one at time) were vertically clamped firmly to a metal frame built especially for these experiments.
5. After about two hours time the thermostat tank temperature reached 25 ±1°C, at this time the peristaltic pump was switched on to circulate water through the column and the organic reservoir jacket.
6. The delivery unit was assembled and connected to the organic reservoir. The valve (V1 in fig. 3.1) was opened to fill the delivery unit with the organic phase and remove any air in this section. The unit was then attached firmly to the lower end of the column.
7. The aqueous solution was poured over gently into the top of the column and the liquid level was controlled by the valve connected to the aqueous reservoir, (V2 in fig. 3.1).
8. The column was lowered so that the polyethylene tube (which connected the organic reservoir to the delivery unit) was immersed in the water bath.

9. A small pressure was developed at the organic reservoir by allowing nitrogen gas to flow in. The valve V_1 was then opened and the flow of drops was adjusted to approximately 80 drops per minute by increasing or decreasing gas flow from the fine pressure controller which was attached to the cylinder.

10. The drops rising time was measured by using digital stopwatch.

3.4.3 Procedure for the rate of mass transfer measurement

The rate of mass transfer in the single drop experiments was determined by assuming that all the drops are uniformly spherical. Then the interfacial area of each single drop can be calculated from the known a volume of the capillary tube and the number of the drops required to fill such volume using the following equations:

$$V_c = V_d \times N_{AB}$$

$$V_c = \frac{4}{3} r_d^3 \pi N_{AB}$$

$$r_d = \left(\frac{3}{4 \pi N_{AB}} \right)^{1/3} \qquad 3.1$$

The surface area of a single spherical drop is given by:

$$A_d = 4\pi r_d^2 \qquad 3.2$$

Substitution of equation 1 in 2 gives:

$$A_d = 4\pi \left(\frac{3}{4\pi N_{AB}} \right)^{2/3} \qquad 3.3$$

Where $V_c = 1\ cm^3$ is the volume of the capillary tube, (section AB in fig. 3.1).

V_d = is the volume of single drop (cm^3).

N_{AB} = the number of drops required to fill section AB of the capillary tube.

r_d = the drop radius (cm).

A_d = the drop surface area, (the interfacial area, cm^2).

The concentration of copper extracted by the droplet of the organic phase was determined by collecting a volume of 1 cm^3 of the loaded organic drops at the capillary tube. This volume was then transferred into 50 cm^3 flask and stripped with 20 cm^3 (2M H_2SO_4). The stripped solution was analysed by atomic spectrophotometer and copper concentration was determined from the calibration curve, (Appendix 1). The overall rate of mass transfer per unit area per unit time was calculated as follows:

$$\text{Rate} = \frac{\text{Mass of copper extracted in single drop}}{\text{drop rising time} \times \text{drop surface area}} \qquad 3.4$$

$$Rate\ .(N_a) = \frac{(C_{Cu_{org}} \times V_{org}) / N_{AB}}{t_r \times A_d}$$

Where $C_{Cu\ org}$ = copper concentration at the droplet organic phase at the top of the column, (g/cm^3).

V_{org}= volume of the loaded organic phase in the capillary tube section, (cm^3).

N_a = the rate of mass transfer, (g/cm^2s).

The main results of single drop experiments in four different columns are summarised in chapter four and thoroughly analysed.

3.5 Fabrication of Free Dispersion Liquid-Liquid Extraction Unit

A dispersion-free unit based on a microporous hydrophobic hollow fibre membrane was built in the laboratory. The main objective of building this unit is to study mass transfer of copper or any metal from an aqueous phase to an organic phase without any disturbances of the interface. Further to that, the unit was designed in such a way that mass transfer can be studied at very low or high flow rates, which has not been studied before. This unit consists of the following apparatus:

1. A wooden base and panel board.

2. Two magnetic drive gear pumps with a body, gears and bearings made out of 316 stainless steel, which has been purchased from Cole-Parmer, USA. These pumps are single-phase electric supply with a performance of 0.25-2.5 litres/min at 30 PSI.

3. Two stainless steel Rotametres, equipped with fine tuning valves, model 65 mm which have a maximum flow rate of 1.5 litres/min and maximum pressure of 120 PSI. These Rotametres were purchased from Gilmont instruments, USA.

4. Four polypropylene tanks, two of them with a capacity of 40 litres of an aqueous or organic phase used as the feed tanks to the unit. While the other two tanks 20 litres capacity each were used to collect the products. These tanks were supplied by Merlin C4 T&D, UK. Specially modified covers made of Perspex glass were manufactured in our workshop to cover the feed tanks which were fitted with special inlets and outlets for the recycled and bypass stream.

5. Four polypropylene fine tuning valves purchased from Cole-Parmer, USA.

6. Fittings and connections are all made of polypropylene with size of 1/4 x 1/8 and 1/4 x 1/4 NPTF. These were purchased from Cole-Parmer, USA.

7. Ten metres of polypropylene tubing with 1/8" inside diameter and 1/4" outside diameter and maximum pressure of 120 PSI. The tubing is purchased from Cole-Parmer (Lot. 06757).

8. Hydrophobic microporous hollow fibre (MPHF) membrane module (Celgard^{TR} 2400, X10) made by Hoechst Celanece Separation Division, Aktiengesellschaft, Germany. The module contained hydrophobic microporous polypropylene hollow fibres with epoxy tube sheets in nylon casing. The details of the module are given in Table 3.1.

All the above components were used to build a free dispersion liquid-liquid extraction unit, which is capable of working under wide range of variable flow rates and pressures. Full details of the experimental rig set-up and its main parts are given in Appendix 3.

Table 3. 1: The full details of the microporous hollow fibre membrane module.

Specifications of the module:	
Overall length of module including endcaps	30 cm
Case length	20 cm
Case Diameter	2.5 cm
Maximum differential operating pressure	410 KPa
Maximum operating temperature	60°C
Case material	Polypropylene
Effective surface area	0.23 m^2
Effective area/volume	40 cm^2/cm^3
Fibre's specification:	
Number of fibres	2100
Effective fibre length	16 cm
Fibre internal diameter	0.024 cm
Fibre wall thickness	0.003 cm
Effective pose size	0.05 μm
Porosity	30%

* Hoechst Celanese Corporation in Germany provided these specifications [120].

3.5.1 Start-up procedure of dispersion-free liquid-liquid extraction unit

Experiments were carried out by, first running both pumps on full circulation mode where the aqueous and organic inlet valves to the MPHF module were closed and the by-pass valves opened. After five minutes the valve on the aqueous by-pass line was slowly closed till the inlet pressure gauge was reached 300 KPa. Then the aqueous inlet valve to the MPHF module was opened slowly while the outlet valves for both phases remained closed until the pressure reached 250 KPa on the aqueous side. The aqueous outlet valve at the other end of the MPHF module was opened gradually and the by-pass valve adjusted till

the required pressure and flow rate were achieved. The same steps were followed on running the organic phase through the MPHF membrane apart from operating the organic outlet valve, which was slightly opened before opening the inlet valve to the MPHF module to avoid any pressure build up. The aqueous inlet pressure was in the range between 240-260 KPa and the outlet pressure was 375-395 KPa. While the organic phase inlet pressure was kept in the range between 200-230 KPa and the outlet pressure between 60-100 KPa. The MPHF pores were always wetted by the organic phase, therefore the aqueous side pressure was always kept higher than the organic phase pressure to avoid any organic break-through to the aqueous side. The main parts of this unit are outlined in figure 3.2 and full description of the unit is given in Appendix 3.

3.5.2. Procedure for continuous extraction in a dispersion-free contactor

In this process, 30 litres of the aqueous phase was prepared by dissolving a known amount of $CuSO_4$ in de-ionised water to obtain the required concentration in a make-up tank where it was mixed thoroughly for 10 hours. The same volume of the organic phase was prepared in a separate make-up tank by diluting a known volume of the fresh LIX984® in Escaid110™ to obtain the required reagent concentration. The organic solution was also mixed for 10 hours. Then both phases were poured into the feed tanks and circulated for 15 minutes in a close loop mode without pumping through the MPHF module by using the by-pass line. The aqueous phase containing copper ions was first pumped through the fibre tubes or in the shell side until the required flow and pressure was reached. Then the organic phase was pumped co-currently or counter-currently on the shell or the tube side. The inlet pressure difference between both phases was always kept around 30-40KPa and a difference of 295-310 KPa was maintained between the outlet sides. In this mode of

operation the organic phase wetted the fibre tubes walls and the interface area was kept at the pores mouth.

This process could be run to process larger volumes of the aqueous phase if the feed tanks were supplied with fresh solutions all the times. The process was run until one or both feed tanks contents were at low level. The low level indication on the feed tanks are safety measurements to protect the pumps from running dry. The products i.e. the extract and the raffinate were collected in separate tanks, where they were sampled regularly at 5 minutes intervals. The experimental set-up of this process is similar to that described in Figure 3.2.

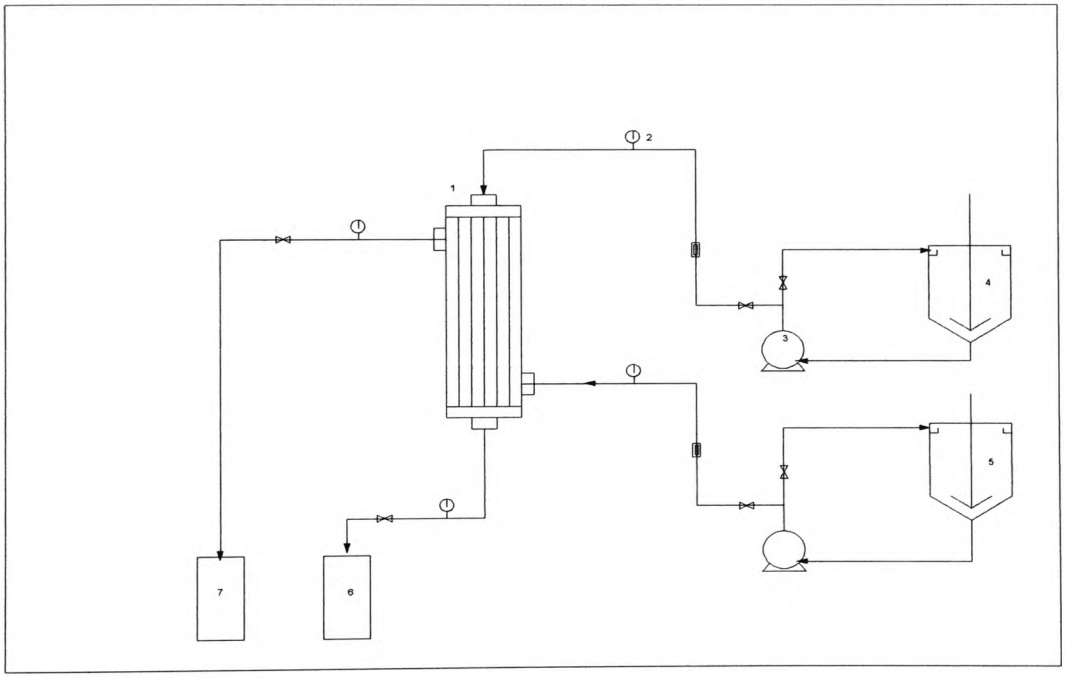

Figure 3. 2: A flow diagram of continuos mode extraction in a dispersion-free unit; (1) the hollow fibre membrane module, (2) pressure gauge, (3) gear pump, (4) the aqueous phase feed tank, (5) the organic phase feed tank, (6) the raffinate phase collection tank and (7) the extract phase collection tank.

3.5.3 Procedure for batch extraction in a free dispersion contactor

The feed solutions were prepared in a similar way to that outlined in section 3.5.2, but in smaller volumes i.e. 5-10 litres of each of the aqueous and organic phases were prepared separately and transferred to the feed tanks. A period of 15 minutes of full circulation from and into the feed tanks through the by-pass line precede the experimental run. The aqueous phase was first pumped through the MPHF module tube side or shell side depending on the flow arrangement. The aqueous outlet line from the MPHF membrane unit was connected back to the aqueous feed tank. In a similar manner the organic phase was pumped co-currently or counter-currently in the shell or tube side from where the output product was returned into the feed tank. This close loop mode process was carried out for a range of flows and concentrations for both phases. The process was carried out for a period of 3-5 hours. The time required to complete this type of batch extraction depends on the processed volumes, phase flow ratios and feed and raffinate concentrations. Figure 3.3 provides a schematic flow diagram of this process set-up.

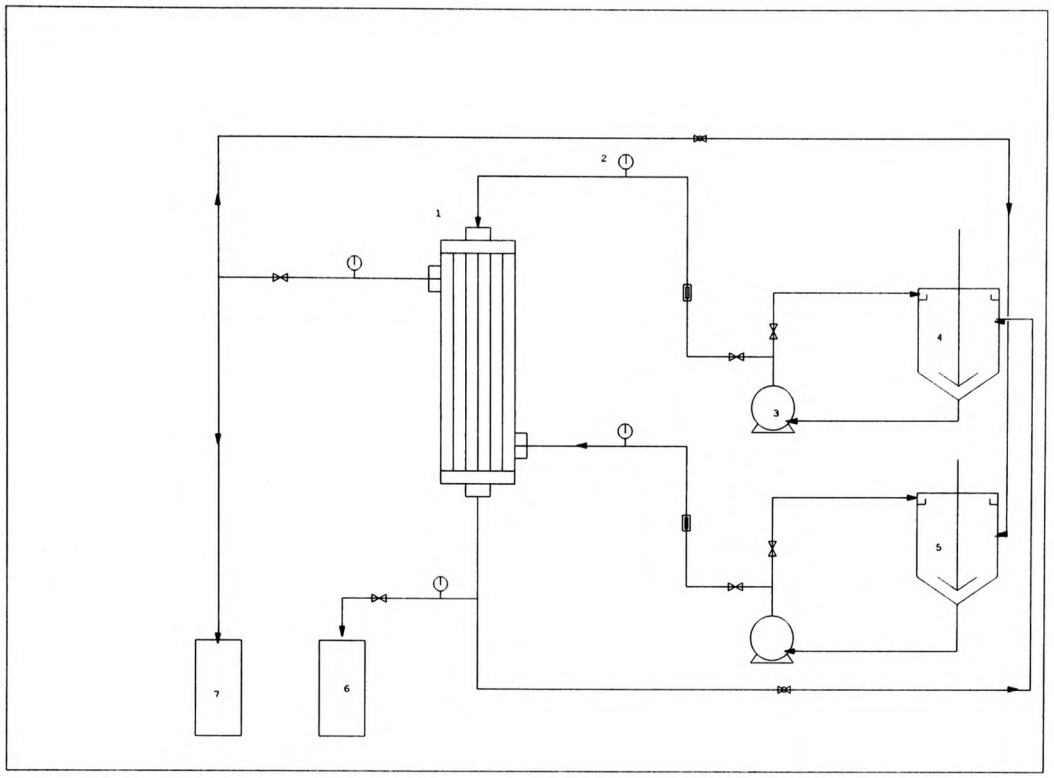

Figure 3. 3: A flow diagram of the close-loop batch extraction in a dispersion-free unit; (1) the hollow fibre membrane module, (2) pressure gauge, (3) gear pump, (4) the aqueous phase feed tank, (5) the organic phase feed tank, (6) the raffinate phase collection tank and (7) the extract phase collection tank.

3.5.4 Procedure for batch stripping in dispersion-free contactors

Copper recovery from the organic phase and concentration into an aqueous solution is defined as stripping and considered is to be one of the most important steps in metal extraction. In this study an acidic solution (0.5 molar H_2SO_4 stripping phase) was prepared from a concentrated solution of 99.9 % H_2SO_4 stock solution by diluting the required volume with de-ionised water in a polypropylene make-up tank with continuous mixing for 5-7 hours. A known volume of the LIX984 was pre-loaded with copper in a special batch extraction process. The loading of LIX984 with copper was achieved by contacting an aqueous solution of known concentration with LIX984 of known concentration at a specific aqueous/organic flow rate ratio through the MPHF module. The obtained extract was

analysed thoroughly by using Atomic Absorption spectroscopy, as described earlier. In some experiments the required copper concentration at the organic phase was achieved by mixing the two phases in equal volumes in a tank until they reach the equilibrium conditions. Then the loaded organic phase (extract) was further contacted co-currently or counter currently against the acidic stripping phase in a close-loop mode. The contacting mode in this process is similar to that in section 3.5.3. But in this process the copper ions transfer in the opposite direction to that of the extraction process. In this stripping process copper transferred from the organic phase which wetted the hollow fibres walls into the aqueous acidic solution. Both phases were contacted in the MPHF module and circulated from and into the feed tanks until the organic phase copper content reduced the required concentration. This type of transport and its results will be presented and discussed in details in chapters four and five of this study.

The flow diagram of this process is similar to that detailed in section 3.5.3 except that the aqueous feed tank contained acid solution while the fresh organic tank contained LIX984 loaded with copper.

3.5.5 Procedure for continuous stripping in dispersion-free contactors

Both phases feed solutions were prepared in a similar manner to that described in section 3.5.4, but larger volumes of both phases were used (30 litres of each phase). The solutions were first circulated from and into the feed tanks through the by-pass lines. Then the stripping acid solution (0.5M H_2SO_4) was pumped into the MPHF module fibre or shell side. When the required aqueous flow and pressure were achieved the organic phase was pumped into the shell or the fibre tubes counter-currently to the aqueous flow. The two phases were always partitioned by the hollow fibre tubes walls of 30μm thickness. The contact process between the copper rich organic and the acidic stripping solution was

taking place at the pores mouths of the aqueous side. The organic phase always wetted the hydrophobic fibres walls, therefore, the aqueous side was kept at higher pressure than the organic side to prevent any organic breakthrough. The membrane module outlet streams (i.e. products) were collected in separate tanks where they analysed. This once-through non-dispersive stripping has been carried out for a wide range of flow rates for both phases. The flow diagram of this process is similar to that outlined in section 3.5.2 but the feed tanks contain acidic solution and LIX984 solution pre-loaded with copper instead of copper solution and fresh LIX984 solution respectively. The results of this operation will be illustrated and discussed in chapters four and five.

3.5.6 Procedure for variable flow rates in dispersion-free continuous extraction

To establish the facts of how the two phases flow rate could effect the local resistance i.e. the film resistance on either side across the membrane fibre walls, a set of experiments were carried out. In these experiments one of the phases (the aqueous or the organic phase) was pumped at a constant flow rate i.e. low or high while the other phase was pumped at either a similar flow or on an increasing order of flow as follows:

Case 1. *Organic at Low flow rate against increasing aqueous flow rate*

First the feed tanks were filled with 30 litres of known concentration solutions of both phases. The two phases were circulated from and into the feed tanks using the by-pass line for 15-20 minutes. Then the aqueous phase was pumped through the fibre tubes or the shell side of the MPHF module at $50cm^3$/min flow rate and 240-260 KPa. After 10 minutes of starting the aqueous phase flow, the organic phase was pumped into the free-side of the MPHF module co-currently or counter-currently to the aqueous phase. This operation was

carried out until the organic phase started changing colour (from amber to dark brown) which is an indication of solute copper transferred from the aqueous to the organic phase. This mass transfer process showed a steady state condition after 5 minutes from the starting time and was left for 5 minutes further before sampling. Then the aqueous phase flow rate was increased to 100 cm^3/min while the organic phase remained constant at 50 cm^3/min. The contact process was carried out for another 5-10 minutes before increasing the aqueous phase flow rate another 100 cm^3/min. This process was continued until the aqueous phase flow reached 600 cm^3/min. After each increase on any of the phases flow rate, the raffinate and the extract streams were analysed on 5 minutes intervals.

Case 2. *High organic flow rate against increasing aqueous flow rate*

This set of experiments were carried out with similar feed concentrations to those in case-1 and in a similar start-up procedure. But the organic phase flow rate started at 600 cm^3/min and remained at this level throughout the experiment run. While the aqueous phase flow rate was started at 50 cm^3/min and increased in 100 cm^3/min each time to reach 600 cm^3/min. In these experiments large volume of the organic phase (40 litres) was required while lesser volume of the aqueous phase feed 25-30 litres was used due to the high flow rate of the organic side.

Case 3. *Low aqueous phase flow rate against increasing organic flow rate*

The same start-up procedure, used with the two previous sets of experiments was used here in a similar concentration range. The MPHF was operated with the aqueous phase on the fibre tubes of shell side flowing rate of 50-100 cm^3/min. While the organic phase was pumped through the MPHF with a gradual increase of 100 cm^3/min on its flow rate every 5-10 minutes from 50 cm^3/min to 600 cm^3/min. The organic phase high flow rate of 600

cm^3/min was achieved after 30-45 minutes of continuous extraction and continued for another 10 minutes before final samples were taken.

Case 4. *High aqueous phase flow rate against increasing organic flow rate*

These experiments required larger volumes of the aqueous phase (40 litres) in contrast to experiments on case 3 where smaller volume was used (20 litre). The concentrations of feed solutions were similar to that used in case 3 experiments. The aqueous phase was maintained at 600 cm^3/min flow rate and an outlet pressure of 380-395 KPa. While the organic phase flow rate was increased gradually between 50-600 cm^3/min while its outlet pressure of 70-100 KPa adjusted to remain constant by closing slowly the by-pass line. In this experiment and all the previous cases both phases outlet products were collected in separate collection tanks and analysed.

3.5.7 Procedure for dispersion-free batch and continuous extraction at constant flow

The start-up procedure and the arrangement of these experiments are the same as described in section 3.5.1. In batch extraction process both phases were pumped at the same flow rate from and into the feed tanks through the MPHF membrane unit. In each run the experiment was continued until the required raffinate concentration was reached.

In the batch extraction process, both phases were circulated at constant flow rate (high or low) through the MPHF membrane. The experimental procedure for this process can be described as follows:

4 litres of both phases was placed in the feed tanks. The experiments started by pumping both phases at constant flow rate e.g. 100 cm^3/min 3 hours or until there was no significant changes in the outlet concentrations. The outlets were circulated into the feed tanks and

sampling was carried out in 5 minutes intervals. When the required concentration was achieved, then the experiment was terminated.

The batch and the continuous mode experiments at constant flow were used to investigate the effect of minimising and maximising the boundary layer thin film resistance and mass transfer characteristics in non-dispersive apparatus. Full discussion of these experiments and their results are detailed on chapters four and five.

3.5.8 Copper concentration measurements in a dispersion-free unit

The sampling procedure used for both phases in and out the MPHF module depends on the mode of the extraction operation i.e. batch or continuous extraction. In batch extraction the starting concentration at the feed tanks for both phases were known but after 5 minutes of circulation through the MPHF membrane, the copper concentration at the shell and tubes inlet and outlets were changed. Therefore, samples were taken from both inlets and outlets at both phases after 10-15 minutes of starting time. Samples (10 cm^3) of the aqueous inlet and outlet streams were collected at 15 minutes intervals. These samples were placed in a 100 cm^3 flask and diluted with de-ionised water to complete 100 cm^3 volume. These samples then were analysed in the atomic absorption spectrometer where their absorptions were recorded.The corresponding aqueous concentrations were obtained from a calibration curve obtained at the same time and under the same conditions. The organic and aqueous outlet samples were collected at the same time i.e. at 10-15 minutes intervals. Samples (5 cm^3) of the organic inlet and outlet streams were withdrawn each time and placed into 50 cm^3 flasks. Then 30 cm^3 of acid (2M H_2SO_4) was added into each flask. The mixtures were shaken for 30 minutes and then separated using separation funnels. The stripped aqueous

solutions were analysed by using the AA technique and the corresponding copper concentrations were found from the calibration curve.

In continuous non-dispersive extraction the aqueous and organic phases were passed through the MPHF unit only once. The sampling procedure for this operation was only for the aqueous and organic outlet streams, because the inlet concentration did not change at the feed tanks. The analysis procedure was similar to that used in the batch process above.

In all continuous dispersion-free experiments where one of the phases was pumped with variable flow rates, samples were taken from both outlets after 10 minutes of each change on the flow rate. The results and discussion of these experiments are summarised in chapter 4 and discussed in detail in chapter 5.

3.6 Shut-Down and Cleaning Procedure for The Dispersion-free Solvent Extraction Unit.

After each experiment, all apparatus in the non-dispersive unit were cleaned thoroughly. The following steps were used:

1. Both pumps electric supply was turned off, and
2. Immediately the valve at the aqueous outlet stream was shut-off to keep small pressure build-up, which was enough to prevent any organic leaking into the aqueous side.
3. The remained of both phases in the MPHF membrane, connection lines and in the feed tanks was drained through the outlet and the by-pass streams and collected in special disposal containers.
4. The feed tanks were disconnected and washed thoroughly with distilled and di-ionised waters. Then reconnected back to the unit.

5. The aqueous feed tank was filled with di-ionised water while the organic feed tank was filled with Escaid 110.

6. The by-pass values were opened for short time to flush out any remains in the lines. Then they were connected back to the feed tanks.

7. The aqueous side (di-ionised water) inlet value was opened slowly while the outlet valve remained close until the pressure gauge reached 260 kPa. At this pressure the outlet on the aqueous side was opened slowly to let the di-ionised water clean the MPHF membrane tubes or shell of any copper remains. After 10-20 minutes the solvent Escaid110 was pumped through the MPHF membrane with an inlet pressure of 200kPa to clean any organic phase left-over. Both sides were pumped through with a flow ratio of 600 cm^3/300 cm^3; di-ionised water /Escaid110 for 20 minutes, then the outlet lines were connected back to the feed tanks to run on a close loop mode. This process was carried out for 2-4 hours or until no traces of any organic (LIX984) or copper were noticed on the unit.

8. After this period the pumps were switched-off and the feed tanks drained and dried ready for the next experimental run.

CHAPTER FOUR

RESULTS

4 INTRODUCTION

In this chapter the experimental results obtained through out this research work are presented. Results of copper-LIX system equilibria are presented first due to the importance of equilibrium factors in designing the extraction process and in choosing suitable techniques. The results of two different techniques (i.e. single rising drop and microporous hollow fibre membrane), which are used in this study to evaluate mass transfer characteristics and determine its main parameter, are also listed below.

4.1 Experimental Results of Copper-Hydroxyoxime Extraction Equilibria

Extraction equilibria experiments were carried out using three different chelating hydroxyoxime reagents namely LIX84, LIX860 and LIX984 in Escaid110. Two samples of the organic active reagent were used with concentrations of 10 and 20 v/v%. While the aqueous phase concentration ranging between 0.25 to 20 g/l. Each experiment was repeated five times and it has been found that data reproducibility was consistent with small margin of error. The aim of studying more than one extractant equilibrium behaviour with the same aqueous solution (copper sulfate) was to establish essential information on the organic solvent extraction capacity, as well as to investigate the right conditions for mass transfer study on LIX reagents. These reagents are new and have not been studied in detail before. The results of two runs of each equilibrium experiment are listed in the tables below.

4.1.1 Extraction of copper with LIX84

These experiments were carried out into two batches. First a set of aqueous solution samples (50cm^3 each) with concentrations ranging between 0.25 to 20 g/l were mixed with 50cm^3 of 10v/v% LIX84 organic phase. Then a similar set of the aqueous samples were mixed with 20v/v% LIX84. Both phases were analysed using an atomic absorption spectrophotometer to find out the copper content. The results of these experiments are listed in tables 4.1.A and B below:

Table 4.1. A: The distribution of copper between the organic phase LIX84 (10v/v%) and the raffinate aqueous phase.

Aqueous feed concentration g/l	Feed pH	Copper concentration at the raffinate phase g/l		Copper concentration at the extract phase g/l		pH at equilibrium	
		1st run	2nd run	1st run	2nd run	1st run	2nd run
0.25	2.5	0.050	0.0019	0.200	0.237	1.73	1.61
1.00	2.5	0.087	0.088	0.913	0.922	1.50	1.23
2.00	2.5	0.185	0.161	1.815	1.839	1.48	1.36
3.00	2.5	0.530	0.762	2.470	2.238	1.50	1.2
4.00	2.5	1.047	1.129	2.953	2.871	1.48	1.34
5.00	2.5	1.670	1.596	3.330	3.404	1.30	1.51
7.00	2.5	3.079	3.069	3.921	3.931	1.30	1.38
9.00	2.5	4.700	4.678	4.300	4.322	1.20	1.51
12.00	2.5	7.330	7.210	4.670	4.790	1.22	1.34
15.00	2.5	10.040	10.132	4.960	4.868	1.30	1.45
17.00	2.5	11.847	11.828	5.153	5.172	1.38	1.51
20.00	2.5	14.747	14.658	5.253	5.342	1.40	1.53

Table 4.1. B: The distribution of copper between the organic phase LIX84 (20v/v%) and the raffinate aqueous phase

Aqueous feed concentration g/l	Feed pH	Copper concentration at the raffinate phase g/l		Copper concentration at the extract phase g/l		pH at equilibrium	
		1st run	2nd run	1st run	2nd run	1st run	2nd run
0.25	2.5	0.001	0.0002	0.249	0.2498	1.70	1.92
1.00	2.5	0.090	0.005	0.910	0.995	1.48	1.83
2.00	2.5	0.057	0.049	1.943	1.951	1.38	1.75
3.00	2.5	0.085	0.074	2.915	2.926	1.50	1.21
4.00	2.5	0.160	0.115	3.840	3.885	1.50	1.46
5.00	2.5	0.520	0.542	4.480	4.458	1.35	1.61
7.00	2.5	1.644	1.591	5.356	5.409	1.28	1.58
9.00	2.5	3.125	3.318	5.875	5.682	1.25	1.53
12.00	2.5	5.621	5.567	6.379	6.433	1.25	1.56
15.00	2.5	8.230	8.411	6.770	6.589	1.33	1.41
17.00	2.5	10.010	10.226	6.989	6.774	1.38	1.42
20.00	2.5	12.849	12.914	7.151	7.086	1.37	1.40

4.1.2 Extraction of copper with LIX860

These experiments were carried out under similar conditions to those used with LIX84 and the aqueous phase samples used here were prepared from the same aqueous stock solution. Two sets of samples of the aqueous phase with wide range of copper concentrations (0.25 to 20 g/l) were contacted with 10v/v% and 20v/v% LIX860 solution separately in $50cm^3/50cm^3$ volume ratio. The results of these experiments are listed in tables 4.2.A and B as follows:

Table 4.2. A: The distribution of copper between the organic phase LIX860 (10v/v%) and the raffinate aqueous phase.

Aqueous feed concentration g/l	Feed pH	Copper concentration at the raffinate phase g/l		Copper concentration at the extract phase g/l		pH at equilibrium	
		1st run	2nd run	1st run	2nd run	1st run	2nd run
0.25	2.5	0.052	0.038	0.198	0.212	1.50	1.61
1.00	2.5	0.200	0.187	0.800	0.813	1.20	1.25
2.00	2.5	0.250	0.235	1.750	1.765	1.30	1.38
3.00	2.5	0.640	0.664	2.360	2.336	1.50	1.22
4.00	2.5	1.260	1.313	2.740	2.687	1.48	1.53
5.00	2.5	1.980	1.887	3.020	3.113	1.30	1.25
7.00	2.5	3.500	3.513	3.500	3.487	1.20	1.21
9.00	2.5	5.030	5.011	3.970	3.989	1.20	1.34
12.00	2.5	7.370	7.532	4.630	4.468	1.22	1.27
15.00	2.5	9.800	9.690	5.200	5.310	1.20	1.32
17.00	2.5	11.470	11.399	5.530	5.601	1.31	1.28
20.00	2.5	14.240	14.190	5.760	5.810	1.40	1.51

Table 4.2. B: The distribution of copper between the organic phase LIX860 (20v/v%) and the raffinate aqueous phase.

Aqueous feed concentration g/l	Feed pH	Copper concentration at the raffinate phase g/l		Copper concentration at the extract phase g/l		pH at equilibrium	
		1st run	2nd run	1st run	2nd run	1st run	2nd run
0.25	2.5	0.001	0.003	0.2490	0.247	1.52	1.65
1.00	2.5	0.070	0.048	0.9300	0.952	1.00	1.43
2.00	2.5	0.051	0.011	1.9490	1.989	1.30	1.34
3.00	2.5	0.085	0.162	2.9250	2.838	1.35	1.38
4.00	2.5	0.115	0.483	3.8950	3.517	1.40	1.34
5.00	2.5	0.346	0.856	4.6548	4.144	1.22	1.26
7.00	2.5	1.064	1.491	5.9356	5.509	1.12	1.15
9.00	2.5	2.125	2.125	6.8750	6.722	1.10	1.21
12.00	2.5	3.830	3.830	8.1700	8.193	1.14	1.24
15.00	2.5	5.740	5.544	9.2600	9.456	1.25	1.21
17.00	2.5	7.130	6.878	9.8700	10.122	1.37	1.26
20.00	2.5	9.510	9.354	10.490	10.646	1.50	1.25

4.1.3 Extraction of copper with LIX984

The chelating agent (LIX984) is defined by Henkel Corporation mineral industry as the most suitable extractant for copper extraction from an acidic leach solution [30]. In this experiment the LIX984 (LOT number 2984037) was used after dilution with Escaid110 to make-up 10v/v% and 20v/v% solutions. Two sets of samples of the same aqueous stock solution used with LIX84 and LIX860 were contacted with a $50cm^3$ of one the LIX984 solutions separately. The mixture was contacted for the same period and the same conditions used to study (LIX84 and LIX860-Copper sulphate) equilibria. The two phases were analysed for their copper content and the equilibrium results can be summarised in tables 4.3.A and B as follows:

Table 4.3. A: The distribution of copper between the organic phase LIX984 (10v/v%) and the raffinate aqueous phase.

Aqueous feed concentration g/l	Feed pH	Copper concentration at the raffinate phase g/l		Copper concentration at the extract phase g/l		pH at equilibrium	
		1st run	2nd run	1st run	2nd run	1st run	2nd run
0.25	2.5	0.050	0.045	0.200	0.215	1.60	1.53
1.00	2.5	0.239	0.248	0.761	0.752	1.41	1.43
2.00	2.5	0.523	0.513	1.477	1.487	1.48	1.38
3.00	2.5	1.132	1.163	1.868	1.837	1.32	1.33
5.00	2.5	2.830	2.857	2.170	2.143	1.29	1.38
7.00	2.5	4.430	4.383	2.570	2.617	1.12	1.35
12.00	2.5	8.376	8.482	3.624	3.518	1.08	1.26
15.00	2.5	10.880	10.761	4.120	4.239	1.11	1.18
17.00	2.5	12.510	12.613	4.490	4.387	1.16	1.35
18.50	2.5	13.823	13.431	4.677	4.569	1.15	1.37
20.00	2.5	15.150	15.203	4.850	4.797	1.40	1.16

Table 4.3. B: The distribution of copper between the organic phase LIX984 (20v/v%) and the raffinate aqueous phase.

Aqueous feed concentration g/l	Feed pH	Copper concentration at the raffinate phase g/l		Copper concentration at the extract phase g/l		pH at equilibrium	
		1st run	2nd run	1st run	2nd run	1st run	2nd run
0.25	2.5	0.002	0.003	0.248	0.247	1.51	1.65
1.00	2.5	0.007	0.058	0.993	0.952	1.52	1.23
2.00	2.5	0.039	0.013	1.961	1.987	1.44	1.34
3.00	2.5	0.135	0.163	2.865	2.837	1.30	1.38
5.00	2.5	0.573	0.857	4.427	4.143	1.21	1.34
7.00	2.5	1.370	2.033	5.630	4.967	1.10	1.26
12.00	2.5	5.020	6.482	6.980	5.518	1.03	1.15
15.00	2.5	7.250	7.561	7.750	7.439	1.15	1.21
17.00	2.5	8.700	8.818	8.300	8.182	1.11	1.14
18.50	2.5	9.700	9.485	8.800	9.015	1.11	1.12
20.00	2.5	10.800	10.678	9.200	9.322	1.20	1.12

Based on the equilibrium results tabled above the equilibrium constant (K_{eq}) for each LIX-copper sulphate system was calculated. The equilibrium constants of LIX84, LIX860 and LIX984 in copper sulphate aqueous solution are calculated and summarised in Appendix 4.1.A,B and C and discussed in detail in chapter five of this work.

4.2 Experimental Results of Copper-Hydroxyoxime Stripping Equilibria

The stripping equilibrium experiments were carried out using a concentrated acidic solution (sulphuric acid) as a stripping phase. Two samples ($1000cm^3$) each with concentration of 0.5 and 2 molar H_2SO_4 were prepared first. Two sets of copper rich organic phase (extract) samples were prepared by contacting $50cm^3$ of 10v/v% LIX984 with $50cm^3$ of an aqueous solution with known concentration. A sample ($20cm^3$) of the loaded organic was mixed with $20cm^3$ of 0.5 and 2 molar H_2SO_4 in two separate batches. A sample ($10cm^3$) of the stripping phase was withdrawn and analysed using atomic absorption spectrophotometer. Copper concentration at the stripped organic phase was calculated by subtracting the resultant aqueous concentrations from those concentrations of

the feed organic phase (extract). These experiments were repeated for five times and it has been found that data reproducibility contains margin of error in the range of (±0.2). The results of two runs of each stripping equilibrium experiment are summarised in table 4.4.A and B as follows:

Table 4.4. A: The distribution of copper between the stripped organic phase LIX984 (10v/v%) and 0.5 molar H_2SO_4 a stripping aqueous phase.

Copper concentration at the :						
Aqueous feed **g/l**	Feed pH	Organic extract **g/l**	Organic phase after Stripping **g/l**		Aqueous stripping phase **g/l**	
			1st run	2nd run	1st run	2nd run
0.25	2.5	0.200	0.014	0.044	0.186	0.156
1.00	2.5	0.761	0.109	0.219	0.652	0.542
2.00	2.5	1.477	0.298	0.464	1.179	1.013
3.00	2.5	1.868	0.410	0.570	1.458	1.298
5.00	2.5	2.170	0.514	0.559	1.656	1.611
7.00	2.5	2.570	0.641	0.719	1.929	1.851
12.00	2.5	3.624	1.037	1.277	2.587	2.347
15.00	2.5	4.120	1.269	1.736	2.851	2.384
17.00	2.5	4.490	1.428	1.278	3.062	3.212
18.50	2.5	4.677	1.506	1.396	3.171	3.281
20.00	2.5	4.850	1.594	1.694	3.256	3.156

Table 4.4. B: The distribution of copper between the stripped organic phase LIX984 (10v/v%) and 2 molar H_2SO_4 a stripping aqueous phase.

Copper concentration at the :						
Aqueous feed **g/l**	Feed pH	Organic extract **g/l**	Organic phase after Stripping **g/l**		Aqueous stripping phase **g/l**	
			1st run	2nd run	1st run	2nd run
0.25	2.5	0.200	0.009	0.011	0.191	0.189
1.00	2.5	0.761	0.029	0.045	0.732	0.716
2.00	2.5	1.477	0.073	0.088	1.404	1.389
3.00	2.5	1.868	0.084	0.153	1.784	1.715
5.00	2.5	2.170	0.109	0.127	2.061	2.043
7.00	2.5	2.570	0.128	0.184	2.442	2.386
12.00	2.5	3.624	0.195	0.227	3.429	3.397
15.00	2.5	4.120	0.261	0.295	3.859	3.825
17.00	2.5	4.490	0.331	0.358	4.159	4.132
18.50	2.5	4.677	0.38	0.365	4.297	4.310
20.00	2.5	4.850	0.442	0.449	4.408	4.401

4.3 Mass Transfer Results Using Rising Drop Technique

The experimental work carried out in this study by using rising single drops was set to measure the overall rate of mass transfer and the overall mass transfer coefficient in the process of copper extraction from an aqueous solution to a LIX reagent. Four different column heights were used in these mass transfer experimental measurements. The experimental work using the rising drop technique was designed to determine all major factors controlling mass transfer characteristics in and around the interface area of a single drop in a continuous-dispersed phases contact system. The experimental work includes investigation of column height, the continuous phase (the aqueous phase) concentration, the drop size and drop flow rate effect on the rate of metal mass transfer and calculations of the system overall mass transfer coefficient.

4.3.1 Copper concentration variations in rising drops at different columns

Columns with height of 55,95,149 and 187 cm and diameter of 2.5 cm were used to study rising drop of LIX984 behaviour and mass transfer properties. In this set of experiments the drops flow rate produced at the tip of 21-gauge hypodermic needle was kept at (80 drops/min) by controlling the nitrogen gas pressure at the organic phase reservoir. A minimum of five experiments was repeated in each column under the same conditions in each experimental run. The initial concentrations of the aqueous (continuous) and the organic (dispersed) phases were kept constant for all experiments. The continuous phase concentration was 3g/l and pH of 2 while the dispersed phase concentration was 20v/v% LIX984. The concentration of extracted copper at the organic phase was found by stripping a collected volume ($10cm^3$) of the rising organic drops with 2M H_2SO_4, then analysing the stripped solution in an atomic absorption spectrophotometer. The results of each column experimental run are given in table 4.5.

Table 4. 5: The results of rising drop experiments in four different columns.

C_L cm	d_f cm	d_p cm	A_d cm^2	N_{AB} Drops	C_{aq}^{in} g/cm^3 $\times 10^3$	C_{org}^{out} g/cm^3 $\times 10^3$	t_r s
55	80	0.33	0.342	53	3	0.32	5.0
	81	0.33	0.356	50	3	0.319	5.1
	77	0.33	0.356	51	3	0.317	5.3
	83	0.33	0.342	53	3	0.325	4.9
95	82	0.33	0.356	51	3	0.561	8.8
	76	0.33	0.356	51	3	0.546	8.65
	81	0.33	0.342	51	3	0.559	8.70
	79	0.33	0.356	50	3	0.553	8.68
	80	0.33	0.356	50	3	0.547	8.69
149	75	0.33	0.356	51	3	0.843	13.35
	83	0.33	0.342	53	3	0.872	13.52
	81	0.33	0.356	51	3	0.852	13.45
	80	0.33	0.347	51	3	0.869	13.50
	81	0.33	0.347	50	3	0.822	13.46
187	80	0.33	0.356	50	3	1.056	16.86
	80	0.33	0.356	50	3	1.05	16.87
	83	0.33	0.342	53	3	1.042	16.71
	77	0.33	0.356	50	3	1.063	16.91
	80	0.33	0.356	51	3	1.055	16.85

C_L = is the column height in cm.

d_f = is the drop flow rate (drops per minutes).

d_p = drop diameter (cm)

A_d = drop surface area (cm^2).

N_{AB} = the number of drops sufficient to fill $1cm^3$ volume of the capillary tube, (section AB in figure 3.1).

C^{in}_{aq} = initial copper concentration at the aqueous phase (g/cm^3).

C_{org}^{out} = copper concentration at the droplet organic phase at the top of the column (g/cm^3).

t_r = is rising drop travelling time between the tip of the needle and the collection capillary tube.

4.3.2 Calculation procedure for the rate of mass transfer of copper in the single drop technique

The rate of mass transfer of copper in the single drop experiments was determined by assuming that all the drops are uniformly spherical. Then the interfacial area of each single drop can be calculated from the known volume of the capillary tube and the number of the drops required to fill such volume using the following equations:

$V_c = V_d \times N_{AB}$

$$V_c = \frac{4}{3} r_d^3 \pi N_{AB}$$

$$r_d = \left(\frac{3}{4\pi N_{AB}} \right)^{1/3} \qquad 4.1$$

The surface area of a single spherical drop is given by:

$$A_d = 4\pi r_d^2 \qquad 4.2$$

Substitution of equation 1 in 2 gives:

$$A_d = 4\pi \left(\frac{3}{4\pi N_{AB}} \right)^{2/3} \qquad 4.3$$

Where $V_c = 1\ cm^3$ is the volume of the capillary tube, (section AB in figure. 3.1).

V_d = is the volume of single drop (cm^3).

N_{AB} = the number of drops required to fill section AB of the capillary tube.

r_d = the drop radius (cm).

A_d = the drop surface area, (the interfacial area, cm^2).

The concentration of copper extracted by the droplet organic phase was determined by collecting a volume of $10cm^3$ of the loaded organic drops from the capillary tube. This

volume was then transferred into $50cm^3$ flask and stripped with 20 to $30cm^3$ (2M H_2SO_4). The stripped solution was analysed by atomic spectrophotometer and copper concentration was determined from the calibration curve, (Appendix 1). The overall rate of mass transfer per unit area per unit time was calculated as follows:

$$\text{Rate} = \frac{\text{Mass of copper extracted in single drop}}{\text{drop rising time} \times \text{drop surface area}}$$

$$(N_a) = \frac{(C_{org}^{out} \times V_{org}) / N_{AB}}{t_r \times A_d} \qquad 4.4$$

Where:

C_{org}^{out} = copper concentration at the droplet organic phase (LIX984) at the top of the column, (g/cm^3).

V_{org}= volume of the loaded organic phase in the capillary tube section, (cm^3).

N_a = the rate of mass transfer of copper between the two phases, (g/cm^2.sec.).

The main results of copper rate of mass transfer between the continuous phase and the dispersed phase, which are obtained from 20 experimental runs summarised in table 4.6 below:

Table 4. 6: The calculated overall rate of mass transfer results in single drop technique

C_L cm	d_f cm	d_p cm	A_d cm^2	N_{AB} Drops	C_{aq}^{in} g/cm^3 $\times10^3$	C_{org}^{out} g/cm^3 $\times10^3$	t_r s	M_{Cu} g $\times10^5$	N_a g/cm^2s $\times10^6$
55	80	0.33	0.342	53	3	0.32	5	1.77	3.531
	81	0.33	0.356	50	3	0.319	5.1	1.80	3.536
	77	0.33	0.356	51	3	0.317	5.3	1.75	3.294
	83	0.33	0.342	53	3	0.325	4.9	1.79	3.659
95	82	0.33	0.356	51	3	0.561	8.8	3.11	3.536
	76	0.33	0.356	51	3	0.546	8.65	3.01	3.477
	81	0.33	0.342	51	3	0.559	8.7	3.21	3.686
	79	0.33	0.356	50	3	0.553	8.68	3.11	3.579
	80	0.33	0.356	50	3	0.547	8.69	3.08	3.540
149	75	0.33	0.356	51	3	0.843	13.35	4.64	3.478
	83	0.33	0.342	53	3	0.872	13.52	4.81	3.558
	81	0.33	0.356	51	3	0.852	13.45	4.69	3.489
	80	0.33	0.347	51	3	0.869	13.5	4.91	3.637
	81	0.33	0.347	50	3	0.822	13.46	4.74	3.520
187	80	0.33	0.356	50	3	1.056	16.86	5.93	3.519
	80	0.33	0.356	50	3	1.053	16.87	5.90	3.497
	83	0.33	0.342	53	3	1.042	16.71	5.74	3.440
	77	0.33	0.356	50	3	1.063	16.91	5.97	3.532
	80	0.33	0.356	51	3	1.055	16.85	5.81	3.449

M_{Cu} = total mass of copper extracted in single drop of the organic phase (g).

N_a = the overall rate of mass transfer per unit area per unit time (g/cm^2sec).

Based on the above results the following calculations were carried out:

4.3.3 The relation between the rate of mass transfer of copper and its concentration at the continuous phase

In this set of experiments one column (95cm) height and 2.5cm diameter was used. A continuous (aqueous) phase copper concentration ranging between 2 to 7 g/l was used in 10 experiments. The organic (dispersed) phase concentration used in these experiments was 20v/v% LIX984. The hypodermic needle used in this experiment was 21-gauge size and the drop flow rate was kept constant at 80±1 drops/minutes. The following results were obtained:

Table 4. 7: The continuous phase concentration and its relation to the rate of mass transfer in rising drops.

C_{aq}^{in} g/cm^3 x10^3	d_f drop/min	d_p cm	A_d cm^2	N_{AB} Drops	C_{org}^{out} g/cm^3 x10^3	tr s	Na g/cm^{2}s x 10^6
2	80	0.33	0.351	51	0.386	8.70	2.48
	81	0.33	0.356	50	0.459	8.69	2.97
	77	0.33	0.356	50	0.469	8.69	3.03
3	82	0.33	0.356	51	0.561	8.80	3.51
	76	0.33	0.356	51	0.546	8.65	3.48
	81	0.33	0.342	51	0.559	8.70	3.68
5	80	0.33	0.356	50	0.599	8.69	3.87
	75	0.33	0.356	51	0.616	8.70	3.90
	83	0.33	0.342	53	0.601	8.65	3.83
6	80	0.33	0.347	51	0.624	8.68	4.06
	81	0.33	0.347	50	0.635	8.70	4.21
	80	0.33	0.356	50	0.657	8.71	4.24
7	83	0.33	0.342	53	0.695	8.72	4.40
	77	0.33	0.356	50	0.711	8.68	4.60
	80	0.33	0.356	51	0.698	8.70	4.42

4.3.4 The relation between the dispersed phase drops size and the rate of mass transfer in copper extraction

Three different sizes of hypodermic needles (17, 21 and 25 gauge size) were used to investigate the drop size relation to the rate of copper extraction in rising drops technique. These experiments were carried out at the same column height (95cm). The continuous and dispersed phases concentrations and the drop flow rate were kept constant through out this experiment. The results of this experiment are summarised in table 4.8 below:

Table 4. 8: The relation between rising drop size and rate of mass transfer of copper.

Needle size Gauge	C_L cm	d_f drop/min	d_p cm	A_d cm^2	N_{AB} drop	C_{aq}^{in} g/cm^3 $x10^3$	C_{org}^{out} g/cm^3 $x10^3$	t_r s	N_a $g/cm^2.s$ $x10^6$
17	95	80	0.362	0.412	40	3	0.589	9.82	3.64
	95	78	0.348	0.38	45	3	0.575	9.54	3.52
	95	81	0.372	0.437	37	3	0.593	10	3.67
21	95	82	0.330	0.342	51	3	0.561	8.8	3.65
	95	76	0.331	0.356	50	3	0.546	8.65	3.55
	95	81	0.331	0.356	50	3	0.559	8.72	3.60
25	95	79	0.229	0.342	157	3	0.538	9.12	1.10
	95	80	0.233	0.356	150	3	0.552	9.7	1.07
	95	80	0.235	0.356	147	3	0.560	9.2	1.166

4.3.5 Calculation of the overall mass transfer coefficient

The overall mass transfer coefficient (K_{ov}) is an important factor in the assessment of copper transfer from the aqueous phase to the organic phase. Therefore the four columns were used to conduct the experimental work of evaluating the overall mass transfer coefficient of rising drops at different height. All the experiments were carried out with a constant copper concentration at the continuous (aqueous) phase (3g/l) and 20v/v% of

LIX984 at the dispersed phase. The following equations were used to determine the value of K_{ov}:

$$N_a = K_{ov}\,\Delta C_{LM}, \qquad K_{ov} = \frac{N_a}{\Delta C_{LM}} \qquad 4.5$$

where N_a = is the overall rate of mass transfer per unit area per unit time (g/cm^2sec)

K_{ov} = is the overall mass transfer coefficient (cm/sec).

ΔC_{LM} = is the logarithmic-mean value of copper concentration profile during drop rising in the column and is calculated by:

$$\Delta C_{LM} = \frac{\Delta C_1 - \Delta C_2}{\ln \frac{\Delta C_1}{\Delta C_2}} \qquad 4.6$$

where : $\Delta C_1 = (C_{aq}^{in} - C_{org}^{in})$

$\Delta C_2 = (C_{aq}^{out} - C_{org}^{out}/m)$

ΔC_1 = copper concentration profile at the bottom of the column.

ΔC_2 = copper concentration profile at the top of the column.

C_{aq}^{in} = copper concentration in the aqueous phase at the bottom of the column.

C_{org}^{in} = copper concentration in the organic phase at the head of the delivery unit.

C_{aq}^{out} = copper concentration in the aqueous phase at time (t) in this case at the top of the column.

C_{org}^{out} = copper concentration in the organic phase at time (t) in this case at the top of the column.

C^*_{aq} =is copper concentration at the aqueous phase which in equilibrium corresponds to the C_{org}^{out} at the interface.

C_{org}^{in} = copper concentration in the extractant at the tip of the delivery unit, as the extractant is fresh, C_{org} =0.

$C_{aq}^{out} = C_{aq}^{in}$ = 3 g/l (negligible changes in the continuous bulk phase concentration).

equation 4.6 can be written as $$\Delta C_{LM} = \frac{C_{aq}^{*}}{\ln \frac{C_{aq}^{in}}{C_{aq}^{in} - C_{aq}^{*}}} \qquad 4.7$$

with this $$K_{ov} = N_a / \frac{C_{aq}^{*}}{\ln \frac{C_{aq}^{in}}{C_{aq}^{in} - C_{aq}^{*}}} \qquad 4.8$$

The values of the overall mass transfer coefficient (K_{ov}) are calculated for all the experimental work by using equation 4.8. Sample of the results obtained in four different height columns are summarised in Table 4.9.

Table 4. 9: The overall mass transfer coefficient of copper-LIX984 system in rising drops technique.

C_L cm	d_f drop	C_{aq}^{in} g/cm^3 $\times 10^3$	C^{*}_{aq} g/cm^3 $\times 10^4$	C^{out}_{org} g/cm^3 $\times 10^3$	ΔC_{LM} g/cm^3 $\times 10^3$	t_r s	N_a g/cm^2.s $\times 10^6$	K_{ov} cm/s $\times 10^3$
55	80	3	2.047	0.320	2.977	5	3.530	1.185
	80	3	2.046	0.325	2.896	4.9	3.659	1.263
95	80	3	2.026	0.561	2.897	8.8	3.539	1.221
	80	3	2.028	0.546	2.897	8.65	3.540	1.221
149	80	3	2.027	0.843	2.897	13.35	3.544	1.223
	80	3	2.034	0.872	2.897	13.52	3.520	1.215
187	80	3	2.028	1.056	2.897	16.86	3.542	1.226
	80	3	2.027	1.053	2.897	16.87	3.518	1.214

4.4 Results Of The Dispersion-Free Based Extraction Process

In this section the results of copper extraction and recovery (stripping) in a microporous hollow fibre (MPHF) membrane will be presented. These include a detailed study of all variables that could influence the rate of mass transfer of the metal (copper) from the aqueous phase into the chelating organic phase (LIX984) and the system's overall mass transfer coefficient characteristics. The experimental work was carried out under a wide range of operating conditions using two types of extraction modes in the same MPHF unit (i.e. continuous extraction and batch extraction). The results of these processes can be summarised as follows:

4.4.1 Results of the continuous counter current extraction process in MPHF module

In this process both phases were continuously pumped through the MPHF module in a counter current type of flow from the feed tanks. The copper concentration in the aqueous feed tank was set during the preparation while the organic feed tank (LIX984) was copper free. In this mode of extraction the effect of range of counter current flow pattern were studied. The experimental conditions were outlined in chapter three and their corresponding results are listed below:

4.4.1.1 Dispersion free extraction at high flow rates of both phases

The aqueous phase was pumped through the MPHF membrane tube side while the organic phase was pumped through the shell side in a co-current or counter current mode of flow. This experiment was designed to study ways of minimising the boundary layer resistance to mass transfer within the MPHF module. The organic feed (LIX984) concentration was kept constant at 10v/v% while the aqueous phase was varied on the range of 0.25 to 4 g/l. The results of these experiments are summarised in table 4.10.

Table 4. 10: Results of copper extraction at high flow rates of both phases in a MPHF (the average results of five experiments).

F_{org} cm^3/min	F_{aq} cm^3/min	C^{in}_{aq} g/cm^3 $x10^3$	C^{out}_{aq} g/cm^3 $x10^3$	C^{out}_{org} g/cm^3 $x10^3$
600	600	0.250	0.195	0.117
600	600	0.250	0.135	0.115
600	600	0.500	0.337	0.163
600	600	0.500	0.341	0.159
600	600	0.750	0.586	0.164
600	600	0.750	0.589	0.161
600	600	1.000	0.825	0.175
600	600	1.000	0.831	0.169
600	600	1.000	0.809	0.191
600	600	2.000	1.621	0.379
600	600	2.000	1.604	0.396
600	600	2.000	1.635	0.365
600	600	3.000	2.495	0.505
600	600	3.000	2.411	0.589
600	600	3.000	2.436	0.564
600	600	4.000	3.287	0.713
600	600	4.000	3.325	0.675

Where:

F_{org} = is the organic solvent volumetric flow rate through the MPHF module.

F_{aq} = is the aqueous phase volumetric flow rate through the MPHF module.

C^{in}_{aq}= is the initial copper concentration at the aqueous feed stream.

C^{out}_{aq}= is copper concentration at the aqueous outlet stream (the raffinate).

C^{out}_{org}= is copper concentration at the organic outlet stream (the extract).

4.4.1.2 Dispersion free extraction at low flow rates of both phases

In these experiments, the influence of low flow rates in both sides of the MPHF membrane on copper extraction by LIX984 was studied. The aqueous phase was pumped at 100cm^3/min through the fibre lumen with initial concentration ranging between 0.25 to 4 g/l. While the organic phase was pumped through the shell at constant flow of 100cm^3/min

and initial concentration of 10v/v% LIX984 in Escaid110. The results of these experiments are summarised in table 4.11.

Table 4. 11: Results of copper extraction at low flow rates of both phases in a MPHF (the average results of five experiments).

F_{org} cm^3/min	F_{aq} cm^3/min	C^{in}_{aq} g/cm^3 $x10^3$	C^{out}_{aq} g/cm^3 $x10^3$	C^{out}_{org} g/cm^3 $x10^3$
100	100	0.250	0.208	0.042
100	100	0.250	0.210	0.040
100	100	0.500	0.413	0.087
100	100	0.500	0.420	0.080
100	100	0.750	0.638	0.112
100	100	0.750	0.636	0.114
100	100	1.000	0.871	0.129
100	100	1.000	0.848	0.152
100	100	2.000	1.648	0.352
100	100	2.000	1.624	0.376
100	100	3.000	2.520	0.480
100	100	3.000	2.498	0.502
100	100	4.000	3.424	0.576
100	100	4.000	3.440	0.560

4.4.1.3 Dispersion free extraction at variable flow rates for both of the phases

This set of experiments was amid to study ways of eliminating or minimising the boundary layer resistance on the tube and shell side during metal extraction in MPHF module. One of the phases (the aqueous solution or the organic solvent) was pumped at fixed flow rate (high or low) and constant initial concentration, while the other phase was pumped at increasing variable flow rate but with constant initial concentration. This process was carried out in the following flow pattern:

4.4.1.3.1 Copper extraction under high aqueous flow rate and variable organic flow rate in a MPHF membrane

The aqueous solution was pumped in the tube side at a constant flow rate (600 cm^3/min) throughout each experiment while the organic phase (LIX984) was pumped through the shell side with gradually increasing flow rate between 100 to 600 cm^3/min in a counter current mode. The results of this study are listed in table 4.12

Table 4. 12: The experimental results of copper extraction in a MPHF module under high aqueous flow rate and variable organic flow rate (average results of five experiments).

Copper concentrations at the aqueous feed stream		**0.250 $g/cm^3 \times 10^{-3}$**		**0.750 $g/cm^3 \times 10^{-3}$**		**1.000 $g/cm^3 \times 10^{-3}$**		**2.000 $g/cm^3 \times 10^{-3}$**		**3.000 $g/cm^3 \times 10^{-3}$**	
Outlet streams specifications		C^{out}_{aq}	C^{out}_{org}	C^{out}_{aq}	C^{out}_{org}	C^{out}_{aq}	C^{out}_{org}	C^{out}_{aq}	C^{out}_{org}	C^{out}_{aq}	C^{out}_{org}
F_{org} $\frac{cm^3}{min}$	F_{aq} $\frac{cm^3}{min}$	$g/cm^3 \times 10^3$	$g/cm^3 \times 10^3$	$g/cm^3 \times 10^3$	$g/cm^3 \times 10^3$	$g/cm^3 \times 10^3$	$g/cm^3 \times 10^3$	$g/cm^3 \times 10^3$	$g/cm^3 \times 10^3$	$g/cm^3 \times 10^3$	$g/cm^3 \times 10^3$
100	600	0.234	0.096	0.708	0.252	0.952	0.288	1.921	0.474	2.840	0.960
200	600	0.227	0.069	0.691	0.177	0.924	0.228	1.844	0.468	2.730	0.810
300	600	0.224	0.052	0.674	0.153	0.898	0.204	1.780	0.440	2.680	0.640
400	600	0.221	0.044	0.662	0.132	0.863	0.201	1.760	0.360	2.630	0.555
500	600	0.204	0.055	0.653	0.117	0.834	0.199	1.720	0.336	2.570	0.516
600	600	0.197	0.053	0.637	0.113	0.807	0.193	1.680	0.320	2.538	0.462

4.4.1.3.2 Copper extraction under low aqueous flow rate and variable organic flow rate in a MPHF membrane

In this set of experiments the aqueous solution flow rate was kept constant and low at 100cm^3/min while the organic solvent flow rate increased gradually (from 100cm^3 in 5 minutes intervals until it reached 600cm^3/min). In this scheme of contact the aqueous phase was pumped through the hollow fibres side while the organic (10v/v% LIX984) was pumped in the shell side. The results of this study are outlined in table 4.13.

Table 4. 13: The results of copper extraction in a MPHF membrane under variable organic phase flow rate and low aqueous flow rate (average results of five experiments).

Copper concentrations at the aqueous feed stream		**0.250 g/cm^3 x 10^{-3}**		**0.50 g/cm^3 x 10^{-3}**		**1.000 g/cm^3 x 10^{-3}**		**2.000 g/cm^3 x 10^{-3}**		**3.000 g/cm^3 x 10^{-3}**	
Outlet streams specifications		C^{out}_{aq}	C^{out}_{org}	C^{out}_{aq}	C^{out}_{org}	C^{out}_{aq}	C^{out}_{org}	C^{out}_{aq}	C^{out}_{org}	C^{out}_{aq}	C^{out}_{org}
F_{org} $\frac{cm^3}{min}$	F_{aq} $\frac{cm^3}{min}$	g/cm^3 x 10^3	g/cm^3 x 10^3	g/cm^3 X 10^3	g/cm^3 x 10^3	g/cm^3 x 10^3	g/cm^3 x 10^3	g/cm^3 x 10^3	g/cm^3 x 10^3	g/cm^3 x 10^3	g/cm^3 x 10^3
100	100	0.210	0.040	0.413	0.087	0.891	0.109	1.816	0.184	2.658	0.342
200	100	0.203	0.024	0.385	0.058	0.798	0.106	1.680	0.160	2.470	0.265
300	100	0.197	0.018	0.364	0.045	0.725	0.092	1.532	0.156	2.300	0.233
400	100	0.192	0.015	0.350	0.038	0.685	0.079	1.457	0.136	2.138	0.216
500	100	0.190	0.012	0.338	0.032	0.634	0.073	1.338	0.132	1.975	0.205
600	100	0.189	0.010	0.329	0.028	0.612	0.065	1.230	0.124	1.807	0.199

4.4.1.3.3 Copper extraction under high organic flow rate and variable aqueous flow rate in a MPHF membrane

The aim of these experiments was to determine the flow pattern effect on the extraction process under high organic flow rate and variable aqueous flow rate. The process was carried out in a counter current mode where the aqueous in the tube side and the organic in the shell side. The organic solvent concentration was kept constant in all runs (10v/v% LIX984) while the aqueous phase copper concentration was ranging between 0.25 g/l to 3 g/l. The organic phase was pumped at a constant flow of 600 cm^3/min while the aqueous solution flow rate was varied between 100 cm^3/min to 600 cm^3/min. The results of these experiments are listed in table 4.14.

Table 4. 14: The results of copper extraction in a MPHF membrane under variable aqueous phase flow rate and high organic flow rate (average results of five experiments).

Copper concentrations at the aqueous feed stream		**0.250 $g/cm^3 \times 10^{-3}$**		**0.50 $g/cm^3 \times 10^{-3}$**		**1.000 $g/cm^3 \times 10^{-3}$**		**2.000 $g/cm^3 \times 10^{-3}$**		**3.000 $g/cm^3 \times 10^{-3}$**	
Outlet streams specifications		C^{out}_{aq}	C^{out}_{org}	C^{out}_{aq}	C^{out}_{org}	C^{out}_{aq}	C^{out}_{org}	C^{out}_{aq}	C^{out}_{org}	C^{out}_{aq}	C^{out}_{org}
F_{aq} $\frac{cm^3}{min}$	F_{org} $\frac{cm^3}{min}$	$g/cm^3 \times 10^3$	$g/cm^3 \times 10^3$	$g/cm^3 \times 10^3$	$g/cm^3 \times 10^3$	$g/cm^3 \times 10^3$	$g/cm^3 \times 10^3$	$g/cm^3 \times 10^3$	$g/cm^3 \times 10^3$	$g/cm^3 \times 10^3$	$g/cm^3 \times 10^3$
100	600	0.153	0.016	0.298	0.034	0.511	0.082	1.153	0.141	1.740	0.210
200	600	0.182	0.023	0.355	0.048	0.709	0.091	1.500	0.166	2.181	0.273
300	600	0.203	0.024	0.401	0.050	0.793	0.104	1.630	0.185	2.320	0.340
400	600	0.212	0.025	0.419	0.054	0.839	0.107	1.700	0.200	2.408	0.395
500	600	0.218	0.027	0.435	0.055	0.869	0.110	1.750	0.208	2.489	0.426
600	600	0.223	0.028	0.454	0.056	0.887	0.113	1.788	0.212	2.547	0.453

4.4.1.3.4 Copper extraction under low organic flow rate and variable aqueous flow rate in a MPHF membrane

In this set of experiments, the aqueous solution was pumped through the tube side of the MPHF module with flow rate increasing by 100 cm^3 in 5 minutes intervals from 100 cm^3/min to 600 cm^3/min. In contrast the organic solvent (10v/v% LIX984) was pumped constantly at 100cm^3 flow rate at the shell side. The effect of varying the aqueous side flow rate and concentration on the outlet copper concentrations in both sides (the aqueous side and the organic) was studied in this work. The results are tabled in below:

Table 4. 15: The results of copper extraction in a MPHF membrane under variable aqueous phase flow rate and low organic flow rate (average results of five experiments).

Copper concentrations at the aqueous feed stream		**0.250 $g/cm^3 \times 10^{-3}$**		**0.50 $g/cm^3 \times 10^{-3}$**		**1.000 $g/cm^3 \times 10^{-3}$**		**2.000 $g/cm^3 \times 10^{-3}$**		**3.000 $g/cm^3 \times 10^{-3}$**	
Outlet streams specifications		C^{out}_{aq}	C^{out}_{org}	C^{out}_{aq}	C^{out}_{org}	C^{out}_{aq}	C^{out}_{org}	C^{out}_{aq}	C^{out}_{org}	C^{out}_{aq}	C^{out}_{org}
F_{org} cm^3/min	F_{aq} cm^3/min	$g/cm^3 \times 10^3$	$g/cm^3 \times 10^3$	$g/cm^3 \times 10^3$	$g/cm^3 \times 10^3$	$g/cm^3 \times 10^3$	$g/cm^3 \times 10^3$	$g/cm^3 \times 10^3$	$g/cm^3 \times 10^3$	$g/cm^3 \times 10^3$	$g/cm^3 \times 10^3$
100	100	0.208	0.042	0.423	0.077	0.891	0.109	1.816	0.184	2.658	0.342
100	200	0.222	0.056	0.448	0.104	0.896	0.208	1.821	0.358	2.673	0.654
100	300	0.227	0.069	0.454	0.138	0.911	0.267	1.843	0.471	2.681	0.957
100	400	0.231	0.076	0.459	0.164	0.920	0.320	1.858	0.570	2.710	1.160
100	500	0.233	0.085	0.464	0.180	0.934	0.330	1.865	0.672	2.750	1.250
100	600	0.234	0.096	0.469	0.186	0.940	0.360	1.876	0.747	2.778	1.332

4.4.2 Results of the continuous co-current extraction process in MPHF module

In this section co-current flow was used to study the behaviour and the effect of both phases parallel flow on mass transfer properties in MPHF membrane. The two phases were pumped under range of flow arrangements where the aqueous was pumped in the fibre lumen side and the organic in the shell side of the MPHF membrane. These flow arrangements and their results can be addressed as follows:

4.4.2.1 Co-current dispersion free extraction at high flow rates of both phases

The aqueous phase and the organic phase were pumped co-currently through the MPHF membrane at flow rate of 600/600 cm^3/min. These experiments were designed to study the characteristics of co-current high flow of both phases in MPHF membrane and its relation to all factors controlling mass transfer within the membrane module. The organic feed (LIX984) concentration was kept constant at 10v/v% while the aqueous phase was changed on the range between 0.25 to 4 g/l in set of separate experiments. The results of these experiments are summarised in table 4.16.

Table 4. 16: Results of copper extraction under co-current high flow rates of both phases in a MPHF membrane (average results of 3 experimental runs).

F_{org} cm^3/min	F_{aq} cm^3/min	C^{in}_{aq} g/cm^3 $x10^3$	C^{out}_{aq} g/cm^3 $x10^3$	C^{out}_{org} g/cm^3 $x10^3$
600	600	0.250	0.170	0.080
600	600	0.500	0.388	0.112
600	600	0.500	0.367	0.133
600	600	0.750	0.631	0.119
600	600	1.000	0.832	0.167
600	600	1.000	0.834	0.166
600	600	2.000	1.643	0.367
600	600	2.000	1.645	0.355
600	600	2.000	1.642	0.358
600	600	3.000	2.498	0.502
600	600	3.000	2.502	0.498
600	600	3.000	2.488	0.512
600	600	4.000	3.369	0.631
600	600	4.000	3.350	0.650

4.4.2.2 Co-current dispersion free extraction at low flow rates of both phases

In this section, the influence of co-current flow arrangement combined with low flow rates of both phases on copper extraction by LIX984 was studied. The aqueous phase was pumped through the fibre lumen at constant flow of 100cm^3/min while its initial concentration was changed in each experimental run (0.25,0.5,1,2,3 and 4 g/l). The organic phase was pumped through the shell at constant flow of 100cm^3/min and initial concentration of 10v/v% LIX984 in Escaid110. The results of these experiments are summarised in table 4.17.

Table 4. 17: Results of co-current flow copper extraction under low flow rates of both phases in a MPHF (average results of 3 experimental runs).

F_{org} cm^3/min	F_{aq} cm^3/min	C^{in}_{aq} g/cm^3 x10^3	C^{out}_{aq} g/cm^3 x10^3	C^{out}_{org} g/cm^3 x10^3
100	100	0.250	0.212	0.038
100	100	0.250	0.215	0.035
100	100	0.500	0.418	0.083
100	100	0.500	0.430	0.070
100	100	0.750	0.664	0.086
100	100	0.750	0.646	0.104
100	100	1.000	0.884	0.116
100	100	1.000	0.876	0.124
100	100	2.000	1.683	0.317
100	100	2.000	1.695	0.305
100	100	3.000	2.631	0.369
100	100	3.000	2.642	0.358
100	100	4.000	3.629	0.371
100	100	4.000	3.571	0.429

4.4.2.3 Co-current dispersion free extraction at variable flow rates of both phases

The aim of this flow arrangement was to study the effect of co-current variable flow of one of the phases on the outcome of the metal extraction process in MPHF module. One of the phases (the aqueous solution or the organic solvent) was pumped at a fixed flow rate (high or low) and a constant initial concentration. While the other phase flow rate was increased gradually in intervals (i.e. increase of $100cm^3$ each 5 minutes). A range of initial concentrations for the aqueous phase was studied under the same conditions. This process can be outlined as follows:

4.4.2.3.1 Co-current dispersion free extraction under high aqueous flow rate and variable organic flow rate in a MPHF membrane

Five experiments were carried out at the following conditions: the aqueous solution flow rate was kept constantly high at $600cm^3$/min throughout all experiments and in each run a different aqueous concentration was used (0.25,0.5,1,2, or 3g/l). The organic phase (10v/v% LIX984) flow rate was increased $100cm^3$ each five minutes from 100 to $600cm^3$/min. a summary of the results is outlined in table 4.18.

Table 4. 18: The results of copper extraction in a MPHF module under high aqueous flow rate and variable organic flow rate (average results of 5 experimental runs).

Copper concentrations at the aqueous feed stream		**0.250 $g/cm^3 \times 10^{-3}$**		**0.50 $g/cm^3 \times 10^{-3}$**		**1.000 $g/cm^3 \times 10^{-3}$**		**2.000 $g/cm^3 \times 10^{-3}$**		**3.000 $g/cm^3 \times 10^{-3}$**	
Outlet streams specifications		C^{out}_{aq}	C^{out}_{org}	C^{out}_{aq}	C^{out}_{org}	C^{out}_{aq}	C^{out}_{org}	C^{out}_{aq}	C^{out}_{org}	C^{out}_{aq}	C^{out}_{org}
F_{org} $\frac{cm^3}{min}$	F_{aq} $\frac{cm^3}{min}$	$g/cm^3 \times 10^3$	$g/cm^3 \times 10^3$	$g/cm^3 \times 10^3$	$g/cm^3 \times 10^3$	$g/cm^3 \times 10^3$	$g/cm^3 \times 10^3$	$g/cm^3 \times 10^3$	$g/cm^3 \times 10^3$	$g/cm^3 \times 10^3$	$g/cm^3 \times 10^3$
100	600	0.238	0.072	0.475	0.150	0.953	0.282	1.928	0.432	2.852	0.888
200	600	0.232	0.054	0.465	0.105	0.925	0.225	1.857	0.429	2.763	0.711
300	600	0.231	0.038	0.460	0.080	0.913	0.174	1.814	0.372	2.720	0.560
400	600	0.225	0.037	0.455	0.068	0.903	0.146	1.803	0.296	2.699	0.451
500	600	0.227	0.027	0.452	0.058	0.898	0.122	1.798	0.242	2.692	0.370
600	600	0.228	0.022	0.450	0.050	0.894	0.106	1.794	0.206	2.687	0.313

4.4.2.3.2 Co-current dispersion free extraction under low aqueous flow rate and variable organic flow rate in a MPHF membrane

The extraction process was carried out by pumping the aqueous solution at a constant low flow rate of $100cm^3/min$ throughout all experiments. While the organic solvent was pumped co-currently at an increasing flow rate (i.e. the increase in the shell side flow was made in the order of $100cm^3$ after five minutes of steady contact at each of the indicated flow rates). The results of this study are outlined in table 4.19.

Table 4. 19: The results of co-current copper extraction in a MPHF membrane under variable organic phase flow rate and low aqueous flow rate (average results of 3 experimental runs).

Copper concentrations at the aqueous feed stream		**0.250 $g/cm^3 \times 10^{-3}$**		**0.50 $g/cm^3 \times 10^{-3}$**		**1.000 $g/cm^3 \times 10^{-3}$**		**2.000 $g/cm^3 \times 10^{-3}$**		**3.000 $g/cm^3 \times 10^{-3}$**	
Outlet streams specifications		C^{out}_{aq}	C^{out}_{org}	C^{out}_{aq}	C^{out}_{org}	C^{out}_{aq}	C^{out}_{org}	C^{out}_{aq}	C^{out}_{org}	C^{out}_{aq}	C^{out}_{org}
F_{org} $\frac{cm^3}{min}$	F_{aq} $\frac{cm^3}{min}$	$g/cm^3 \times 10^3$	$g/cm^3 \times 10^3$	$g/cm^3 \times 10^3$	$g/cm^3 \times 10^3$	$g/cm^3 \times 10^3$	$g/cm^3 \times 10^3$	$g/cm^3 \times 10^3$	$g/cm^3 \times 10^3$	$g/cm^3 \times 10^3$	$g/cm^3 \times 10^3$
100	100	0.220	0.030	0.423	0.077	0.912	0.088	1.838	0.162	2.711	0.289
200	100	0.212	0.019	0.417	0.042	0.874	0.063	1.713	0.144	2.616	0.192
300	100	0.206	0.015	0.395	0.035	0.821	0.060	1.602	0.133	2.442	0.186
400	100	0.198	0.013	0.380	0.030	0.793	0.052	1.524	0.119	2.228	0.180
500	100	0.195	0.011	0.353	0.029	0.746	0.050	1.437	0.113	2.130	0.174
600	100	0.190	0.010	0.335	0.027	0.698	0.049	1.398	0.100	1.979	0.170

4.4.2.3.3 Co-current dispersion free extraction under high organic flow rate and variable aqueous flow rate in a MPHF membrane

In this set of experiments the organic phase was pumped continuously at 600cm^3/min flow rate. While the aqueous flow rate in the tube side was increased gradually from 100 to 600cm^3/min. In these experiments the organic solvent concentration was kept constant in all runs (10v/v% LIX984) while the aqueous phase copper concentrations used were 0.25,0.5,1,2 and 3 g/l. The results of these experiments are listed in table 4.20.

Table 4. 20: The results of co-current copper extraction in a MPHF membrane under variable aqueous phase flow rate and high organic flow rate (average results of 4 experimental runs).

Copper concentrations at the aqueous feed stream		**0.250 g/cm^3 x 10^{-3}**		**0.50 g/cm^3 x 10^{-3}**		**1.000 g/cm^3 x 10^{-3}**		**2.000 g/cm^3 x 10^{-3}**		**3.000 g/cm^3 x 10^{-3}**	
Outlet streams specifications		C^{out}_{aq}	C^{out}_{org}	C^{out}_{aq}	C^{out}_{org}	C^{out}_{aq}	C^{out}_{org}	C^{out}_{aq}	C^{out}_{org}	C^{out}_{aq}	C^{out}_{org}
F_{aq} cm^3/min	F_{org} cm^3/min	g/cm^3 x 10^3	g/cm^3 x 10^3	g/cm^3 x 10^3	g/cm^3 x 10^3	g/cm^3 x 10^3	g/cm^3 x 10^3	g/cm^3 x 10^3	g/cm^3 x 10^3	g/cm^3 x 10^3	g/cm^3 x 10^3
100	600	0.208	0.007	0.320	0.030	0.518	0.080	1.394	0.101	1.761	0.206
200	600	0.214	0.012	0.401	0.033	0.713	0.096	1.670	0.110	2.191	0.269
300	600	0.224	0.013	0.430	0.035	0.803	0.099	1.764	0.118	2.374	0.313
400	600	0.227	0.015	0.443	0.038	0.845	0.103	1.820	0.120	2.512	0.325
500	600	0.231	0.016	0.452	0.040	0.874	0.105	1.852	0.123	2.583	0.347
600	600	0.233	0.017	0.459	0.041	0.893	0.107	1.872	0.128	2.611	0.389

4.4.2.3.4 Co-current dispersion free extraction under low organic flow rate and variable aqueous flow rate in a MPHF membrane

In these experiments, the aqueous solution flow rate was increased progressively in the tube side of the MPHF module with flow rate increased 100 cm^3 in 5 minutes intervals from 100 cm^3/min to 600 cm^3/min. In the shell side the organic solvent (10v/v% LIX984) was pumped constantly and co-currently at a low flow rate of 100cm^3/min. The effect of varying the aqueous side flow rate and concentration on the outlet copper concentrations in both sides (the aqueous raffinate and the organic extract) was studied in this work. The results are tabled in below:

Table 4. 21: The results of co-current copper extraction in a MPHF membrane under variable aqueous phase flow rate and low organic flow rate (average results of 4 experimental runs).

Copper concentrations at the aqueous feed stream		**0.250 g/cm³ x 10⁻³**		**0.50 g/cm³ x 10⁻³**		**1.000 g/cm³ x 10⁻³**		**2.000 g/cm³ x 10⁻³**		**3.000 g/cm³ x 10⁻³**	
Outlet streams specifications		C^{out}_{aq}	C^{out}_{org}	C^{out}_{aq}	C^{out}_{org}	C^{out}_{aq}	C^{out}_{org}	C^{out}_{aq}	C^{out}_{org}	C^{out}_{aq}	C^{out}_{org}
F_{org} $\frac{cm^3}{min}$	F_{aq} $\frac{cm^3}{min}$	g/cm³ x 10³	g/cm³ x 10³	g/cm³ x 10³	g/cm³ x 10³	g/cm³ x 10³	g/cm³ x 10³	g/cm³ x 10³	g/cm³ x 10³	g/cm³ x 10³	g/cm³ x 10³
100	100	0.211	0.039	0.427	0.073	0.901	0.099	1.819	0.181	2.713	0.287
100	200	0.229	0.042	0.451	0.098	0.912	0.176	1.826	0.348	2.477	0.523
100	300	0.235	0.045	0.459	0.123	0.933	0.201	1.851	0.447	2.284	0.816
100	400	0.237	0.052	0.462	0.152	0.938	0.248	1.862	0.552	2.998	1.002
100	500	0.238	0.060	0.467	0.165	0.949	0.255	1.870	0.650	2.846	1.154
100	600	0.240	0.062	0.471	0.174	0.956	0.264	1.881	0.714	2.800	1.200

The results of the co-current and counter current continuous extraction process of copper in MPHF membrane will be further analysed in details in chapter five of this study.

4.4.3 Results of the batch extraction process of copper in MPHF module

In this process both phases were pumped continuously in a counter current closed loop mode operation where the aqueous solution was circulated in the tube side and the organic solvent in the shell side. A known volume of both phases with a known initial copper concentration in the case of the aqueous solution was placed in the feed tanks. Then the two sides were circulated through the membrane module as described in section (3.5.7). The flow arrangements used in this study and their results can be outlined as follows:

4.4.3.1 Batch extraction of copper in MPHF membrane under high flow of both phases

In this process the aqueous solution and the organic solvent were contacted in close loop mode under high flow rate 600cm^3/min. Equal volumes of both phases (4 litre of each) were placed in the feed tanks. The aqueous concentrations used in these experiments ranged between 0.25 to 3 g/l while the organic solvent concentration was kept constant at 10v/v%. The extraction process was continued under these conditions for about 2 hours and 30 minutes of continuous contact time (t_c) or until no significant concentration changes were observed at the outlet streams. The results of these experiments are summarised in table 4.22.

Table 4. 22: Results of batch extraction of copper in a MPHF membrane under high flow rates of both phases (average results of 3 experimental runs).

Copper concentrations at the aqueous feed stream			**0.250 $g/cm^3 \times 10^{-3}$**		**0.50 $g/cm^3 \times 10^{-3}$**		**1.000 $g/cm^3 \times 10^{-3}$**		**2.000 $g/cm^3 \times 10^{-3}$**		**3.000 $g/cm^3 \times 10^{-3}$**	
Outlet streams specifications			C^{out}_{aq}	C^{out}_{org}	C^{out}_{aq}	C^{out}_{org}	C^{out}_{aq}	C^{out}_{org}	C^{out}_{aq}	C^{out}_{org}	C^{out}_{aq}	C^{out}_{org}
t_c min	F_{org} $\frac{cm^3}{min}$	F_{aq} $\frac{cm^3}{min}$	$g/cm^3 \times 10^3$	$g/cm^3 \times 10^3$	$g/cm^3 \times 10^3$	$g/cm^3 \times 10^3$	$g/cm^3 \times 10^3$	$g/cm^3 \times 10^3$	$g/cm^3 \times 10^3$	$g/cm^3 \times 10^3$	$g/cm^3 \times 10^3$	$g/cm^3 \times 10^3$
5	600	600	0.218	0.032	0.439	0.061	0.859	0.141	1.723	0.277	2.501	0.499
15	600	600	0.192	0.058	0.408	0.092	0.801	0.199	1.589	0.411	2.350	0.650
30	600	600	0.171	0.079	0.365	0.135	0.707	0.293	1.401	0.599	2.060	0.940
60	600	600	0.129	0.121	0.274	0.226	0.523	0.477	1.020	0.980	1.570	1.430
80	600	600	0.095	0.155	0.205	0.295	0.440	0.560	0.830	1.170	1.370	1.630
100	600	600	0.083	0.167	0.165	0.335	0.350	0.650	0.681	1.319	1.256	1.744
120	600	600	0.063	0.187	0.136	0.364	0.300	0.700	0.630	1.370	1.201	1.799
140	600	600	0.058	0.192	0.115	0.385	0.290	0.710	0.590	1.410	1.199	1.801
160	600	600	0.053	0.197	0.112	0.388	0.270	0.730	0.570	1.430	1.191	1.809

4.4.3.2 Batch extraction of copper in MPHF membrane under low flow of both phases

This set of experiments was carried out under low flow rate ($100cm^3/min$) of both sides. A range of initial copper concentrations at the aqueous phase were studied against the same organic phase concentration (10v/v% LIX984 in Escaid110). The contact time (t_c) and the volumes of aqueous and organic solutions used in these experiments were similar to that used in section 4.4.3.1. The results of these experiments are highlighted in table 4.23 below:

Table 4. 23: Results of batch extraction of copper in a MPHF membrane under low flow rate of both phases (average results of 3 experimental runs).

Copper concentrations at the aqueous feed stream			**0.250 $g/cm^3 \times 10^{-3}$**		**0.50 $g/cm^3 \times 10^{-3}$**		**1.000 $g/cm^3 \times 10^{-3}$**		**2.000 $g/cm^3 \times 10^{-3}$**		**3.000 $g/cm^3 \times 10^{-3}$**	
Outlet streams specifications			C^{out}_{aq}	C^{out}_{org}	C^{out}_{aq}	C^{out}_{org}	C^{out}_{aq}	C^{out}_{org}	C^{out}_{aq}	C^{out}_{org}	C^{out}_{aq}	C^{out}_{org}
t_c min	F_{org} $\frac{cm^3}{min}$	F_{aq} $\frac{cm^3}{min}$	$g/cm^3 \times 10^3$	$g/cm^3 \times 10^3$	$g/cm^3 \times 10^3$	$g/cm^3 \times 10^3$	$g/cm^3 \times 10^3$	$g/cm^3 \times 10^3$	$g/cm^3 \times 10^3$	$g/cm^3 \times 10^3$	$g/cm^3 \times 10^3$	$g/cm^3 \times 10^3$
5	100	100	0.215	0.035	0.440	0.06	0.884	0.116	1.695	0.305	2.642	0.358
15	100	100	0.197	0.053	0.408	0.092	0.801	0.199	1.589	0.411	2.490	0.510
30	100	100	0.185	0.065	0.365	0.135	0.740	0.260	1.500	0.500	2.330	0.670
60	100	100	0.178	0.072	0.341	0.159	0.680	0.320	1.370	0.630	2.180	0.820
80	100	100	0.172	0.078	0.332	0.168	0.660	0.340	1.344	0.656	2.100	0.900
100	100	100	0.163	0.087	0.313	0.187	0.651	0.349	1.321	0.679	2.060	0.940
120	100	100	0.151	0.099	0.311	0.189	0.649	0.351	1.300	0.700	2.040	0.960
140	100	100	0.148	0.102	0.309	0.191	0.643	0.357	1.290	0.710	2.020	0.980
160	100	100	0.145	0.105	0.306	0.194	0.635	0.365	1.285	0.715	2.010	0.990

4.4.3.3 Batch extraction in MPHF membrane under low aqueous flow rate and high organic flow rate

The batch extraction of copper was studied under constant aqueous flow rate of $100cm^3/min$ and organic flow rate of $600cm^3/min$ in close loop mode. The initial concentrations of copper in the feed tank for these experiments were between 0.25 to 3 g/l while the organic solvent concentration was 10v/v%. These experiments were designed to study the effect of the low flow rate of either phase on the extraction process its mass transfer properties. The results of these experiments are listed in table 4.24.

Table 4. 24: Results of batch extraction of copper in a MPHF membrane under low aqueous flow rate and high organic flow rate (average results of 3 experimental runs).

Copper concentrations at the aqueous feed stream			**0.250 $g/cm^3 \times 10^{-3}$**		**0.50 $g/cm^3 \times 10^{-3}$**		**1.000 $g/cm^3 \times 10^{-3}$**		**2.000 $g/cm^3 \times 10^{-3}$**		**3.000 $g/cm^3 \times 10^{-3}$**	
Outlet streams specifications			C^{out}_{aq}	C^{out}_{org}	C^{out}_{aq}	C^{out}_{org}	C^{out}_{aq}	C^{out}_{org}	C^{out}_{aq}	C^{out}_{org}	C^{out}_{aq}	C^{out}_{org}
t_c min	F_{org} $\frac{cm^3}{min}$	F_{aq} $\frac{cm^3}{min}$	$g/cm^3 \times 10^3$	$g/cm^3 \times 10^3$	$g/cm^3 \times 10^3$	$g/cm^3 \times 10^3$	$g/cm^3 \times 10^3$	$g/cm^3 \times 10^3$	$g/cm^3 \times 10^3$	$g/cm^3 \times 10^3$	$g/cm^3 \times 10^3$	$g/cm^3 \times 10^3$
5	600	100	0.208	0.007	0.402	0.016	0.654	0.058	1.394	0.101	1.863	0.190
15	600	100	0.199	0.009	0.389	0.019	0.627	0.062	1.297	0.117	1.784	0.203
30	600	100	0.187	0.011	0.346	0.026	0.583	0.070	1.178	0.137	1.670	0.222
60	600	100	0.148	0.017	0.287	0.036	0.503	0.083	1.012	0.165	1.520	0.247
80	600	100	0.120	0.022	0.252	0.041	0.453	0.091	0.924	0.179	1.446	0.259
100	600	100	0.092	0.026	0.214	0.048	0.406	0.099	0.845	0.193	1.372	0.271
120	600	100	0.084	0.028	0.175	0.054	0.366	0.106	0.782	0.203	1.321	0.280
140	600	100	0.073	0.030	0.149	0.059	0.327	0.112	0.743	0.210	1.254	0.291
160	600	100	0.071	0.030	0.133	0.061	0.308	0.115	0.709	0.215	1.201	0.300

4.4.3.4 Batch extraction in MPHF membrane under high aqueous flow rate and low organic flow rate

In these experiments the effect of low organic flow rate on the batch extraction of copper in a MPHF membrane was studied. A range of initial copper concentrations (0.25 to 3 g/l) were used to eliminate any resistance could be caused by the boundary layer inside the fibre tubes. The flow rate of the aqueous solution was kept constantly high at $600cm^3/min$ throughout all these experiments while the organic solvent was kept at $100cm^3/min$. These experiments were carried out for the same length of time as that used to study the batch process under high flow of both phases. The results of this study are outlined in table 4.25.

Table 4. 25: Results of batch extraction of copper in a MPHF membrane under high aqueous flow rate and low organic flow rate (average results of 3 experimental runs).

Copper concentrations at the aqueous feed stream			**0.250 g/cm³ x 10⁻³**		**0.50 g/cm³ x 10⁻³**		**1.000 g/cm³ x 10⁻³**		**2.000 g/cm³ x 10⁻³**		**3.000 g/cm³ x 10⁻³**	
Outlet streams specifications			C^{out}_{aq}	C^{out}_{org}	C^{out}_{aq}	C^{out}_{org}	C^{out}_{aq}	C^{out}_{org}	C^{out}_{aq}	C^{out}_{org}	C^{out}_{aq}	C^{out}_{org}
t_c min	F_{aq} $\frac{cm^3}{min}$	F_{org} $\frac{cm^3}{min}$	g/cm^3 x 10^3	g/cm^3 x 10^3	g/cm^3 x 10^3	g/cm^3 x 10^3	g/cm^3 x 10^3	g/cm^3 x 10^3	g/cm^3 x 10^3	g/cm^3 x 10^3	g/cm^3 x 10^3	g/cm^3 x 10^3
5	600	100	0.241	0.054	0.483	0.102	0.968	0.192	1.950	0.300	2.845	0.930
15	600	100	0.232	0.108	0.467	0.198	0.946	0.324	1.887	0.678	2.792	1.248
30	600	100	0.228	0.132	0.454	0.276	0.930	0.420	1.860	0.840	2.769	1.386
60	600	100	0.225	0.150	0.447	0.318	0.901	0.594	1.840	0.960	2.751	1.494
80	600	100	0.223	0.162	0.445	0.330	0.897	0.618	1.839	0.966	2.732	1.608
100	600	100	0.220	0.180	0.440	0.360	0.892	0.648	1.803	1.182	2.729	1.626
120	600	100	0.218	0.192	0.439	0.366	0.887	0.678	1.801	1.194	2.72	1.680
140	600	100	0.216	0.204	0.437	0.378	0.881	0.714	1.786	1.284	2.713	1.722
160	600	100	0.215	0.210	0.434	0.396	0.879	0.726	1.765	1.410	2.701	1.794

4.5 Calculation Procedure Of The Rate Of Mass Transfer In MPHF Membrane Based Liquid-Liquid Extraction

The rate of mass transfer of copper from the aqueous phase in the tube side to the organic solvent in the shell side across the membrane wall was calculated based on the analytical copper content found at the outlet and the volumetric flow rate of both phases. From the known initial concentrations of copper on the feed side and by choosing a suitable volumetric flow rate through the MPHF module, a mass balance of copper content at both ends of the membrane could be devised as follows:

$$F_{aq} (C_{aq}^{in} - C_{aq}^{out}) = F_{org} (C_{org}^{out} - C_{org}^{in}) \qquad 4.9$$

In the case when fresh LIX984 was used its copper concentration will be (0)

then $C_{org}^{in} = 0$

Therefore; $F_{aq}(C_{aq}^{in} - C_{aq}^{out}) = F_{org}C_{org}^{out}$ 4.10

The rate of mass transfer as defined earlier is the mass of metal transferred per unit area per unit time. And since the surface area of the membrane (A) where mass transfer takes place was known from the manufacturer specifications, then the rate of mass transfer of copper in the MPHF module based on the aqueous side could be written as follows:

Rate of mass transfer of copper = $N_a = \frac{[F_{aq}(C_{aq}^{in} - C_{aq}^{out})]}{A}$ 4.11

4.5.1 The relation between the rate of mass transfer and aqueous phase concentration

In this study equation (4.11) was used to calculate the rate of mass transfer of copper from the aqueous solution to the organic solvent. The influence of the initial aqueous phase concentration on the rate of metal transport was examined. A set of experiments were devised to study this connection by contacting the two phases counter currently through the MPHF module at two levels of equal flow rates (100/100 cm^3/min and 600/600 cm^3/min aqueous/organic). The organic solvent concentration was kept constant at 10v/v% LIX984 while the aqueous feed concentration was changed in each experiment. The results of this study are summarised in table 4.26.

Table 4. 26: The relationship between the aqueous phase concentration and the rate of mass transfer in MPHF module at equal flow rate of both phases.

Volumetric flow rate of: Aqueous phase / organic phase	**100/100** cm^3/min / cm^3/min			**600/600** cm^3/min / cm^3/min		
C^{in}_{aq} **Aqueous phase inlet copper concentrations** $g/cm^3 x\ 10^3$	**Outlet streams specifications**					
	C^{out}_{aq} $g/cm^3 x\ 10^3$	C^{out}_{org} $g/cm^3 x\ 10^3$	N_a $g/cm^2.s x\ 10^7$	C^{out}_{aq} $g/cm^3 x\ 10^3$	C^{out}_{org} $g/cm^3 x\ 10^3$	N_a $g/cm^2.s x\ 10^7$
0.250	0.208	0.042	0.289	0.195	0.055	2.391
0.500	0.413	0.087	0.630	0.388	0.112	4.870
1.00	0.835	0.165	1.196	0.821	0.179	7.783
2.00	1.648	0.352	2.551	1.731	0.269	11.70
3.00	2.52	0.480	3.478	2.678	0.322	14.00

4.5.2 The relation between the rate of mass transfer and the organic phase concentration

The organic solvent (LIX984) concentration effect on the rate of mass transfer of copper in a MPHF membrane based liquid-liquid extraction was investigated in this work. The same flow rate levels used to study the system properties with variable aqueous phase concentrations was used in this part (i.e. 100/100cm^3/min and 600/600cm^3/min aqueous/organic). Four batches of the organic phase with LIX984 initial concentrations of; 5v/v%, 10v/v%, 15v/v% and 20v/v% were contacted against three batches of the aqueous solution with concentrations of 1, 2 and 3g/l in set of experiments. Each batch of the organic solvent was pumped against each one of the above aqueous solution concentrations at both of the two levels flow rate. The results of these experiments are outlined in table 4.27.

Table 4. 27: The average results of three experiments outline the relationship between the organic phase concentration and the rate of mass transfer in MPHF module.

Copper concentrations at the aqueous feed stream			**1.000 $g/cm^3 \times 10^{-3}$**			**2.000 $g/cm^3 \times 10^{-3}$**			**3.000 $g/cm^3 \times 10^{-3}$**		
outlet streams specifications			C^{out}_{aq}	C^{out}_{org}	N_a	C^{out}_{aq}	C^{out}_{org}	N_a	C^{out}_{aq}	C^{out}_{org}	N_a
C_{HR} v/v%	F_{aq} $\frac{cm^3}{min}$	F_{org} $\frac{cm^3}{min}$	$g/cm^3 \times 10^3$	$g/cm^3 \times 10^3$	$g/cm^2.s \times 10^7$	$g/cm^3 \times 10^3$	$g/cm^3 \times 10^3$	$g/cm^2.s \times 10^7$	$g/cm^3 \times 10^3$	$g/cm^3 \times 10^3$	$g/cm^2.s \times 10^7$
5	100	100	0.948	0.052	0.3768	1.798	0.202	1.464	2.668	0.332	2.406
5	600	600	0.91	0.09	3.913	1.798	0.202	8.783	2.747	0.253	11.00
10	100	100	0.889	0.111	0.8043	1.743	0.257	1.862	2.642	0.358	2.594
10	600	600	0.884	0.116	5.043	1.723	0.277	12.04	2.683	0.317	13.78
15	100	100	0.886	0.114	0.8261	1.737	0.263	1.906	2.641	0.359	2.601
15	600	600	0.867	0.133	5.783	1.684	0.316	13.74	2.639	0.361	15.70
20	100	100	0.875	0.125	0.9058	1.726	0.274	1.986	2.635	0.365	2.645
20	600	600	0.859	0.141	6.130	1.674	0.326	14.17	2.632	0.368	16.00

Where C_{HR}= is the LIX984 concentration (v/v%) at the organic phase.

4.6 Calculation Procedure Of The Overall Mass Transfer Coefficient In MPHF Membrane Based Liquid-Liquid Extraction

The overall mass transfer coefficient (K_{ov}) was calculated based on the aqueous phase, using the following relationships:

The overall rate of mass transfer equation can be expressed as:

$$F_{aq} (C_{aq}^{in} - C_{aq}^{out}) = K_{ov} A_c \Delta C_{LM} \qquad 4.12$$

Where:

A_c=is the surface area where the contact between the two phase occurs (cm^2).

ΔC_{LM}= is the logarithmic mean driving force for copper concentration at both ends

of the MPHF membrane contactor.

For a counter-current flow arrangement ΔC_{LM} will be:

$$\Delta C_{LM} = \frac{\Delta C_1 - \Delta C_2}{\ln \frac{\Delta C_1}{\Delta C_2}} \qquad 4.13$$

where $\Delta C_1 = C_{aq}^{in} - C_{org}^{out}$

and since the calculation is based on the aqueous film side then:

$\Delta C_1 = C_{aq}^{in} - (C_{org}^{out} / m)$

$$\Delta C_1 = C_{aq}^{in} - C_{aq}^{*} \qquad 4.14$$

$$\Delta C_2 = C_{aq}^{out} - C_{org}^{in}$$

In continuous mode extraction fresh LIX984 was used $C_{org}^{in} = 0$

Then $\Delta C_2 = C_{aq}^{out}$ 4.15

Substitute equations 4.14 and 4.15 in equation 4.13 will result:

$$\Delta C_{LM} = \frac{[(C_{aq}^{in} - C_{aq}^{out})] - C_{aq}^{out}}{\ln \frac{(C_{aq}^{in} - C_{aq}^{*})}{C_{aq}^{out}}} \qquad 4.16$$

Substitution of equation 4.16 into equation 4.12 will result in:

$$K_{ov} = \frac{[F_{aq}(C_{aq}^{in} - C_{aq}^{out})]}{\left[A\left\{\frac{(C_{aq}^{in} - C_{aq}^{*}) - C_{aq}^{out}}{\ln \frac{C_{aq}^{in} - C_{aq}^{*}}{C_{aq}^{out}}}\right\}\right]} \qquad 4.17$$

or $K_{ov} = \frac{N_a}{\Delta C_{LM}}$

The values of K_{ov} found experimentally were calculated using equation 4.17 where the flow rates of both phases were chosen and copper concentrations found by analysing both phases' outlet using atomic absorption spectrophotometer.

4.6.1 The relation between the overall mass transfer coefficient and the aqueous phase concentration

In this work, the effect of the aqueous feed stream initial concentration on the overall mass transfer coefficient (K_{ov}) was studied. Many experiments were devised in this study to examine the connection between K_{ov} and the aqueous phase flowing inside the fibre lumen of the MPHF contactor. In this section a range of aqueous copper solutions were prepared with concentrations ranging between 0.25 to 3g/l. These solutions were contacted against an organic solvent (LIX984) of 10v/v% concentration in Escaid110 which was kept constant throughout all experimental runs. These experiments were carried out in a counter-current flow arrangement and under two ranges of equal flow rates (100/100cm^3/min and 600/600cm^3/min aqueous/organic). The average of three experimental runs results at each concentration are listed in table 4.28 and more a detailed discussion of these results and others will be addressed in chapter five.

Table 4. 28: Results outlined the relationship between the aqueous phase concentration and the overall mass transfer coefficient in MPHF module (average of three experimental runs).

Volumetric flow rate of: Aqueous phase / organic phase	**100/100** cm^3/min / cm^3/min				**600/600** cm^3/min / cm^3/min			
C^{in}_{aq} **Aqueous phase inlet copper concentrations** $g/cm^3 x\ 10^3$	**Outlet streams specifications**							
	C^{out}_{aq} $g/cm^3 x\ 10^3$	C^{out}_{org} $g/cm^3 x\ 10^3$	N_a $g/cm^2.s x\ 10^7$	K_{ov} $cm/s x\ 10^4$	C^{out}_{aq} $g/cm^3 x\ 10^3$	C^{out}_{org} $g/cm^3 x\ 10^3$	N_a $g/cm^2.s x\ 10^7$	K_{ov} $cm/s x\ 10^4$
0.250	0.210	0.040	0.2899	1.271	0.229	0.021	0.913	4.946
0.500	0.415	0.085	0.6159	1.361	0.451	0.049	2.130	5.181
1.00	0.824	0.176	1.275	1.400	0.88	0.120	5.217	5.752
2.00	1.631	0.369	2.674	1.485	1.729	0.271	11.78	6.526
3.00	2.410	0.590	4.275	1.560	2.59	0.410	17.83	6.604

4.6.2 The relation between the overall mass transfer coefficient and the organic phase concentration

The relationship between the organic solvent (LIX984) concentration and the overall mass transfer coefficient (K_{ov}) during copper extraction process in a MPHF membrane was studied intensively in this work. All the experiments were carried out in a counter-current mode at two flow rate levels (i.e. 100/100cm^3/min and 600/600cm^3/min aqueous/organic). The aqueous solution was pumped in the tube side with initial concentrations of 1g/l or 3g/l. In contrast, the organic phase concentration was changed in each experiment. The studied concentrations were 5v/v%, 10v/v%, 15v/v% and 20v/v% of LIX984 in Escaid110. The results (an average of three experimental runs in each case) are outlined in table 4.29. Some of these experiments was carried out for about 30 minutes under the same conditions

and the extract phase (the copper rich LIX984 product) of each experiment was stored in separate tank for further study in the stripping process.

Table 4. 29: Experimental results which reflect the relationship between the organic phase concentration and the overall mass transfer coefficient (average results of 3 experiments).

Copper concentrations at the aqueous feed stream			**1.000 $g/cm^3 \times 10^{-3}$**				**3.000 $g/cm^3 \times 10^{-3}$**			
outlet streams specifications			C^{out}_{aq}	C^{out}_{org}	N_a	K_{ov}	C^{out}_{aq}	C^{out}_{org}	N_a	K_{ov}
C_{HR} v/v%	F_{aq} $\frac{cm^3}{min}$	F_{org} $\frac{cm^3}{min}$	$g/cm^3 \times 10^3$	$g/cm^3 \times 10^3$	$g/cm^2.s \times 10^7$	$cm/s \times 10^4$	$g/cm^3 \times 10^3$	$g/cm^3 \times 10^3$	$g/cm^2.s \times 10^7$	$cm/s \times 10^4$
5	100	100	0.913	0.087	0.630	0.660	2.661	0.339	2.457	0.871
5	600	600	0.912	0.088	3.826	4.013	2.712	0.288	12.52	4.398
10	100	100	0.849	0.151	1.094	1.191	2.465	0.535	3.877	1.430
10	600	600	0.884	0.116	5.043	5.376	2.627	0.373	16.22	5.790
15	100	100	0.818	0.182	1.319	1.462	2.397	0.603	4.370	1.634
15	600	600	0.867	0.133	5.783	6.225	2.584	0.416	18.09	6.512
20	100	100	0.811	0.189	1.370	1.525	2.373	0.627	4.543	1.708
20	600	600	0.861	0.139	1.878	6.784	2.568	0.432	18.78	6.784

4.7 Results Of The Stripping Process In MPHF Membrane Contactor

The extracted metal (copper) can be recovered from the organic solvent through a re-extraction process (stripping) against a suitable acidic solution. In this work sulphuric acid was chosen for the recovery of copper from the LIX984 solution in a MPHF membrane based stripping process. This process was studied using two types of operations i.e. batch stripping and continuous stripping type of operation. The results of both operations and their conditions can be outlined as follows:

4.7.1 Continuous stripping process of copper from LIX984 in MPHF membrane

In this process 30 litres of extract LIX984 containing a known concentration of copper was placed in the organic feed tank while similar volume of 0.5 molar H_2SO_4 solution was placed in the aqueous feed tank in each experimental run. The two phases were circulated from and into these tanks for 10 minutes through the by-pass line. In this study the extract phase produced during studying the organic solution concentration effect on the MPHF membrane based extraction was used (section 4.6.2). In each experiment the initial concentration of the LIX984 in the organic phase was set and the extracted copper concentration was predetermined by analysis and from the average concentrations of the solutions obtained in table 4.29. The continuous mode stripping process was carried out at two flow rate levels where both phases were pumped at the equal flow rate; these were 100 cm^3/min and 600 cm^3/min and each experiment was repeated two or three times. The copper concentrations at the outlet steams were determined by analysing both phases outlet using atomic absorption spectrophotometer. The rate of mass transfer of copper transfer from the organic solution to the acidic strip phase was determined by mass balance at both ends of the MPHF membrane using the following equation:

$$F_{aqs} (C_{aqs}^{in} - C_{aqs}^{out}) = F_{orge} (C_{orge}^{in} - C_{orge}^{out})$$

Since the stripping solution is initially copper free then $C_{aqs}^{in}=0$

Then rate of mass transfer for the stripping process can be expressed as follows:

$$\textbf{Rate of mass transfer of copper} = N_s = \frac{[F_{aqs}C_{aqs}^{out}]}{A} = \frac{[F_{aq}(C_{orge}^{in} - C_{orge}^{out})]}{A} \qquad 4.18$$

Where F_{aqs}= is the stripping phase volumetric flow rate.

C_{aqs}^{in} , C_{aqs}^{out} = are copper concentrations at the stripping phase flowing into and out of the MPHF membrane.

F_{orge} = is the rich copper organic (extract) phase volumetric flow rate and

(C_{orge}^{in} , C_{orge}^{out}) = are copper concentrations at the organic (extract) phase flowing into and out the MPHF membrane.

In this work a counter current continuous mode stripping process was carried out over a range of known copper concentrations in the organic phase. The initial LIX984 concentrations before the extraction stage are also known. The results of these experiments are summarised in table 4.30.

Table 4. 30: Results of continuous mode stripping process in MPHF membrane (average of three experimental runs).

Volumetric flow rate of: stripping phase / organic phase	**100/100** cm^3/min / cm^3/min				**600/600** cm^3/min / cm^3/min			
outlet streams specifications	C^{in}_{orge}	C^{out}_{orge}	C^{out}_{aqs}	N_a	C^{in}_{orge}	C^{out}_{orge}	C^{out}_{aqs}	N_a
C_{HR} v/v%	g/cm^3 x 10^3	g/cm^3 x 10^3	g/cm^3 x 10^3	$g/cm^2.s$ x 10^8	g/cm^3 x 10^3	g/cm^3 x 10^3	g/cm^3 x 10^3	$g/cm^2.s$ x 10^8
5	0.087	0.077	0.010	0.725	0.087	0.079	0.0080	3.478
10	0.151	0.131	0.020	1.464	0.151	0.1373	0.0137	5.957
15	0.182	0.159	0.023	1.659	0.182	0.1665	0.0155	6.739
20	0.189	0.166	0.023	1.696	0.189	0.1733	0.0157	6.826

4.7.2 Results of the batch stripping process of copper in MPHF module

In this study a batch stripping process was carried out by contacting the loaded organic phase and the fresh acid solution for 2 to 3 hours in a close loop mode operation during which the organic phase copper concentration reduced to a low value. In each experiment equal volumes of both phase were used (3 litres of each). In this process the organic extract used had the same specifications to that studied in the continuous mode operation in regard to its copper content. The strip phase was of the same stock used in the continuous stripping experiments (0.5 molar H_2SO_4). The batch stripping process was carried out under two sets of counter current flow conditions; a high flow rate of 600cm^3/min and a low flow rates of 100cm^3/min for both sides. The average results of two experimental runs under each set of condition are summarised in tables 4.31 and 4.32 below.

Table 4. 31: The results of batch stripping process at equal high flow rates of both phases (average results of three experimental runs).

Copper concentrations at the feed organic phase			**0.087 g/cm^3 x 10^{-3}**		**0.151 g/cm^3 x 10^{-3}**		**0.182 g/cm^3 x 10^{-3}**		**0.189 g/cm^3 x 10^{-3}**	
Outlet streams specifications			C^{in}_{orge}	C^{out}_{aqs}	C^{in}_{orge}	C^{out}_{aqs}	C^{in}_{orge}	C^{out}_{aqs}	C^{in}_{orge}	C^{out}_{aqs}
t_c min	F_{org} cm^3/min	F_{aq_3} cm^3/min	g/cm^3 x 10^3	g/cm^3 x 10^3	g/cm^3 x 10^3	g/cm^3 x 10^3	g/cm^3 x 10^3	g/cm^3 x 10^3	g/cm^3 x 10^3	g/cm^3 x 10^3
5	600	600	0.079	0.008	0.137	0.014	0.166	0.016	0.173	0.017
15	600	600	0.069	0.018	0.122	0.029	0.166	0.016	0.170	0.019
30	600	600	0.058	0.029	0.101	0.050	0.141	0.041	0.138	0.051
60	600	600	0.032	0.055	0.068	0.083	0.122	0.060	0.123	0.066
80	600	600	0.021	0.066	0.051	0.100	0.090	0.092	0.087	0.102
100	600	600	0.010	0.077	0.032	0.119	0.071	0.111	0.069	0.120
120	600	600	0.002	0.085	0.021	0.130	0.052	0.130	0.050	0.139
140	600	600	0.001	0.086	0.016	0.135	0.043	0.139	0.041	0.148
160	600	600	-	-	0.005	0.146	0.035	0.147	0.036	0.153

Table 4. 32: The results of batch stripping process at equal low flow rates of both phases (average results of three experimental runs).

Copper concentrations at the feed organic phase			**0.087 $g/cm^3 \times 10^{-3}$**		**0.151 $g/cm^3 \times 10^{-3}$**		**0.182 $g/cm^3 \times 10^{-3}$**		**0.189 $g/cm^3 \times 10^{-3}$**	
Outlet streams specifications			C^{in}_{orge}	C^{out}_{aqs}	C^{in}_{orge}	C^{out}_{aqs}	C^{in}_{orge}	C^{out}_{aqs}	C^{in}_{orge}	C^{out}_{aqs}
t_c min	F_{org} $\frac{cm^3}{min}$	F_{aq_3} $\frac{cm^3}{min}$	$g/cm^3 \times 10^3$	$g/cm^3 \times 10^3$	$g/cm^3 \times 10^3$	$g/cm^3 \times 10^3$	$g/cm^3 \times 10^3$	$g/cm^3 \times 10^3$	$g/cm^3 \times 10^3$	$g/cm^3 \times 10^3$
5	100	100	0.077	0.010	0.135	0.016	0.159	0.023	0.166	0.023
15	100	100	0.069	0.018	0.127	0.024	0.153	0.029	0.154	0.035
30	100	100	0.063	0.024	0.120	0.031	0.141	0.041	0.143	0.046
60	100	100	0.051	0.036	0.102	0.049	0.123	0.059	0.123	0.066
80	100	100	0.044	0.043	0.091	0.060	0.112	0.070	0.109	0.080
100	100	100	0.035	0.052	0.084	0.067	0.103	0.079	0.104	0.085
120	100	100	0.031	0.056	0.078	0.073	0.097	0.085	0.098	0.091
140	100	100	0.028	0.059	0.075	0.076	0.095	0.087	0.096	0.093

The results in table 4.31 and 4.32 clearly represent the relation between the organic phase copper content and the ability of the stripping phase to recover the required amount of the metal content under these conditions.

The results outlined in this chapter will be discussed in thorough details in chapter five of this thesis.

CHAPTER FIVE

DATA ANALYSIS AND DISCUSSION

5 INTODUCTION

In this chapter the experimental results are analysed in detail. This includes the findings and observations on the results listed in chapter three. Further a thorough illustration and analysis of the experimental data is carried out using mathematical models which are developed in this study for the treatment of equilibrium data and mass transfer parameter in single drop and hollow fibre membrane techniques.

5.1 Discussion Of The Equilibrium Data

The following points were observed during the generation of the extraction equilibrium data listed in tables 4.1 to 4.3:

1. The loading capacity at the end of the equilibrium experiments of LIX860® in Escaid110™ is slightly higher than the loading capacity of LIX84® and LIX984® in the same diluent. Further, in some experiments it has been noticed that LIX84 and LIX860 suffer to some degree of discolouring when contacted against concentrated acid solutions during metal recovery (stripping) which required further investigation.

2. The acidity of the aqueous phase increases (pH decreases) during the contacting process until equilibrium is reached. This is due to the fact that as the reaction proceeds protons from the reacting extractant molecules are released and diffused into the aqueous phase, which can been seen from the reaction equation below:

$$Cu^{2+}_{aq.} + 2(HR)_{org} \rightleftharpoons (CuR_2)_{org.} + 2\,H^{+}_{aq}$$

3. Copper concentration in the extract phase increased with an increase of copper content in the aqueous feed solution.

4. The higher the LIX reagent concentration the more copper extracted under fixed pH and temperature conditions.

In the stripping equilibrium results listed in table 4.4.A and B, It has been observed that the concentration of stripped copper was a function of the stripping acid concentration and increased with the increase of H_2SO_4 concentration in the stripping solution, see figure 5.1. However, it has been noticed that some experiments the increase of the acid concentration at the stripping phase (higher than 2 molar) led to discolouring of the organic solvent, especially LIX860 and LIX84, which I think deserves further investigation.

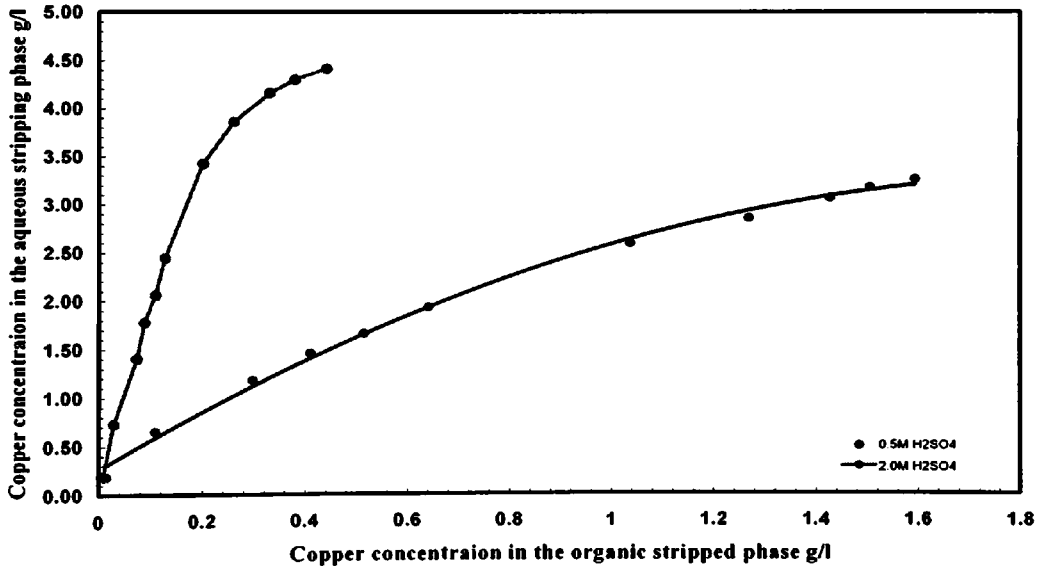

Figure 5. 1: Copper concentration in the stripped organic phase and the stripping aqueous phase as a function of acid concentration in the stripping phase.

5.2 Mathematical Modelling Of The Equilibrium Results

Two mathematical models were developed in this study to treat copper sulphate-LIX system's equilibrium data and predict copper concentration at the extraction equilibrium stage. One of the models is chemically based, while the other is a semi-empirical model.

5.2.1 Chemical based model

The chemical model is basically based on applying the mass action law to equation (5.1). This equation represents the final stage of the reaction between the dissociated metal Cu^{2+} in the aqueous phase and the active species of the chelating reagent which will be referred to here and after as (HR). The extraction reaction equation can be expressed as follows:

$$(Cu^{2+} + SO_4^{2-})_{aq.} + 2(HR)_{org.} \rightleftharpoons (CuR_2)_{org.} + (2H^+ + SO_4^{2-})_{aq.} \qquad 5.1$$

In this extraction process, the concentration of copper in the organic phase depends on the metal's initial concentration and the pH of the aqueous phase. The equilibrium data of the (copper-LIXs) system used to test the chemical model were experimentally obtained in the laboratory and is summarised in Tables 4.1.B, 4.2.B and 4.3.B. The initial copper concentration in the feed aqueous solutions varied between 0.25-20 g/l and the solution pH was between 2 to 2.5. The concentration of the organic solvent was 20v/v% of LIX84®, LIX860® or LIX984® in Escaid 110.

Applying the mass action law to equation (5.1) will give:

$$K_{eq} = \frac{[Cu^{2+}]_{org}[H^+]^2_{aq}}{[Cu^{2+}]_{aq.}[HR]^2_{org}} \qquad 5.2$$

The concentration of the complex formed after the reaction ($[CuR_2]_{org}$) could be related to the concentration of reacted copper ($[Cu^{2+}]_{org}$) or to the predicted number of moles of copper to be extracted (α^*) per the organic phase volume which can be written as follows:

$$[CuR_2]_{org} \equiv [Cu^{2+}]_{org} = (\alpha^*)/V_o \qquad 5.3$$

While copper concentration at the raffinate phase ($[Cu^{2+}]_{aq}$) could be expressed in the form of the number of moles of copper in the raffinate phase (R) per its unit volume as follows:

$$[Cu^{2+}]_{aq.} = (R)/V_a \qquad 5.4$$

At equilibrium the organic phase concentration can be related to its initial concentration (B) as follows:

B = The reacted $[HR]_r$ to form CuR_2 + The unreacted $[HR]_{org}$ at equilibrium

equation (5.1) shows that to produce one mole of CuR_2, would require 2 moles of HR and one mole of Cu^{2+} therefore :

$$[HR]_{org} = B - 2\,[HR]_r \qquad 5.5$$

The reacted regent concentration $[HR]_r$ could be related to the extracted copper as follows:

$$[HR]_{org} = (B-2\alpha^*)/V_o \qquad 5.6$$

$$[H^+]^2_{aq} = (H^+)^2/\,V_a^{\,2} \qquad 5.7$$

Substitution of equations 5.3, 5.4, 5.6 and 5.7 into equation 5.2 will result:

$$K_{eq} = \frac{\frac{(\alpha^*)}{V_o} \times \frac{(H^+)^2}{V_a^2}}{\frac{(R)}{V_a} \times \frac{(B-2\alpha^*)^2}{V_o^2}} \qquad 5.8$$

$$\frac{K_{eq} \times R(B^2 - 4B\alpha^* + 4\alpha^{2^*})}{V_a V^2{}_o} = \frac{\alpha^*(H^+)^2}{V_o V^2{}_a}$$

$$K_{eq} R V_a (B^2 - 4B\alpha^* + 4\alpha^{2^*}) - V_o (H^+)^2 \alpha^* = 0$$

$$4K_{eq} R V_a \alpha^{2^*} - \alpha^* (4K_{eq} R V_a B + V_o (H^+)^2) + K_{eq} R V_a B^2 = 0$$

$$\alpha^* = \frac{(4K_{eq} R V_a B + V_o (H^+)^2) \pm \sqrt{(4K_{eq} R V_a B + V_o (H^+)^2)^2 - (4K_{eq} R V_a B)^2}}{8K_{eq} R V_a} \qquad 5.9$$

To simplify equation 5.9 the following parameters were defined:

$$\theta = 4K_{eq}RV_aB + V_o(H^+)^2 \qquad 5.10$$

$$\psi = (4K_{eq}RV_aB)^2 \qquad 5.11$$

$$\varepsilon = 8K_{eq}RV_a \qquad 5.12$$

Substitution of equations 5.10, 5.11 and 5.12 into equation 5.9 will result in:

$$\alpha^* = \frac{\theta \pm \sqrt{\theta^2 - \psi}}{\varepsilon} \qquad 5.13$$

Where:

K_{eq} = is the equilibrium constant.

B = is the number of initial moles of the organic solvent (LIX) at the organic phase.

R = the number of moles of unextracted copper at the aqueous phase (raffinate).

α^* = the number of moles of copper predicted to be extracted by the chemical model

$B-2\alpha^*$ = the number of moles of unreacted LIX reagent in the organic solvent.

V_a, V_o = are the aqueous solution and the organic solvent volumes respectively.

[ ] = refers to the molar concentration (mole /litre).

Ec = the concentration of copper predicted by the chemical model in (g/l).

Equation (5.13) is a direct modelling equation which represents all the variables in the copper-LIX system, namely:

$[Cu^{2+}]_{org.}$, $[Cu^{2+}]_{aq}$, $[B-2\alpha^*]_{org}$ and $[H^+]_{aq}$ or the system pH.

To calculate copper concentration at equilibrium conditions, by using the positive root of equation (5.13), set of experimental runs are required to establish a preliminary idea of the system parameters. An average value of the equilibrium constant (K_{eq}) was used in the

chemical model calculations. This model was set in such a way to account for any changes in concentrations of the main equilibrium parameters. Therefore, it gives the system's evaluator the freedom of simulating the equilibrium data at any set of conditions by assuming one or more of the equilibrium parameters. The calculations and the predicted results were set to be processed automatically through a model spreadsheet which was designed in this study to handle the equilibrium data.

The results of fitting equation (5.13) to the equilibrium data of the three LIX extractants (LIX84, LIX860 and LIX984) are shown in figure 5.2.A, B and C. In these figures the dots represent the experimental results, while the bold lines represent the best equilibrium curve fit that can be obtained from the chemical model. The corresponding data to these figures are tabulated in Appendix 5.A,B and C.

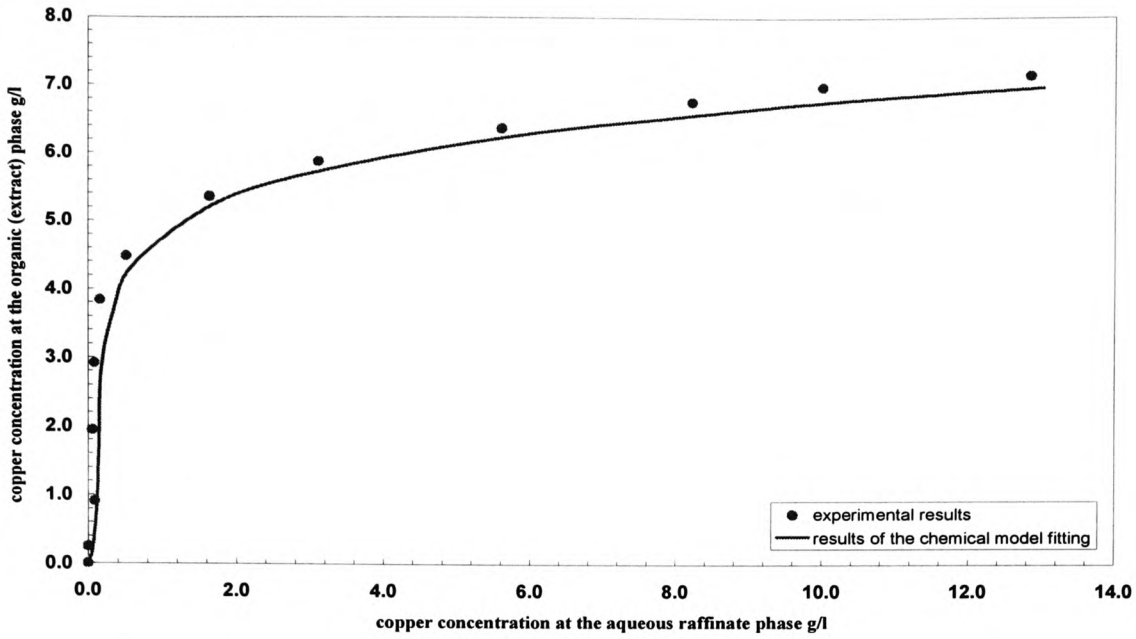

Figure 5.2. A: The result of fitting the chemical model to the equilibrium data of $CuSO_4$-LIX84.

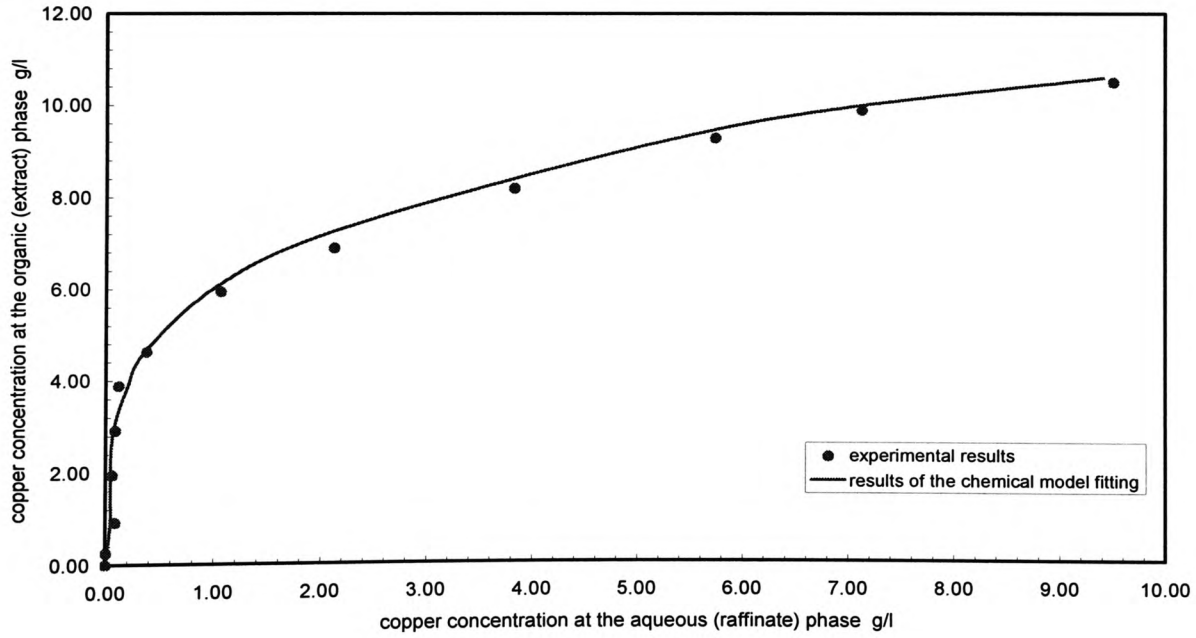

Figure 5.2. B: The result of fitting the chemical model to the equilibrium data of $CuSO_4$-LIX860.

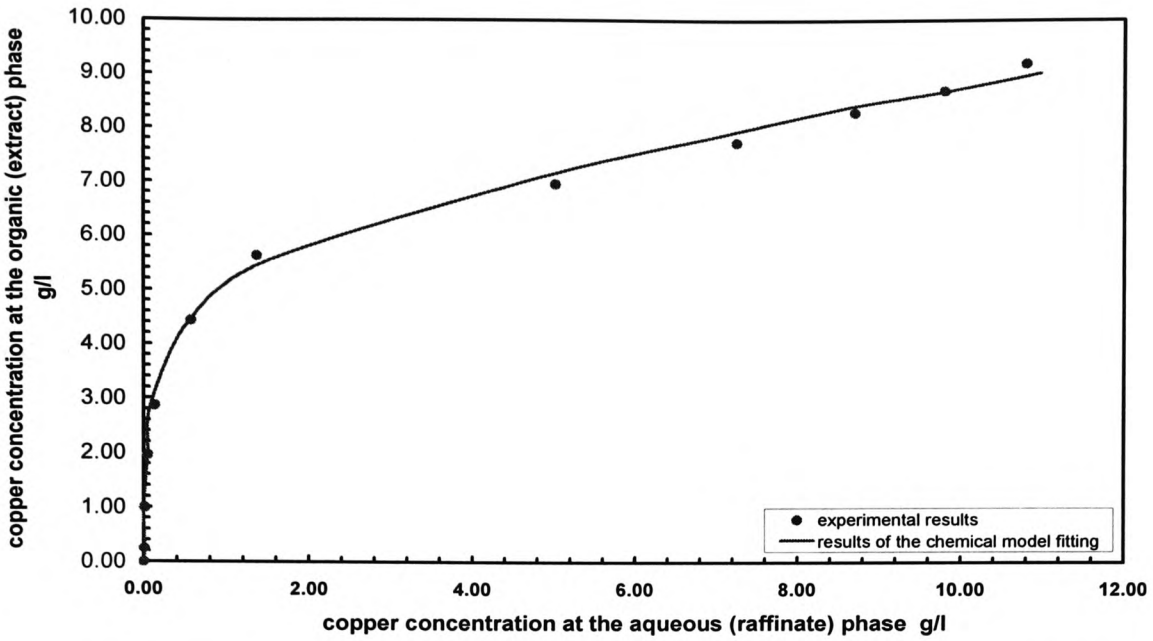

Figure 5.2. C: The result of fitting the chemical model to the equilibrium data of $CuSO_4$-LIX984.

5.2.2 A semi-empirical model

The semi-empirical model proposed in this study was obtained through Freundlich's equation, which is usually used to treat the equilibrium isotherms of binary gases or liquids during an adsorption process [1]. The equation can be used to represent the equilibrium distribution of a metal between the aqueous and the organic phases as follows:

$$Y = MX^n \qquad 5.14$$

Taking Log on both sides of equation (5.14) will result:

$$\text{Log } Y = n \text{ Log } X + \text{Log } M \qquad 5.15$$

Equation 5.14 could be rearranged as:

$$X=(Y/M)^{1/n} \qquad 5.16$$

Where X = copper concentration in the organic phase g/l.

Y = copper concentration in the aqueous phase g/l.

M, n = constants which represent the intercept and the line slope respectively.

The values of the intercept and the slope (M, n) of equation 5.15, have to be found experimentally under well define conditions. Hence a set of experimental runs are required to determine the constants values by utilising equation 5.15. Based on the determined or assumed values of (M, N), equation 5.14 can be used to predict the equilibrium data of a metal extraction stage. In this study the values of the constants (M, n) were calculated from applying equation 5.15 to the experimental data. The results of these calculation steps are summarised in appendix 6.1,6.2 and 6.3.

The calculated values of M and n from appendix 6 were substituted in equation 5.16 to predict the equilibrium copper concentrations of $CuSO_4$-LIX984, LIX860 and LIX84 in this study. This equation (5.14) was used to determine the concentrations of copper at equilibrium corresponding to the raffinate concentration found experimentally and the constant values of M, n for each system. The predicted equilibrium curves for $CuSO_4$-LIXs systems by this semi-empirical model are given in figure 5.3.A, B and C. In these figures the dots are referring to the experimental equilibrium results, while the bold line represents the results of fitting this model. The corresponding data for these figures are tabulated in appendix 7.

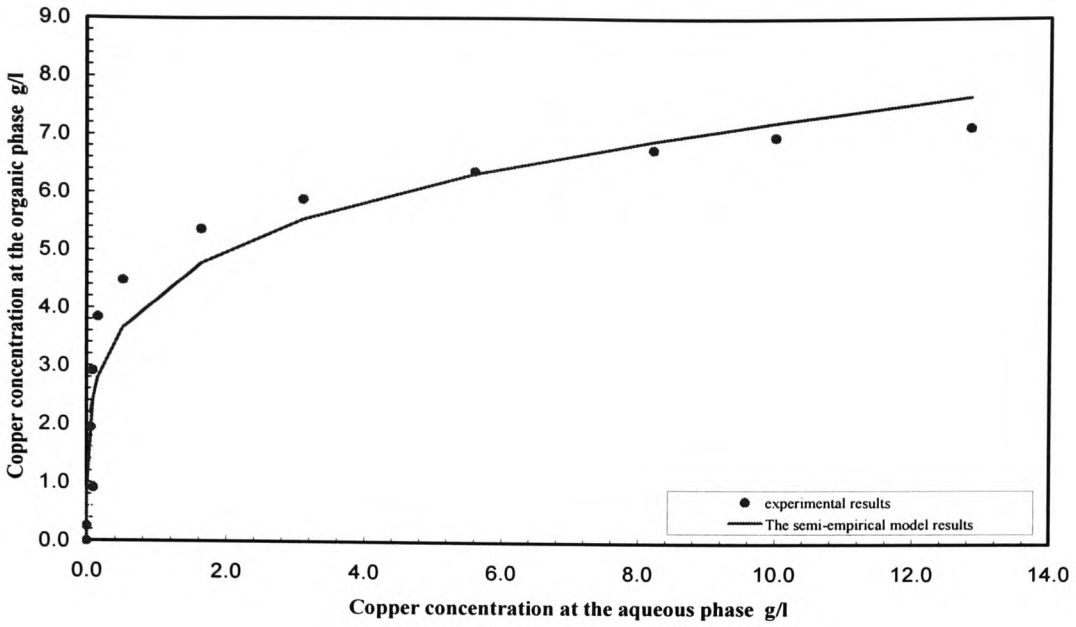

Figure 5.3. A: The result of fitting the semi-empirical model to the equilibrium data of $CuSO_4$-LIX84.

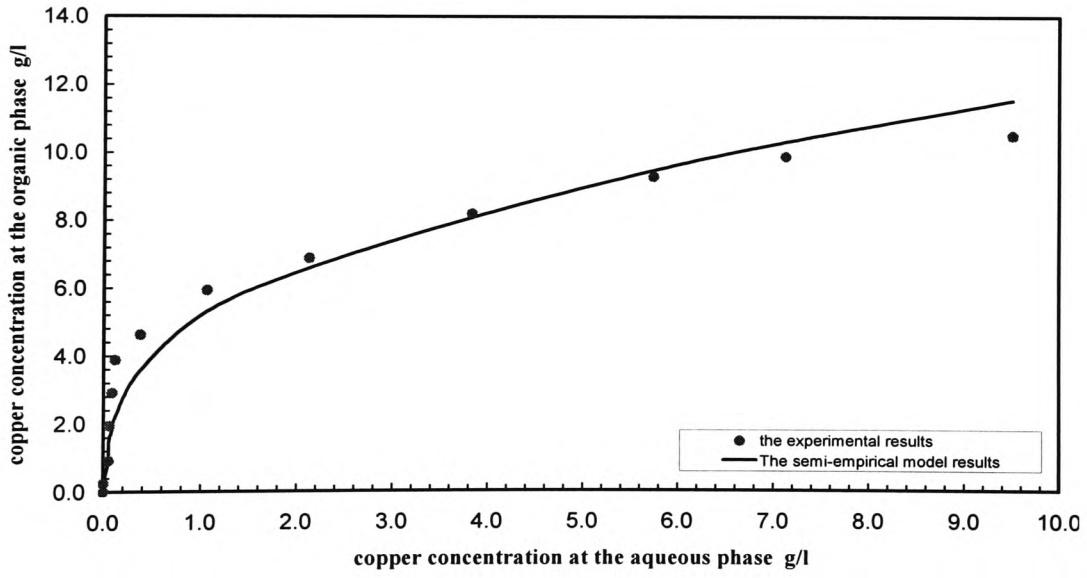

Figure 5.3. B: The result of fitting the semi-empirical model to the equilibrium data of $CuSO_4$-LIX860.

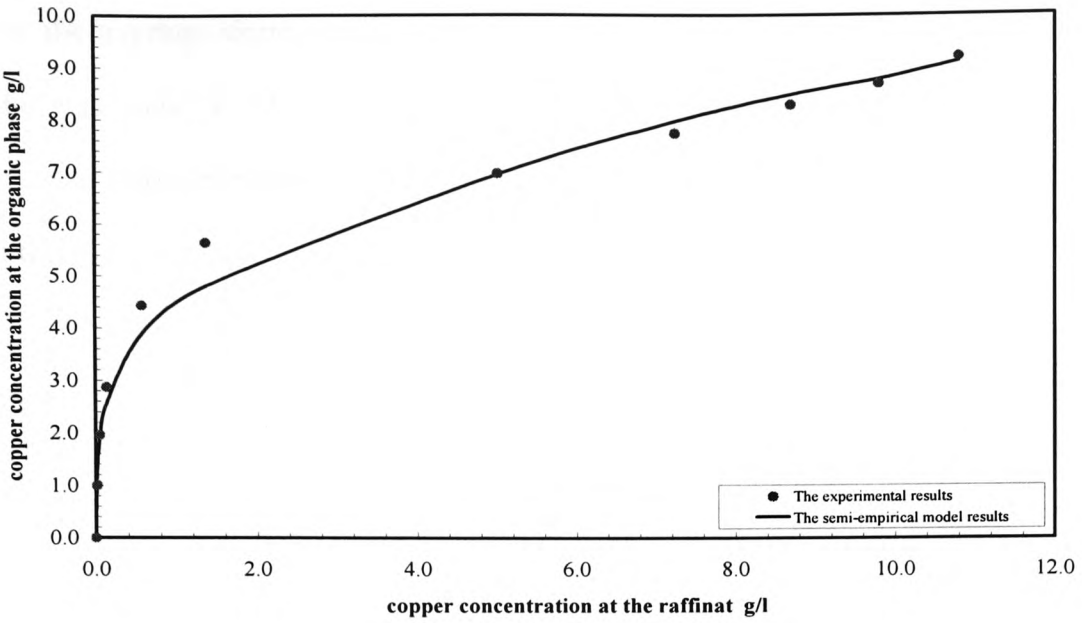

Figure 5.3. C: The result of fitting the semi-empirical model to the equilibrium data of $CuSO_4$-LIX984.

The results obtained from both models (the chemical based model and the semi-empirical model) show clearly that these models can be used to predict copper concentrations in the extract phase under set conditions. The chemical model appears to be more suitable to predict the systems equilibria. This is due to the fact that the chemical model includes all the process variables such as pH, the concentration of the chelating reagent and the metal concentration at the raffinate phase. While the semi-empirical model fit matches less of the experimental data points and therefore could be less precise in predicting the same systems equilibria. This could be attributed to the mathematical relationship used to calculate the values of (M, n) in equation 5.16, which have to be calculated from logarithm graphic relationships of the equilibrium data. These graphic relationships (appendices 6.1.1, 6.2.1 and 6.3.1) show that equilibrium data would be far from a straight logarithm linear relation especially at high aqueous phase concentrations where the equilibrium data form plateau.

Therefore the average slope which was taken in this model for the equilibrium data could effect the out come of the model fit to the data. Therefore, more investigation into modifying the semi-empirical model is required especially when the equilibrium data near or reach the plateau stage.

Based on the experimental results and the observations of the three LIX reagents extraction equilibrium data the following points could be highlighted:

1. The three organic solvents LIX984, LIX84 and LIX860 gave a favourable equilibrium curves and were efficient in extracting copper in reasonable contact time.
2. Some of the stripping experiments where LIX84 and LIX860 were stripped with concentrated acid (higher than 2M of H_2SO_4) led to discolouring of the organic phase used which visually observed and I feel it required further investigation.

These characteristics added to the published recommendations by the manufacturing company (Henkel Co.[30]) have made LIX984 the choice of this study in the determination of mass transfer properties using rising single drop and hollow fibre membrane techniques.

5.3 Rising Drops Data Analysis

In this section the results of single rising drops, which have been experimentally obtained in chapter four, will be discussed in detail. This includes discussion of all measures taken to account for the local and overall mass transfer coefficients characteristics in the dispersion based (rising drop) technique.

5.3.1 The effect of column height in single drop overall mass transfer

The aim of using four different column heights was to examine in addition to rising drops mass transfer properties if there was any end effects caused by mass transfer during drop formation at the tip of the needle or during coalescence at the capillary tube. In this work the rising drops flow rate was chosen by trial and error method and kept constant at (80±1 drops per minute). This flow rate was sufficient to make negligible any end effect during the formation stage at the bottom of the columns and during coalescence in the capillary tube at the top of the columns (see figure 5.4). This figure shows that the relation between the extracted mass of copper and the travel time of the rising drop is a straight-line relationship start at the origin point. This proves that the end effect, which would appear as an intercept at the Y co-ordinate is insignificant. Further this figure also represents a graphical relationship which could be used to calculate the overall rate of mass transfer. It shows a straight-line relationship between the drop rising time in four different columns' height and the mass of copper extracted in (cm^2) at the drop surface. This line starts at the origin point and has a constant slope, which represents the constant overall rate of mass transfer in all the columns. This figure also shows that the amount of copper extracted per single drop increases with the column's height, which may reflects that the concentrations driving force of the reactants and the product at reaction interface (the drops surface) was not effected by the column's height or drop's rising time. The results are given in table 4.5.

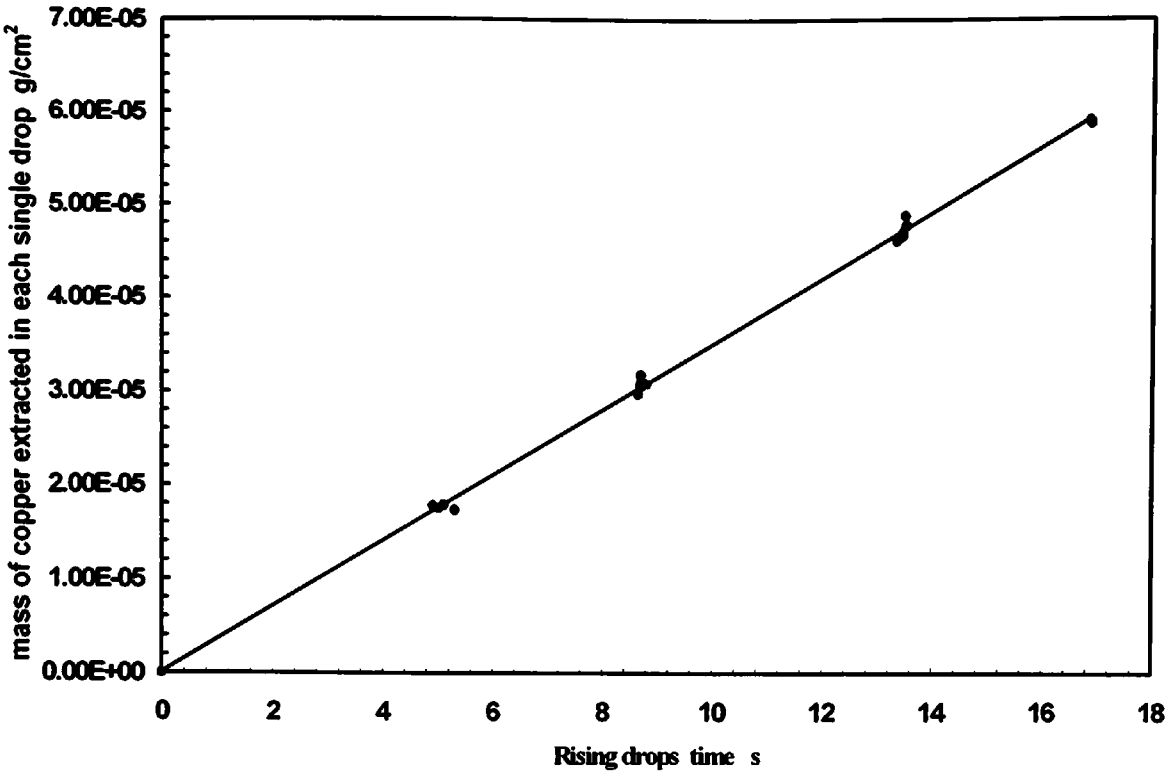

Figure 5. 4: The relationship between the column height expressed as rising drop travel time and the mass of copper extracted in four different columns

5.3.2 Mathematical models to calculate the local mass transfer coefficients in the continuous and dispersed phases in rising drop technique

Due to the difficulty in finding the interfacial concentrations of copper at the interface zone by analysis, it will be more difficult to determine the values of the local resistances in both phases experimentally. In dispersion based liquid-liquid extraction, mass transfer coefficients at the dispersed and the continuous phases are essential factors in accounting for the overall mass transfer coefficient (i.e. the location of the main resistance to species transfer). In this work, dimensionless groups were used to calculate local mass transfer coefficients in both phases (the continuous and dispersed phases).

5.3.2.1 Calculation of the continuous phase mass transfer coefficients

To calculate the continuous phase (the aqueous phase) mass transfer coefficient (k_c) an empirical equation was proposed in this study based on the equation suggested by Elzinga et al. and reported by Treybal[1]. This equation utilises two of the dimensionless groups for the aqueous solution contained in the rising drop columns and can be expressed for the current system ($CuSO_4$-LIX984) as follows:

$$N_{shc} = 5.52\left(\frac{\mu_c + \mu_D}{2\mu_c + 3\mu_D}\right)^{3.47}\left(\frac{d_p \sigma \rho_c}{\mu_c^2}\right)^{0.056} N_{Pec}^{0.5} \qquad 5.17$$

Where N_{shc} = the continuous phase Sherwood number = $k_c \cdot d_p/D_c$

N_{Pec} = the continuous phase Peclet number = $V_t.d_p/D_c$

Expanding the Sherwood and Peclet numbers and substituting them in equation (5.17) results in:

$$\frac{k_c d_p}{D_c} = 5.52\left(\frac{\mu_c + \mu_D}{2\mu_c + 3\mu_D}\right)^{3.47} \times \left(\frac{d_p \sigma \rho_c}{\mu_c^2}\right)^{0.056} \times \left(\frac{V_t . d_p}{D_c}\right)^{0.5} \qquad 5.18$$

D_c = Diffusivity of copper ion in the aqueous phase, the average value reported by Komasawa et al[58]. = 7.05×10^{-10} m^2/sec.

d_p = average drop diameter =0.33 cm =0.33×10^{-2} m.

d_c = The column internal diameter = 0.025 m.

V = The drop's average linear velocity = 0.11 m/sec.

V_t = the drop's terminal velocity = 0.1127 m/sec, and is calculated by:

$$V = V_t\left[1 - \left(\frac{d_p}{d_c}\right)^2\right]^{1.43}$$

μ_c = the continuous phase viscosity = 1Cp = 10^{-3}N.sec/m^2.

μ_D = the dispersed phase viscosity = 165×10^{-3}N.sec/m^2.

ρ_c = the continuous phase density = 1000 kg/m^3.

σ = the continuous phase interfacial tension = 0.0323 N/m^2.

The calculated results of the continuous phase mass transfer coefficient in four different height columns are tabulated in Table 5.1.

Table 5. 1: The calculated results of the continuous phase mass transfer coefficient using equation 5.18 in four different height columns.

C_L m	d_f	N_{AB} Drop	d_p m	d_c m	D_c cm^2/s x10^{10}	t_r s	V m/s	V_t m/s	μ_c Ns/m^2	μ_d Ns/m^2	σ N/m	k_c cm/s x10^3
0.55	80	50	0.0033	0.0254	7.051	5.00	0.110	0.112	0.001	0.165	0.0323	3.65
	80	50	0.0033	0.0254	7.05	4.90	0.112	0.115	0.001	0.165	0.0323	3.68
0.95	80	50	0.0033	0.0254	7.05	8.80	0.107	0.110	0.001	0.165	0.0323	3.61
	80	50	0.0033	0.0254	7.05	8.65	0.109	0.112	0.001	0.165	0.0323	3.64
1.49	80	50	0.0033	0.0254	7.05	13.3	0.111	0.114	0.001	0.165	0.0323	3.67
	80	50	0.0033	0.0254	7.05	13.5	0.110	0.112	0.001	0.165	0.0323	3.65
1.87	80	50	0.0033	0.0254	7.05	16.8	0.110	0.113	0.001	0.165	0.0323	3.66
	80	50	0.0033	0.0254	7.05	16.8	0.110	0.113	0.001	0.165	0.0323	3.66

5.3.2.2 Calculation of the dispersed phase mass transfer coefficients

The mass transfer coefficient at the organic dispersed phase (k_D) was calculated using the following equation:

$$N_a = k_D(C_{HR}^{in} - C_{HR}^{i}) \qquad 5.19$$

However, equation (5.19) can not be applied directly to the experimental results unless the interfacial concentration of the organic droplet phase was calculated. Therefore, an empirical relationship is proposed in this study based on equation propound by Kronig et al. and reported by Tryebal[1]. This equation was set to utilise the dispersed phase (LIX984)

concentrations at three zones (at the bulk phase, at the interface and at the final complex product) and can be written as follows:

$$\frac{C^{r}_{HR}}{C^{in}_{HR} - C^{i}_{HR}} = \{1 - \exp[\frac{-9D_{HR}\pi^2 t_r}{d_p^2}]\}^{0.5} \qquad 5.20$$

Where: C^{in}_{HR} = the initial concentration of the droplet organic phase LIX984 in Escaid110, (g/cm^3)

C^{r}_{HR} = the reacted concentration of LIX984 to form the metal-organic complex, (g/cm^3), which was calculated from the stoichiometric relationship with the extracted copper.

C^{i}_{HR} = the interfacial concentration of LIX984 at time (t), (g/cm^3)

D_{HR} = the diffusivity coefficient of LIX984 in Escaid 110 = 4.9196×10^{-6} cm^2/sec,

which was calculated by using Wilk-Changs' and Vignes equations as reported by Ried et at.[135].

Wilk-Chang equation for the current copper-LIX complex is:

$$D^{o}_{HR} = 7.4\times10^{-8}\frac{(\theta_f M_s)^{0.5}T}{\mu_s v_{HR}}$$

D^{o}_{HR} = the mutual diffusivity coefficient of species.

M_s = the molecular weight of Escaid110 =175

T = the room temperature during experiment time, in Kelvin =298 K

v_{HR} = the molar volume of LIX984 calculated by using Le Bas method reported by Ried et at.[135] = 420

μ_s = the viscosity of Escaid 110 = 1.653 Cp.

t_r = drop rising time in seconds.

θ_f = association factor of the organic solvent = 1 for Escaid110.

The calculated results of mass transfer coefficient at the organic phase in four different columns are summarised in Table 5.2:

Table 5. 2: The calculated results of the dispersed phase mass transfer coefficient by using equation 5.20.

C_L cm	d_p cm	C^{in}_{HR} g/cm^3	D_{HR} cm^2/s x10^6	C^{r}_{HR} g/cm^3	t_r s	C^{in}_{aq} g/cm^3 x10^3	C^{out}_{org} g/cm^3 x10^3	N_a g/cm^{2}s x10^6	C^{i}_{HR} g/cm^3	k_D cm/s x10^3
55	0.33	0.1	4.920	0.0033	5.00	3	0.321	3.531	0.0768	1.555
55	0.33	0.1	4.920	0.0033	5.10	3	0.319	3.536	0.0771	1.578
55	0.33	0.1	4.920	0.0032	5.30	3	0.317	3.294	0.0776	1.508
55	0.33	0.1	4.920	0.0033	4.90	3	0.325	3.659	0.0762	1.571
95	0.33	0.1	4.920	0.0056	8.65	3	0.546	3.477	0.0698	1.176
95	0.33	0.1	4.920	0.0057	8.70	3	0.559	3.686	0.0691	1.221
95	0.33	0.1	4.920	0.0057	8.68	3	0.553	3.579	0.0694	1.197
95	0.33	0.1	4.920	0.0056	8.69	3	0.547	3.540	0.0698	1.198
95	0.33	0.1	4.920	0.0086	13.35	3	0.843	3.478	0.0622	0.942
149	0.33	0.1	4.920	0.0089	13.52	3	0.872	3.558	0.0612	0.937
149	0.33	0.1	4.920	0.0087	13.45	3	0.852	3.489	0.0620	0.938
149	0.33	0.1	4.920	0.0089	13.5	3	0.869	3.637	0.0613	0.961
149	0.33	0.1	4.920	0.0084	13.46	3	0.822	3.520	0.0633	0.981
149	0.33	0.1	4.920	0.0108	16.86	3	1.056	3.519	0.0578	0.852
187	0.33	0.1	4.920	0.0107	16.87	3	1.05	3.497	0.0580	0.852
187	0.33	0.1	4.920	0.0107	16.71	3	1.042	3.440	0.0581	0.840
187	0.33	0.1	4.920	0.0109	16.91	3	1.063	3.532	0.0576	0.851
187	0.33	0.1	4.920	0.0108	16.85	3	1.055	3.449	0.0578	0.835

5.3.3 Calculation of the reaction rate constant in rising drops technique

The chemical reaction between copper ions and LIX984 at the interface zone represents another resistance to metal mass transfer between the continuous and the dispersed phases. Therefore, in this study two general mathematical equations were proposed to calculate and evaluate the reaction resistance at the interface area in single drop technique as follows:

1. In the current system ($CuSO_4$-LIX984) the overall resistance to the metal transfer can be expressed in form of the relation between the overall mass transfer coefficient and the individual coefficients. This can be represented by the sum of local resistances as follows:

$$\frac{1}{K_{ov}} = \frac{1}{k_c} + \frac{1}{mk_D} + \frac{1}{k_r}$$

$$\text{Then } \frac{1}{k_r} = \frac{1}{K_{ov}} - \frac{1}{k_c} - \frac{1}{mk_D} \qquad 5.21$$

Where: k_r = is the reaction rate constant.

From equation (5.21) the resistance at the reaction zone ($1/k_r$) was determined in set of experiments were all conditions of; drop flow rate, the two phases initial concentrations and the drops size were kept constant in four columns. The calculated results of the reaction resistance and the reaction rate constant for four different height columns are listed in table 5.3. :

Table 5. 3: The calculated results of the reaction rate constant and the reaction resistance as a function of the overall resistance.

C_L cm	d_f	d_p cm	C^{out}_{org} g/cm^3 x10^3	t_r s	N_a g/cm^{3}s x10^6	K_{ov} cm/s x10^3	$1/k_{ov}$ s/cm	k_c cm/s x10^3	$1/k_c$ s/cm	k_D s/cm x10^3	$1/mk_D$ s/cm	k_r s/cm x10^3	$1/k_r$ cm/s
55	80	0.33	0.32	5.00	3.531	1.19	843.88	3.65	274.33	1.56	28.965	1.85	540.59
	80	0.33	0.325	4.90	3.659	1.26	791.77	3.68	271.57	1.57	28.671	2.03	491.52
95	80	0.33	0.561	8.80	3.536	1.22	819.00	3.61	276.91	1.17	38.363	1.99	503.72
	80	0.33	0.546	8.65	3.477	1.22	819.00	3.64	274.54	1.18	38.301	1.98	506.16
149	80	0.33	0.843	13.3	3.478	1.22	817.66	3.67	272.34	0.942	47.805	2.01	497.51
	80	0.33	0.872	13.5	3.558	1.22	823.05	3.65	274.07	0.938	48.037	2.00	500.94
187	80	0.33	1.056	16.8	3.519	1.23	815.66	3.66	273.20	0.852	52.854	2.04	489.61
	80	0.33	1.05	16.8	3.497	1.21	823.72	3.66	273.28	0.852	52.870	2.01	497.58

2. In systems where the reaction between the metal ions and the chelating agent is slow, the reaction resistance will be the main controlling factor on the rate of mass transfer. In the current system it is clear that the reaction resistance is higher than the diffusional resistances in the continuous and dispersed phase as table (5.3) shows. Based on the results listed in table (5.3), a general equation was devised to account for the reaction rate constant (k_r) by assuming that the $CuSO_4$-LIX984 system was controlled by chemical reaction rate. The general form of this equation is as follows:

$$N_a = k_r \frac{C^i_{Cu_{aq}} - (C^i_{HR})^n}{C_{H^+}} \qquad 5.22$$

The interfacial concentrations of copper ($C^i_{Cu\ aq}$) was calculated after substituting the calculated value of the continuous phase mass transfer coefficient (k_c) from equation (5.18) into the following relationship:

$$N_a = k_c(C^{in}_{Cu} - C^i_{Cu}) \qquad 5.23$$

While the interfacial concentration of the LIX984 active reagent (C^i_{HR}) was calculated from the equation (5.20). After substituting the calculated values of ($C^i_{Cu\ aq}$ and C^i_{HR}) in equation (5.22), it was found that the value of the exponent (n) would be (1.4). This value is in agreement with the finding of Flett et al.[38] who reported similar value in LIX65N and suggested that hydroxyoximes could suffer some form of polymerisation during a chelating reaction. Therefore, equation (5.22) can be rewritten for the current system as follows:

$$N_a = k_r \frac{C^i_{Cu_{aq}} - (C^i_{HR})^{1.4}}{C_{H^+}} \qquad 5.24$$

The calculated values of (k_r) by using equation (5.24) are summarised in table 5.4 below:

Table 5. 4: The calculated results of k_r by applying equation (5.24) to the experimental data.

C_L cm	d_f	d_p cm	C^{in}_{aq} g/cm^3 x10^3	C^{out}_{org} g/cm^3 x10^3	C^{i}_{HR} g/cm^3	t_r s	N_a g/cm^{3}s x10^6	K_{ov} cm/s x10^3	$1/k_{ov}$ s/cm	$k_r^{calculated}$ cm/s x10^3
55	80	0.33	3	0.32	0.077	5.00	3.531	1.19	843.88	1.79
	80	0.33	3	0.325	0.076	4.90	3.659	1.26	791.77	1.90
95	80	0.33	3	0.561	0.069	8.80	3.536	1.22	819.00	2.09
	80	0.33	3	0.546	0.070	8.65	3.477	1.22	819.00	2.00
149	80	0.33	3	0.843	0.062	13.3	3.478	1.22	817.66	2.34
	80	0.33	3	0.872	0.061	13.5	3.558	1.22	823.05	2.49
187	80	0.33	3	1.056	0.058	16.8	3.519	1.23	815.66	2.65
	80	0.33	3	1.05	0.058	16.8	3.497	1.21	823.72	2.61

From the data in tables (5.1, 5.2, 5.3 and 5.4) the following points can noticed:

- The mass transfer coefficient at the aqueous phase (k_c) remains constant through out all columns. This could be attributed to the negligible changes occur during the diffusional mass transfer of copper from the continuous bulk phase to the interface area due to the high concentration used in the columns.

- The mass transfer coefficient at the dispersed organic phase side (k_D) has slightly decreases with the increase in column height. This is could be due to the significant decrease of the active reagent (HR) interfacial concentration during drop rising time inside the columns which could be caused by a form of adsorption of the CuR_2 complex at the interface.

- The current system appears to be controlled by the reaction rate at the drops surfaces, and that the reaction rate constant was not affected by the drops rising time. Further,

the proposed equation to calculate (k_r) from the interfacial concentration gave very close results to those calculated from the overall resistance relation.

5.3.4 The continuous phase concentration effect on the rate of mass transfer

In this study the influence of the continuous phase (the aqueous solution's) copper concentration on the rate of metal transfer to the dispersed phase was examined. The copper concentration in the continuous phase was varied between 2 and 7 g/l in a set of experiments, which were carried out at the same column height (95 cm) and constant initial organic phase concentration and drop flow rates. These changes resulted in a small increase in the rate of mass transfer of copper (see figure 5.5). This could be attributed to the fact that mass transfer between the two phases seems to be influenced by the interfacial area and the reaction kinetics and not by the bulk aqueous phase resistance or its concentrations.

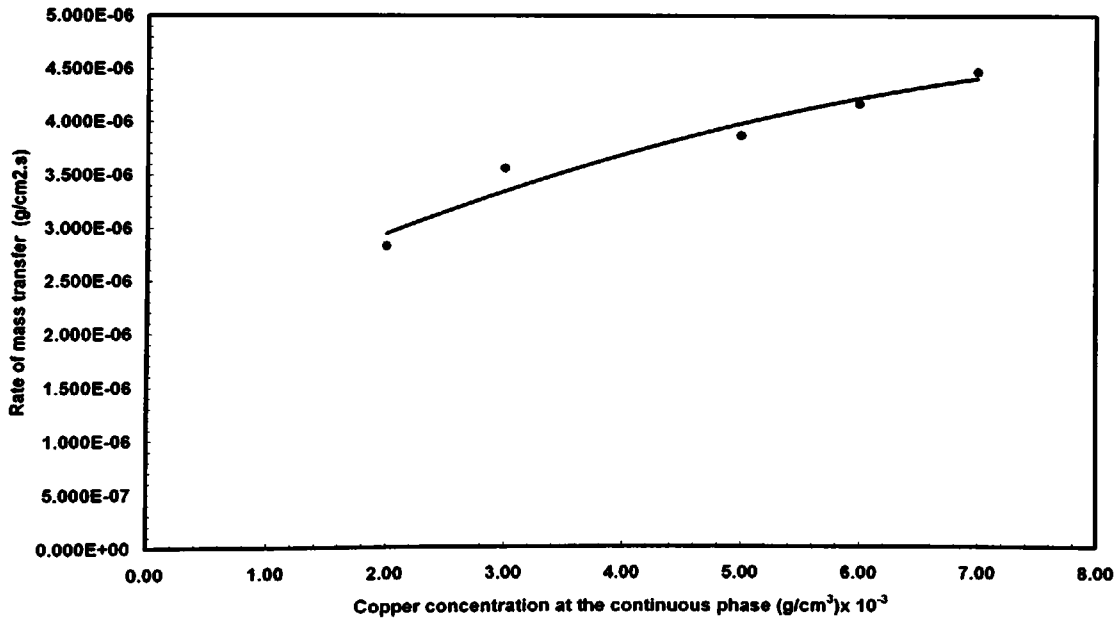

Figure 5. 5: The continuous phase concentration effect on rate of mass transfer

5.3.5. The dispersed phase concentration effect on the rate of mass transfer

In this work the organic droplet phase initial concentration was studied at two organic concentrations 20 and 60 v/v%LIX984 in Escaid110. The results listed in table 5.5 show considerable increase in the rate of mass transfer of copper from the continuous phase to the dispersed phase when the organic phase concentration is increased. This pattern of increase was also noticed on the overall mass transfer coefficient, this could be related to a significant decrease on the droplet phase resistance and the availability of the LIX reactive species (HR) at the organic side of the interface. The results of the dispersed phase effect at different concentrations of LIX984 are summarised in table 5.5 below.

Table 5. 5: The dispersed phase concentration effect on the rate of mass transfer

v/v%LIX984	d_f drop/min	N_{AB}	d_f cm	A_d cm^2	C^{in}_{aq} g/cm^3 $x10^3$	C^{out}_{orq} g/cm^3 $x10^3$	t_r s	Na g/cm^2s $x10^6$
20	82	51	0.33	0.356	3	0.561	8.80	3.511
20	76	51	0.33	0.356	3	0.546	8.65	3.477
20	81	51	0.33	0.342	3	0.559	8.70	3.684
20	79	50	0.33	0.356	3	0.553	8.68	3.579
60	77	50	0.33	0.356	3	0.864	8.90	5.454
60	80	50	0.33	0.356	3	0.732	8.80	4.676
60	80	51	0.33	0.356	3	0.709	8.70	4.494
60	81	50	0.33	0.356	3	0.871	8.69	5.633
60	82	49	0.33	0.356	3	0.865	8.70	5.700

5.3.6 The effect of drop size and drop flow rate on the overall mass transfer coefficient

Three different size needles were used to study the effect of formed drops on mass transfer characteristics. The experiments were carried out with 20 v/v% LIX984 concentration and 3g/l aqueous phase copper concentration in a column of 95cm height. It has been observed that needle size (17 gauge) produced slightly larger drops than those produced in needle size 21 or 25 gauge. At needle size (25 gauge) the smallest drops in these experiments were produced and large number of them (about 150 drops) were required to fill the capillary tube. The calculated results of the rate of mass transfer show a sharp decline in both the amount of copper extracted in small drops and the overall mass transfer coefficient. The conclusion from this would be that large drops (produced in 17 gauge needle size) facilitate a form of inner circulation which enhanced the rate of copper transfer and reduced the over all resistance to mass transfer. In contrast, the small drops (produced in 25 gauge needle size) acted as rigid spheres which eliminate or minimise any inner drop circulation which resulted in a sharp decrease on the amount of copper transferred per drop. These results are listed in table 5.6.

Drop flow rate effect on mass transfer characteristics was also examined in this work. Experiments were designed to increase the drop flow rate (150-200 drop/min) using the same needle size (21 gauge needle size) used in those experiments carried out at flow rate of 80 drops/min. This was achieved by increasing the nitrogen pressure on the organic phase reservoir. These experiments resulted in very small drops, which in size were more like those produced in a 25 gauge needle size, and hence the mass transfer properties were similar to those obtained in small rigid-like spheres listed in table 5.6 below:

Table 5. 6: The results of the drop size effect on the rate of mass transfer and the overall mass transfer coefficient.

Needle size	C_L cm	d_f	d_p cm	A_d cm^2	N_{AB} drop	t_r s	C^{in}_{aq} g/cm^3 $x10^3$	C^{out}_{org} g/cm^3 $x10^3$	N_a g/cm^2 $x10^6$	K_{ov} cm /s $x10^6$
17	95	80	0.362	0.412	40	9.82	3	0.589	3.64	1.22
17	95	78	0.348	0.38	45	9.54	3	0.575	3.52	1.18
17	95	81	0.372	0.437	37	10.1	3	0.593	3.67	1.23
21	95	82	0.331	0.342	51	8.80	3	0.561	3.65	1.22
21	95	76	0.331	0.356	50	8.65	3	0.546	3.55	1.19
21	95	81	0.331	0.356	50	8.72	3	0.559	3.60	1.21
25	95	79	0.229	0.164	160	9.12	3	0.538	2.25	0.752
25	95	80	0.233	0.171	150	9.71	3	0.552	2.22	0.743
25	95	80	0.235	0.173	147	9.23	3	0.561	2.40	0.803
21	95	157	0.236	0.175	145	9.34	3	0.562	2.37	0.794
21	95	180	0.229	0.166	157	9.65	3	0.539	2.15	0.721
21	95	200	0.228	0.163	161	9.65	3	0.538	2.12	0.711

5.4 MICROPOROUS HOLLOW FIBRE MEMBRANE DATA ANALYSIS

This section discusses in detail the results of copper extraction and stripping in a MPHF membrane. The results listed in chapter four are analysed in line with the main objective of this work which highlights the main factors governing the extraction process in a hollow fibre membrane contactor. Thus, this section will cover the changes in operating conditions and their effect, if any, on the main extraction process parameters such as both phases outlet concentrations, the rate of mass transfer of the metal and the overall resistance in a membrane based reactive extraction. Further this part also contains proposed mathematical models for the design of a MPHF membrane extractor for copper recovery from wastewater streams.

5.4.1 The effect of the aqueous and the organic phase flow rate on the outlet steams concentrations

The results of studying the effect of the two phases counter current flow rate pattern on the extract and raffinate streams' concentrations can be divided in to the following areas:

Case one: *high flow rate of both phases*

The results obtained at 600cm^3/min at both sides show a linear increase in copper concentration at the organic extract outlet with an increase of the metal concentration in the feed stream, see figure 5.6. This could be attributed to the fact the at high flow of both phases the availability of the metal ions and the chelating active reagent at the interface (the pores mouths) would be at their highest. Then the only factors affecting the metal transport would be the reaction mechanism and the membrane thickness.

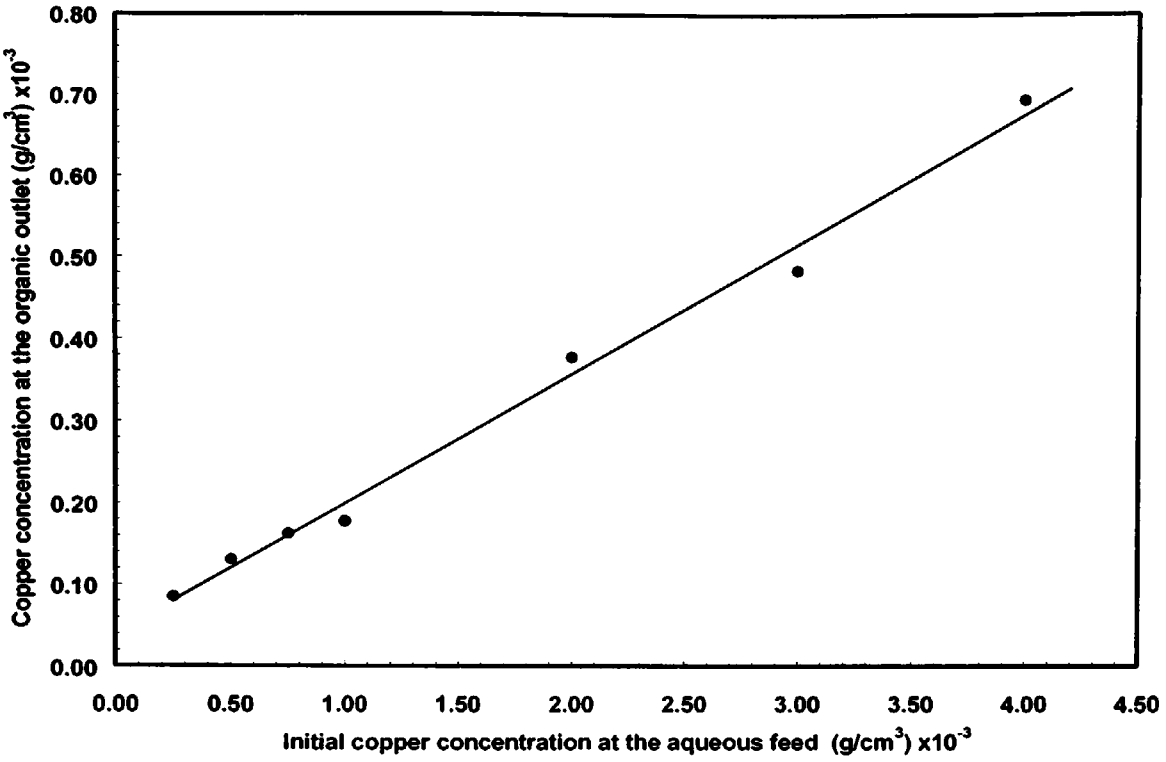

Figure 5. 6: The relationship between copper concentration at the aqueous feed and its concentration at the organic extract under high flow rate of both phases.

Case two: *low flow rate of both phases*

In this part the two phases were pumped at low flow rate of a 100 cm^3/min. The effect of this type of flow rate can clearly be observed in figure 5.7. Where the concentration of copper intake to the extract phase was in some experiments 75% less than the concentration obtained under high flow rate conditions. Figure 5.7 also shows that the straight-line relationship between the initial metal concentration and its concentration at the organic outlet has a different gradient from that resulted for high flows. This may be caused by the boundary layer thin film resistance which could be formed under low flow rates. The thickness of the thin films inside and outside the hollow fibres would be significant at low flow rate and have a direct effect on hindering or reducing the mobility

of the reactive species and the formed (Cu-LIX) complex into and away from the interface area respectively, and consequently reduces the rate of mass transfer across the membrane surface.

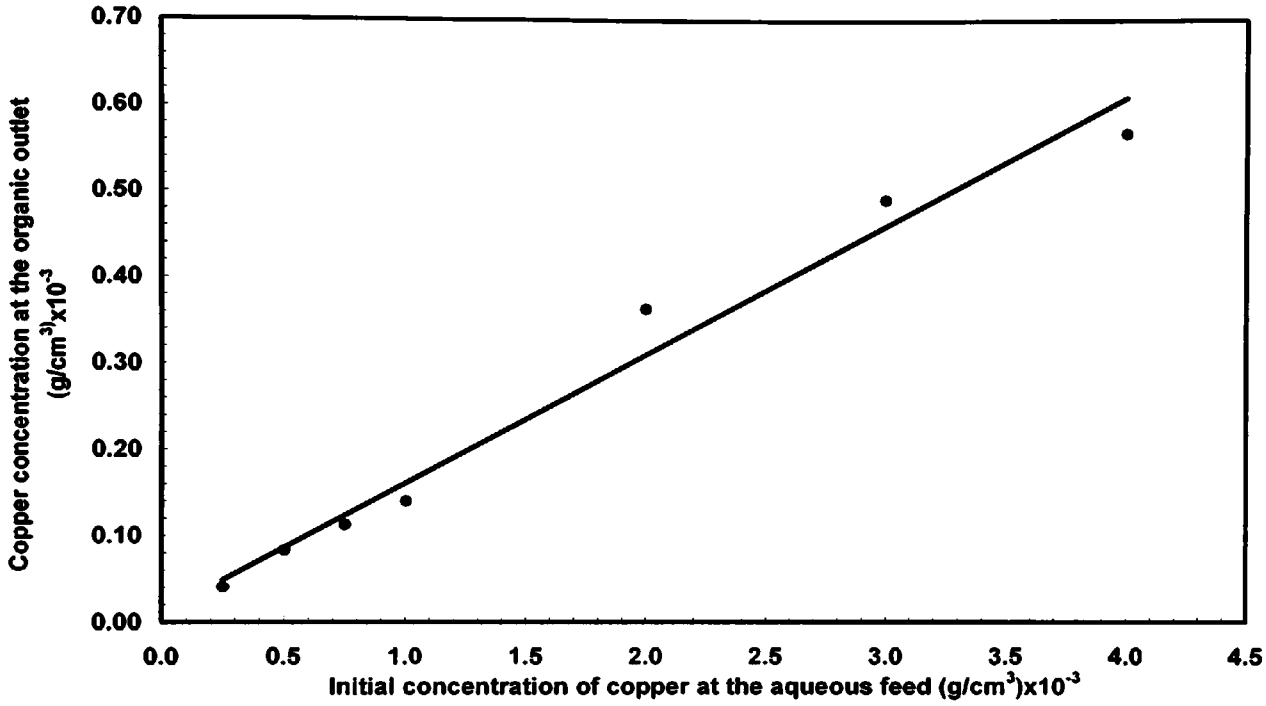

Figure 5. 7: The relationship between copper concentration at the aqueous feed and its concentration at the organic extract at low flow rate of both phases.

***Case three**: one phase at high flow rate while the other phase has a variable flow rate*

The effect of gradual flow rate increase at one side i.e. in the tube side or the shell side while the opposite side flow was kept constantly under a high flow rate have been studied thoroughly in this work. The objective of this excise was to determine which of the two phases would have the most resistance to mass transfer and under what flow rate conditions. Beside the gradual variation in flow rate studied here, the metal concentration at the feed aqueous phase was also taken into consideration, hence coupled low flow and low copper concentration at the feed side would result in more resistance to mass transfer.

The experimental work in this area focussed on detecting the outlet stream copper concentrations changes at the high flowing phase with the variations on the opposite phase flow rate. These results can be explained as follows:

1. In the case of high aqueous flow rate and gradually increasing organic flow rate it has been found that copper concentrations at the raffinate side were decreasing with every increase in the organic phase flow rate. However, these decreases varied with the initial aqueous phase copper concentrations. In experiments with a low aqueous feed initial metal concentration, the raffinate phase metal concentrations decreased in only small magnitude with each increase in the organic flow rate side. In contrast copper concentrations were decreased significantly at the outlets of highly concentrated initial aqueous phase, see figure 5.8A. These variations in the amount of unextracted copper could be related to the fact that for an aqueous feed with low initial metal concentrations the availability of metals ions at the interface will be minimal. Therefore, in spite of the aqueous feed high flow rate the gradual increases in the organic phase flow rate beyond 300cm^3/min would not be beneficial or effective for the extraction of metal from low initial concentration stream. But it seems that high flow rate in both sides 600cm^3/min would be very effective for copper extraction from a highly concentrated aqueous phase.

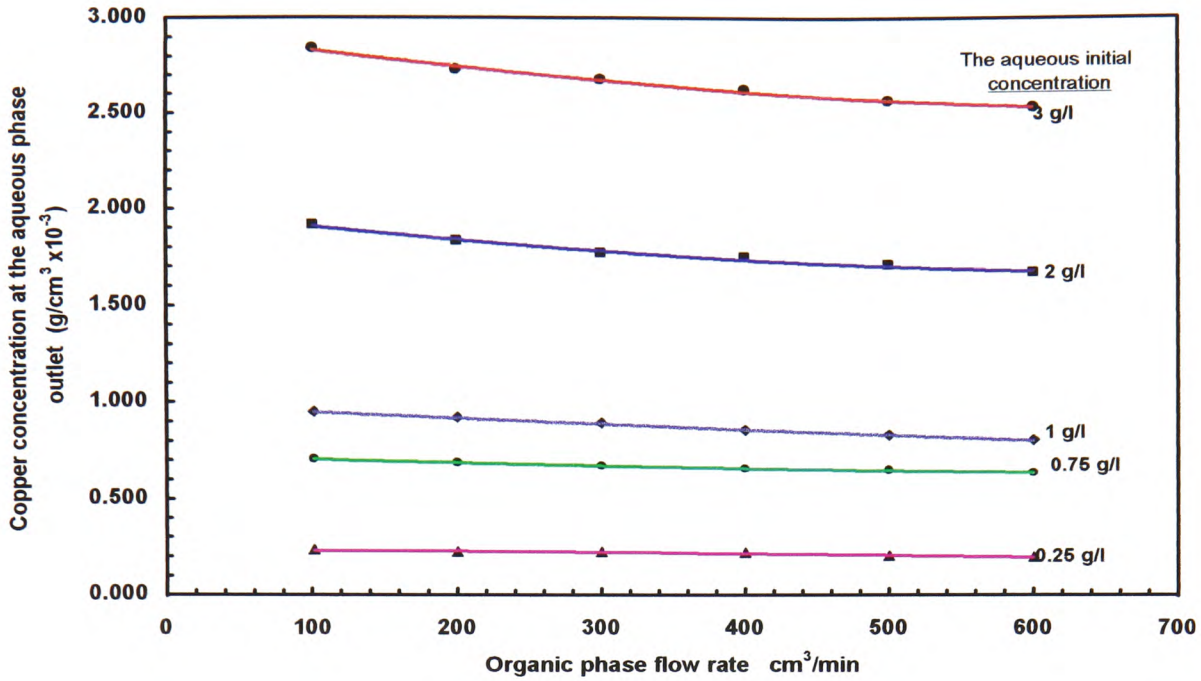

Figure 5.8. A: The relation between the aqueous phase outlet copper concentrations at high aqueous flow rate and gradually increasing organic phase flow rate.

2. In the case of high organic flow rate and the gradually increasing aqueous flow rate, the relationship between copper concentrations at the extract side and the increasing aqueous flow rate shows that each aqueous flow rate increase will result in a corresponding increase at the organic outlet (extract) metal concentration. The results obtained under these conditions show that even at low aqueous feed flow rate and low initial concentration the organic solvent could still extract between 10 to 40% of the inlet copper concentration. This could be attributed to the reduction of the resistance at the organic side of the MPHF membrane where the high organic flow could eliminate most of the thin layer film in the shell side. While the gradual increase on the aqueous phase flow rate would lead to the reduction of the film resistance at the tube side. Figure 5.8.B, shows that further increases in the aqueous side flow rate beyond

500cm^3/min did not lead to a large increase in the extracted copper concentration at the organic outlet especially when the aqueous phase initial concentration was low. This could be caused by the presence of some limiting resistance at the aqueous side even under high flow rate conditions.

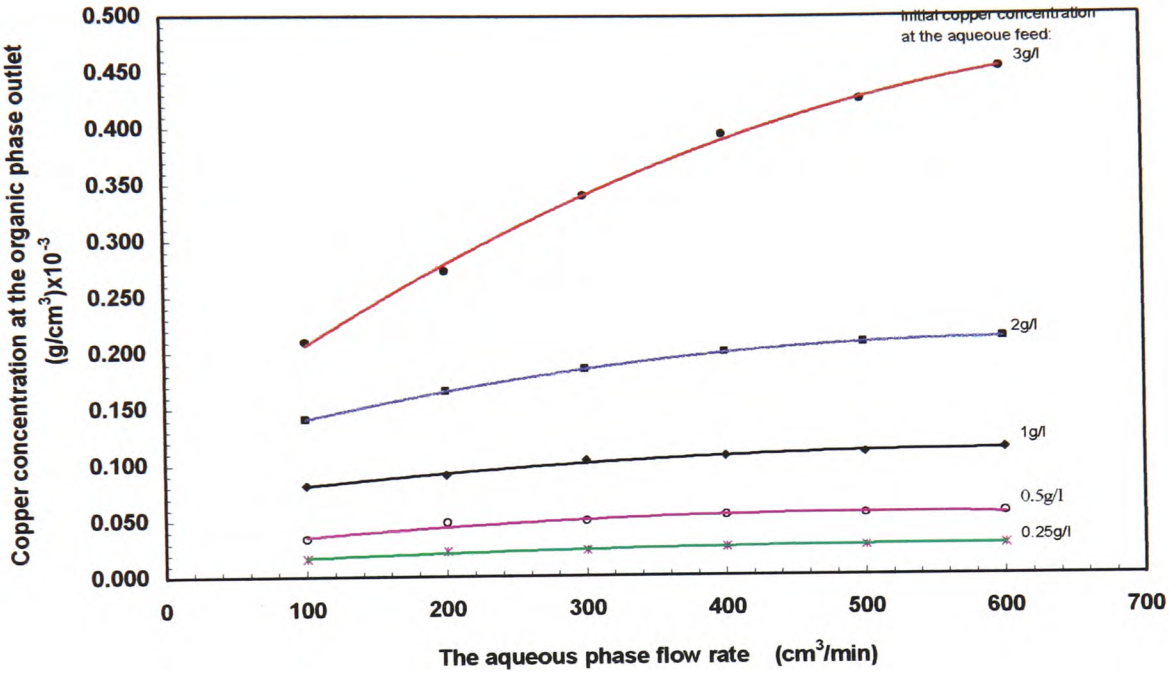

Figure 5.8. B: The relation between the organic phase outlet copper concentrations at high organic flow rate and the gradually increasing aqueous phase flow rate.

Case four: one phase at low flow rate while the other phase at variable flow rate

In this study low flow rate effects on metal extraction process efficiency through the MPHF module have been investigated. The results of this process can be summarised as follows:

In the case of low aqueous flow rate and gradually increasing organic phase flow rate it has been found that with each increase in the organic flow rate the raffinate metal concentration declined sharply. The relationship between the aqueous outlet (raffinate)

copper concentration and the organic phase flow rate appears to be a straight line relationship when the feed aqueous solution copper content is high and takes a non-linear form under low initial aqueous phase concentrations as in figure 5.9.A. This could be interpreted in relation to the resistance inside the tubes which had little effect on metal transfer when the metal initial concentrations are high and it caused non linear pattern when the initial metal concentrations were low. Therefore, the higher the organic solvent flow rate the more copper could be extracted. While at low concentrations i.e. 0.25 to 1g/l the resistance at the tube side appeared to have visible influence on reducing the metal transfer across the membrane.

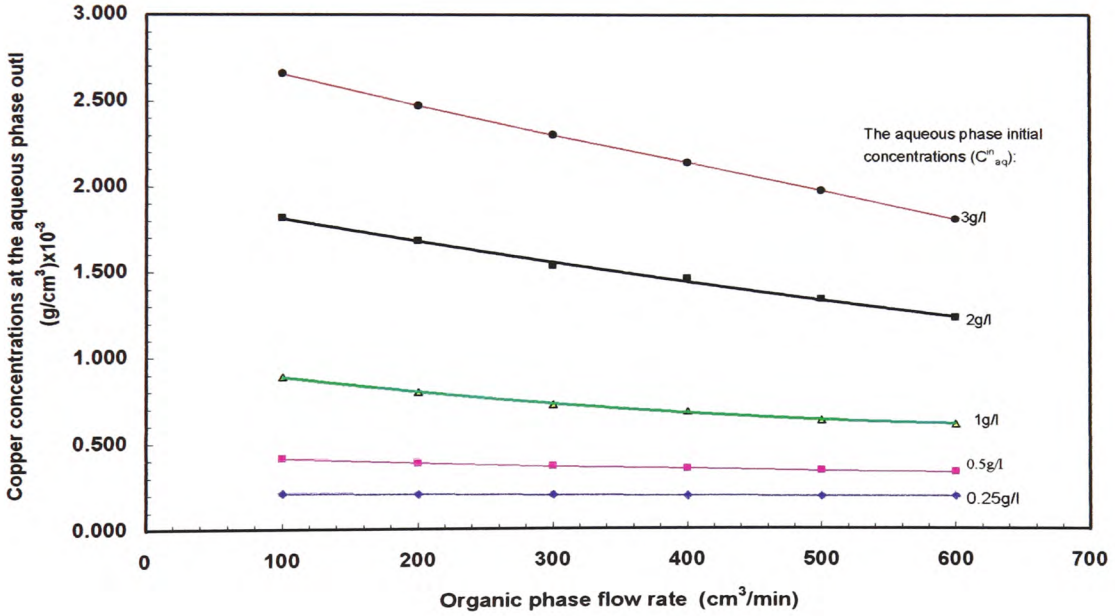

Figure 5.9. A: The relation between the aqueous phase outlet copper concentrations at low aqueous flow rate and changing organic phase flow rate.

1. The results of low organic flow rate and gradually increasing aqueous flow rate show that the extracted metal concentration at the organic phase outlet (extract) has increased with each increase at the aqueous feed stream, see figure 5.9.B. However, the extracted

amount of copper in this case was less than that obtained under high organic flow rate and increasing aqueous flow rate discussed earlier. The copper concentrations at the extract phase resulted under this flow arrangement would be higher than that obtained under high organic flow rate and varied aqueous flow rate due to the low organic phase flow rate. Further, the relationship between the extract phase copper concentrations and the aqueous feed increasing flow rate resulted in a non-liner relationship which reflected small changes in copper concentrations at the organic outlet, especially at the flow rate region between 500 to 600cm^3/min. This non-linear relationship could reflect two predictions: (a) that the availability of the organic active species at the interface was scarce due to the limited volumetric flow and/or (b) that due to the low flow rate condition at the shell side a thin organic boundary layer developed which caused significant resistance to metal transfer across the membrane wall to the organic bulk phase.

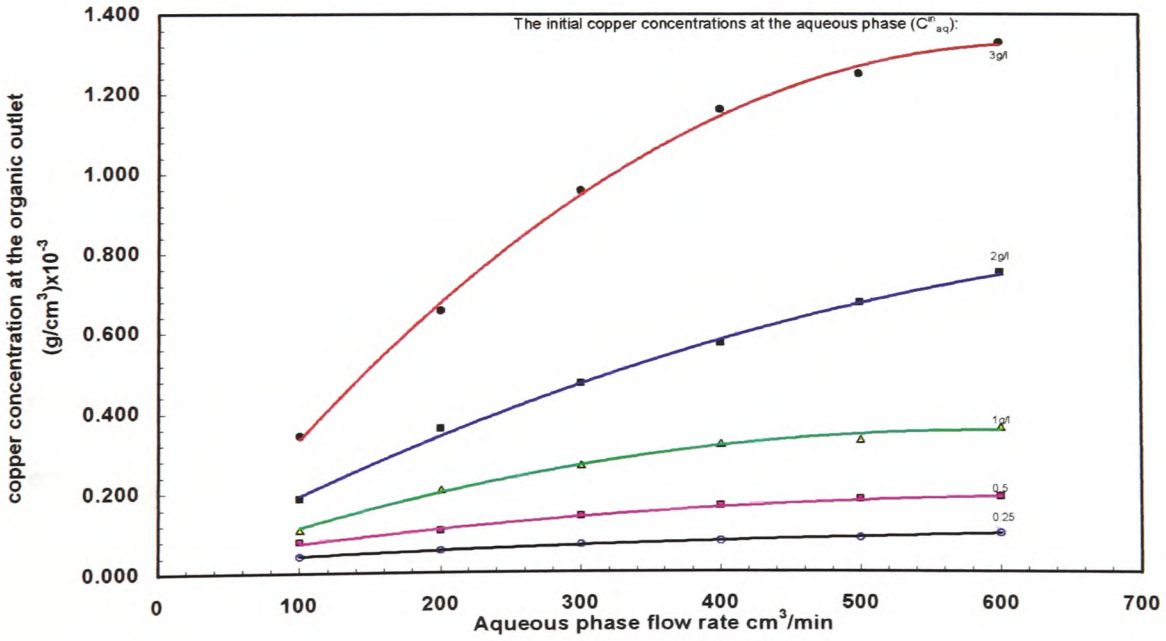

Figure 5.9. B: The relation between the organic phase outlet copper concentrations at low organic flow rate and the gradually increasing aqueous phase flow rate.

5.4.2 The effect of changing the flow direction and the two phases positions in the MPHF membrane based extraction process

The effects of changing the two phases flow pattern at the MPHF module from counter current to co-current on copper extraction have been examined in this study. Further the influence of switching the two phases positions within the module (i.e. the aqueous phase was pumped in the shell side instead of the tubes lumen while the organic solvent was pumped in the tube side) has also been investigated. The results of this co-current continuous extraction process were listed in tables 4.16 to 4.21. These results can be explained as follows:

1. Under high flow rate condition of both phases the continuous co-current extraction resulted in a straight-line relationship when the initial concentrations of metal at the aqueous phase were drawn against the corresponding extracted concentrations at the organic outlet, see figure 5.10. However, it has been found that the amount of copper extracted under these conditions was about 2% less than that extracted using the counter current process from aqueous feed with low initial concentrations. Furthermore, the amount of copper extracted in the co-current arrangement was found to be around 4% less than counter current process at high aqueous feed concentrations. This variation could be attributed to the general fact that counter current flow arrangement gives higher driving force which reflected in form of transfer rate and hence a higher extract concentration along the contact surface area.

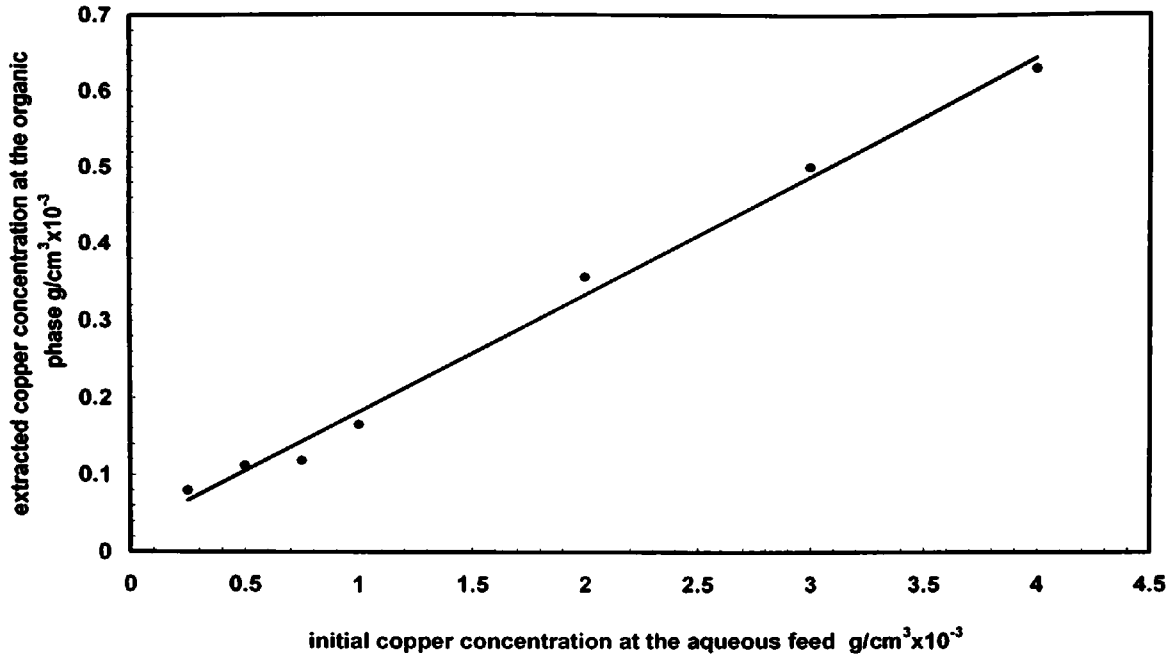

Figure 5. 10: The relationship between copper concentration at the aqueous feed and its concentration at the organic extract under co-current high flow rate of both phases.

2. The aqueous phase initial copper concentrations drawn verses the organic outlet copper content under low flow rate co-current extraction, gave a non-linear relationship, see figure 5.11. In addition it has been found that the amount of copper extracted from low concentrated feed solutions was about 4% to 5% less than that extracted in counter current arrangement from the same feed and approximately 16% less in the case of high concentrations feed solutions. The departure from the linear relationship found under these conditions could be related to the influence of both phases' resistances which would be apparent under low flow conditions. While the variations of the extracted copper concentrations from that observed in the counter current arrangement could be attributed to the weakness of the driving force between the bulk phases and the reaction interface inside the pores mouths.

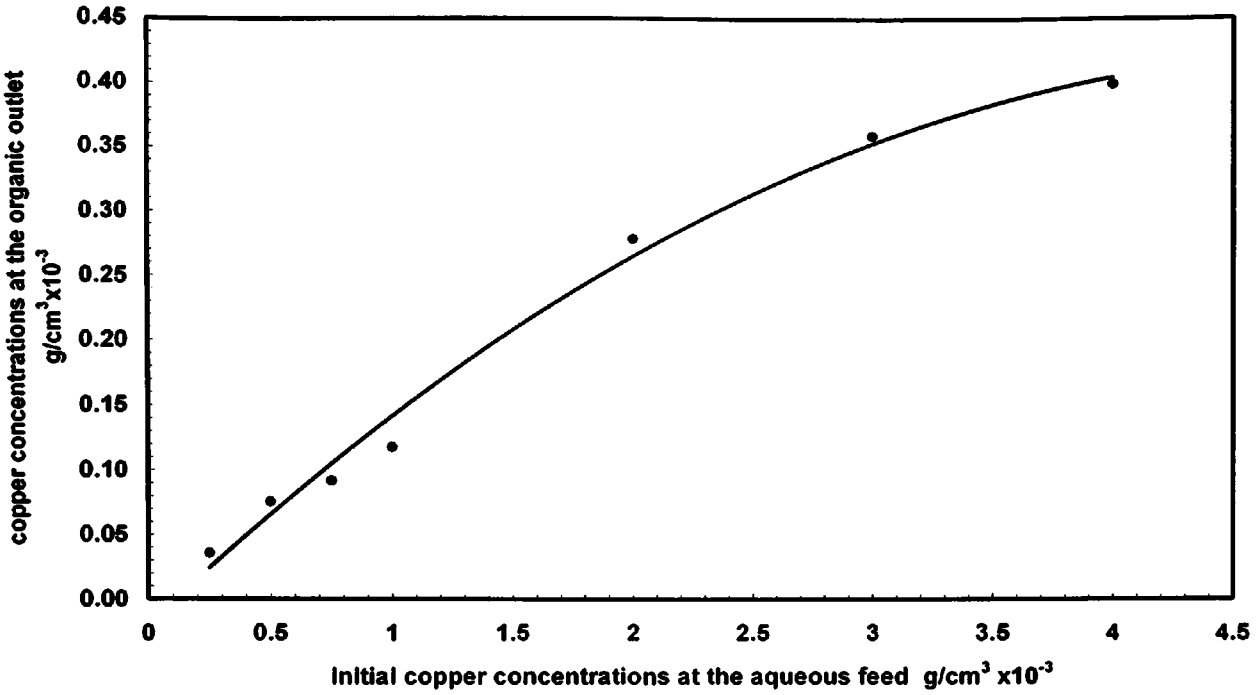

Figure 5. 11: The relationship between copper concentrations at the aqueous feed and its concentration at the organic outlet at co-current low flow rate of both phase.

3. The results of co-current extraction carried out under constant flow rate (high or low) of one phase while the other phase flow rate increased gradually can be described as follows:

(a) In the case of a high flow rate of aqueous feed and gradually increasing organic solvent flow, the relationship obtained for the organic flow rate against the copper raffinate concentrations was similar to that illustrated in figure 5.8.A. However, the copper concentrations in the raffinate solution produced in the co-current extraction appeared to be slightly higher than those obtained under counter current extraction. A similar pattern of results were observed when the process was carried out under a high organic flow rate and gradually increasing aqueous feed flow, see tables 4.18 and 4.20.

(b) In the case of one phase at a constant low flow rate ($100cm^3/min$) and the opposing phase flow rate gradually increased, it has been found that the main resistances to mass transfer would be the availability of the reactive species at the low flowing phase boundary near the interface. Further the boundary layer thickness in the shell or tube side during low flow seems had an added effect in reducing the amount of extracted copper during co-current extraction in comparison to that amount extracted at counter current.

The experimental work on switching the two phases positions within the MPHF module produced similar results to those obtained under co-current conditions in particular when the organic phase was pumped at high flow rate. However, under relatively high organic phase concentration 20v/v% LIX984 and beyond the extraction process showed no large increase in the amount of copper extracted, see table 5.7. This shortcoming could be attributed to the increase in the organic phase viscosity at high LIX content, which might have resulted in increasing the boundary layer thickness in the tubes side and consequently increasing the resistance to metal transfer from the shell to the tube side. Further, the relationship between the initial aqueous phase copper concentrations and copper concentrations at the extract phase appeared to be non-liner as illustrated in figure 5.12.

Table 5. 7: Results of copper extraction under co-current high flow rates of both phases when the aqueous flows at the shell side and the organic in the tube side of the MPHF membrane (average of runs).

Organic phase concentrations:		**10v/v%LIX984**			**20v/v%LIX984**	
F_{org} cm^3/min	F_{aq} cm^3/min	C^{in}_{aq} g/cm^3 $x10^3$	C^{out}_{aq} g/cm^3 $x10^3$	C^{out}_{org} g/cm^3 $x10^3$	C^{out}_{aq} g/cm^3 $x10^3$	C^{out}_{org} g/cm^3 $x10^3$
600	600	0.250	0.178	0.072	0.158	0.092
600	600	0.500	0.393	0.107	0.365	0.135
600	600	0.750	0.641	0.109	0.598	0.152
600	600	1.000	0.854	0.146	0.802	0.198
600	600	2.000	1.657	0.343	1.579	0.421
600	600	3.000	2.538	0.462	2.468	0.532
600	600	4.000	3.476	0.524	3.419	0.581

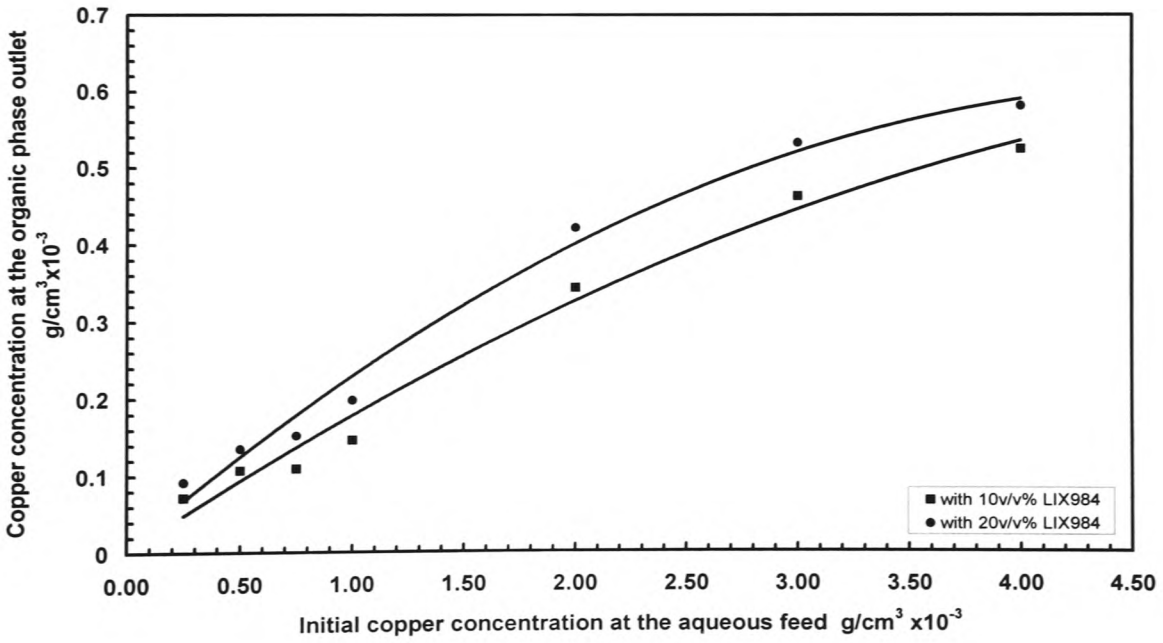

Figure 5. 12: The relationship between the aqueous feed initial copper concentrations and extracted copper concentrations at the organic phase outlet when the aqueous phase flows co-currently at the shell side while the organic at the tube side.

5.4.3 The effect of both phases flow rates on the batch extraction process performance of a MPHF membrane

The effect of the two phases flow rate patterns on the effectiveness of the batch extraction of copper in a MPHF module have been investigated in this work. The results of this process (Batch extraction under different flow rates conditions) are summarised in tables 4.22 to 4.25 and can be analysed as follows:

(a) In the case of counter current batch extraction with high flow rates at both sides of the MPHF the process has resulted in the recovery of 60% to 80% of the feed copper content in two hours and 40 minutes. However, it has been noticed that the reduction on the raffinate copper concentrations was significantly low after 2 hours of continuous extraction, see figure 5.13. This could be caused, in the case of a low concentration aqueous feed, by the lack of copper ions availability at the interface area after a large portion of them have been extracted in the early stages of the process. While in the case of high concentration aqueous feeds the small concentration changes in the raffinate phase after 2 hours could be caused by the near-saturated organic phase. In the latter case the metal-LIX complex may have formed a thin film layer on the shell side, which in turn could lead to the reduction of mass transfer. In this stage of the batch extraction improved performance may be obtained either by adding fresh LIX to the organic feed tank or using a more concentrated organic phase.

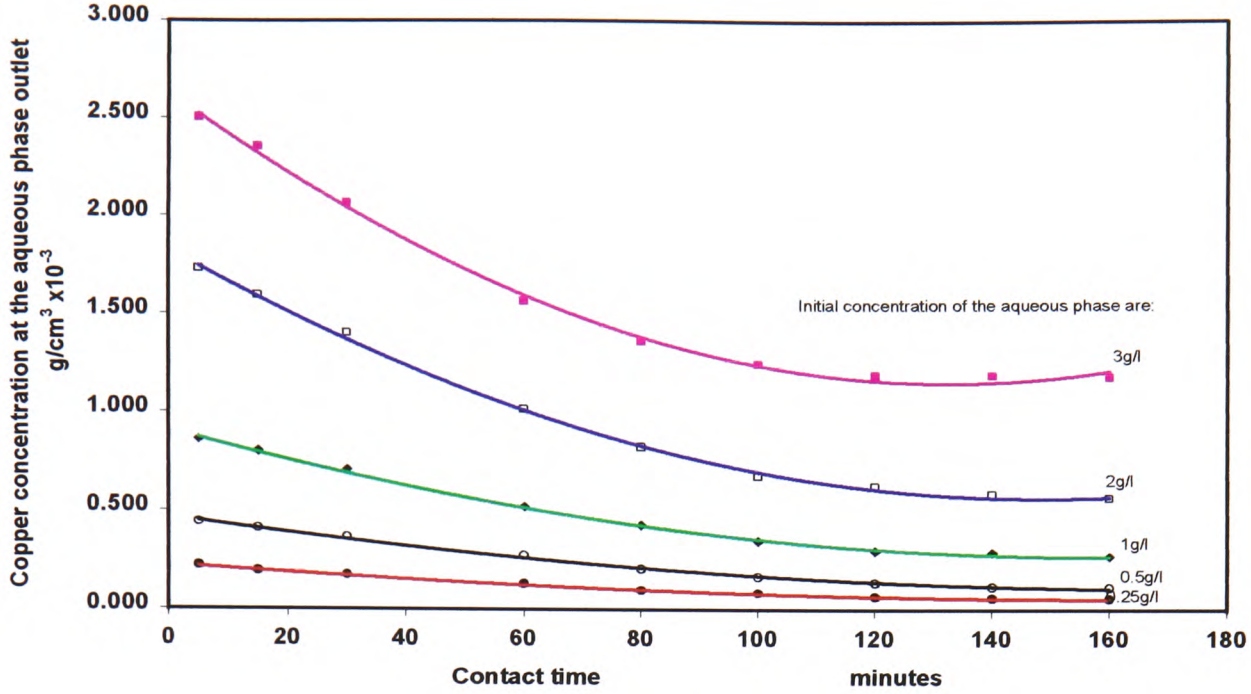

Figure 5. 13: The relation between copper concentrations in the raffinate and the contact time of batch extraction under high flow rates of both phases and at different aqueous feed concentrations.

(b) While in the case of batch extraction of copper under low flow rate of both phases it has been found that copper concentrations at the raffinate phase would remain higher than those obtained at the same contact time under high flow condition, see figure 5.14.A. These results could be attributed the presence of high resistance caused by the thin film layer at both sides of the MPHF membrane. It has also been observed that the reduction at the aqueous phase outlet concentrations was very little beyond the first two hours of continuous extraction. This pattern was noticed at all studied levels of aqueous feed concentrations and could be caused by the lack of sufficient diffusion of the active organic species from the organic bulk in the shell side to the interface area inside the pores.

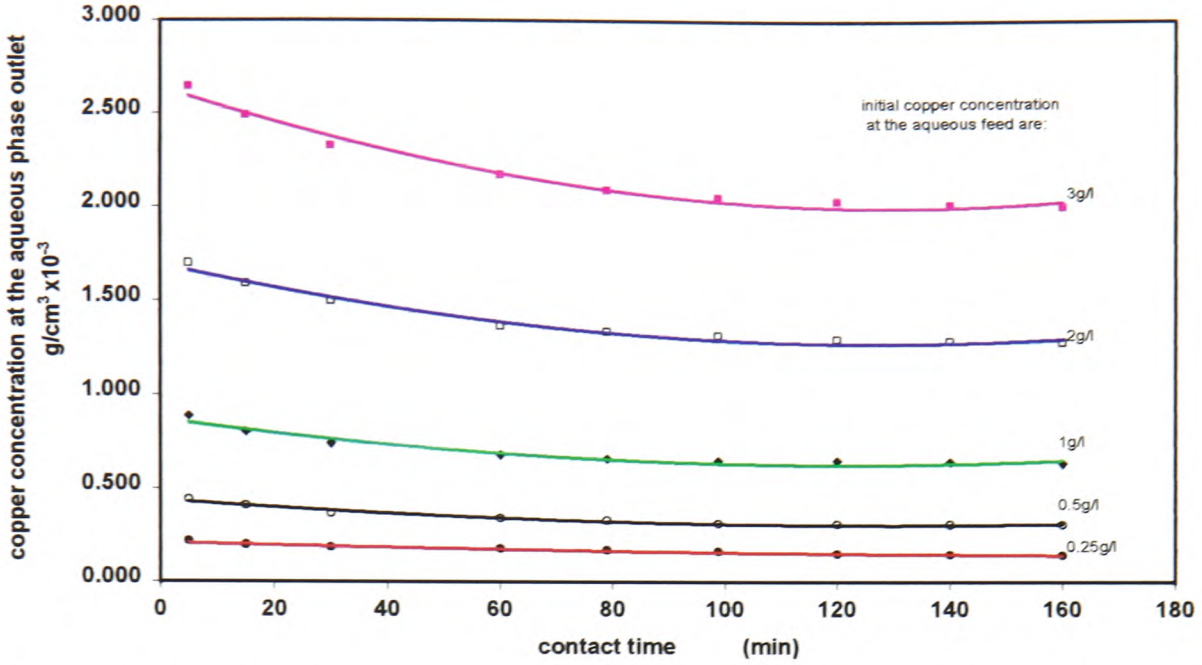

Figure 5.14. A: The relation between copper concentrations at the raffinate and the contact time of batch extraction under low flow rate of both phases and at different aqueous feed concentrations.

(c) Batch extraction was also studied in this work under a high flow rate for one of the phases while the opposite phase flow rate was kept low throughout the process. The result of this process can be summarise as follows:

1. In the case of a high organic flow rate contacted against a low aqueous phase flow rate over wide range of aqueous feed initial concentrations, it has been found that between 50 to 70% of the feed copper concentrations were removed over 2 hours to 2 and a half hours. This may be as a result of the high flowing organic phase, which could eliminate the resistance at the shell side of the MPHF membrane, see table 4.24 and figure 5.14.B. Further the high flowing organic facilitated easy diffusional mass transfer of

the extracted copper and the active LIX reagent into and from the bulk organic phase respectively.

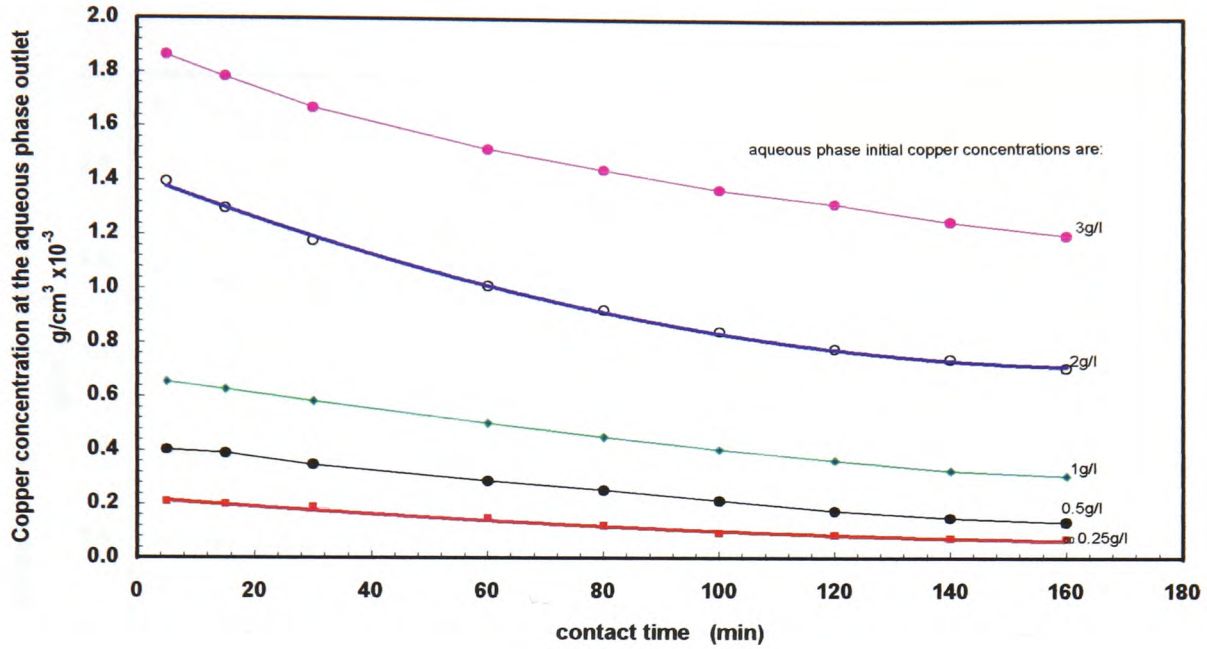

Figure 5.14. B: The relation between copper concentrations in the raffinate and the contact time of a batch extraction under a high organic phase flow rate and a low aqueous feed flow rate over range of aqueous feed initial concentrations.

2. When the organic phase flow rate was kept low while the aqueous phase flow rate was high it has been found that only approximately 10 to 15% of the aqueous feed copper content was extracted for the same range of feed concentrations studied above, see table 4.25. Further it has also been noticed that the metal concentrations in the aqueous outlet stream changed very little in the last hour of the extraction process, see figure 5.14.C. This pattern of results was also noticed in the co-current and counter current continuous extraction system and can be attributed to the high resistance at the organic

side which it seems in this work has the most noticeable effect on the two phases outlet concentrations.

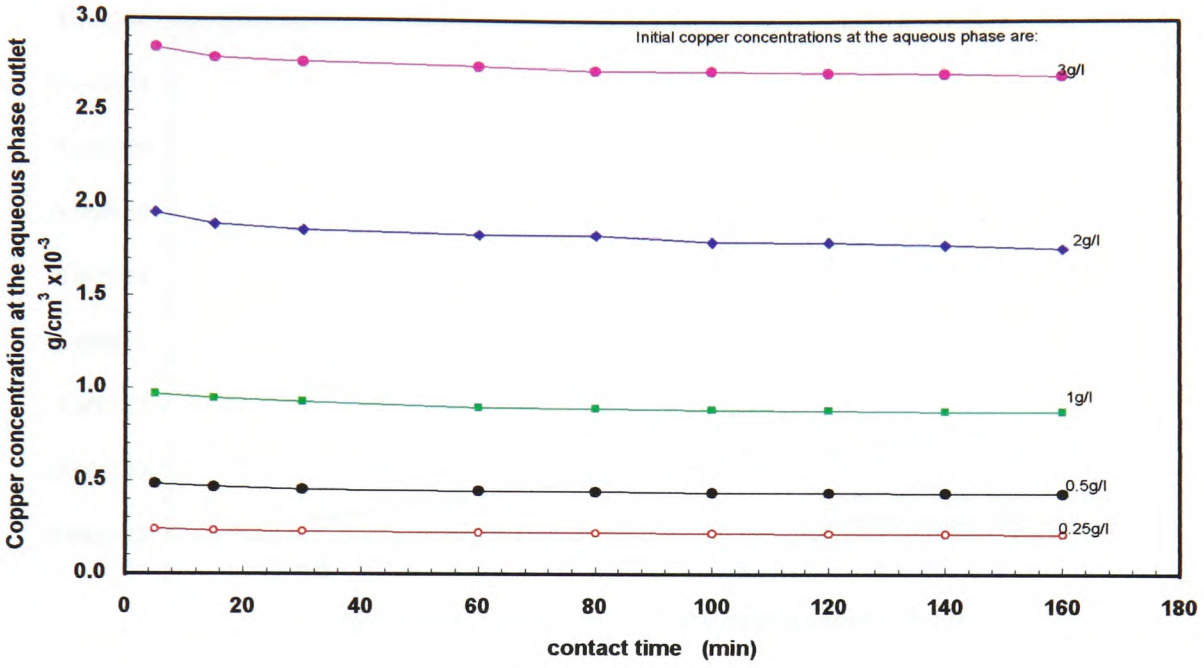

Figure 5.14. C: The relation between copper concentrations in the raffinate and the contact time of a batch extraction under a low organic phase flow rate and a high aqueous feed flow rate over range of aqueous feed initial concentrations.

5.4.4 The relationship between the two phases initial concentrations and the rate of mass transfer in MPHF membrane based extraction

The effect of both phases' initial concentrations on the rate of mass transfer of copper in a continuous extraction process using the MPHF membrane was studied intensively in this work. It has been found that increasing the aqueous feed initial concentration always led to direct increase in the rate of mass transfer of copper across the membrane wall. Noticeably the rate of mass transfer under high flow rates of both phases was approximately 5 to 8 times higher than that obtained under low flow rate conditions, see table 4.26 and figure

4.15.A. This large increase in the rate of metal transport may be related to the local thin film resistances at the shell and tube sides, which could be reduced significantly under high flow rate at both sides.

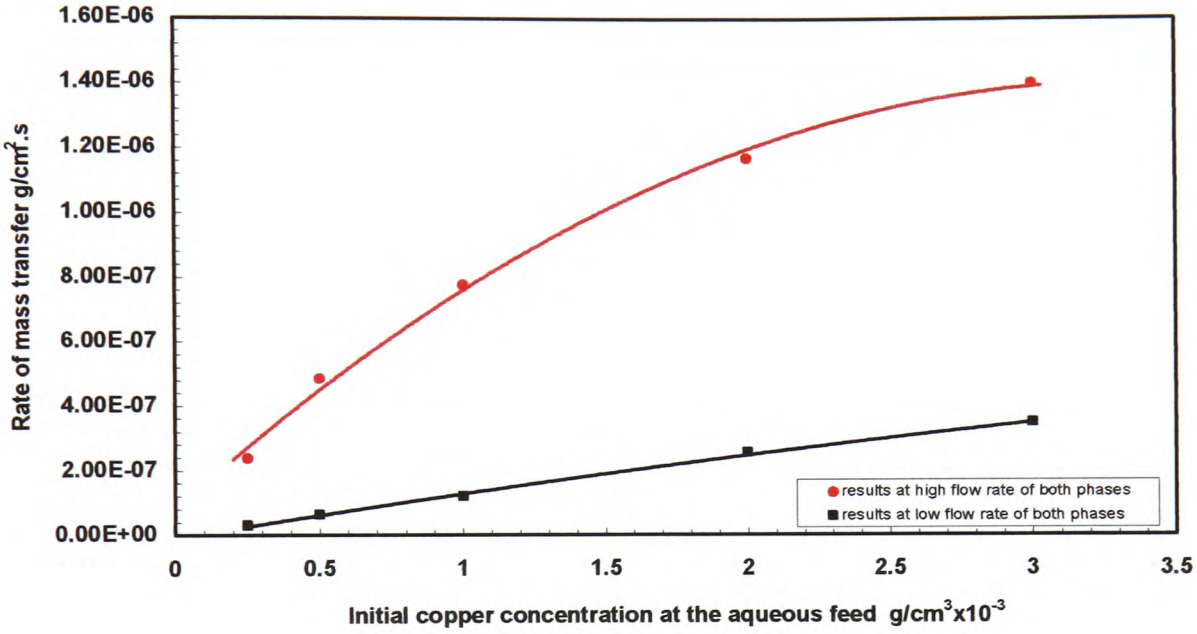

Figure 5.15. A: The relation between the aqueous feed initial concentrations and the rate of mass transfer of copper under high and low flow rate conditions at the shell and tube sides.

In the case of the organic phase (LIX984) initial concentration variations, the effects on the rate of mass transfer of a MPHF membrane based continuous extraction process can be drawn from figure 5.15.B and table 4.27 and summarised in following points:

1. The rate of copper transport through the membrane porous surface initially increased with each increase in the LIX984 concentrations at the organic phase. However the rate magnitude increased very little when the LIX984 concentration ranges between 15 to 20v/v% and beyond.

2. At high flow rates of both phases (600cm^3/min aqueous/600cm^3/min organic), it has been found that the rate of copper transfer has increased approximately 5 to 7 fold to the rate obtained under low flow rate conditions, see table 4.27.

3. The relation between the rate of mass transfer and the organic phase initial concentration was found to be non-linear especially when the aqueous phase was at a high flow rate and a high concentration, see figure 5.15.B.

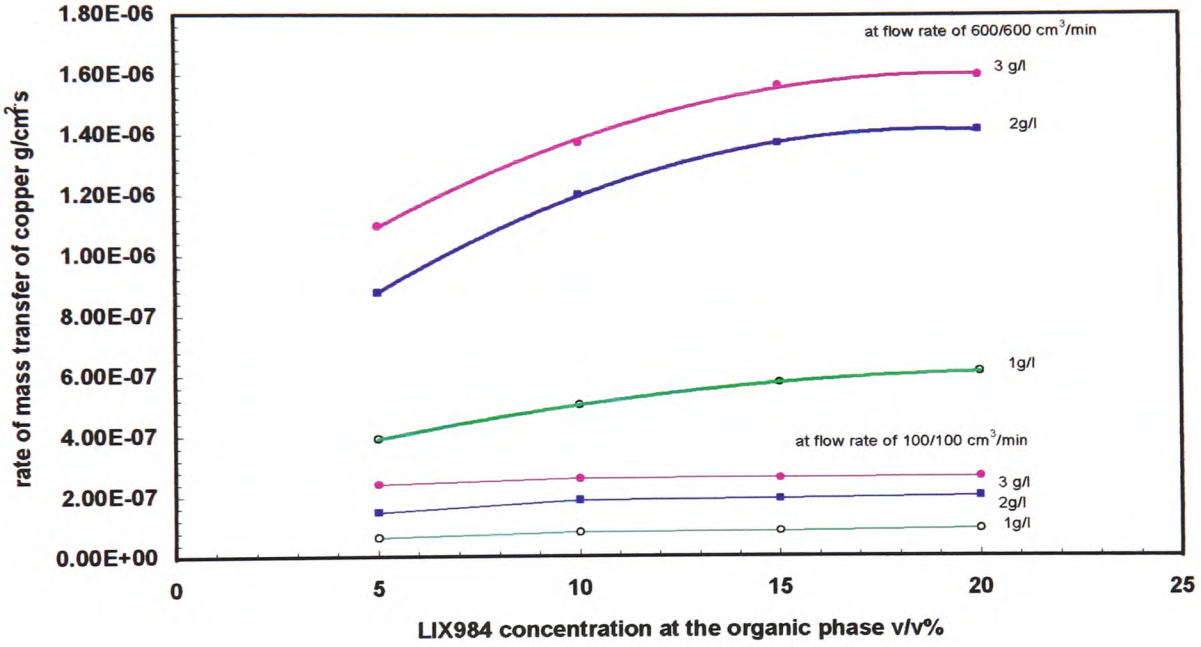

Figure 5.15. B: The relation between the organic phase initial concentrations and the rate of mass transfer of copper under high and low flow rate conditions at the shell and tube sides.

5.4.5 A generalised mathematical model to predict the overall mass transfer coefficient in a MPHF membrane base extraction

In a MPHF membrane-base liquid-liquid extraction system, the overall mass transfer coefficient (K_{ov}) can be treated as function of the individual mass transfer coefficients in the feed phase, at the reaction interface, across the membrane wall and in the organic phase. Therefore, resistance to copper transfer from the tube side to the shell side in a MPHF membrane can be expressed in form of the sum of all resistances as follows:

$$\frac{1}{K_{ov}} = \frac{1}{k_{aq}} + \frac{1}{mk_m} + \frac{1}{k_r} + \frac{1}{mk_{org}} \qquad 5.25$$

Previous studies on the calculation of the overall mass transfer coefficient across immobilised aqueous-organic interface in membranes have dealt only with either non reactive extraction or specific set of physical conditions [111,132,133] and empirical correlations [119] to account for the overall mass transfer coefficient and local coefficients.

In this study a model was developed based on the thin film theory and the previously cited literature to predict the overall mass transfer coefficient of membrane based extraction. This model was devised to account for all individual local coefficients under a wide range of conditions for a counter current continuous mode extraction process. From the results discussed in the earlier section (5.4.1) it has been noticed that there was a direct relation between the two phases flow rates and the rate of metal extracted which was attributed to the effect of the phases flow pattern on the local resistances. Based on these findings a relationship is proposed using Wilson's method [134] and the experimental data to relate the overall resistance ($1/K_{ov}$) and the flow rates of both the aqueous phase at the tube side ($1/F^n_{aq}$) and the organic phase at the shell side ($1/F^n_{org}$). Plotting the relationship between ($1/K_{ov}$) and $1/F^n_{aq}$ or $1/F^n_{org}$) with the exponent n value ranging between (0.1 to 0.9)

resulted in a straight-line relation only when the value of n was 0.33 for the tube side and 0.75 for the shell side.

The MPHF membrane wall resistance ($1/k_m$) was reported by Kiani et al.,[122] and Prasad et al.,[125] to be proportional to: the diffusion coefficient (D_{Cu}) of the solute (Cu-LIX complex) in the organic solvent which wetted the hydrophobic fibres, the fibres thickness (t_m), their porosity (ε_m) and the pores tortuosity (τ_m). Therefore, the membrane module resistance at any point across the fibres' wall can be calculated as follows:

$$\frac{1}{k_m} = \frac{t_m \tau_m}{D_{Cu} \varepsilon_m} \qquad 5.26$$

Where D_{Cu}: is the diffusion coefficient of copper in the organic solvent (LIX984), cm^2/s.

t_m: is the membrane fibre wall thickness, ($t_m = d_{ot} - d_{it}/2$), cm.

d_{ot}: the fibre outer diameter, cm.

d_{it}: the fibre inner diameter, cm.

ε_m: is the membrane porosity.

τ_m: is the tortuosity of the membrane pores.

In this work it has been observed that under a combination of high flow rate and high concentrations of both phases, the rate of mass transfer would be at its highest value. Therefore, it could be presumed that the thin films boundary layers resistance at the shell side and the fibre tubes side are at their lowest under these conditions and hence could be neglected when accounting for the system resistances from the overall resistance equation. This will reduce equation 5.25 to:

$$\frac{1}{K_{ov}} = \frac{1}{m k_m} + \frac{1}{k_r} \qquad 5.27$$

Therefore, under these conditions the system's reaction resistance at the interface can be calculated from equation 5.27. For instance when a counter current extraction process was

carried out under a high aqueous phase flow rate of 600cm^3/min and a copper concentration of 3g/l at the tube side and a similar organic phase flow rate of 20v/v% LIX984 concentration at the shell side. The following resistance results were found:

- The overall resistance ($1/K_{ovf}$) found experimentally =1550.387 s/cm.
- The diffusion coefficient of copper (D_{Cu}) was calculated using the Wilk-Chang equation and was found to be = 4.19196×10^{-6} cm^2/s.
- The membrane porosity of and tortuosity were taken from the literature [107] as 0.3 and 2.3 respectively. While the distribution coefficient of copper ions at the interfaces (m) was taken as an average value of 21.222.
- Then the resistance across the membrane wall ($1/mk_m$) was calculated from equation 5.26 and found to be = 220.315 s/cm.
- This value was used in equation 5.27 to calculate the reaction resistance at the interface area: $1/k_r$ =1330.072 s/cm.

These values of the membrane wall resistance and the reaction resistance would not fluctuate under changes in concentrations or flow pattern of both sides. Therefore the value of $1/mk_m$ and $1/k_r$ were kept constant when used in Wilson's plot which was used to account for boundary layer resistances at the tube and shell sides under variation of flow and concentration conditions at the shell and tube sides.

Figure (5.16) and appendix 8 show Wilson's plot results of an aqueous phase flowing under variable flow rate against a constant high flow rate and high concentration organic phase. Under these conditions the boundary layer thickness would be minimal, hence the local resistance at the shell side could be neglected. Consequently the intercept of the relation ($1/K_{ov}$ vs $1/F_{aq}^{0.33}$) would represent the combined resistance of the aqueous phase boundary layer inside the fibre tubes, the membrane wall resistance and the reaction resistance. From

this intercept and the constant value of ($1/mk_m + 1/k_r$), the magnitude of the aqueous phase thin film resistance was determined over range of conditions, see appendix 8.

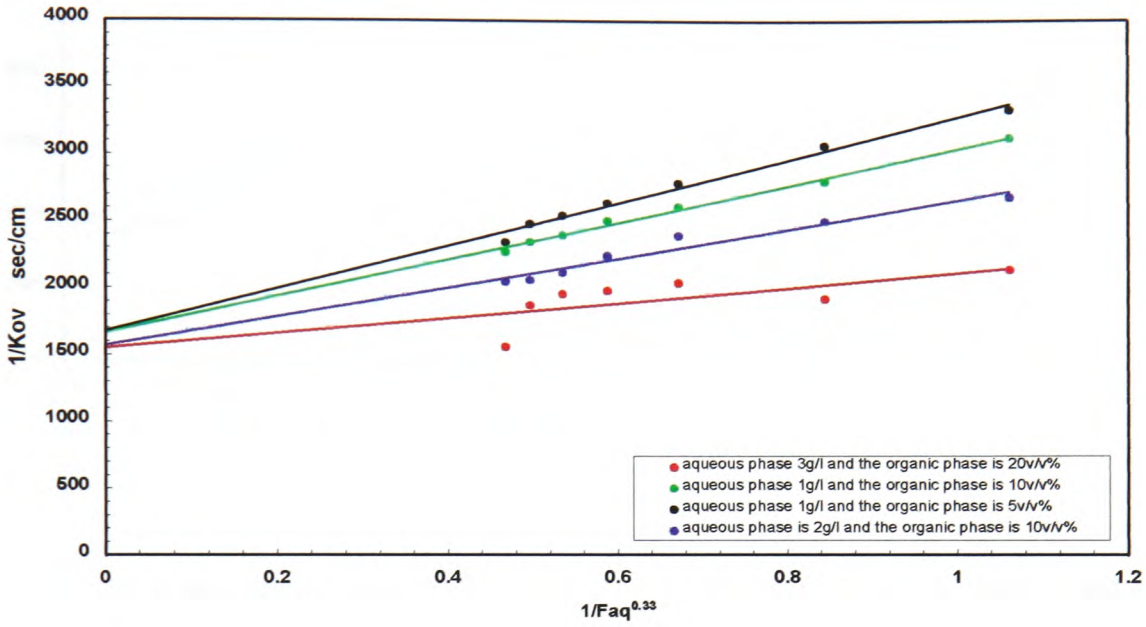

Figure 5. 16: Wilson's plot results for the tube side aqueous flow rate under different concentrations.

Figure (5.17) and appendix 9 show the results Wilson's plot for the shell side. In these experiments the organic phase flow rate and concentration were varied while the aqueous phase flow rate and concentration was kept high and constant to minimise or even eliminate any resistance at the tube side. The intercept of the straight-line relationship of ($1/K_{ov}$ vs $1/F_{org}^{0.75}$) would represent the combined resistance of the organic thin film boundary layer in the shell side, the membrane wall resistance and the reaction resistance. Then from this intercept and the constant value of membrane wall resistance and the reaction resistance, which was calculated earlier, the magnitude of the organic phase thin film resistance was determined under set of conditions, see appendix 9.

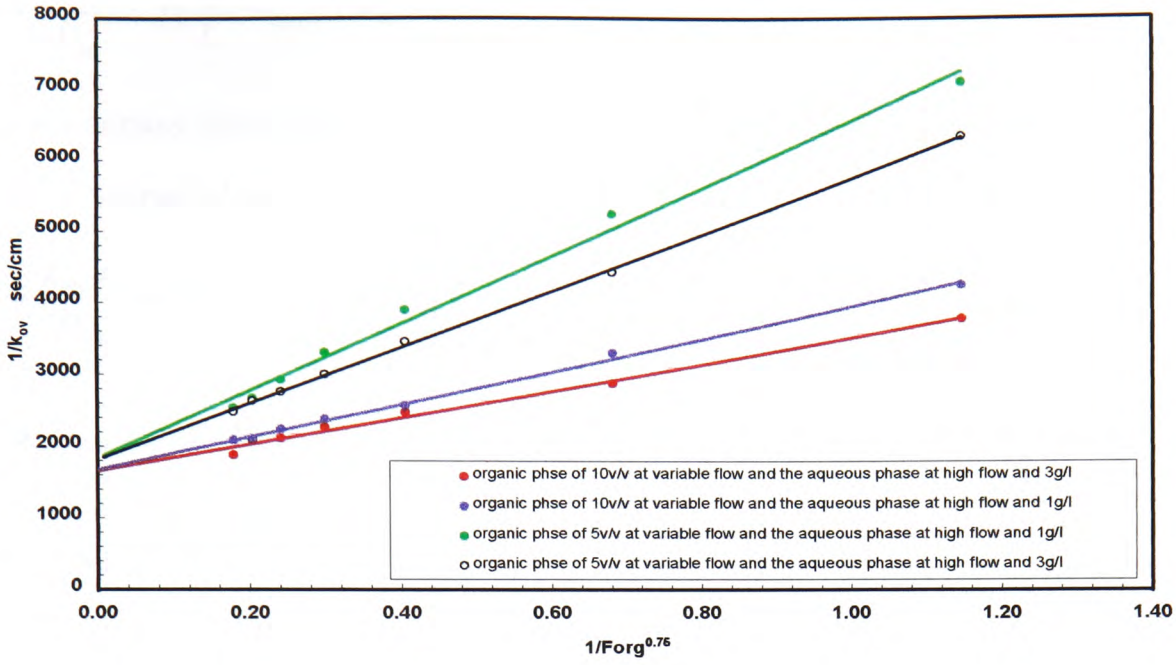

Figure 5. 17: Wilson's plot results for the shell side organic flow rate under different concentrations.

However, the use of Wilson's plot is not enough to predict local resistances especially when both phases flow rates were low or the concentrations of copper at the aqueous phase and the active reagent at the organic solvent were low. Therefore, the data gained from the relationship between the overall mass transfer coefficient and the flow rates of both phases ($1/K_{ov}$ vs $1/F^{n}_{aq}, 1/F^{n}_{org}$) were used to correlate and predict the overall mass transfer coefficient by using a dimensionless groups based model. This model was linked to the two phase's physical properties and the system's parameters using a form of Leveque equation to correlate more precisely the local coefficients at any set of conditions. This became effective by making use of Reynolds, Schmit and Sherwood numbers at both side of the MPHF membrane module.

The aqueous phase mass transfer (k_{aq}) in the tube side could be expressed in the form of the Sherwood number as follows:

$$N_{Sht} = \frac{k_{aq} d_{it}}{D_{aq}} = \gamma[\frac{d_{it}}{L}(N_{Ret})^a (N_{Sct})^b] \quad 5.28$$

While the organic phase mass transfer coefficient (k_{org}) in the shell side could be expressed in form of Sherwood number as follow:

$$N_{Shs} = \frac{k_{org} d_h}{D_{org}} = \beta[\frac{d_h}{L}(N_{Res})^a (N_{Scs})^b] \quad 5.29$$

Where: N_{Ret} = is the Reynolds number of the aqueous phase inside the fibre tube = $\frac{4F_{aq}}{\pi d_{it}\eta}$

N_{Res}= is the Reynolds number of the organic phase in the shell side = $\frac{4F_{org}}{\pi d_h \eta}$

N_{Sct} = is Schmidt number of the aqueous phase inside the fibre tube = $\frac{\eta}{D_{aq}}$

N_{Scs} = is Schmidt number of the organic phase in the shell side = $\frac{\eta}{D_{org}}$

N_{Sht}, = is Sherwood number of the aqueous phase inside the fibre tube = $\frac{k_{aq} d_{it}}{D_{aq}}$

N_{Shs} = is Sherwood number of the organic phase in the shell side = $\frac{k_{org} d_h}{D_{org}}$

F_{aq}, F_{org} = are the volumetric flow rates of the aqueous and organic phases Respectively, cm^3/s.

D_{aq}, D_{org} = is the diffusion coefficient of copper at the aqueous phase and the organic phase respectively, cm^2/s.

η = kinematic viscosity, cm^2/s.

L = is the membrane module length, cm.

d_{it} = is the fibre tubes internal diameter, cm.

d_h= is the shell hydraulic diameter which can be expressed as follows:

$$d_h = \frac{4 \times \text{the cross - sectional area of flow}}{\text{wetted perimetre (the outer circumference of the fibre tubes)}} = \frac{(d_{is}^2 - d_{ot}^2 \times n)}{d_{ot} \times n}$$

d_{is} = is the inner diameter of the membrane shell, cm.

d_{ot}= is the outer diameter of fibre tube, cm.

n = number of fibre tubes inside the membrane module.

a, b, γ and β = are constants.

The value of the exponent (a) was used as 0.33 for the fibre tube side and 0.75 for the shell side which was in line with the exponent of the flow found experimentally and used in drawing Wilson's plot earlier. These values also are in agreement with similar values suggested in the literature which have reported a value of 0.33 for laminar flow in tube side and a value of (0.6 to 0.8) for turbulent flow in the shell side [101,107]. The Schmit number in both phases has been reported to be unaffected by the flow pattern and to be relatively constant ranging between (0.3-0.33) [107], a value of 0.33 was used in this study.

The values of the constants (γ) and (β) in equations 5.28 and 5.29 respectively are proportional to: the packing fraction of membrane module, the hydraulic diameter and the module length and are found experimentally by drawing N_{Sht} vs $[d_{it}/L\ (N_{Ret})\ (N_{Sct})]^{0.33}$ for the tube side or N_{Shs} vs $[(d_h/L)(N_{Res})^{0.75}\ (N_{Scs})^{0.33}\ ]$ for the shell side. The (γ) value was found to range between 0.2 to 0.295 and was influenced to some extent by the solute concentration and the flow rate pattern inside the tubes. Therefore a more refined correlation was established in this study by calculating the slopes (the real γ values) of the relation N_{Sht} vs $[d_{it}/L(N_{Ret})(N_{Sct})]^{0.33}$ at each individual point and then plotting the calculated slope values against the aqueous phase flow rate. This correlation resulted in the following relations:

$\gamma = 0.147F_{aq} + 2.298$ for highly concentrated aqueous phase and

$\gamma = 0.105F_{aq} + 1.747$ for low concentration aqueous phase.

These relations were then used to calculate the value of (γ) which then substituted in equation 5.28 to account for $1/k_{aq}$ at any conditions. The variations on (γ) could be attributed to the effect of aqueous phase concentration and flow rate pattern on diffusivity of the copper ions from the bulk aqueous phase to the boundary layer inside the tubes and within the thin film layer near the pores' mouths at aqueous side. This effect could not be represented in equation 5.28 and therefore, the relation between (γ) and the aqueous phase properties gave more precise prediction to the overall mass transfer coefficient, see figures 5.18.A and B.

Using the same technique as above, the value of (β) was found to range between (0.0139 to 0.0156) for experiments carried out with low organic phase concentration and (0.023 to 0.0295) for experiments with highly concentrated organic phase. These values were substituted in equation (5.29) to account for the local resistance ($1/k_{org}$) under any flow conditions. The calculated local coefficients in combination with the earlier found values of $1/k_r$ and $1/mk_m$ were used to calculate the overall system resistance and the corresponding overall mass transfer coefficient ($1/K_{ovc}$). The results of fitting this model to the experimental data at tube and shell sides are illustrated in figures (5.18) and (5.19) and appendices 10.a,b and 11.a,b.

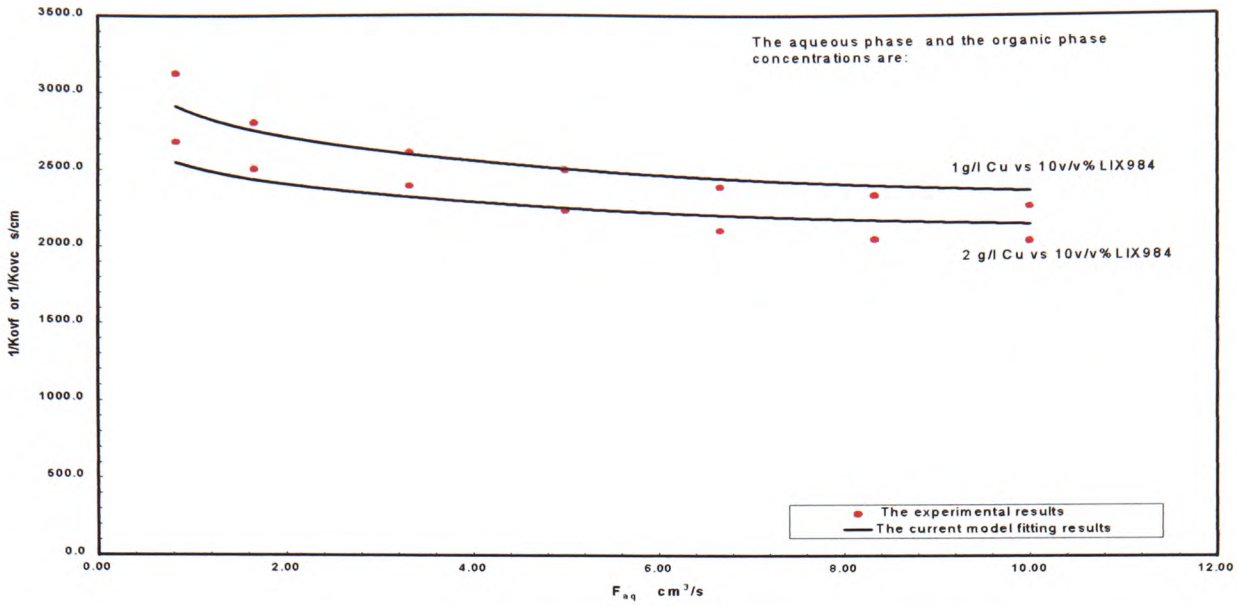

Figure 5.18.A: The results of fitting the generalised model using the average γ value to calculate the overall resistance, where the aqueous phase at variable flow rate and the organic at relatively high flow rate.

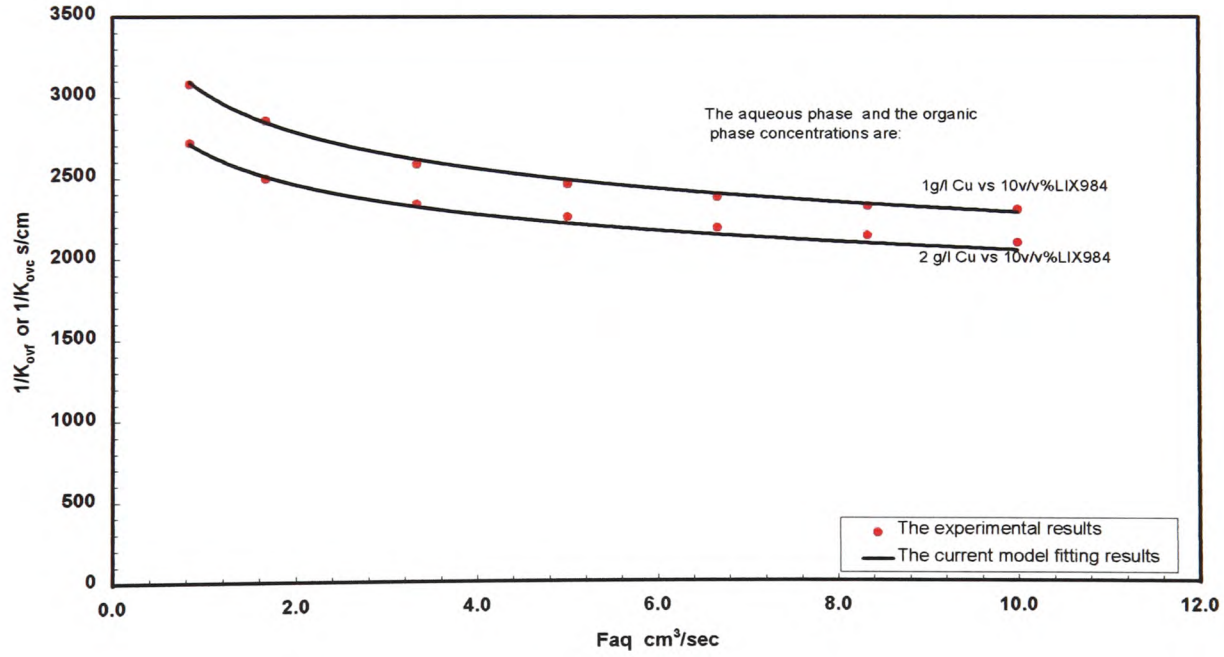

Figure 5.18.B: The results of fitting the generalised model using the refined correlation to calculate the overall resistance, where the aqueous phase at variable flow rate and the organic at relatively high flow rate.

In Figure 5.18 where the aqueous phase at variable flow rate and concentration was contacted counter currently against high flow organic phase at two different concentrations. The overall resistance was calculated from the combination of equations 5.28 and equation 5.29 and taking $(1/mk_m+1/k_r)$ as constant at (1550). The results show that the aqueous phase local resistance $(1/k_{aq})$ was the dominant and varying with the flow while the organic phase resistance $(1/k_{org})$ was constant and relatively low. In contrast when the aqueous phase was kept at high flow rate and constant concentration while the organic flow rate and concentration was varied, the resistance at the shell side became more important, see figure 5.19.

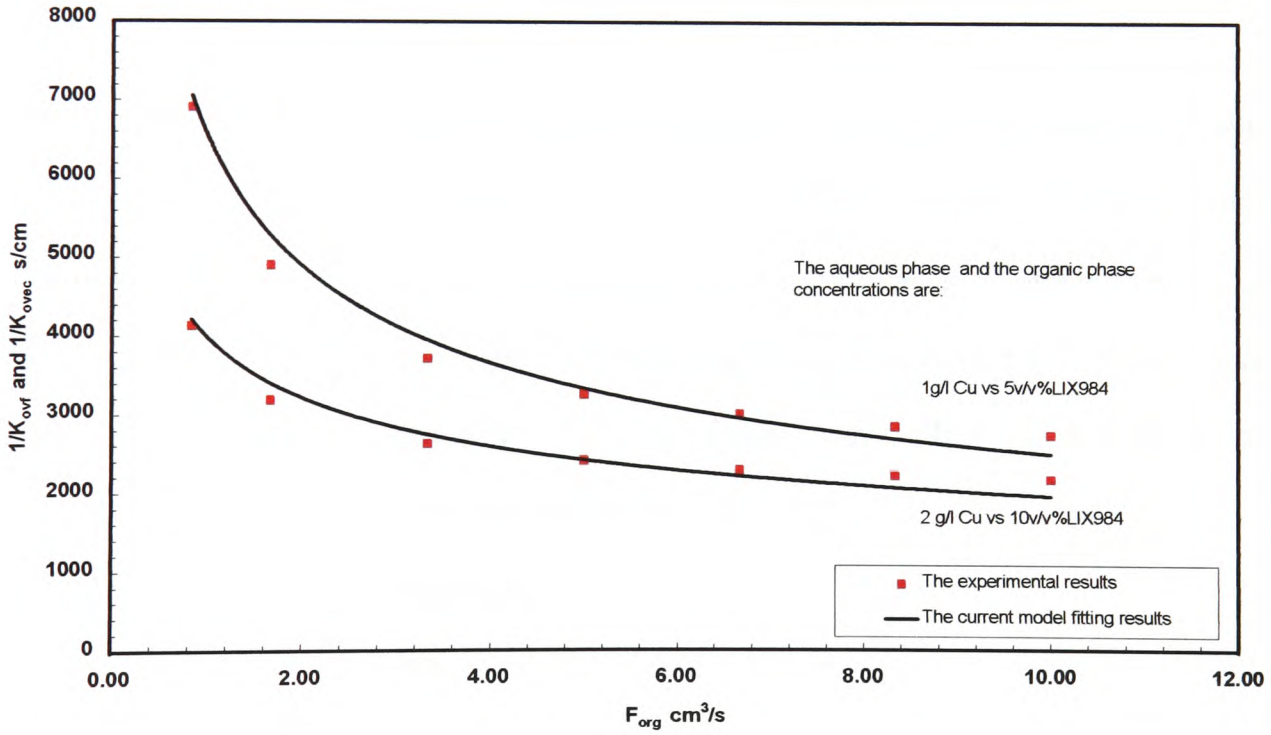

Figure 5.19: The results of fitting the generalised model to calculate the overall resistance, where the organic phase at variable flow rate and the aqueous phase at relatively high flow rate.

As it is apparent from figures 5.18, 5.19 and appendices 10 and 11 that the model proposed in this study is more effective in predicting the local resistances in comparisons to the models suggested by Prasad et. al.,[121] and Yang et. al.,[136].

Further intensive investigation is required to determine the relationship between the overall mass transfer coefficient and the local coefficients using the dimensionless groups. In addition to that a more accurate correlation for the constants (γ) and (β) using different membrane modules under wider operating conditions would help in predicting the precise overall resistance and hence would make membrane extractor design more reliable.

5.5 A Comparison Between Rising Drop and MPHF Membrane Based Liquid-Liquid Extraction

In this study the rising drop and MPHF membrane techniques were used to establish important factors of copper extraction process using highly reactive chelating agents in particular LIX984. The rising drop technique was chosen instead of others to study and assess the mass transfer characteristics of this extraction process for the following reasons:

1. Well defined interfacial area and easy to calculate especially when the rising drops have consistent shapes and constant flow rate.
2. Easy to build, modify and operate.
3. Small energy consumption.

However, this technique has shortcomings, which can be listed as follows:

1. The difficulty on controlling the rising drops size and flow rate especially at low flow rate when the pressurising gas flow rate should be precise to eliminate any fluctuation in drops formation rate.

2. It requires many trail and error experiments to establish the right flow rate for a specific drop size to eliminate any end effect (i.e. to eliminate any mass transfer during drops formation and coalescence.
3. Limitations on the quantities it could process and the difficulty in controlling the rising drops travelling path.

Therefore, a MPHF membrane module system was designed and built to be used to study the same extraction process. This technique has offered tremendous advantages over the rising drop's technique which can be summarised as follows:

1. A large and well define surface area in a compact and easy to operate system.
2. Capable of facilitating the extraction process with no dispersion or coalescence between the two phases.
3. Can be used to operate under a wide range of flow rate conditions ranging from small flow rate of 0.05 l/min to 4 l/min and a pressure over 400 KPa.
4. Can be operated in a batch or a continuous extraction mode process and can be used to process large volumes of both phases.
5. Easy and independent control on both phases flow rates and concentrations.
6. Does not suffer any loading or flooding problems.

However, this technique still has limiting feature, which in comparison to other techniques could be minimal. This limiting feature is represented by the extra resistance of the membrane wall thickness, which could effect the rate of mass transfer of a liquid-liquid extraction process.

CHAPTER SIX

CONCLUSIONS AND RECOMMENDATIONS

6.1 CONCLUSIONS

The extraction of copper from a copper sulfate medium using three different chelating reagents (LIX984®, LIX84® and LIX860®) was carried out in this study. The experimental work covers the equilibrium behaviour of the three reagents and mass transfer characteristics of the copper-chelating reagent complex in dispersion based and non-dispersive techniques.

1. The extraction equilibrium study was planned first to determine the equilibrium behaviour of the three extractants separately. Their equilibrium properties with respect to copper sulfate solutions have not been reported in the literature and the findings of this study can be summarised as following:

(a) The main observation of the equilibrium results is that all the three reagents gave favourable equilibrium curves and efficient in extracting copper under the studied conditions

(b) The acidity of the aqueous phase increases (pH decreases) dramatically after a few minutes of contacting the two phases. This is due to the fact that as the reaction proceeds protons from the reacting extractant molecules are released and diffused into the aqueous phase, which can be seen from the reaction equation below:

$$Cu^{2+}_{aq} + 2(HR)_{org} \rightleftharpoons (CuR_2)_{org} + 2\,H^{+}_{aq}$$

(c) In the stripping equilibrium results listed in table 4.4.A and B, It has been observed that the concentration of stripped copper was a function of the stripping acid concentration and increased with the increase of H_2SO_4 concentration in the stripping solution. However, it has been noticed that any increase in the acid concentration at the stripping phase (higher than 2 molar) could lead to the organic solvent instability, especially LIX860 and LIX84.

2. Mathematical models (chemical based model and semi-empirical based model) were developed in this work to predict copper concentration in the organic phase at equilibrium. The chemical model is based on the mass action law of the reaction equation between the metal ions and the organic active species. This model is found to fit the experimental data of the three systems.

   The semi-empirical model based on the Freundlich's adsorption equation fitted to the same results does not fit all the experimental data as well as the chemical based model. This could be attributed to the constants values (M,n) of Freundlich's equation which have been calculated from graphical relationships of copper concentrations in both phases at the equilibrium stage.

3. Mass transfer and kinetic characteristics of copper transfer from the aqueous phase into the organic phase in a dispersion based rising drop technique were thoroughly examined in this study. The aqueous solution was used as a continuous phase while the organic phase was dispersed in form of drops over a wide range of both phases' concentrations. The following conclusions can be drawn from the mass transfer study in this technique:

(a) The rate of mass transfer (N_a) and the overall mass transfer coefficient (K_{ov}) remain constant in all four columns used.

(b) Due to the difficulty in finding the interfacial concentrations of both phases experimentally and consequently the difficulty of assessing which of the two phases has the most resistance to mass transfer, a dimensionless-based mathematical model was developed in this study based on the experimental results and equations proposed by Elzinga and reported by Treybal [1]. This model also utilises the use of the overall mass transfer coefficient and the two-film theory to account for the reaction resistance.

(c) The calculated mass transfer coefficient at the continuous (aqueous) phase (k_c) remains constant in all columns. While the calculated mass transfer coefficient at the dispersed (organic) phase side (k_D) slightly decreases with an increase in the column's height.

(d) The calculated value of the reaction rate constant (k_r) remained relatively constant for all columns. However, calculations of (k_r) from a reaction controlled mass transfer equation (5.24) resulted in a power relationship with an order of (1.412) of the organic phase concentration. While the relationships with the interfacial copper and hydrogen concentrations were of first order.

4. A dispersion-free technique using a microporous hollow fibre membrane was also used in this work to study mass transfer properties in non-dispersive extraction. An intensive and a through experimental work was carried out to determine the extraction and the stripping processes main characteristics under wide range of operational conditions. The findings of this study on MPHF membrane effectiveness for copper extraction and recovery from an acidic copper sulfate solution can be summarised as follows:

4.1. On studying the counter current flow rate pattern effects on mass transfer of copper from the aqueous phase in the tube side to the organic phase in the shell side the following points were observed:

(a) The continuous counter current extraction process at 600 cm^3/min on both sides gave a linear increase in copper concentration at the organic extract outlet with each increase of the metal concentration in the feed stream. This was attributed to the fact that with a relatively high flow of both phases the availability of the metal ions and the chelating active reagent at the interface would be at their highest. Then the only factors affecting the metal transport would be the reaction mechanism and the membrane thickness.

(b) At low flow rate of both phases (100 cm^3/min) using a counter current extraction process resulted in small amounts of copper extraction and in some experiments this was 75% less than the concentrations obtained under high flow rate conditions. It was also observed that the relationship between the feed metal concentrations and the metal concentrations at the organic outlet is far from the linear relationship that resulted for high flows.

(c) In a counter current extraction with gradual flow rate increases at one side (i.e. in the tube side or the shell side) while the opposite side flow rate was kept constantly under relatively high flow rate: The results show that in the case of a relatively high (600cm^3/min) and constant aqueous flow rate and gradually increasing organic flow rate, the copper concentrations at the raffinate side were decreasing with each increase in the organic phase flow rate (from 100 to 600cm^3/min). However, these decreases varied with the initial aqueous phase copper concentrations.

In the case of a relatively high organic flow rate (600cm^3/min) and gradually increasing aqueous flow rate: The relationship between copper concentrations at the extract side and the increasing aqueous flow rate shows that each aqueous flow rate increase resulted in a corresponding increase at the organic outlet (extract) metal concentration. The results of this process also show that even at low aqueous feed flow

rate and low initial concentration the organic solvent could still extract between 10 to 40% of the inlet copper concentration.

(d) For a constant and relatively low flow rate ($100cm^3/min$) in one side and a gradually increasing flow rate (from 100 to $600cm^3/min$) in the opposite side. The counter current continuous extraction process results show that, if the aqueous phase flow rate was kept low in the tube side and the organic flow rate gradually increased in the shell side each increase in the organic flow rate leads to significant decline in the raffinate metal concentration. This relationship between the aqueous outlet (raffinate) copper concentration and the organic phase flow rate appears to be a straight line relationship when the feed aqueous solution copper content is high but the relationship takes a non-linear form when low initial aqueous phase concentrations were used.

If on the other hand, the organic phase had a relatively low flow rate and the aqueous phase flow rate was gradually increased, the results show that the extracted metal concentration at the organic phase outlet (extract) increased with each increase in the aqueous feed metal content. But the amount of copper extracted in this case was less than that obtained for a relatively high organic flow rate with a gradually increasing aqueous flow rate. The relationship between the extract phase copper concentrations and the gradually increasing aqueous feed flow rate resulted in a non-linear relationship for low flow rates of the organic phase.

4.2. Changing the flow arrangement of both phases from counter current to co-current resulted in a reduced amount of copper extracted under any of the set conditions examined in the counter current case. For instance the amount of copper extracted in the co-current arrangement was found to be ranging between 4% to 16% less than that extracted in counter current process under relatively high flow rate of both phases and low flow rates of both phase respectively.

4.3. The results of switching the two phases positions within the MPHF module (i.e. the organic phase flows to the tube side and the aqueous phase flows to the shell side gave similar results to those obtained under co-current conditions. In this arrangement the extraction process required a higher pressure in the shell side than that on the tube side to prevent any organic breakthrough.

4.4. A counter current batch extraction process under relatively high flow rates ($600cm^3/min$) in both sides of the MPHF membrane resulted in the recovery of 60% to 80% of the feed copper content in two hours and 40 minutes. However, it was noticed that the reduction of the raffinate copper concentrations was significantly low after 2 hours of continuous extraction. Whereas, the same process under relatively low flow rates of both phases ($100\ cm^3/min$) resulted in a less extracted copper concentrations than that obtained under relatively high flow rate conditions.

4.5. In relation to the two phases initial concentrations effect on the rate of mass transfer properties at $600\ cm^3/min$ flow rates of both phases. The results show a linear increase in copper concentration at the organic extract outlet with the increase of the initial metal concentration in the feed stream. While the results obtained under $100\ cm^3/min$ of both phases show a non-linear relationship between the initial metal concentration and its concentration at the organic outlet. These phenomenon could be caused by the boundary layers resistances in the path of metal transfer from the bulk aqueous phase to the bulk organic phase.

4.6. A continuous counter current stripping process resulted in very good recovery results of copper from the loaded organic phase (LIX984) in a MPHF membrane module. This process, it seems depends to a large extent on the aqueous stripping phase concentrations, (in other words the more acidic the stripping solution the more it is capable of recovering the metal especially under high flow rates of both phases). It has

also been found that a concentrated stripping solution (2 M H_2SO_4) could extract approximately 80% of the organic phase copper content in about 2 hours in a batch process.

4.7. The rate of mass transfer results in a non-dispersive MPHF membrane technique show a direct relation between the two phases flow rates and the rate of metal extracted which was attributed to the effect of the two phases flow pattern on the local resistances. Based on these findings a generalised mathematical model was developed in this study which utilised Wilson's method [134], the experimental data, some dimensionless groups and the two-film theory to account for local resistances and predict the system's overall mass transfer coefficient. This model was linked to the two phase's physical properties and the system's parameters using a form of Leveque equation which relate the two phases local coefficients (Sherwoods' numbers) to their Reynolds' and Schmits' numbers as follows:

$$N_{Sht} = \frac{k_{aq} d_{it}}{D_{aq}} = \gamma[\frac{d_{it}}{L}(N_{Ret})(N_{Sct})]^{0.33} \qquad \text{For the tube side}$$

$$N_{Shs} = \frac{k_{org} d_h}{D_{org}} = \beta[\frac{d_h}{L}(N_{Res})^{0.75}(N_{Scs})^{0.33}] \qquad \text{For the shell side}$$

The values of the constants (γ) and (β) in these relations were proportional; to the packing fraction of membrane module, the hydraulic diameter and the module length. The average (γ) value was found to range between 0.2 to 0.295 and was influenced to some extent by the solute concentration and the flow rate pattern inside the tubes. Therefore, a more refine correlation was established in this study by calculating the slopes (the real γ values) of the relation N_{Sht} vs $[d_{it}/L(N_{Ret})(N_{Sct})]^{0.33}$ at each individual point and then plotting the calculated slope values against the aqueous phase flow rate. This correlation enabled the model to fit all the experimental data.

The value of (β) was found to range between (0.0139 to 0.0156) for experiments carried out with low organic phase concentration and (0.023 to 0.0295) for experiments with a highly concentrated organic phase. The values of (γ) and (β) were substituted in equations (5.28 and 5.29) to account for the local resistance of ($1/k_{aq}$ and $1/k_{org}$) respectively and then in combination with the calculated values of ($1/k_r$ and $1/k_m$) were used to predict the value of the system's overall mass transfer coefficient ($1/K_{ov}$) under any flow rate conditions.

4.8. This study has proven that microporous hollow fibre membrane extractor has the ability to overcome many operational and technical limitations associated with conventional dispersion based extraction techniques. It is also apparent from this study that the MPHF contactor is capable of functioning as an effective extractor under unlimited operating conditions for the extraction and recovery of heavy metals from weak leach liquor and its applicability to the extraction of wide range of materials merit further investigation.

6.2 Recommendations for Future Work

1. In this study most of the experimental work has been focussed on finding the optimum theoretical and operational conditions for the extraction and recovery of copper using chelating agents and in particular LIX984. It is important to emphases here that the extraction abilities and behaviours of the other two LIX reagents (LIX84 and LIX986) merit further investigations.
2. In mass transfer studies using a dispersion based rising drops technique the use of smaller diameter columns could give clearer indications to changes in the continuous phase concentration during the extraction process and worth further examination.

3. An attempt has been made in this work to study and determine the main factors affecting the reactive extraction process of copper in a dispersion-free technique using MPHF membrane. However, this work is merely the tip of the iceberg of non-dispersive extraction process. Further studies are required to examine the exact phenomena of one metal or one mixture of metals ions transfer near and inside the pores of a MPHF membrane extractor.

4. This intensive work has only covered small area of the potentially promising features of the dispersion-free extraction technique. The author believes that this technique has great future applications which have to be thoroughly examined by researchers and industrialists alike. For instance its application in the treatment of circuit board industry wastewater streams (the etching waste) should be taken seriously and its application for CO_2 gas absorption from cars exhaust emission should be studied.

REFERENCES

1. Treybal, R. E.,"Liquid Extraction", Second edition, McGraw-Hill, NewYork, 1963.
2. Pratt, H. R. C.,"Counter-current Separation Processes", Elsevier's Publishing, Amsterdam,1967.
3. Schwezer, P. A., "Handbook of Separation Techniques For Chemical Engineering", McGraw-Hill, 1979.
4. Roger, W. C., Pierre, F., Don, G., Chem. Eng. Feb. 1991.
5. King, C. J., " Separation processes", McGraw-Hill, New York, 1971.
6. Coulson, J. M., Richardson, J. F., Backhurst, J. R., Harker, J. H., "Chemical Engineering", Vol.2, Fourth edition, Pergamon press, Oxford, 1991.
7. Hennico, A., Vermeulen, T.V., AIChEJ.,Vol. 8, 394, 19
8. Jackson, R., J. Chem. Eng. Progr., Vol. 62, 82, 1966.
9. Davies, J. T., J. Chem. Eng. Progr., Vol. 62, 89, 1966.
10. Doulah, M.S., Ind. Eng. Chem. Funnd. Vol. 14, 137, 1975.
11. Bailes, P.J., Hanson, C., Hughes, M.A., J. Chem. Eng., January, 1976.
12. Jimmy, L., Humphrey, J., Antonio, R., James, R.F., Chem. Eng., September, 1984.
13. Laddha, G.S., Degaleesan, T.E., "Transport Phenomena In Liquid extraction", Tata McGraw-Hill, New Delhi, 1976.
14. Thornton, J.D., Anderson, T.J. Javed, K.H., Achwal, S.K., AIChJ., Vol. 31, 1069, 1985.
15. Cusack, R.W., Fermeaux, P., Glatz, D., J. Chem., February, 1991.
16. Baird, M.H.I., Cand. J. Chem. Eng., Vol, 69, 1287, 1991.
17. Marcus, Y., Chem. Rev., Vol. 63, 139, 1963.
18. Marcus, Y., Kertes, A.S., "Ion-exchange and solvent extraction of metal complexes", Wiley-Interscience, London, 1967.
19. Hanson, C., (editor), "Recent advances in liquid-liquid extraction", Pergamon press, Oxford, 1971.
20. Morrison, G.H., Freiser, H., "Solvent extraction in analytical chemistry", Wiley, New York, 1957.
21. Stary, J., "The solvent extraction of metal chelats", Pergamon, 1964.
22. Lo, T.C., Baird, M.H.I., Hanson,C., (Editors), "Handbook of solvent extraction", Wiley, New York, 1967.

23. Ritcey, G.M., Ashbrook, A.W., "Solvent extraction principles and applications to process metallurgy", Part II, Elsevier, Amsterdam, 1979.
24. Lamborn, R.H., "The metallurgy of copper", Lockwood, London, 1875.
25. Ritcey, G.M., Ashbrook, A.W., "Solvent extraction principles and applications to process metallurgy", Part I, Elsevier, Amsderdam, 1984.
26. Drew, T.B., Cokelet, G.R., Hoopes, J.W., Vermeulen, T., (Editors), "Advances in chemical engineering", Vol. 9, Academic press, New York, 1974.
27. Power, K.L., ISEC.71, PP. 1409, 1971.
28. Ray, M.S., Ibid., Vol. 29, 2203, 1994
29. Komasawa, I., Otake, T. Ymada, A., J. Chem. Eng. Japan, Vol. 13, 130, 1980
30. Henkel Corporation mineral industry division,"Private communications"
31. Marcus, Y., Chem. Rev., Vol. 63, 139, 1963
32. Baes, C.F., J. Inorg. Nucl. Chem., Vol. 24, 707, 1962
33. Robinson, C.G., Paynter, J.C., ISEC 71. Society Of Chemical Industry, London, paper number 24, 1971
34. Mikhlim, E.V., ISEC 80., paper number 24, 1980
35. Baes, C.F., Coleman, C.F., Zingaro, R.A., J. Phys. Chem. Vol. 62, 2, 1958
36. Madigan, D.C., Aust. J. Chem. Vol.13, 58, 1960
37. Forrest, C., Hughes, M.A., Hydrometallurgy, Vol. 1, 139, 1975
38. Flett , D.S., Okuhara, D.N., Spink, D.R., J. Inorg. Nucl. Chem., Vol.35, 247, 1973
39. Renon, H., "Deviation from ideality in electrolyte solutions, in Foundation computer aided chemical process design", Engineering foundation, New York, 1981
40. Brisk, M.L., McManameny, W., IChemE. Symposium series, Vol.26, 21,1967.
41. Brisk, M.L., McManameny, W., J. Appl.Chem.,Vol.19, 103, 1969.
42. Bromley, L. A., J. Chem. Thermodynamics, Vol. 4, 669,1972.
43. Bromley, L. A., AIChEJ., Vol. 19, 313, 1973.
44. Flory, P. J., J. Chem. Phys., Vol. 9,660,1941.
45. Huggins, M.L., J. Chem. Phys. Vol. 9, 440, 1941.
46. Mahmood, Z., Ph.D., Thesis, Teesside Polytechnic, 1987.
47. Marcus, Y., "Thermodynamics of solvent extraction, in Alegret, S (editor), Developments in solvent extraction", Ellis Horwood Ltd., Chichester, 1988.
48. Ellis, D.A., Ind. Eng. Chem., Vol.52, 251. 1960.
49. Ioannou, T.K., Bautista, G., Smutz, M., ISEC'71. Soc. Ind. Chem., London, 1971.
50. Sharp, B.M., Smutz, M., Ind. Eng. Chem. Proc. Des. Develop., Vol. 4, 49, 1965.

51. Goto, T., ISEC'71. Soc. Ind. Chem., London, paper number 73, 1971.
52. Alegrat, S., (editor), "Developments in solvent extraction", Ellis Horwood Ltd., Chichester, 1988.
53. Cox, M., Flett, D.S., "Metal extraction chemistry", Chapter 2.2 in Handbook of solvent extraction, Lo, T.C., Baird, M.H.I., Hanson, C., (editors), Wiley, New York, 1983.
54. Cox, M., "Development in solvent extraction, new reagent", Chapter 8, in Alegret, S., (editor), Ellis Horrid Ltd., Chichester, 1988.
55. Whewell, R.J., Hughes, M.A., Hanson, C., J. Inorg. Nucl. Chem., Vol. 37, 2303,1975.
56. Akibar, K. Freiser, H., Anal.Chem.Acta., Vol. 136, 329, 1982.
57. Harada, M., Kishada, M., ISEC'90.,in Sekine, T. Kusakabe, S., (editors), "Proceeding to international solvent extraction, part A", Elsevier, Amsterdam, pp.777, 1992.
58. Komasawa, I., Otake, T., Muraoka, T., J. Chem. Eng. Japan, Vol. 13, 204, 1980.
59. Komasawa, I., Otake, T., Yamada, A., J. Chem. Eng. Japan, Vol. 13, 209,1980.
60. Hanson, C., J. Appl. Chem. Biotech., Vol. 28, 426, 1958.
61. Kojima, T., Miyauchi, T., In. Chem. Fundam., Vol. 20, 14, 1981
62. Inoue, K., Okubo, H., Nakashio, F., J. Chem. Eng. Japan, Vol. 12, 19, 1979.
63. Jamarack, W.D., " Rear metals extraction by chemical engineering techniques", Pergamon press, 1963.
64. Rudberg, J., Reinhardt, H., Liljensin, J.O., in Marinsky, J.A., Marcus, Y., (Editors), "Ion-exchange and solvent extraction", Marcel Dekker, New York, Vol. 3, pp.111, 1973.
65. Lewis, J.B., Chem. Eng. Sci., Vol. 3, 248, 1954.
66. Silva Cassa, J.C., Monhenius, A.J., "Kinetics of extraction of Iron (III) from chloride solution by Trioctylamine, in Bautista, R.G., (Editor), Hydrometallurigical process fundamentals", Plenum, New York, 1984.
67. Hughes, M.A., Middlebrook, P.D., Int. J. Min. Proc., Vol. 5, 229, 1978.
68. Freeman, R.W., Tavlarides, L.L., Chem. Eng. Sci., Vol. 35, 559, 1980.
69. Chapman, T.W., "Solvent extraction of metals-metal transfer rates and contactor design, in Bautista, R.G., (Editor), Hydrometallurigical process fundamentals", Plenum, New York, 1984.
70. Pratt, H.R.C., Murdoch, R, Trans. Inst. Chem. Eng., Vol. 31, 307, 1953.
71. Baumgärtner, F., Finsterwalder, L., J. Phys. Chem., Vol. 74, 108, 1970.

72. Treybal, R. E., "Mass transfer operation", Third edition, McGraw Hill, New York, PP. 537, 1980.
73. Astarita, G, " Mass transfer with chemical reaction", Elsevier, Amsterdam, 1967.
74. Whitman, W.G., Chem. Met. Eng., Vol. 29. 147, 1923
75. Whitman, W.G., Lewis, W.K., Ind. Eng. Chem. Vol. 16, 1215, 1924.
76. Higbie, R. Trans. Am. Inst. Cem. Engrs. Vol. 31, 365, 1935.
77. Danckwerts, P.V., AIChEJ., Voll. 1, 456, 1955.
78. Hadamard, J., Compt, rend., Vol.154, 109, 1912.
79. Hughes, M.A., Ipinmoroti, K.O., Hydrometallurgy, Vol. 24, 255, 1990.
80. Pratt, J.M., Tilley, R.I., Hydrometallurgy, Vol. 5, 29, 1979.
81. Danesi, P.R., Horwitz, E.P., Vandegrift, G.F., Chiarizia, R., Sep. Sci.Tech., Vol. 16, 201, 1981.
82. Harada, M., Miyake, Y., J. Chem. E.ng. Japan., Vol. 19, 196, 1986.
83. Danckwerts, P.V., "Gas-liquid reactions", McGrow Hill, New York, 1970.
84. Coulson, J.M., Richardson, J.F., Backhurst, J.R., Harker, J.H., "Chemical Engineering", Vol. I, Fourth edition, Pergamon press, Oxford, 1990.
85. Hughes, M.A., Rod, V., Faraday Discuss. Chem. Soc., Vol. 77, 75, 1984.
86. Scott, K., Editor, "Handbook of industrial membranes", First edition, Elsevier Advanced Technology, Oxford, UK, pp. 633, 1995.
87. Lee, C. T., Ho, S. W., Liu, J. K., Membrane solvent extraction, U.S. Patent 3, 956, 112, May 11, 1976.
88. Baker, R. W., Tuttle, M. E., Kelly, D. J., Lonsdale, H. K., J. Mem. Sci., Vol. 2, pp. 213, 1977.
89. Lee, K. H., Evans, D. F., Cussler, E. L., AlchEJ, Vol. 24, pp. 860, 1978.
90. Largman, T., Sifniades, S., Hydrometallurgy, Vol. 3, pp. 153, 1978.
91. Cussler, E. L., Evans, D. F., J. Mem. Sci., Vol. 6, pp. 113, 1980.
92. Danesi, P. R., Horwitz, E. P., Vandergift, G. F., Chiarizia, R., Sep. Sci. Tech., Vol. 16, pp. 201, 1981.
93. Kataoka. T., Nishki, T., Ueyama, K., Bull. Chem. Soc., Japan, Vol. 55, pp. 1306, 1982.
94. Chiarizia, R., Castanogla, A., Danesi, P. R., J. Mem. Sci., Vol. 14, pp. 161, 1983.

95. Danesi, P. R., Sep. Sci. Tech., Vol. 19, pp. 857, 1985.

96. Danesi, P. R., Yinger, L. R., Rickert, P. G., J. Mem. Sci., Vol. 31, pp. 147, 1987.

97. Izatt, R. M., Bruening, R. L., Christensen, J. J., ACS. Symp. Sers., Vol. 347, pp. 98, 1987.

98. Winston Ho, W. S., Sirkar, K. K., (Editors), Membrane Handbook, Van Nostrand Reinhold, New York, pp. 633-763, 1992.

99. Cecille, L. Toussaint, J. C., (Editors), Future industrial prospects of membrane processes, Elsevier applied Science, New York, 1989.

100. Flett, D. S., (Editor), Ion exchange membranes, Ellis, Horwood Ltd., Chichester, UK, 1983.

101. Meares, P., (Editor), Membrane separation process, Elsevier Advanced Technology, Oxford, 1976.

102. Prasad, R., Sirkar, K. K., Sep. Sci. Tech., Vol. 22, No. (2,3), pp. 619-640, 1987.

103. Alexander, P. R., Calahan, R. W., J. Mem. Sci., Vol. 35, pp. 57, 1987.

104. Cooney, D. O., Jin, C. L., Chem. Eng. Commun., Vol. 37, pp. 173, 1985.

105. Prasad, R., Sirkar, K. K., J. Mem. Sci., Vol. 47, pp. 255, 1989.

106. Keurentjes, T. F., Sluijs, T. M., Robert Jan, H. F., Klaus, V. R., Ind. Eng. Chem. Res., Vol. 31, pp. 581, 1992.

107. Chang, H. Y., Prasad, R., Guha, A. K., Sirkar, K. K., Ind. Eng. Chem. Res., Vol. 32, pp. 1186, 1993.

108. Cussler, E. L., AlchEJ, Vol. 17, No. 6, pp. 1300, 1971.

109. Cahn, R. P., Frankenfeld, J. W., Li, N. N., Naden, D., Subramanian, K. N., Recent developments in separation sciences, Vol. 6, Chapter 4, pp. 51, 1981.

110. Haan, A. B., Bartels, P. V., Graauw, J., J. Mem. Sci., Vol. 45, pp. 281-297, 1989.

111. Prasad, R., Sirkar, K. K., AIchJ., Vol. 33, No. 7, pp. 1057, 1987.

112. Teramoto, M., Tohno, N., Ohnisi, N., Matsuyama, H., Sep. Sci. Tech., Vol. 24, No. 12-13, pp. 981, 1989.

113. Takahashi, K., Takeuchi, H., J. Chem. Eng. Japan, Vol. 18, No. 3, pp. 205, 1985.

114. Noble, R. D., Koval, C. A., Chem. Eng. Prog., March, pp. 58, 1989.

115. Danesi, P. R., Rickert, P. G., J. Solvent extraction and ion exchange, Vol. 4, pp. 149, 1986.

116. Sengupta, A., Basu, R., Sirkar, K. K., AlChEJ., Vol. 34, pp. 1698, 1988.

117. Majumdar, S., Guha, A. K., Sirkar, K. K., AlChEJ., Vol. 34, pp. 1135, 1988.

118. Majumdar, S., Guha, A. K., Lee, Y. T., Sirkar, K. K., J. Memb. Sci., Vol. 43, pp. 259, 1989.

119. Guha, A. K., Yun, C. H., Basu, R., Sirkar, K. K., AlChEJ., Vol. 40, pp. 1223, 1994.

120. Hoechst Celanese Corporation, Germany, Separation Product Division, privet communication in hollow fibre modules and systems.

121. Prasad, R., Sirkar, K. K., AlChEJ., Vol. 34, No. 2, pp. 177, 1988.

122. Kiani, A., Bhave, R. R., Sirkar, K. K., J. Memb. Sci., Vol. 20, pp. 125, 1984.

123. Kim, M. B., J. Mem. Sci., Vol. 21, pp. 5, 1984.

124. Product and Applications Catalogue of Intersep Filtration System, Intersep Ltd., Wokingham, UK.

125. Prasad, R., Bhave, R. R., Kiani, A., Sirkar, K. K., J. Memb. Sci., Vol. 26, pp. 79, 1986.

126. Way, J. D., Noble, D. R., Bateman, B., Selection of supports for immobilised liquid membranes, in: Lloyd, D. R., (Editor), "Material Science of synthetic membranes", American chemical society, Washington, D.C., pp. 118-128, 1985.

127. Teramoto, M., Tanimoto, H., Sep. Sci. Tech., Vol. 18, pp. 871, 1983.

128. Danesi, P. R., J. Mem. Sci., Vol. 20, pp. 231, 1984.

129. Danesi, P. R., J. Solvent Ext. Ion. Exch., Vol. 2, pp. 115, 1984.

130. Way, J. D., Noble, D. R., ACS Symp. Ser., Vol. 347, pp. 123, 1987.

131. Noble, D. R., Koval, A. C., Chem. Eng. Progress, March 1989.

132. Prasad, R., Sirkar, K. K., J. Mem. Sci., Vol. 50, pp. 153, 1990.

133. Ortiz, I., Galan, B., Irabien, A., J. Mem., Sci. , Vol. 118, pp. 213, 1996.

134. McAdams, H. W., "Heat transmission", McGraw Hill. New York, pp. 343, 1954.

135. Reid, C. R., Prausnitz, M. J., Sherwood, K. T., "The properties of gaes and liquids", third edition, McGraw-Hill, New York, 1977.

136. Yang, M.C., Cussler, E. L., AIChE, Vol. 32, No. 11, pp. 1914, 1986.

Appendix 1: Sample of calibration curves used for equilibrium and mass transfer studies.

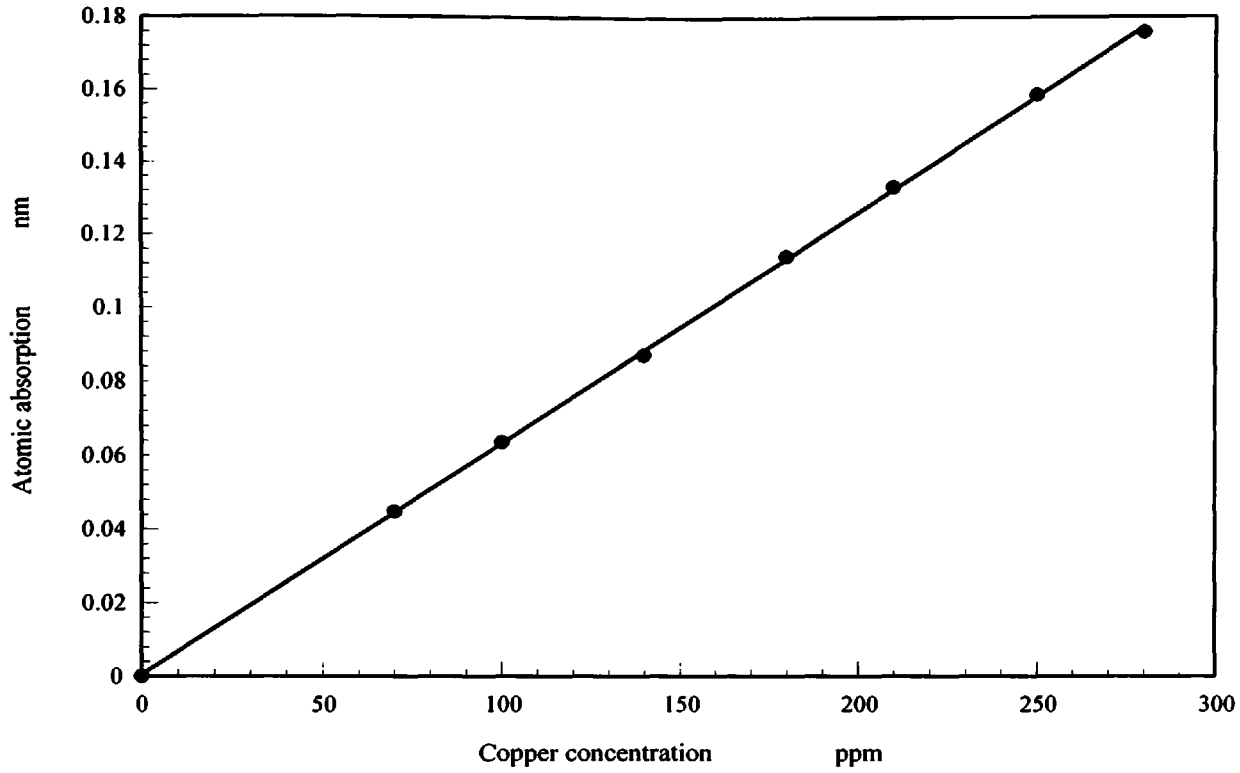

Appendix 2: The rising drops experimental rig set up.

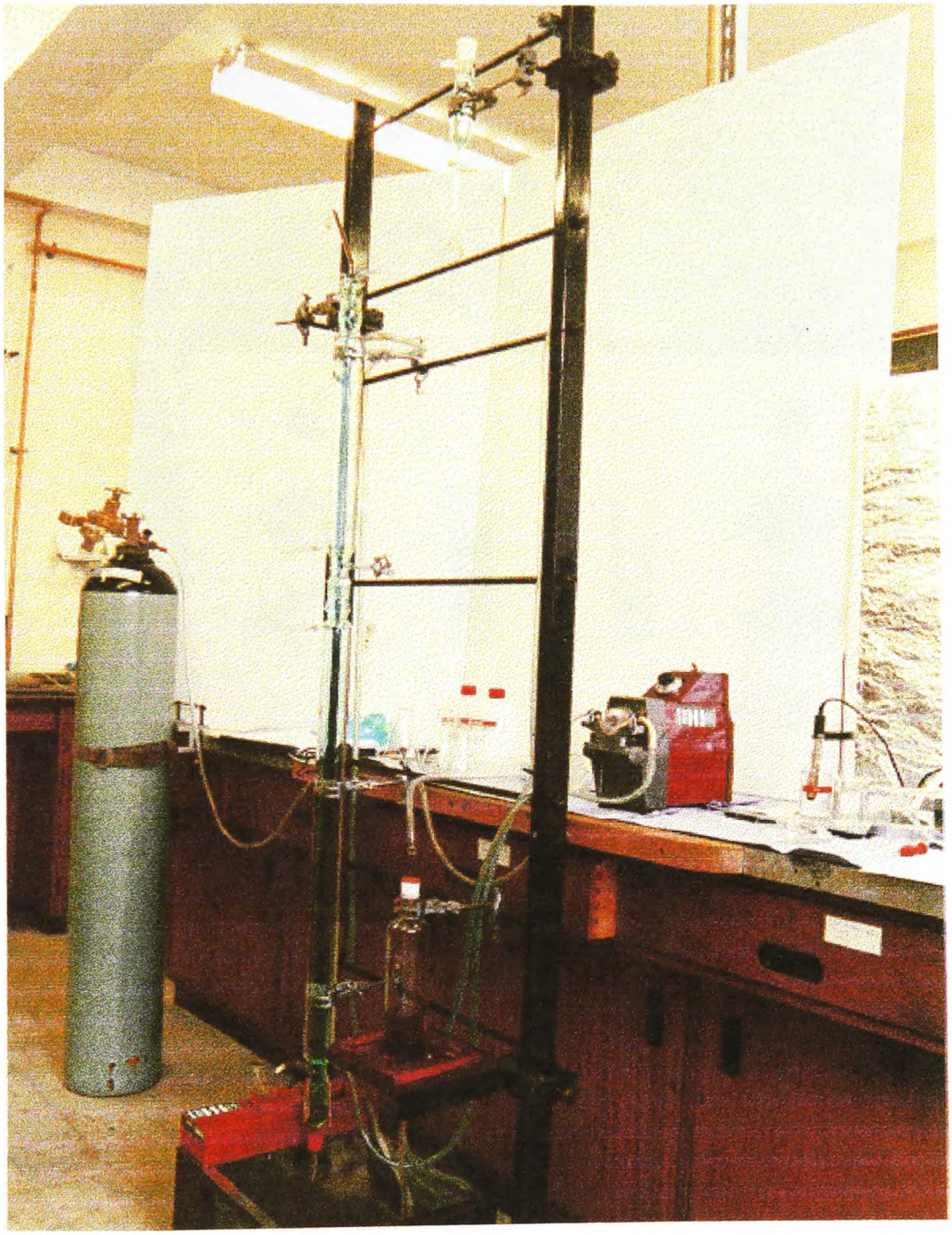

Appendix 3: The dispersion-free extraction unit and its main apparatus.

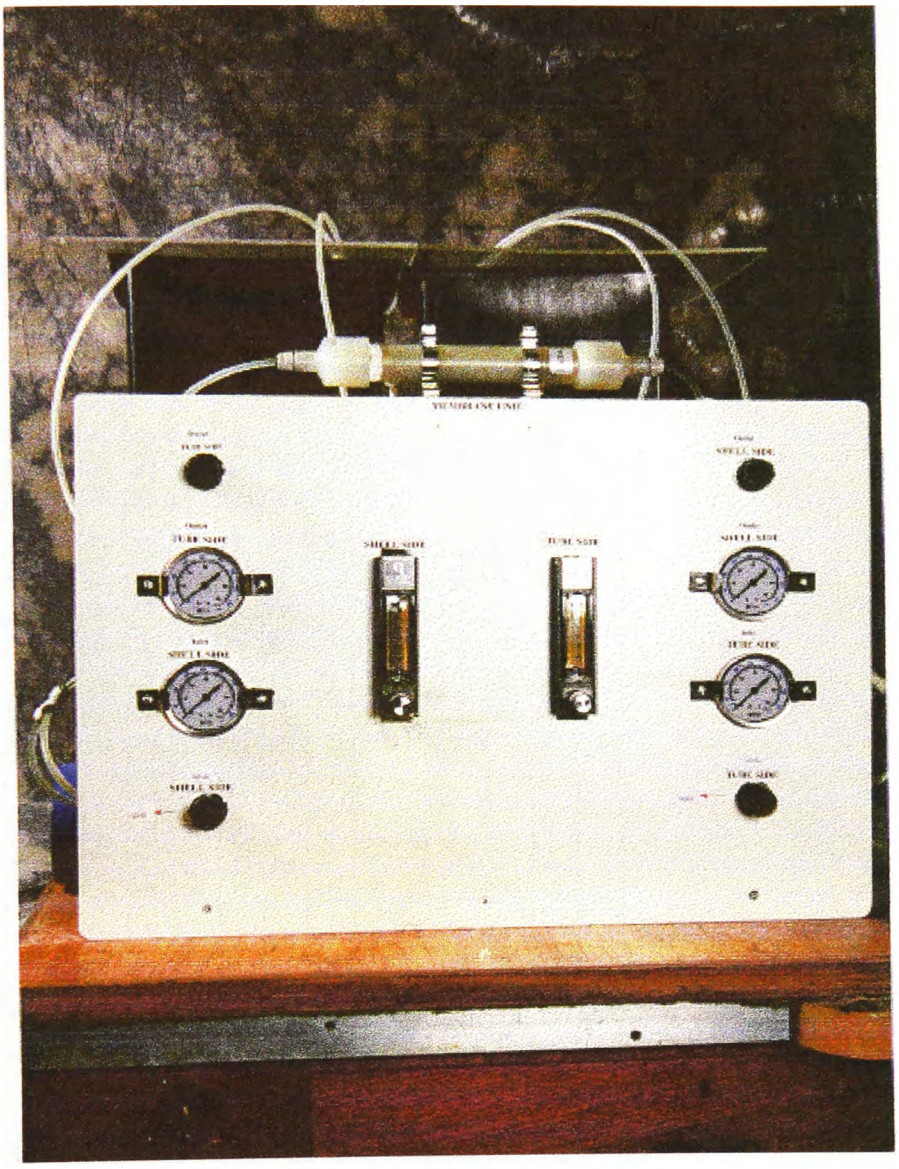

Appendix 4.A: The experimental results of the equilibrium constant of LIX84-Copper Sulphate system.

$[Cu_{in}]$ g/l	$[Cu_{in}]$ molar	HR_{in} mole	V_{org} Litre	$[CuR_2]$ g/l	$x = Cu_{react}$ mole	$HR_{react} = 2x$ mole	$[x] = x / V_{org}$ molar	$[Cu_{raffinat}]$ molar	$[HR_{eq}]$ molar	$[HR_{eq}]^2$ $molar^2$	pH_{eq}	$[H_{eq}]^2$ $molar^2$	K_{eq}
0.250	3.94E-03	0.012	0.05	0.2492	0.0002	0.0004	0.004	1.276E-05	0.2395	0.057	1.73	3.5E-04	1.860
1.000	1.57E-02	0.012	0.05	0.9873	0.0008	0.0016	0.016	2.000E-04	0.2162	0.047	1.50	1.0E-03	1.663
2.000	3.15E-02	0.012	0.05	1.9430	0.0015	0.0031	0.031	8.976E-04	0.1861	0.035	1.48	1.1E-03	1.079
3.000	4.72E-02	0.012	0.05	2.9150	0.0023	0.0046	0.046	1.339E-03	0.1555	0.024	1.50	1.0E-03	1.418
4.000	6.30E-02	0.012	0.05	3.8400	0.0030	0.0060	0.060	2.520E-03	0.1264	0.016	1.48	1.1E-03	1.648
5.000	7.87E-02	0.012	0.05	4.4800	0.0035	0.0071	0.071	8.189E-03	0.1062	0.011	1.30	2.5E-03	1.918
7.000	1.10E-01	0.012	0.05	5.3561	0.0042	0.0084	0.084	2.589E-02	0.0786	0.006	1.30	2.5E-03	1.324
9.000	1.42E-01	0.012	0.05	5.8750	0.0046	0.0093	0.093	4.921E-02	0.0623	0.004	1.20	4.0E-03	1.930
12.000	1.89E-01	0.012	0.05	6.3790	0.0050	0.0100	0.100	8.852E-02	0.0464	0.002	1.22	3.6E-03	1.913
15.000	2.36E-01	0.012	0.05	6.7700	0.0053	0.0107	0.107	1.296E-01	0.0341	0.001	1.30	2.5E-03	1.778
17.000	2.68E-01	0.012	0.05	6.9899	0.0055	0.0110	0.110	1.576E-01	0.0272	0.001	1.38	1.7E-03	1.644
20.000	3.15E-01	0.012	0.05	7.1510	0.0056	0.0113	0.113	2.023E-01	0.0221	0.0005	1.40	1.6E-03	1.807
													1.7

Appendix 4.B: The experimental results of the equilibrium constant of LIX860-Copper Sulphate system.

$[Cu_{in}]$ g/l	$[Cu_{in}]$ molar	HR_{in} mole	V_{org} Litre	$[CuR_2]$ g/l	$x = Cu_{react}$ mole	$HR_{react} = 2x$ mole	$[x] = x / V_{org}$ molar	$[Cu_{raffinate}]$ molar	$[HR_{eq}]$ molar	$[HR_{eq}]^2$ $molar^2$	pH_{eq}	$[H_{eq}]^2$ $molar^2$	K_{eq}
0.250	3.94E-03	0.018	0.05	0.2490	0.0002	0.0004	0.004	1.575E-05	0.3582	0.128	1.50	0.0010	1.941
1.000	1.57E-02	0.018	0.05	0.9140	0.0007	0.0014	0.014	1.354E-03	0.3372	0.114	1.20	0.0040	0.372
2.000	3.15E-02	0.018	0.05	1.9430	0.0015	0.0031	0.031	8.976E-04	0.3048	0.093	1.30	0.0025	0.922
3.000	4.72E-02	0.018	0.05	2.9150	0.0023	0.0046	0.046	1.339E-03	0.2742	0.075	1.50	0.0010	0.456
4.000	6.30E-02	0.018	0.05	3.8840	0.0031	0.0061	0.061	1.827E-03	0.2437	0.059	1.48	0.0011	0.618
5.000	7.87E-02	0.018	0.05	4.6248	0.0036	0.0073	0.073	5.909E-03	0.2203	0.049	1.30	0.0025	0.638
7.000	1.10E-01	0.018	0.05	5.9356	0.0047	0.0093	0.093	1.676E-02	0.1791	0.032	1.20	0.0040	0.692
9.000	1.42E-01	0.018	0.05	6.8750	0.0054	0.0108	0.108	3.346E-02	0.1495	0.022	1.20	0.0040	0.577
12.000	1.89E-01	0.018	0.05	8.1700	0.0064	0.0129	0.129	6.031E-02	0.1087	0.012	1.22	0.0036	0.656
15.000	2.36E-01	0.018	0.05	9.2600	0.0073	0.0146	0.146	9.039E-02	0.0743	0.006	1.20	0.0040	1.162
17.000	2.68E-01	0.018	0.05	9.8700	0.0078	0.0155	0.155	1.123E-01	0.0551	0.003	1.31	0.0024	1.092
20.000	3.15E-01	0.018	0.05	10.4900	0.0083	0.0165	0.165	1.498E-01	0.0356	0.0013	1.40	0.0016	1.379
											$K_{eq.}$ average =		0.9

Appendix 4.C: The experimental results of the equilibrium constant of LIX984-Copper Sulphate system.

$[Cu_{in}]$ g/l	$[Cu_{in}]$ molar	HR_{in} Mole	V_{org} Litre	$[CuR_2]$ g/l	$x = Cu_{react}$ mole	$HR_{react} = 2x$ mole	$[x] = x / V_{org}$ molar	$[Cu_{raffinate}]$ molar	$[HR_{eq}]$ molar	$[HR_{eq}]^2$ $molar^2$	pH_{eq}	$[H_{eq}]^2$ $molar^2$	K_{eq}
0.250	0.003937	0.01701	0.05	0.248	0.000195	0.000391	0.003906	0.00003	0.332509	0.11056	1.5	0.001	1.12154
1.000	1.57E-02	0.01701	0.05	0.993	0.000782	0.001564	0.015638	0.0001	0.309044	0.095508	1.5	0.00079	1.52165
2.000	3.14E-02	0.01701	0.05	1.961	0.001544	0.003088	0.030882	0.0006	0.278556	0.077594	1.4	0.00151	1.06684
3.000	4.72E-02	0.01701	0.05	2.865	0.002256	0.004512	0.045118	0.0021	0.250084	0.062542	1.3	0.00288	1.01406
5.000	7.86E-02	0.01701	0.05	4.427	0.003486	0.006972	0.069717	0.0089	0.200887	0.040356	1.2	0.00501	0.97286
7.000	1.10E-01	0.01701	0.05	5.630	0.004433	0.008866	0.088661	0.0214	0.162997	0.026568	1.1	0.00631	0.98385
12.000	1.89E-01	0.01701	0.05	6.980	0.005496	0.010992	0.109921	0.0788	0.120477	0.014515	1.0	0.01000	0.96156
15.000	2.36E-01	0.01701	0.05	7.750	0.006102	0.012205	0.122047	0.1138	0.096226	0.009259	1.1	0.00794	0.92002
17.000	2.67E-01	0.01701	0.05	8.300	0.006535	0.013071	0.130709	0.1366	0.078903	0.006226	1.1	0.00631	0.96987
18.500	2.91E-01	0.01701	0.05	8.800	0.006929	0.013858	0.138583	0.1523	0.063155	0.003989	1.1	0.00525	1.19730
20.000	3.14E-01	0.01701	0.05	9.200	0.007244	0.014488	0.144882	0.1696	0.050556	0.002556	1.3	0.00275	0.92062
											K_{eq} average =		1.05911

Appendix 5.A: The calculated results of fitting the chemical model on LIX84-Copper sulphate equilibrium data.

HR_{in} mole	V_{org} L	V_{aq} L	$R=Cu_{in}-Cu_{react}$ mole	$[H]^2$	$(H)^2$	K_{eq}	θ	θ^2	Ψ	ε	α*	Ec
0.012	0.05	0.05	3.28E-07	0.000398	1.0E-06	1.700	5.1E-08	2.6E-15	1.8E-18	2.2E-07	0.0001	0.100
0.012	0.05	0.05	8.76E-06	0.001096	2.7E-06	1.700	1.7E-07	3.0E-14	1.3E-15	6.0E-06	0.0006	0.797
0.012	0.05	0.05	4.24E-05	0.001738	4.3E-06	1.700	3.9E-07	1.5E-13	3.0E-14	2.9E-05	0.0014	1.782
0.012	0.05	0.05	6.32E-05	0.001000	2.5E-06	1.700	3.8E-07	1.5E-13	6.7E-14	4.3E-05	0.0023	2.951
0.012	0.05	0.05	1.21E-04	0.001000	2.5E-06	1.700	6.2E-07	3.8E-13	2.4E-13	8.2E-05	0.0030	3.794
0.012	0.05	0.05	4.03E-04	0.001995	5.0E-06	1.700	1.9E-06	3.6E-12	2.7E-12	2.7E-04	0.0035	4.423
0.012	0.05	0.05	1.29E-03	0.002754	6.9E-06	1.700	5.6E-06	3.1E-11	2.8E-11	8.7E-04	0.0042	5.314
0.012	0.05	0.05	2.45E-03	0.003162	7.9E-06	1.700	1.0E-05	1.1E-10	1.0E-10	1.7E-03	0.0045	5.757
0.012	0.05	0.05	4.41E-03	0.003162	7.9E-06	1.700	1.8E-05	3.4E-10	3.2E-10	3.0E-03	0.0049	6.182
0.012	0.05	0.05	6.46E-03	0.002188	5.5E-06	1.700	2.7E-05	7.1E-10	7.0E-10	4.4E-03	0.0052	6.599
0.012	0.05	0.05	7.86E-03	0.001738	4.3E-06	1.700	3.2E-05	1.0E-09	1.0E-09	5.3E-03	0.0053	6.783
0.012	0.05	0.05	1.01E-02	0.001820	4.5E-06	1.700	4.1E-05	1.7E-09	1.7E-09	6.9E-03	0.0054	6.860

Appendix 5.B: The calculated results of fitting the chemical model on LIX860-Copper sulphate equilibrium data.

HR_{in} mole	V_{org} L	V_{aq} L	$R=Cu_{in}-Cu_{react}$ mole	$[H]^2$	$(H)^2$	K_{eq}	θ	θ^2	Ψ	ε	α*	Ec
0.018	0.0500	0.0500	7.87E-07	0.000912	2.3E-06	1.04	1.2E-07	1.4E-14	9.0E-18	3.3E-07	0.0001	0.149
0.018	0.0500	0.0500	5.51E-05	0.010000	2.5E-05	1.04	1.5E-06	2.1E-12	4.4E-14	2.3E-05	0.0007	0.839
0.018	0.0500	0.0500	4.02E-05	0.002512	6.3E-06	1.04	4.7E-07	2.2E-13	2.3E-14	1.7E-05	0.0015	1.956
0.018	0.0500	0.0500	5.91E-05	0.001995	5.0E-06	1.04	4.7E-07	2.2E-13	5.1E-14	2.5E-05	0.0023	2.929
0.018	0.0500	0.0500	8.27E-05	0.001585	4.0E-06	1.04	5.1E-07	2.6E-13	9.9E-14	3.4E-05	0.0031	3.985
0.018	0.0500	0.0500	2.72E-04	0.003631	9.1E-06	1.04	1.5E-06	2.2E-12	1.1E-12	1.1E-04	0.0037	4.699
0.018	0.0500	0.0500	8.38E-04	0.005754	1.4E-05	1.04	3.9E-06	1.5E-11	1.0E-11	3.5E-04	0.0047	6.009
0.018	0.0500	0.0500	1.67E-03	0.006310	1.6E-05	1.04	7.2E-06	5.1E-11	4.1E-11	7.0E-04	0.0056	7.100
0.018	0.0500	0.0500	3.02E-03	0.005248	1.3E-05	1.04	1.2E-05	1.5E-10	1.3E-10	1.3E-03	0.0065	8.300
0.018	0.0500	0.0500	4.52E-03	0.003162	7.9E-06	1.04	1.8E-05	3.1E-10	3.0E-10	1.9E-03	0.0074	9.382
0.018	0.0500	0.0500	5.61E-03	0.001820	4.5E-06	1.04	2.2E-05	4.7E-10	4.6E-10	2.3E-03	0.0079	10.044
0.018	0.0500	0.0500	7.49E-03	0.001000	2.5E-06	1.04	2.9E-05	8.2E-10	8.1E-10	3.1E-03	0.0083	10.582

Appendix 5.C: The calculated results of fitting the chemical model on LIX984-Copper sulphate equilibrium data.

HR_{in} mole	V_{org} L	V_{aq} L	$R=Cu_{in}-Cu_{react}$ mole	$[H]^2$	$(H)^2$	K_{eq}	θ	θ^2	Ψ	ε	α*	Ec
0.017016	0.05	0.05	1.57E-06	0.001000	2.5E-06	1.059	1.3E-07	1.71E-14	3.2E-17	6.7E-07	0.0002	0.235
0.017016	0.05	0.05	4.27E-06	0.000794	1.99E-06	1.059	1.1E-07	1.32E-14	2.4E-16	1.8E-06	0.0006	0.729
0.017016	0.05	0.05	2.82E-05	0.001514	3.78E-06	1.059	2.9E-07	8.46E-14	1.0E-14	1.2E-05	0.0015	1.951
0.017016	0.05	0.05	1.03E-04	0.002884	7.21E-06	1.059	7.3E-07	5.33E-13	1.4E-13	4.3E-05	0.0023	2.938
0.017016	0.05	0.05	4.45E-04	0.005012	1.25E-05	1.059	2.2E-06	4.97E-12	2.6E-12	1.9E-04	0.0036	4.584
0.017016	0.05	0.05	1.07E-03	0.006310	1.58E-05	1.059	4.6E-06	2.16E-11	1.5E-11	4.5E-04	0.0045	5.760
0.017016	0.05	0.05	3.94E-03	0.010000	0.000025	1.059	1.5E-05	2.38E-10	2.0E-10	1.7E-03	0.0056	7.123
0.017016	0.05	0.05	5.69E-03	0.007943	1.99E-05	1.059	2.1E-05	4.62E-10	4.2E-10	2.4E-03	0.0062	7.925
0.017016	0.05	0.05	6.83E-03	0.006310	1.58E-05	1.059	2.5E-05	6.45E-10	6.1E-10	2.9E-03	0.0066	8.394
0.017016	0.05	0.05	7.61E-03	0.005248	1.31E-05	1.059	2.8E-05	7.9E-10	7.5E-10	3.2E-03	0.0068	8.687
0.017016	0.05	0.05	8.48E-03	0.003981	9.95E-06	1.059	3.1E-05	9.65E-10	9.3E-10	3.6E-03	0.0071	9.023

Appendix 6

The results of applying equation 5.15 to the equilibrium data of $CuSO_4$-LIX84, $CuSO_4$-LIX860 and $CuSO_4$-LIX984 systems are summarised in appendix 6.1, 6.2 and 6.3 respectively. These results were then used to draw the logarithm graphic relationship between copper concentrations at the aqueous and organic phases which can be illustrated in appendices 6.1.1, 6.2.1 and 6.3.1 as follows:

Appendix 6.1: The results of applying equation 5.15 to the equilibrium data of $CuSO_4$-LIX84 system.

g/l Copper concentration at the :				
Feed	**aqueous**	**Organic**	**Log Cu_{org}=logX**	**Log Cu_{aq}=logY**
0.250	0.001	0.2490	-0.6038	-3.000
1.000	0.090	0.9100	-0.0410	-1.046
2.000	0.057	1.9430	0.2885	-1.244
3.000	0.085	2.9150	0.4646	-1.071
4.000	0.160	3.8400	0.5843	-0.796
5.000	0.520	4.4800	0.6513	-0.284
7.000	1.644	5.3561	0.7288	0.216
9.000	3.125	5.8750	0.7690	0.495
12.000	5.621	6.3790	0.8048	0.750
15.000	8.230	6.7700	0.8306	0.915
17.000	10.010	6.9899	0.8445	1.000
20.000	12.849	7.1510	0.8544	1.109

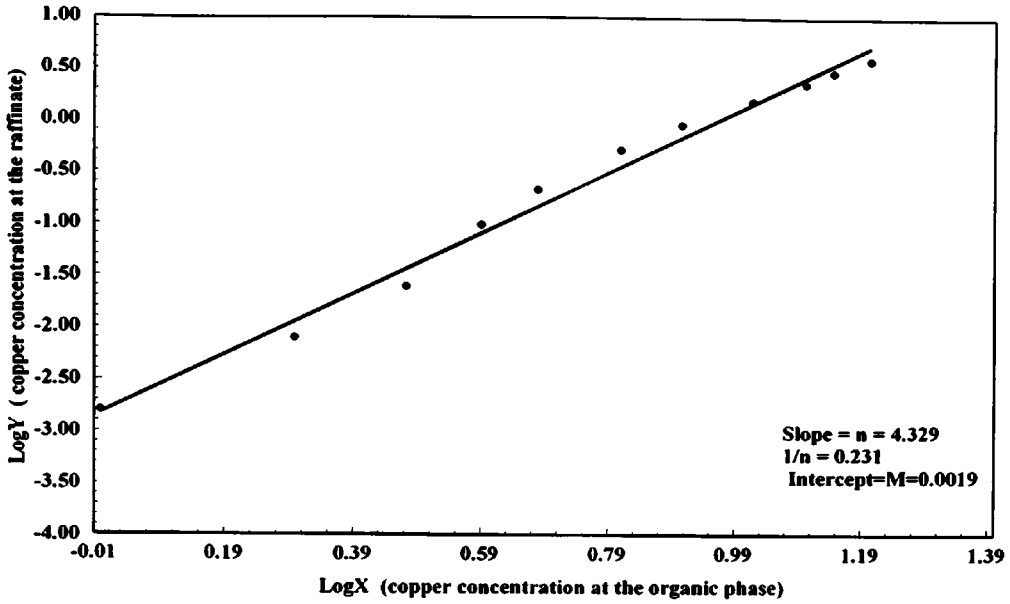

Appendix 6.1.1: The graphic relationship between log X and log Y, which was used to calculate the values of the intercept and the slope from $CuSO_4$-LIX84 equilibrium data.

Appendix 6.2: The results of applying equation 5.15 to the equilibrium data of $CuSO_4$-LIX860 system.

g/l Copper concentration at the :				
Feed	**aqueous**	**organic**	**Log Cu_{org}=logX**	**Log Cu_{aq}=logY**
0.250	0.0010	0.2490	-0.6038	-3.0000
1.000	0.0860	0.9140	-0.0391	-1.0655
2.000	0.0570	1.9430	0.2885	-1.2441
3.000	0.0850	2.9150	0.4646	-1.0706
4.000	0.1160	3.8840	0.5893	-0.9355
5.000	0.3752	4.6248	0.6651	-0.4257
7.000	1.0644	5.9356	0.7735	0.0271
9.000	2.1250	6.8750	0.8373	0.3274
12.000	3.8300	8.1700	0.9122	0.5832
15.000	5.7400	9.2600	0.9666	0.7589
17.000	7.1300	9.8700	0.9943	0.8531
20.000	9.5100	10.4900	1.0208	0.9782

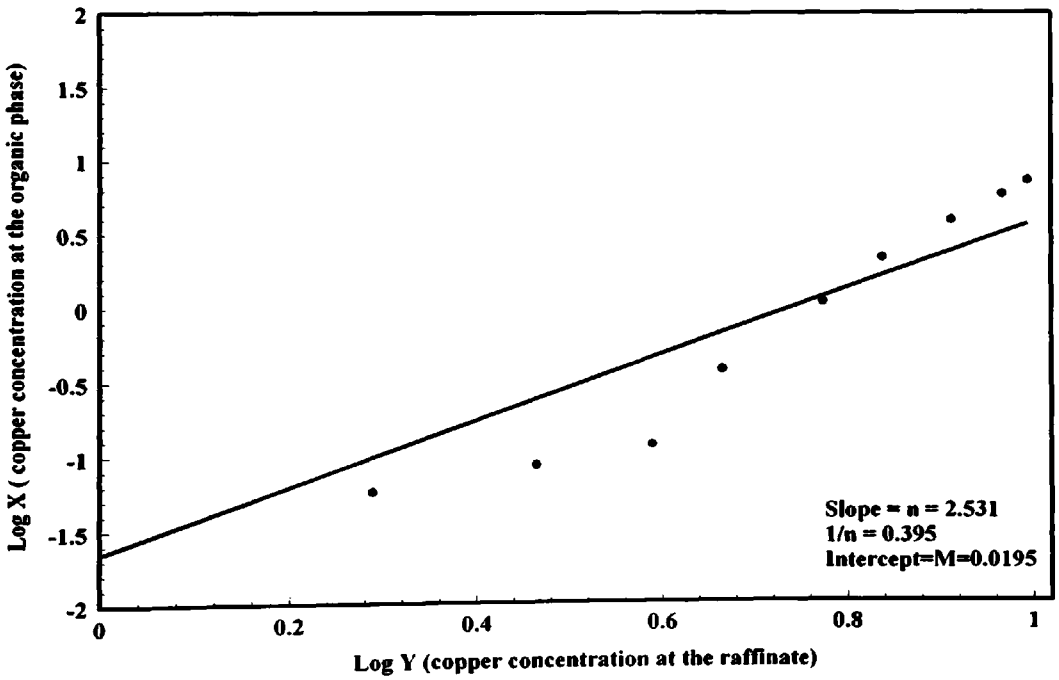

Appendix 6.2.1: The graphic relationship between log X and log Y, which was used to calculate the values of the intercept and the slope from $CuSO_4$-LIX860 equilibrium data.

Appendix 6.3: The results of applying equation 5.15 to the equilibrium data of $CuSO_4$-LIX984 system.

g/l Copper concentration at the :				
Feed	**aqueous**	**organic**	**Log Cu_{org}=logX**	**Log Cu_{aq}=logY**
1.000	0.01	0.99	-0.003	-2.155
2.000	0.04	1.96	0.292	-1.409
3.000	0.14	2.87	0.457	-0.870
5.000	0.57	4.43	0.646	-0.242
7.000	1.37	5.63	0.751	0.137
12.000	5.02	6.98	0.844	0.701
15.000	7.25	7.75	0.889	0.860
17.000	8.70	8.30	0.919	0.940
18.500	9.80	8.70	0.940	0.991
20.000	10.80	9.20	0.964	1.033

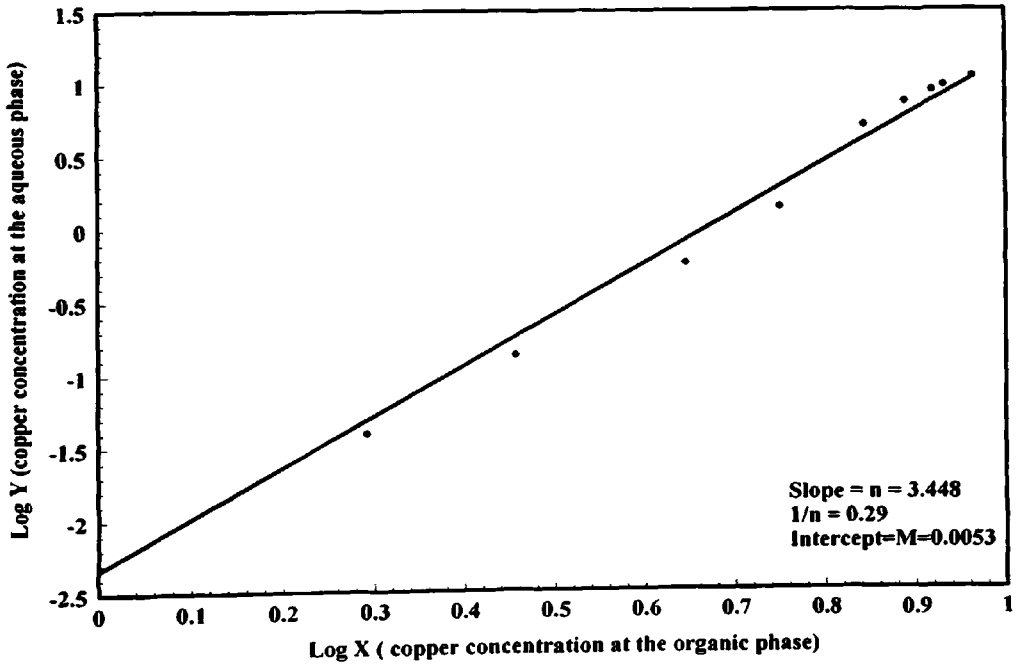

Appendix 6.3.1: The graphic relationship between log X and log Y, which was used to calculate the values of the intercept and the slope from $CuSO_4$-LIX984 equilibrium data.

Appendix 7

In this appendix a summary of the results that the semi-empirical model predicted by applying equation 5.16 to the equilibrium data of $CuSO_4$-LIX84, $CuSO_4$-LIX860 and $CuSO_4$-LIX984 systems. The values of the intercepts and the slopes (M and n) respectively were calculated from appendix 6.

Appendix 7.1: The results of applying freundlich's equation to predict the equilibrium of copper concentration at the organic phase in $CuSO_4$-LIX84 system.

The experimental results			**The semi-empirical model results**			
g/l copper concentration			Values from appendix 6. of:		g/l predicted concentration	
feed	**aqueous**	**organic**	**M**	**n**	**aqueous**	**organic**
0.250	0.001	0.2490	0.0019	4.329	0.0010	0.8622
1.000	0.090	0.9100	0.0019	4.329	0.0900	2.4380
2.000	0.057	1.9430	0.0019	4.329	0.0570	2.1939
3.000	0.085	2.9150	0.0019	4.329	0.0850	2.4060
4.000	0.160	3.8400	0.0019	4.329	0.1600	2.7846
5.000	0.520	4.4800	0.0019	4.329	0.5200	3.6560
7.000	1.644	5.3561	0.0019	4.329	1.6439	4.7695
9.000	3.125	5.8750	0.0019	4.329	3.1250	5.5325
12.000	5.621	6.3790	0.0019	4.329	5.6210	6.3360
15.000	8.230	6.7700	0.0019	4.329	8.2299	6.9193
17.000	10.010	6.9899	0.0019	4.329	10.0100	7.2395
20.000	12.849	7.1510	0.0019	4.329	12.8489	7.6693

Appendix 7.2: The results of applying freundlich's equation to predict the equilibrium copper concentration at the organic phase in $CuSO_4$-LIX860 system.

The experimental results			**The semi-empirical model results**			
g/l copper concentration			Values from appendix 6 of:		g/l predicted concentration	
feed	**aqueous**	**organic**	**M**	**n**	**aqueous**	**organic**
0.250	0.0010	0.2490	0.0199	2.564	0.0451	0.2049
1.000	0.0860	0.9140	0.0199	2.564	0.0472	0.9528
2.000	0.0570	1.9430	0.0199	2.564	0.4727	1.5273
3.000	0.0850	2.9150	0.0199	2.564	1.2116	1.7884
4.000	0.1160	3.8840	0.0199	2.564	1.9779	2.0221
5.000	0.3752	4.6248	0.0199	2.564	1.7850	3.2150
7.000	1.0644	5.9356	0.0199	2.564	2.1465	4.8535
9.000	2.1250	6.8750	0.0199	2.564	2.6224	6.3776
12.000	3.8300	8.1700	0.0199	2.564	3.9516	8.0484
15.000	5.7400	9.2600	0.0199	2.564	5.5568	9.4432
17.000	7.1300	9.8700	0.0199	2.564	6.7123	10.2877
20.000	9.5100	10.4900	0.0199	2.564	8.4726	11.5274

Appendix 7.3: The results of applying freundlich's equation to predict the equilibrium copper concentration at the organic phase in $CuSO_4$-LIX986 system.

The experimental results			**The semi-empirical model results**			
g/l copper concentration			Values from appendix 6 of:		g/l predicted concentration	
feed	**aqueous**	**organic**	**M**	**n**	**aqueous**	**organic**
1.000	0.01	0.99	0.005	3.448	0.009	0.991
2.000	0.04	1.96	0.005	3.448	0.216	1.784
3.000	0.14	2.87	0.005	3.448	0.443	2.557
5.000	0.57	4.43	0.005	3.448	1.111	3.889
7.000	1.37	5.63	0.005	3.448	1.993	5.007
12.000	5.02	6.98	0.005	3.448	4.703	7.297
15.000	7.25	7.75	0.005	3.448	6.882	8.118
17.000	8.70	8.30	0.005	3.448	8.441	8.559
18.500	9.80	8.70	0.005	3.448	9.640	8.860
20.000	10.80	9.20	0.005	3.448	10.887	9.113

Appendix 8: Wilson's plot results of the aqueous phase flowing under variable flow rate against a constantly high flow rate organic phase over rage of concentrations.

The aqueous phase flow properties:		**The overall and the tube side resistances corresponding to the aqueous flow rate pattern and the aqueous and organic phases concentrations**											
		3g/cmx10^{-3} aqueous vs 20v/v% LIX984			2g/cmx10^{-3} aqueous vs 10v/v% LIX984			1g/cmx10^{-3} aqueous vs 10v/v% LIX984			1g/cmx10^{-3} aqueous vs 5v/v% LIX984		
F_{aq} cm^3/s	$1/F_{aq}^{0.33}$	K_{ov}	$1/K_{ov}$ s/cm	$1/k_{aq}$ s/cm	K_{ov} cm/s	$1/K_{ov}$ s/cm	$1/k_{aq}$ s/cm	K_{ov}	$1/K_{ov}$ s/cm	$1/k_{aq}$ s/cm	K_{ov} cm/s	$1/K_{ov}$ s/cm	$1/k_{aq}$ s/cm
0.833	1.062	4.68E-04	2137.666	586.566	3.73E-04	2679.25	1113.95	3.20E-04	3125.0	1461.9	3.00E-04	3333.333	1662.333
1.667	0.845	5.21E-04	1920.000	368.900	4.00E-04	2500.99	935.69	3.57E-04	2801.1	1138.0	3.26E-04	3067.485	1396.485
3.333	0.672	4.90E-04	2040.816	489.716	4.18E-04	2393.56	828.26	3.83E-04	2611.0	947.9	3.59E-04	2785.515	1114.515
5.000	0.588	5.05E-04	1980.198	429.098	4.46E-04	2243.58	678.28	3.99E-04	2506.3	843.2	3.79E-04	2638.090	967.090
6.667	0.535	5.11E-04	1956.947	405.847	4.72E-04	2117.69	552.39	4.17E-04	2398.1	735.0	3.93E-04	2544.529	873.529
8.333	0.497	5.34E-04	1872.659	321.559	4.85E-04	2061.75	496.45	4.26E-04	2347.4	684.3	4.03E-04	2481.390	810.390
10.000	0.468	6.41E-04	1560.062	8.962	4.88E-04	2047.44	482.14	4.40E-04	2272.7	609.6	4.27E-04	2341.920	670.920
The intercept at very low flow rate= $1/K_{ov}$= $1/mk_m+1/k_r+1/mk_{org}+1/k_{aq}$			1551.1			1565.3			1663.1			1671	

Where: $1/k_{aq}=1/K_{ov}-1/mk_{org}-(1/mk_m+1/k_r)$

Appendix 9: Wilson's plot results of the organic phase flowing under variable flow rate against a constantly high flow rate of the aqueous phase over rage of concentrations.

The organic phase flow rate properties:		**The overall and the shell side resistances corresponding to the organic phase flow rate pattern and the aqueous and organic phases concentrations:**											
		3g/cm x10^{-3} aqueous vs 10v/v% LIX984			1g/cm x10^{-3} aqueous vs 10v/v% LIX984			1g/cm x10^{-3} aqueous vs 5v/v% LIX984			3g/cm x10^{-3} aqueous vs 5v/v% LIX984		
F_{aq} cm^3/s	$1/F_{aq}^{0.75}$	K_{ov} cm/s x10^4	$1/K_{ov}$ s/cm	$1/mk_{org}$ s/cm	K_{ov} cm/s x10^4	$1/K_{ov}$ s/cm	$1/mk_{org}$ s/cm	K_{ov} cm/s x10^4	$1/K_{ov}$ s/cm	$1/mk_{org}$ s/cm	K_{ov} cm/s x10^4	$1/K_{ov}$ s/cm	$1/mk_{org}$ s/cm
0.833	1.1469	2.62	3812.281	2150.981	2.33	4284.364	2601.164	1.41	7107.321	5273.72	1.57	6355.956	4538.456
1.667	0.6816	3.44	2904.803	1243.503	3.01	3325.000	1641.800	1.90	5273.000	3439.40	2.25	4454.118	2636.618
3.333	0.4054	4.02	2489.000	827.700	3.87	2584.650	901.450	2.55	3918.500	2084.90	2.88	3474.712	1657.212
5.000	0.2991	4.39	2276.000	614.700	4.18	2392.445	709.245	3.02	3315.300	1481.70	3.32	3009.791	1192.291
6.667	0.2410	4.71	2122.635	461.335	4.45	2249.281	566.081	3.40	2942.244	1108.64	3.62	2764.027	946.5271
8.333	0.2039	4.82	2074.058	412.758	4.74	2109.704	426.504	3.74	2672.110	838.510	3.79	2636.789	819.2891
10.000	0.1778	5.32	1880.000	218.700	4.79	2089.000	405.800	3.94	2539.231	705.631	4.03	2480.172	662.6718
The intercept at very low flow rate = $1/K_{ov}$= $1/mk_m+1/k_r+1/mk_{org}+1/k_{aq}$		1661.3			1683.2			1833.6			1817.5		

Where: $1/k_{aq}=1/K_{ov}-1/mk_{org}-(1/mk_m+1/k_r)$

Appendix 10.A: The experimental results of the overall mass transfer coefficient and the aqueous phase coefficient under high organic phase flow rate and variable aqueous phase flow rate and concentrations.

The aqueous phase concentration is 2g/l vs organic phase of 10v/v% LIX984								The aqueous phase concentration is 1g/l vs organic phase of 10v/v% LIX984				
F_{aq} cm^3/s	$1/f_{aq}^{0.33}$	K_{ovf} cm/s x 10^4	$1/K_{ovf}$ s/cm	$(d_t/l*NRe*NSc)^{0.33}$	$1/k_{aqf}$ s/cm	k_{aqf} cm/s x 10^3	N_{Shtf}	K_{ovf} cm/s x 10^4	$1/K_{ovf}$ s/cm	$1/k_{aq}$ s/cm	k_{aq} x 10^3	N_{Sht}
0.833	1.0621	4.31	2320.0	1.640	769.500	1.30	4.424	3.20	3125	1460.4	0.685	2.331
1.667	0.8448	4.50	2220.0	2.062	669.500	1.49	5.085	3.57	2801.1	1136.5	0.880	2.995
3.333	0.6721	4.90	2040.8	2.592	490.316	2.04	6.943	3.83	2610.9	946.36	1.060	3.597
5.000	0.5879	5.05	1980.1	2.963	429.698	2.33	7.922	3.99	2506.2	841.66	1.19	4.044
6.6667	0.5346	5.11	1956.9	3.258	406.447	2.46	8.376	4.17	2398.0	733.48	1.36	4.641
8.333	0.4967	5.18	1930.5	3.507	380.002	2.63	8.959	4.26	2347.4	682.81	1.46	4.985
10.00	0.4677	5.22	1915.7	3.725	365.209	2.74	9.321	4.40	2272.7	608.12	1.64	5.597

Appendix 10.B: The calculated results of the overall and local mass transfer coefficients using the generalised model for a relatively high organic phase flow rate and variable aqueous phase flow rate and concentrations.

The aqueous phase concentration is 2g/l vs organic phase of 10v/v% LIX984								The aqueous phase concentration is 1g/l vs organic phase of 10v/v% LIX984			
F_{aq} cm^3/s	$1/f_{aq}^{0.33}$	$(d_t/l*NRe*NSc)^{0.33}$	N_{shtc}	$1/k_{aqc}$ s/cm	$1/mk_{orgc}$ s/cm	$1/mk_m+1/k_r$ s/cm	$1/K_{ovc}$ s/cm	N_{shtc}	$1/k_{aqc}$ s/cm	$1/mk_{orgc}$ s/cm	$1/K_{ovc}$ s/cm
0.833	1.0621	1.640	3.969	857.62	309.67	1550	2717.39	3.034	1121.86	408.67	3081.13
1.667	0.8448	2.062	5.361	634.95	309.67	1550	2494.71	3.815	892.36	408.67	2851.62
3.333	0.6721	2.592	7.128	477.59	309.67	1550	2337.36	5.443	625.42	408.67	2584.68
5.000	0.5879	2.963	8.593	396.16	309.67	1550	2255.92	6.845	497.34	408.67	2456.60
6.6667	0.5346	3.258	10.427	326.50	309.67	1550	2186.27	8.146	417.92	408.67	2377.19
8.333	0.4967	3.507	12.275	277.33	309.67	1550	2137.09	9.469	359.50	408.67	2318.76
10.00	0.4677	3.725	14.527	234.35	309.67	1550	2094.11	10.057	338.50	408.67	2297.77

Appendix 11.A: The experimental results of the overall mass transfer coefficient and the organic phase mass transfer coefficient under high aqueous phase flow rate and variable organic phase flow rate and concentrations.

The aqueous phase concentration is 2g/l vs organic phase of 10v/v% LIX984								The aqueous phase concentration is 1g/l vs organic phase of 5v/v% LIX984				
F_{org} cm^3/s	$1/f_{org}^{0.75}$	K_{ovf} cm/s x 10^4	$1/K_{ovf}$ s/cm	$d_h/l*NRe^{0.75}*NSc^{0.33}$	$1/mk_{orgf}$ s/cm	k_{orgf} cm/s x 10^5	N_{Shsf}	K_{ovf} cm/s x 10^4	$1/k_{ovf}$ s/cm	$1/mk_{orgf}$ s/cm	K_{orgf} cm/s x 10^5	N_{Shsf}
0.833	1.147	2.38	4201.681	9.643	2526.58	1.865	0.262	1.41	7107.32	5273.82	0.893	0.126
1.667	0.682	2.90	3448.276	16.225	1773.18	2.657	0.374	1.90	5273.00	3439.50	1.37	0.193
3.333	0.405	3.55	2816.901	27.281	1141.80	4.127	0.580	2.55	3918.50	2085.00	2.26	0.318
5.000	0.299	4.32	2314.815	36.979	639.71	7.366	1.036	3.02	3315.30	1481.80	3.18	0.447
6.6667	0.241	4.65	2150.538	45.885	475.44	9.9	1.394	3.40	2942.24	1108.74	4.25	0.598
8.333	0.204	4.73	2114.165	54.241	439.06	10.73	1.509	3.74	2672.11	838.61	5.62	0.790
10.00	0.178	5.00	2000.000	62.191	324.90	14.50	2.040	3.94	2539.23	705.73	6.68	0.939

Appendix 11.B: The calculated results of the overall and local mass transfer coefficients using the generalised model for a high aqueous phase flow rate and variable organic phase flow rate and concentrations.

The aqueous phase concentration is 2g/l vs organic phase of 10v/v% LIX984								The aqueous phase concentration is 1g/l vs organic phase of 5v/v% LIX984			
F_{org} cm^3/s	$1/f_{org}^{0.75}$	$d_h/l*NRe^{0.75}*NSc^{0.33}$	N_{Shsc}	$1/k_{aqc}$ s/cm	$1/mk_{orgc}$ s/cm	$1/mk_m+1/k_r$ s/cm	$1/K_{ovc}$ s/cm	N_{shtc}	$1/k_{aqc}$ s/cm	$1/mk_{orgc}$ s/cm	$1/K_{ovc}$ s/cm
0.833	1.147	9.643	0.284	252.08	2329.82	1550	4132.00	0.134	410.08	4944.57	6905.153
1.667	0.682	16.225	0.479	252.08	1384.69	1550	3186.87	0.225	410.08	2938.74	4899.318
3.333	0.405	27.281	0.805	252.08	823.53	1550	2625.71	0.379	410.08	1747.78	3708.358
5.000	0.299	36.979	1.091	252.08	607.54	1550	2409.72	0.514	410.08	1289.39	3249.973
6.6667	0.241	45.885	1.354	252.08	489.62	1550	2291.80	0.637	410.08	1039.12	2999.698
8.333	0.204	54.241	1.600	252.08	414.19	1550	2216.38	0.754	410.08	879.05	2839.626
10.00	0.178	62.191	1.835	252.08	361.25	1550	2163.43	0.864	410.08	766.68	2727.258